



January 2017

Mechanisms Of Dopaminergic, Histaminergic, And Glutamatergic Neuromodulation Within The Medial Entorhinal Cortex

Nicholas Ian Cilz

Follow this and additional works at: <https://commons.und.edu/theses>

Recommended Citation

Cilz, Nicholas Ian, "Mechanisms Of Dopaminergic, Histaminergic, And Glutamatergic Neuromodulation Within The Medial Entorhinal Cortex" (2017). *Theses and Dissertations*. 2188.
<https://commons.und.edu/theses/2188>

This Dissertation is brought to you for free and open access by the Theses, Dissertations, and Senior Projects at UND Scholarly Commons. It has been accepted for inclusion in Theses and Dissertations by an authorized administrator of UND Scholarly Commons. For more information, please contact zeinebyousif@library.und.edu.

MECHANISMS OF DOPAMINERGIC, HISTAMINERGIC, AND
GLUTAMATERGIC NEUROMODULATION WITHIN THE MEDIAL
ENTORHINAL CORTEX

by

Nicholas Ian Cilz
Bachelor of Science, North Dakota State University (Fargo), 2010

A Dissertation
Submitted to the Graduate Faculty

of the

University of North Dakota

In partial fulfillment of the requirements

for the degree of

Doctor of Philosophy

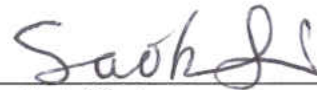
Grand Forks, North Dakota

August

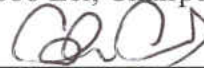
2017

Copyright 2017 Nicholas Ian Cilz

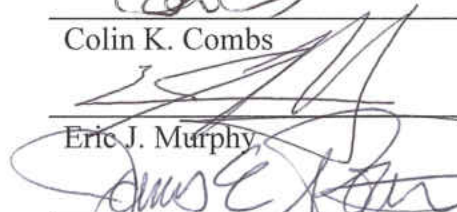
This dissertation, submitted by Nicholas Ian Cilz in partial fulfillment of the requirements for the Degree of Doctor of Philosophy from the University of North Dakota, has been read by the Faculty Advisory Committee under whom the work has been done and is hereby approved.



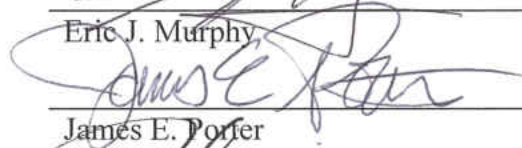
Saobo Lei, Chairperson



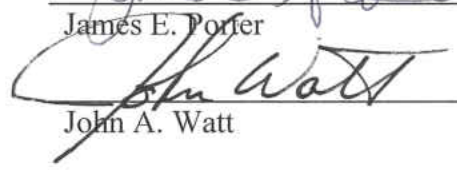
Colin K. Combs



Eric J. Murphy

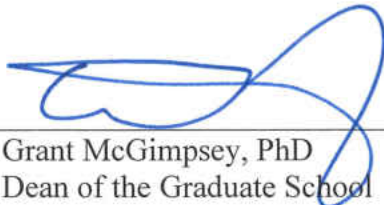


James E. Porter



John A. Watt

This dissertation is being submitted by the appointed advisory committee as having met all of the requirements of the School of Graduate Studies at the University of North Dakota and is hereby approved.



Grant McGimpsey, PhD
Dean of the Graduate School

July 24, 2017

Date

PERMISSION

Title: Mechanisms of Dopaminergic, Histaminergic, and Glutamatergic
 Neuromodulation Within the Medial Entorhinal Cortex

Department: Pharmacology, Physiology, and Therapeutics

Degree: Doctor of Philosophy

In presenting this dissertation in partial fulfillment of the requirements for a graduate degree from the University of North Dakota, I agree that the library of this University shall make it freely available for inspection. I further agree that permission for extensive copying for scholarly purposes may be granted by the professor who supervised my dissertation work, or in his absence, by the Chairperson of the department or the dean of the School of Graduate Studies. It is understood that any copying or publication or other use of this dissertation or part thereof for financial gain shall not be allowed without my written permission. It is also understood that due recognition shall be given to me and to the University of North Dakota in any scholarly use which may be made of any material in my dissertation.

Nicholas Ian Cilz
August, 2017

TABLE OF CONTENTS

LIST OF FIGURES	xi
ACKNOWLEDGEMENTS	xiii
ABSTRACT	xv
CHAPTER	
I. INTRODUCTION	1
Preface.....	1
Memory Systems Reside in the Medial Temporal Lobe	2
Lesions to the MTL Impair Learning and Memory	2
Early Structural and Functional Investigations Aimed at Understanding MTL Parahippocampal- Entorhinal-Hippocampal Regions.....	3
Connectivity of the Rodent Parahippocampal-Entorhinal- Hippocampal System	5
The Medial Entorhinal Cortex	7
Structural Overview of the MEC	7
Principal Cells of Layer I.....	8
Principal Cells of Layer II.....	8
Principal Cells of Layer III	10
Layer IV	12
Principal Cells of Layer V	12
Principal Cells of Layer VI.....	12

	GABAergic Interneurons of MEC	13
	MEC Connectivity with the Hippocampus and Connectivity within MEC	15
	Connections Between MEC and Hippocampus	15
	Connections Within the MEC	18
	Specialized Features of Neurons within the MEC	21
	The MEC and Learning and Memory	22
	Pathological Conditions Related to the EC	24
	Alzheimer’s Disease	25
	Temporal Lobe Epilepsy	29
	Depression and Anxiety	32
	Neuromodulation	35
	General Overview	35
	Dissertation Research Objective	37
II.	METHODS	39
	Acute Slice Preparation	39
	Organotypic Slice Preparation	40
	Electrophysiological Recordings	40
	Recordings of GABA _A Receptor-Mediated sIPSCs, mIPSCs, and eIPSCs	41
	Recordings of Resting Membrane Potentials, Action Potentials, Holding Currents, and Current-Voltage Relationships from Layer III MEC Interneurons	43
	Recordings of APs, RMPs, HCs, and I-Vs from Principal Neurons of the MEC	44

	Western Blot	46
	Immunohistochemistry	47
	Knock-Down of TRPC4 and TRPC5.....	48
	Biolistic Transfection of Organotypic Slice Cultures.....	48
	Data Analysis	49
	Chemicals.....	49
III.	RESULTS	51
	Study 1 – Dopaminergic Modulation of MEC GABAergic Transmission.....	51
	Introduction.....	51
	DA Increases the Frequency Not the Amplitude of sIPSCs Recorded from Entorhinal Neurons Via Activation of $\alpha 1$ Adrenergic Receptors	53
	Endogenously Released DA Also Increases sIPSC Frequency Via Activation of $\alpha 1$ Receptors.....	59
	DA Enhances the Frequency of mIPSCs, But Slightly Reduces the Amplitude of eIPSCs.....	61
	DA Depolarizes GABAergic Interneurons in the EC.....	66
	Ionic Mechanisms Underlying DA-Induced Depolarization of Interneurons	71
IV.	RESULTS	77
	Study 2 - Histaminergic Modulation of MEC GABAergic Transmission.....	77
	Introduction.....	77
	HA Increases the Frequency without Significant Effects on the Amplitude of sIPSCs Recorded from Principal Neurons in the MEC	80

	HA Increases Spontaneous GABAergic Transmission by Facilitating Presynaptic GABA Release.....	82
	HA Increases the Excitability of Local Interneurons in the MEC.....	85
	Both H ₁ and H ₂ Receptors are Involved in HA-Induced Enhancement of Spontaneous GABAergic Transmission.....	88
	Partial Involvement of a Na ⁺ -Permeable Cation Channel in HA-Induced Depolarization of Interneurons.....	97
	HA Inhibits K _{irs} and I _K in MEC Interneurons.....	101
	Extracellular Cs ⁺ Reduces HA-Induced Depolarization and Prevents HA-Elicited Increases in sIPSCs Independent of Changes to I _h	105
V.	RESULTS.....	108
	Study 3 - Group I mGluR Modulation within the Entorhinal Cortex.....	108
	Introduction.....	108
	Study 3 Rationale.....	111
	Activation of Group I mGluRs Increases the Excitability of MEC Principal Neurons and Requires Both mGluR1 and mGluR5.....	112
	DHPG Induces Subthreshold Changes in Principal Cell Excitability.....	115
	Potential Signaling Mechanisms Underlying DHPG- Induced Changes in Subthreshold Excitability.....	116
	DHPG-Induced Changes in Subthreshold Excitability Involve Activation of a Non-Selective Cationic Current.....	119
	Group I mGluRs Activate a TRPC-Like Conductance That May Involve TRPC1, TRPC4, and TRPC5.....	122

VI.	DISCUSSION.....	127
	Study 1 – Dopaminergic Modulation of MEC GABAergic Transmission.....	127
	DA-Induced Facilitation of Transmitter Release Involves T-Type Ca ²⁺ Channels Secondary to RMP Depolarization	128
	Promiscuous Activity of DA Linked to Inhibition of Kirs	131
	DA and MEC GABAergic System: Functional Implications.....	134
	Study 2 – Histaminergic Modulation of MEC GABAergic Transmission.....	135
	Ionic Mechanisms Mediating HA-Induced Increased Excitability of Interneurons	139
	HA and GABAergic Systems	142
	HA and Disease.....	143
	Study 3 – Group I mGluR Modulation within the Entorhinal Cortex.....	144
	Both mGluR 1 and mGluR5 are Functionally Present in the MEC	144
	DHPG-Induced Currents are Mediated by TRPC-Like NSCCs.....	146
	Signaling Mechanism Involved in DHPG-Induced Currents.....	150
	Group I mGluRs and Neuropsychiatric Disorders.....	152
	Limitations of the Work Presented in this Dissertation	154
	APPENDICES	158
	List of Abbreviations	159
	Copyright Clearance	163

REFERENCES 164

LIST OF FIGURES

Figure		Page
1.	DA increases the frequency but not the amplitude of sIPSCs recorded from entorhinal neurons	54
2.	DA facilitates sIPSC frequency via the activation of $\alpha 1$ adrenoreceptors, but not DA receptors	56
3.	Endogenously released DA enhances sIPSC frequency via the activation of $\alpha 1$ receptors.....	60
4.	DA augments the frequency with no effects on the amplitude of mIPSCs recorded in the presence of TTX, but attenuates the amplitude of eIPSC	63
5.	Ca^{2+} influx via T-type Ca^{2+} channels is required for DA-induced facilitation of GABAergic transmission	67
6.	DA depolarizes GABAergic interneurons in the EC	69
7.	DA-induced depolarization of interneurons does not require the function of I_h channels and is independent of extracellular Na^+ and Ca^{2+} , but is affected by intracellular Ca^{2+} concentration	72
8.	DA-induced depolarization of interneurons is mediated by inhibition of Kirs.....	75
9.	HA increases the frequency but not the amplitude of sIPSCs recorded from the principal neurons in the MEC	81
10.	HA-induced augmentation of spontaneous GABAergic transmission is dependent on APs and extracellular Ca^{2+} , but does not involve postsynaptic HA receptors	83
11.	HA depolarizes GABAergic interneurons in the MEC.....	86
12.	HA facilitates sIPSC frequency via activation of H_1 and H_2 but not H_3	89

13.	Both H ₁ and H ₂ are expressed in MEC and co-localize to GABAergic interneurons	94
14.	HA depolarizes MEC interneurons via both H ₁ and H ₂	96
15.	HA-induced depolarization is mediated by a mixed ionic mechanism including activation of a TTX-insensitive Na ⁺ permeable channel	98
16.	HA inhibits both K _{irs} and I _K recorded from Type I and Type II interneurons of the MEC.....	103
17.	Extracellular Cs ⁺ inhibits the depolarization of interneurons and blocks the facilitation of sIPSC frequency in response to HA	106
18.	DHPG significantly increased the AP firing frequency of a layer III pyramidal neurons.....	114
19.	DHPG induced a significant RMP depolarization	116
20.	DHPG-induced inward currents may require G proteins and AC but not PLC or Src	118
21.	DHPG activated a non-selective cationic conductance	120
22.	DHPG-induced currents require Ca ²⁺ signaling but not Ca ²⁺ release and are sensitive to NSCC blockers.....	121
23.	DHPG-induced currents involve a TRPC-like conductance that involves TRPC4 and TRPC5	123
24.	Knock-down of TRPC4 and TRPC5 did not reduce maximal DHPG-induced currents and endogenous group I mGluRs couple to TRPC5	126
25.	Summary figure for Study 1	127
26.	Summary figure for Study 2	137
27.	Summary figure for Study 3	145

ACKNOWLEDGEMENTS

I first wish to express my sincere thanks to my mentor, Dr. Saobo Lei. His dedication to his work and impressive attributes as a scientist are something I have strived to emulate and achieve. Both the professional and personal advice he has offered me throughout my training has been instrumental in my maturation as a graduate student and important toward my becoming an independent scientist. Additionally, I am very grateful for the technical and financial resources he has provided me with throughout my training.

I next want to thank my committee members Dr. Colin Combs, Dr. James Porter, Dr. Eric Murphy, and Dr. John Watt. I would also like to thank my former committee member, Dr. Lucia Carvelli. Each of these members has been a wonderful resource to me in helping me expand my thinking about my own research, troubleshooting methodological issues, and offering sage career advice.

Members of the Department of Biomedical Sciences faculty, staff, and graduate student body have also been influential figures throughout my time in graduate school. I would like to express my thanks to both the primary investigators and members of the laboratories of Dr. James Porter, Dr. Colin Combs, Dr. Brij Singh, Dr. Othman Ghribi, Dr. Jonathan Geiger, Dr. Xuesong Chen, Dr. Keith Henry, Dr. Brown-Borg, Dr. Jyotika Sharma, Dr. Thad Rosenberger, and Dr. Eric Murphy. Each of these labs have provided me with either technical assistance in troubleshooting experiments or through the sharing of equipment, reagents, and consumables. I would also like to thank Jennifer Hershey,

Michael Ullrich, Julie Horn, Deb Krose, and Bonnie Kee for their assistance over the years with various administrative matters. I would like to extend an additional thank-you to Bonnie Kee for her help in answering questions and offering assistance regarding the formatting of this dissertation.

I want to thank my family for everything they have done for me throughout my time in graduate school. My mother, Kathy, has always been a stabilizing force in my life. I am grateful for her love and encouragement. My sister, Jennifer, has always been there to offer me her advice and support. Her husband, Tony, has also been a very positive influence in my life. I cherish my memories of visiting their family every summer over the past six years and spending quality time with my nieces, Reagan and Taylor, and nephew, Jackson.

Lastly, I want to thank my girlfriend, Katie. I do not know what I would have done without her. She has been a source of great encouragement for me to finish graduate school and I am sincerely grateful for everything she has done

For my parents, Kathy and Doug.

ABSTRACT

The medial entorhinal cortex (MEC) is a critical region for both limbic functions as well as learning and memory. In addition to these normal processes, the MEC is also implicated in several disorders including epilepsy, Alzheimer's disease, and several neuropsychiatric disorders. The MEC's function and role in various disorders is intimately related to its underlying cellular activity. The primary neuronal cell types in this region consist of glutamatergic principle cells and GABAergic local inhibitory interneurons. This dissertation consists of three aims related to the neuromodulation of these cells located in the superficial layers of the MEC—the primary input source to the hippocampus. The first aim addresses how dopamine (DA) alters GABAergic transmission. The second aim also considers GABAergic transmission but examines its modulation by histamine (HA). Finally, the third aim investigates mechanisms of group I metabotropic glutamate receptor(mGluR)-induced increases in layer III principal cell excitability.

For Study 1, exogenous application of DA increases spontaneous inhibitory postsynaptic currents (sIPSCs) recorded from layer II neurons. This increase is mediated by a promiscuous interaction with the $\alpha 1$ adrenergic receptors ($\alpha 1$ ARs) found on the MEC interneurons. Application of amphetamine to elevate extracellular DA concentrations mimic these effects in an $\alpha 1$ AR-dependent fashion. Activation of interneuron $\alpha 1$ AR-induced depolarization is mediated by inhibition of inwardly rectifying K^+ channels (Kirs).

For Study 2, exogenous application of HA increases sIPSCs recorded from layer II principal neurons. This increase requires both H1 and H2 receptors located on GABAergic interneurons. The magnitude of HA-induced depolarization is significantly larger within one class of tested interneurons and HA-induced depolarization of interneurons involves both the inhibition of (Kirs) and activation of a TTX-insensitive Na⁺ current.

For Study 3, activation of group I mGluRs increases action potential firing, depolarization and generation of inward currents in layer III pyramidal neurons. This increase is sensitive to antagonists for both mGluR1 and mGluR5, indicating the functional presence of both receptors. The mGluR-induced currents are mediated by a non-selective cation channel that contains TRPC4 and TRPC5 subunits.

CHAPTER I
INTRODUCTION

Preface

The topic of this dissertation is focused on neuromodulatory mechanisms within the entorhinal cortex (EC), a region located within the medial temporal lobe (MTL). The EC is a crucial component for learning and memory processes, as well as a component of the limbic system. Expanding the knowledge base regarding how activity is modulated in this region is necessary to more accurately understand the EC functional role and its role in disease.

Both glutamate and γ -aminobutyric acid (GABA) are the primary neurotransmitters in the EC. The goal of this dissertation is to address some of the gaps in knowledge regarding modulation of glutamatergic and GABAergic transmission within the EC. It is important to have a fundamental appreciation of the cytoarchitecture, anatomical wiring, and both the functional and pathophysiological roles of the EC. This introduction serves to provide the reader with a background of the EC.

For this dissertation, three separate neuromodulatory studies were conducted. The first two concern the monoamines dopamine and histamine and their modulation of the GABAergic system in the EC. The third study concerns glutamatergic transmission and specifically examines group I metabotropic glutamate receptor (mGluR)-dependent modulation of principal cell excitability in the EC. Each results chapter provides additional introductory material relevant to that study.

Memory Systems Reside in the Medial Temporal Lobe

Lesions to the MTL Impair Learning and Memory

A study published in 1957 described treatment outcomes following bilateral surgical excision of a substantial portion of the MTL from a patient suffering from intractable epilepsy. The procedure rendered the patient, referred to as H.M, with partial retrograde and profound anterograde amnesia (Scoville and Milner, 1957). H.M. remained capable of learning new motor tasks (Milner, 1962), suggesting that different memory systems involve different brain regions. The tragic outcome of H.M.'s procedure established that the MTL is an important brain structure involved in the encoding and retrieval of explicit (i.e. episodic- and semantic-based) memories and initiated decades of intense research into the underlying structures of the MTL responsible for these processes.

Both the hippocampus and amygdala were known targets of H.M.'s surgery but how these structures and what—if any—other related regions were impacted remained unknown. Subsequent lesion studies targeting similar MTL structures in non-human primates (Mishkin, 1978; Mahut et al., 1982) and rodents (Olton et al., 1978; Becker et al., 1980) validated the key role of the MTL in learning and memory tasks. Removal of both amygdala and hippocampus produced the most profound cognitive deficits. However, subsequent studies that produced more selective lesions of the amygdala while minimizing damage to adjacent cortical regions did not impact performance on memory tasks (Zola-Morgan et al., 1989a). This finding suggests that the amygdala is not important for lesion-induced memory impairment. An alternative hypothesis was that the resultant damage to the surrounding cortical regions in previous, less-selective lesion

studies where both amygdala and hippocampus were targeted was actually the source of the additive impairment seen, compared to lesioning only the hippocampus. Indeed, selective lesions to only the perirhinal and parahippocampal regions produced significant impairments similar to those originally described in earlier combined hippocampal-amygdala removals (Zola-Morgan et al., 1989b). Thus, it appeared H.M.'s profound memory loss was due to parahippocampal-hippocampal ablations.

Subsequent advances in imaging technologies ultimately demonstrated that smaller than originally conceived portions of the hippocampus and amygdala were removed in patient H.M., whereas all the adjacent EC was removed. The perirhinal and parahippocampal cortex were relatively preserved in H.M.'s surgery (Corkin et al., 1997). These lesion and imaging studies firmly established the medial temporal lobe—specifically the parahippocampal, entorhinal, and hippocampal regions—as being a crucial structure for learning and memory processes.

Early Structural and Functional Investigations Aimed at Understanding MTL Parahippocampal-Entorhinal-Hippocampal Regions

Early descriptions of EC were noted by Santiago Ramon y Cajal and, later, Rafael Lorente de No (Ramon y Cajal, 1902; Lorente de No, 1933). Both noted dense projections extending to the dentate gyrus (DG), indicating a strong connection between the EC and hippocampus. This projection ultimately became known as the perforant pathway, owing its name to the perforating fibers through the subiculum as they extend to the DG. What was unclear was the direction of connections and what upstream sites project to the EC.

Silver impregnation studies in non-human primates demonstrate that several cortical regions converge onto parahippocampal regions, including the EC (van Hoesen et

al., 1972), suggesting that the hippocampus is a site for integration of information from many sensory modalities. Electrophysiological and degeneration studies conducted in the 1960's and 1970's began clarifying the connections of EC-hippocampal structures and led to the establishment of the lamellar hypothesis of the hippocampus (Andersen et al., 1971). This hypothesis essentially held that wiring of the hippocampus was topographically restricted to the transverse plane and that individual lamellae were functional units of the hippocampus. Central to the lamellae was the tri-synaptic circuit which, stated briefly, holds that cortical information is relayed into the hippocampus via excitatory connections from the EC to the DG. Information is then propagated via fibers, referred to as the mossy fiber pathway, that connect the DG to CA3. The next fiber connection—the Schaffer collateral pathway—connects CA3 to CA1. Finally, the CA1 region projects out of the hippocampus to septum, hypothalamus, and contralateral hippocampus (Andersen et al., 1971).

The synapses, of this circuitry are excitatory in nature and exhibit a high degree of plasticity in response to stimuli. The first detailed account of this process described a long-lasting potentiation phenomena at the EC-DG synapse resulting from a brief, high-frequency electrical stimulation of the perforant pathway (Bliss and Lømo, 1973). Such plasticity became considered as the cellular basis for learning and memory. Around the same time, unit-recording in the hippocampus of awake and behaving rats suggested that activity of individual cells corresponded to an animal's specific spatial position (O'Keefe and Dostrovsky, 1971).

These combinatorial approaches involving anatomical, functional, and behavioral experiments provided early evidence of the substrates within the MTL that are important

for learning and memory. The rodent provides a useful model for investigating the anatomical and functional aspects of the parahippocampal-hippocampal system and was the model used in this dissertation. The following section provides a more detailed overview of the anatomical connections of the rodent brain.

Connectivity of the Rodent Parahippocampal-Entorhinal-Hippocampal System

Tracing studies have provided a detailed understanding and working model of the anatomical connections between the parahippocampal and hippocampal regions. The parahippocampal regions consist of the postrhinal (POR) cortex, perirhinal (PER) cortex, EC, parasubiculum, and presubiculum; whereas the hippocampal proper regions consist of DG, CA1-4, and subiculum (Witter et al., 2000; van Strien et al., 2009). Improved anatomical retrograde (e.g. tracing dyes or wheat germ agglutinin conjugated with horseradish peroxidase) or anterograde (e.g. *Phaseolus vulgaris*-leucoagglutinin or biotinylated dextran amine) tracing methods enabled precise and detailed mapping studies to be conducted. From these studies, a standard conventional understanding of information flow into and out of the parahippocampal-entorhinal-hippocampal system has been established.

Under the standard model, convergence of cortical information occurs at the POR and PER cortices, however the sources of cortical input to each region differ considerably. For example, the visual association cortices provide almost 40% of the input to the POR, whereas only about 4% of PER cortical input is derived from visual regions. Conversely, the PER receives more somatosensory, olfactory, and auditory cortical input relative to the POR (Burwell and Amaral, 1998a; b; Furtak et al., 2007). The PER and the POR are extensively interconnected, indicating that integration of visual

and other sensory modalities occurs prior to entry into entorhinal-hippocampal systems. Outputs from layers II, III, and V of the PER and POR connect to superficial layers II and III of the EC (Burwell and Amaral, 1998a). Projections from the PER preferentially connect to the lateral EC (LEC) whereas the POR connects to both the LEC and medial EC (MEC) (Burwell and Amaral, 1998a). However, some studies have indicated an equal amount of PER and POR input to the MEC (Kerr et al., 2007), suggesting that these conventional models are not fully accurate. The standard model holds that the MEC and LEC regions largely handle different sensory information (e.g. LEC more olfactory vs. MEC more visual) and functional evidence is in line with these views. However, because the PER and POR are highly interconnected and because the POR inputs to both EC regions (Burwell and Amaral, 1998a), there may be more integration of inputs than what is conventionally considered (van Strien et al., 2009).

As indicated above, downstream of the PER and POR is the EC. In addition to PER and POR inputs, both EC regions also receive direct inputs from other cortical regions including piriform, insular, temporal, frontal, cingulate, parietal, and occipital regions (Kerr et al., 2007). Cortical information enters the EC primarily at layers II and III, where it is subsequently processed and input into the hippocampus via two distinct input pathways. The superficial layer II LEC and MEC neurons project to the molecular layer of the DG to make up the perforant pathway. Superficial layer III LEC and MEC neurons project stratum lacunosum of area CA1, forming the temporoammonic pathway (Steward, 1976; Steward and Scoville, 1976). There is a topographical distinction worth noting between perforant and temporoammonic inputs with respect to EC origin. Both LEC and MEC perforant efferents converge on to the same DG populations. With the

temporoammonic inputs, LEC efferents preferentially input to distal CA1 and proximal subiculum, whereas MEC temporoammonic efferents preferentially input to proximal CA1 and distal subiculum (Witter et al., 2000, 2006). After information is processed in the hippocampus via either tri-synaptic or monosynaptic inputs, the information is returned to the deeper layers of the EC via connections from CA1 and subiculum (Witter et al., 2000, 2006). Additionally, many hippocampal subfields as well as para- and pre-subicular regions may also provide hippocampal-processed information back to the EC (Kerr et al., 2007), suggesting a high degree of complexity exists with entorhinal-hippocampal connections. Because the EC forms extensive reciprocal connections with regions that provide cortical input to the EC (Kerr et al., 2007), it is generally presumed that the EC then redistributes information back to other cortical areas.

From this conventional understanding of parahippocampal-entorhinal-hippocampal connectivity, it is evident that the EC plays a pivotal role in gating information input and output of the hippocampus. The following section will expand in more detail on the EC, specifically the MEC, and provide descriptions of its neuroanatomy and physiology.

The Medial Entorhinal Cortex

Structural Overview of the MEC

The MEC is transitional zone between the 3-layered allocortex observed in the hippocampus proper and the six-layered neocortex. In this transition, the cytoarchitecture begins to assume a more organized distribution, especially more so relative to the adjacent para and pre-subicular regions (Witter et al., 2000; Canto et al., 2008). Depending on lateromedial and rostrocaudal anatomical positions, the laminar

composition of the MEC is between five and six layers. The transition to a more neocortical-like structure is nearly complete at the MEC/LEC border. While both LEC and MEC are adjacent cortical regions and share similar columnar organization, there are a few subtle morphological and electrophysiological differences between regions, which are most pronounced in layer II (Canto and Witter, 2012a; b). Within each layer of the MEC, there are different cell types with unique morphological and functional features that are likely crucial to MEC function. The primary neurotransmitters of the MEC are glutamate released from the principal cells and γ -aminobutyric acid (GABA) released from the interneurons.

Principal Cells of Layer I

The superficial molecular layer (layer I) is sparsely populated with cell bodies. Two types of cells have been described and are classified as either horizontal or multipolar. These cells have wide-spanning dendritic arbors that are primarily confined to layer I and, to a lesser extent, layer II. The electrophysiological properties are largely consistent with layer II stellate cells (see below) (Canto and Witter, 2012a).

Principal Cells of Layer II

The external granule layer (layer II) of the MEC is densely populated with very large cell bodies. Two broad classes of principal cell types have been consistently described by different labs in this layer (Alonso and Klink, 1993; Canto and Witter, 2012a; Kitamura et al., 2014; Fuchs et al., 2016; Ferrante et al., 2017; Winterer et al., 2017). Generally, principal neurons are referred to as either stellate or pyramidal (non-stellate) cells, although some researchers have established criteria to identify additional related cell types (Canto and Witter, 2012a; Fuchs et al., 2016).

Detailed studies examining morphological and electrophysiological characterizations of layer II MEC principal neurons have revealed several unique features between cell types. Many thick primary dendrites emanate in both apical and basal directions from the soma of stellate cells. The apical span of stellate dendritic arbors tends to be spiny and quite expansive—covering a large area of layer I and II (Klink and Alonso, 1997a). Unlike the multipolar stellate neurons, pyramidal neurons typically exhibit an apical-facing dendrite with spiny branches that span less of a medio-lateral distance (Klink and Alonso, 1997a). These morphological criteria are useful but there is a relatively large degree of variability, as evidenced by the report of intermediate types of stellate and pyramidal neurons (Canto and Witter, 2012a; Fuchs et al., 2016).

Differences between cell types are more apparent with respect to their electrophysiological properties. Both stellate and pyramidal neurons exhibit a “sag” response to subthreshold current injections (Alonso and Klink, 1993; Canto and Witter, 2012a; Fuchs et al., 2016; Winterer et al., 2017). This response reflects the presence of a relatively slow-to-activate hyperpolarization-dependent current (I_h). A ratio of the steady-state membrane potential following a negative current injection over the peak membrane potential early in the injection provides an index of the sag ratio (Canto and Witter, 2012a). The sag ratio is smaller for stellate compared to pyramidal neurons, providing an electrophysiological means for distinction (Canto and Witter, 2012a). Stellate neurons also display pronounced subthreshold membrane potential oscillations (MPOs) at potentials positive to -60 mV but below threshold. Little to no MPOs are detected in pyramidal neurons (Alonso and Klink, 1993; Canto and Witter, 2012a). MPOs require I_h , vary in frequency along the dorso-ventral axis (Giocomo and

Hasselmo, 2008) and may permit spike clustering characteristics typical of these cells (Alonso and Klink, 1993). Finally, a short latency to AP firing, higher AP firing frequency, and the presence of an afterdepolarization are also characteristic features of stellate neurons (Alonso and Klink, 1993; Canto and Witter, 2012a; Fuchs et al., 2016).

The morphological and electrophysiological distinctions between stellate and pyramidal neurons correspond to differential anatomical projections layer II cell-type specific inputs to the hippocampus. Recent studies investigating molecular markers found in layer II principal neurons uncovered two distinct populations (Varga et al., 2010). Layer II pyramidal (non-stellate) neurons express the calcium-binding protein calbindin and exhibit hexagonal patch-like distributions. Their dendritic projections colocalize with acetylcholinesterase and their axons do not innervate the DG (Ray et al., 2014). The endoplasmic reticulum transmembrane protein, wolframin, also colocalizes with calbindin, providing another molecular marker for layer II pyramidal neurons (Kitamura et al., 2014). On the other hand, reelin—an extracellular matrix glycoprotein—predominantly colocalizes with layer II EC principal neurons (Chin et al., 2007) that project to the DG (Varga et al., 2010). Reelin-positive cells do not colocalize with calbindin or wolframin (Kitamura et al., 2014). Because layer II pyramidal neurons (i.e. calbindin- and wolframin-positive cells) exhibit a patch-like distribution, they have come to be referred to as “island” cells (Kitamura et al., 2014). Stellate neurons (i.e. reelin-positive) are defined as “ocean” cells (Kitamura et al., 2015).

Principal Cells of Layer III

The external pyramidal cell layer (layer III) is thicker than layer II but less densely packed. Principal cells of this layer consist of medium to large pyramidal

neurons. Although there are several descriptions of the morphology and electrophysiology of layer III pyramidal neurons (Dickson et al., 1997; Gloveli et al., 1997; Canto and Witter, 2012a; Tang et al., 2015), this layer has received considerably less attention than layer II. Layer III pyramidal neurons are rather uniform and typically exhibit a prominent, apical-facing dendrite that extends into layers II and I. (Dickson et al., 1997; Gloveli et al., 1997; Canto and Witter, 2012a). A classification system employed by Gloveli et al. (1997) distributed principal cells into one of four categories (type I-IV). Type I and type II were considered projection neurons since antidromic APs were generated with deep stimulation. Type III and IV were presumed to be part of the local circuitry since no antidromic AP was elicited, yet these two types still resemble pyramidal morphology (Gloveli et al., 1997). An analysis by Canto and Witter (2012a) identified five distinct morphological types: three pyramidal cell types, a multipolar cell type, and a stellate cell type (Canto and Witter, 2012a). Layer III pyramidal neurons are physiologically distinct from layer II in that they exhibit very little sag (i.e. high sag ratio), are absent of MPOs, have a high input resistance, fire quick and regular action potentials, and can fire rhythmically *in vitro* (Dickson et al., 1997; Canto and Witter, 2012a).

Like layer II, there are unique markers selective for this layer. Purkinje cell protein 4 (PCP4) is a selective marker for deeper layer III and V pyramidal neurons and their apical dendrites (Lein et al., 2007; Tang et al., 2015; Ray et al., 2017). PCP4-positive apical layer III dendrites form clusters between calbindin-positive layer II neurons (Tang et al., 2015) and overlap with zinc-positive modules (Ray et al., 2017), suggesting their inputs preferentially overlap with stellate reelin-positive neurons.

Layer IV

In the MEC, layer IV is a thin, fiber-rich, cell-sparse layer referred to as the lamina dissecans. The lamina dissecans gradually disappears near the LEC border of the MEC and transitions to a more evident layer IV (Canto et al., 2008). Cells in this regions are generally considered to be members of either adjacent layers III or V (Canto and Witter, 2012a).

Principal Cells of Layer V

The internal pyramidal layer (layer V) consists primarily of medium to large-sized principal neurons. The morphology of layer V principal neurons is divided into three types: pyramidal, horizontal, and polymorphic (Hamam et al., 2000); although additional subtypes are also described (Canto and Witter, 2012a). Both pyramidal and horizontal neurons extend an apical dendrite that reaches layers I and II, whereas multipolar dendrites are typically confined to deeper layers. Electrophysiological data obtained from morphologically different cells are variable, resulting in no clear electrophysiological signatures for respective types. Layer V principal cells have the highest input resistance of MEC principal cells and a large sag ratio (Hamam et al., 2000; Canto and Witter, 2012a). MPOs in layer V is thought to be age-dependent (Canto and Witter, 2012a) because there is conflicting evidence either in support (Schmitz et al., 1998; Hamam et al., 2000) or against (Canto and Witter, 2012a) their presence.

Principal Cells of Layer VI

The morphology of layer VI principal neurons has been divided into three types: horizontal pyramidal, tilted pyramidal, and multipolar. Unlike layer V, the dendritic arbors of these three types do not extend apically and are largely confined within layer

VI. Layer VI principal cells have input resistances comparable to layer III, a high sag ratio, and no MPOs. Layer VI show no physiological differences among morphologically different cell groups (Canto and Witter, 2012a).

GABAergic Interneurons of MEC

Inhibitory GABAergic interneurons influence neuronal excitability, shape synaptic inputs, and regulate network mechanisms important for learning and memory. Cortical GABAergic interneurons comprise a broad class of cells with varying morphological, electrophysiological, and neurochemical features (Ascoli et al., 2008). Interneurons of different shapes including ovoid, round, spindle-shaped, bipolar, horizontal, or irregular are distributed throughout all layers of the MEC. There are three different interneuron classes based on molecular marker expression which comprise nearly all cortical GABAergic interneurons. Interneurons may be parvalbumin (PV)-positive, ionotropic serotonin receptor (5HTR3a)-positive, or somatostatin (SOM)-positive. The MEC expresses all three of these classes (Miettinen et al., 1996; Wouterlood and Pothuizen, 2000; Yekhlief et al., 2015; Fuchs et al., 2016; Ferrante et al., 2017), as well as sub-classes of 5HTR3a interneurons. The 5HTR3a subclasses include cholecystokinin (CCK)-positive, vasoactive intestinal polypeptide (VIP)-positive, and neuropeptide Y (NPY)-positive interneurons, the latter of which can be further classified as neurogliaform (NGF) and non-neurogliaform (Non-NGF) (Varga et al., 2010; Ferrante et al., 2017). PV-positive interneurons are generally confined to the layer they occupy, exhibit extensive dendritic arborization, and typically resemble chandelier or basket interneurons (Ascoli et al., 2008; Ferrante et al., 2017). SOM-positive interneurons extend their dendrites to apical layers and can span layers I, II, and III. The morphology

of SOM-positive interneurons typically resembles the Martinotti interneurons (Ascoli et al., 2008; Ferrante et al., 2017). 5HT3Ra-positive interneurons are often bipolar and multipolar interneurons and their dendritic arbors can extend throughout the entire MEC cortical column (Ascoli et al., 2008; Ferrante et al., 2017).

Interneurons are distinguished from principal neurons by electrophysiological markers including a fast-spiking (FS) action potential firing profile, narrow action potential half-width, and a steep after hyperpolarization (Canto and Witter, 2012a). Because interneurons are typically confined to the local circuitry, an additional indicator of an interneuron is a significantly smaller capacitance relative to principal cells. PV-positive interneurons are most often FS interneurons and, in the MEC, this class co-localizes with 80% of regulator of calcineurin 2 (RCan2)-positive neurons (Ferrante et al., 2017). All three classes are relatively abundant in the superficial MEC layers. The FS class is the most abundant GABAergic neuron (~26% of interneurons), followed by 5HT3a-positive (~21%), and SOM-positive (~14%). Some intrinsic properties, such as input resistance or threshold for first AP, are predictive of FS RCan2-positive (and presumably PV-positive) interneurons. Intrinsic properties are more variable for SOM-positive and 5HT3a-positive interneurons (Ferrante et al., 2017). Some general guides for electrophysiological identification are available, however. FS interneurons typically have a lower input resistance relative to SOM-positive interneurons and SOM-positive interneurons are typically endowed with I_h , as evidenced by a pronounced sag-response (Yekhlef et al., 2015; Fuchs et al., 2016; Ferrante et al., 2017). Classification schemes in the MEC have been employed describing type I and type II interneurons (Kumar and Buckmaster, 2006; Lei et al., 2007; Deng and Lei, 2008; Xiao et al., 2009b; Deng et al.,

2010b; Cilz et al., 2014; Zhang et al., 2014b; Cilz and Lei, 2017) and these types likely correspond respectively to PV- and SOM-positive GABAergic interneurons based on similar firing properties reported in molecularly identified interneurons (Yekhlef et al., 2015; Ferrante et al., 2017).

MEC Connectivity with the Hippocampus and Connectivity within MEC

As stated earlier, extrinsic outputs to the hippocampus from the MEC are provided by the superficial layers and consist of either the perforant or temporoammonic pathways. Extrinsic inputs from the hippocampus to the MEC are primarily through the subiculum, parasubiculum, and presubiculum. These connections terminate in layers throughout the MEC but, generally, prefer to terminate in layer V (van Strien et al., 2009). Intrinsic recurrent, intralaminar connections between deeper and superficial MEC layers provide a possible mode for “re-entry” of information back to the hippocampus. The local GABAergic circuitry serves to fine-tune the MEC excitatory activity. This section will expand on the extrinsic connections between the MEC and hippocampus and intrinsic connections within the MEC by highlighting recent work that has uncovered vital details regarding the MEC microcircuitry.

Connections Between MEC and Hippocampus

The perforant pathway arises from layer II neurons of the MEC (Steward and Scoville, 1976). As described above, two cell populations make up layer II: stellate (ocean cells) and pyramidal (island cells). Circuit studies dissecting roles for these two distinct cell populations indicate that layer II ocean cells provide excitatory input to DG and CA3 regions (Kitamura et al., 2015) while layer II island cells provide excitatory input to parvalbumin-expressing interneurons of the CA1 region (Kitamura et al., 2014;

Yang et al., 2016). Thus, modulation of these sub-populations of layer II neurons will differentially influence information input to the hippocampus, whereby an increase in ocean cell activity will presumably increase CA1 activity via the tri-synaptic pathway; whereas island cells will reduce CA1 activity through feed-forward inhibition of CA1. The definitive presence of an island cell-CA1 connection remains unclear (Fuchs et al., 2016). Selective inactivation of layer III pyramidal neurons significantly reduces excitatory drive onto hippocampal CA1 and subiculum regions (Suh et al., 2011), validating the excitatory nature of the temporoammonic pathway (Steward, 1976).

In addition to hippocampal inputs, both layer II and layer III also provide substantial contralateral superficial MEC excitatory input (Varga et al., 2010; Tang et al., 2015; Fuchs et al., 2016). Because there is a high degree of overlap between hippocampal-projecting and contralateral-projecting layer III neurons, it is presumed that distinct projecting cell populations are not present in layer III (Tang et al., 2015). On the other hand, layer II island cells preferentially connect to contralateral MEC ocean cells (Fuchs et al., 2016). Although these studies suggest layer specific wiring diagrams, it is important to recall that early tracing studies suggest that all MEC layers, including—albeit to a lesser degree—deeper layer V neurons, contribute to perforant inputs (Witter et al., 2000). Regardless, these studies underscore the detail and complexity of MEC-MEC and MEC-hippocampal connections.

The terminals of both perforant and temporoammonic pathways exhibit unique topographical distributions (Witter et al., 2006). Perforant terminals from both LEC and MEC, presumably from ocean cells, converge onto different portions of the DG molecular layer but do overlap onto the same population of granule cells. The LEC inputs

are at the outer portion, whereas MEC inputs are at more intermediate sites of the molecular layer. Such differences might suggest the MEC exerts more control over DG excitability. Conversely, inputs from LEC and MEC do not appear to converge in the temporoammonic pathway. The LEC temporoammonic-fibers preferentially synapse onto distal and proximal regions of CA1 and subiculum, respectively; whereas, MEC temporoammonic-fibers synapse on to proximal and distal regions of CA1 and subiculum regions, respectively (Witter et al., 2000, 2006). Both CA1 and subiculum are highly interconnected and maintain parallel streams of information based on respective EC inputs. Once processed, information is ready to be returned to the EC.

Both CA1 (Cenquizca and Swanson, 2007) and subiculum (Kloosterman et al., 2003) provide hippocampal output back to deeper layers V and VI of the MEC. Once again, outputs are largely segregated based on origin and mirror EC inputs, suggesting that parallel streams of information are maintained in entorhinal-hippocampal circuits (Witter et al., 2006). CA1 fields more extensively innervate subiculum relative to EC (Cenquizca and Swanson, 2007), consistent with the subiculum being regarded as the primary output of the hippocampus (Kim and Spruston, 2012). Additionally, the presubiculum and parasubiculum regions are highly interconnected with the subiculum (van Strien et al., 2009) and the presubiculum innervates superficial layers of the MEC (Caballero-Bleda and Witter, 1993). Subiculum provides largely excitatory input to the MEC (Kloosterman et al., 2003) whereas MEC inputs from the presubiculum may include a GABAergic component (van Haeften et al., 1997).

Finally, in addition to the excitatory connections between MEC-hippocampus and hippocampus-MEC described above, long-range GABAergic projections in both

directions also exist (Germroth et al., 1989; Melzer et al., 2012; Zhang et al., 2013a). Many of the GABAergic projections from the MEC are PV-positive, whereas others are molecular marker-unknown. Such projections provide inhibitory input to the stratum lacunosum of CA1 and molecular layer of DG (Melzer et al., 2012). Reciprocal inhibitory connections between hippocampal interneurons and the MEC also exist. Projections arise from interneurons located in the stratum oriens of CA1 and hillus of DG—many of which co-localize with SOM. These long-range hippocampal-MEC interneuron connections preferentially target MEC interneurons (Melzer et al., 2012), suggesting that they provide a source of disinhibition.

Connections Within the MEC

The microcircuitry within the MEC display a rich multitude of intra- and inter-laminar connections. These connections were inferred from an early layer-specific tracing study (Swanson and Kohler, 1986). Intralaminar recurrent excitatory connections provide a mechanism for local amplification that may be important for generation of a cell assemblies involved in working memory tasks (Durstewitz et al., 2000).

Paired-recordings in the MEC indicate a relatively high degree of intralaminar recurrent excitation in layers III and V, whereas recurrent connections were absent in layer II (Dhillon and Jones, 2000). Electrical coupling, presumably via gap junctions, is also present in layer III MEC (Dhillon and Jones, 2000). The absence of layer II recurrent excitation was challenged by experiments using caged-glutamate release at large distances away from the recorded soma, as these conditions elicit EPSCs (Kumar et al., 2007; Beed et al., 2010). While caged-glutamate experiments are not as stringent as paired recordings, the generation of EPSCs resulting from glutamate release at long

distances away from the soma is consistent with layer II axon collaterals extending long distances away horizontally in the MEC (Lingenhohl and Finch, 1991). Subsequent investigations utilizing either paired-recordings or optical activation of layer II neurons are consistent with a lack of stellate to stellate recurrent excitation (Couey et al., 2013; Pastoll et al., 2013), however, neither study completely ruled out their existence. On the basis that two distinct populations exist in layer II and these populations form discrete and periodic patches (Varga et al., 2010; Kitamura et al., 2014), both Fuchs et al. (2016) and Winterer et al. (2017) addressed whether connections existed between specific cell-types (Fuchs et al., 2016; Winterer et al., 2017). In both studies, recurrent excitatory connections were found in layer II. Winterer et al. (2017) found robust excitatory recurrent drive between layer II pyramidal (calbindin-positive) to stellate (reelin-positive) neurons, but the reverse was not true. Furthermore, weaker recurrent excitation was also found between stellate to stellate and pyramidal to pyramidal neurons (Winterer et al., 2017). Thus, input to layer II pyramidal neurons might be expected to encourage stronger activation of perforant versus temporoammonic activities due to layer II pyramidal-mediated inhibition of CA1 activity (Yang et al., 2016) and increased excitation of stellate activity (Winterer et al., 2017).

In addition to intralaminar connections, the MEC displays a high degree of interlaminar excitatory connections between deeper and superficial layer (Dickson and Alonso, 1997; van Haeften et al., 2003; Quilichini et al., 2010). Layer V is interconnected with layer III (Quilichini et al., 2010) and layer III pyramidal neurons drive excitation of layer II stellate neurons (Winterer et al., 2017). In addition to this feed-forward excitation of superficial layers, deep MEC neurons also provide weak feed-forward inhibition to

both layer II and III principal cells via excitation of MEC interneurons (van Haeften et al., 2003). Thus, deeper layers provide a means for information to enter back into the hippocampus, which may play an important function in learning and memory processes.

Inter- and intra-laminar coupling between MEC principal neurons and interneurons is much more commonly observed than is recurrent excitation with paired-recordings. For example, there is a ~40-50% chance of connectivity between layer II FS-to-principal and principal-to-FS cells (Couey et al., 2013). PV-positive or FS interneurons appear to be rather non-discriminant in targeting specific principal cell types (Varga et al., 2010). However, although high degrees of reciprocal connections are observed between FS and stellate neurons, there is considerably less connectivity between FS and pyramidal (Fuchs et al., 2016). The same holds to be largely true for SOM-positive interneurons. Many cortical 5HT3Ra interneurons co-release CCK (Morales and Bloom, 1997). CCK-positive interneurons specifically target principal neurons that are calbindin (pyramidal) but not reelin-positive (stellate) (Varga et al., 2010), which suggests layer II pyramidal cells receive inhibitory input primarily from 5HT3Ra-interneurons. Consistent with Varga et al. (2010), 5HT3Ra-positive interneurons form a high degree of reciprocal inhibitory connections with pyramidal and intermediate cells, although a very low degree of connections with stellate cells was observed (Fuchs et al., 2016). These studies suggest that layer II principal cells might receive differential inhibitory input. Unlike layer II, layer III pyramidal neurons receive robust GABA_A-mediated IPSCs from both SOM-positive or PV-positive interneurons (Yekhlief et al., 2015). The significance of such differential inhibitory inputs between layers remains unclear.

Specialized Features of Neurons within the MEC

Specialized cell types reside within the MEC are modulated by spatial and visual information and may be part of the neural circuitry important for internal representations of surrounding environments (Fyhn et al., 2004). Tetrode-recording in rats reveal cell-firing patterns analogous to hippocampal place cells but with periodic firing distributions that overlap with the animal's environment. Firing maps are distributed about in a hexagonal array and the receptive fields vary in size from small to large along the dorso-ventral axis (Hafting et al., 2005). Grid fields are established rapidly in novel environments, set by external landmarks, and persist after removal of visual inputs. The anchoring of grid fields to external landmarks is illustrated by a 90° rotation of the visual cues resulting in a learning environment immediately corresponding to a 90° rotation of the grid fields (Hafting et al., 2005). Head direction cells, like those seen in the hippocampus, are also found in the MEC. These cells increase their firing frequency when the animal is facing a particular direction (Sargolini et al., 2006). Many MEC cells in deeper layers are conjunctive grid and direction cells. This might suggest cells in deeper layers—layers III and V—are important for integrating both grid and directional elements (Sargolini et al., 2006). Border cells fire near the perimeter border or near one side of a barrier within an animal's environment. Border cells typically display a dominant border firing position (Solstad et al., 2008). Grid cells reside primarily in layer II (Hafting et al., 2005; Sargolini et al., 2006; Tang et al., 2015) and are generally considered to be the stellate neuron type. However, layer II pyramidal neurons also exhibit grid-like activity (Kitamura et al., 2014; Sun et al., 2015) and are modulated by animal speed. Although the majority of grid cells appear to reside in layer II, there is

conflicting evidence documenting their presence throughout all MEC layers (Sargolini et al., 2006; Tang et al., 2015). Understanding how synaptic activity and modulatory processes influence these cells will be useful in understanding how the unique features of these cells arise and may be important to their contribution to animal behavior.

The MEC and Learning and Memory

Activity in the MEC is necessary for multiple forms of learning and memory. Selective lesions to the rat dorso-ventral MEC reduces firing rates in a subpopulation of hippocampal neurons and causes place fields to broaden (Hales et al., 2014). MEC-only lesioned rats also display impaired learning abilities in the Morris water maze, while other hippocampal-dependent memory processes, including novel-object working memory and tone-fear associational memory, are preserved (Hales et al., 2014). Baclofen significantly and long-lastingly reduces layer II stellate neuron excitability (Deng et al., 2009). Pharmacologically-induced suppression of MEC activity with baclofen during Morris water maze acquisition stages significantly increases the latency time to target and impairs recall in rats (Deng et al., 2009). Conversely, the neuropeptide neurotensin (NT) produces a significant, long-lasting increase in layer II excitability (Xiao et al., 2014), facilitates glutamate release onto DG granule cells (Zhang et al., 2015b), and increases DG granule cell excitability (Zhang et al., 2016), indicating NT strongly promotes perforant pathway activity. Consistent with perforant activity in spatial navigation (Kitamura et al., 2015), increasing MEC activity with neurotensin reduces latency time to target in the Barnes maze and enhances recall relative to saline controls (Xiao et al., 2014). Thus, entorhinal inputs are crucial for spatial learning and memory tasks.

Perforant input to the DG and CA3 regions is implicated in another hippocampal-dependent process, pattern separation (Leutgeb et al., 2007). In this paradigm, an animal learns to discern differences between two novel contexts. Place-cell fields at either DG or CA3 will change, or re-map, as a result of exposure to a new environment (Leutgeb et al., 2007). Monitoring activity of MEC layer II ocean cells *in vivo* reveals that different populations of ocean, but not island cells, are active within different contexts and the respective cells are re-activated upon return to the appropriate context (Kitamura et al., 2015). The extent of similarities between the two contexts influences the percentage of cells that are active in both contexts, whereas more differences correspond to less overlapping active cells (Kitamura et al., 2015). Furthermore, inhibition of ocean but not island cells during context-fear conditioning reduces freezing behavior upon re-exposure to the conditioning context (Kitamura et al., 2015). Thus, MEC perforant pathway input is essential for contextual representations.

Temporal associational memory is a component of both episodic and working memory insofar as it provides a means to associate temporally discontinuous events (Suh et al., 2011). At the cellular level, a model for temporal associations is expected to involve prolonged activity of a cell ensemble engaged during an initial encoding event that persists after the sensory information related to that ensemble's activity is terminated. If that activity overlaps with a subsequent encoding event, there is a likelihood that elements of the previous ensemble will be incorporated into the subsequent ensemble, and vice versa. This processes is called persistent firing and is considered to be a cellular model for working memory (Hasselmo and Stern, 2006). In the MEC, cholinergic and group I mGluR agonists induce persistent firing throughout

layers II, III, and V (Klink and Alonso, 1997b; Egorov et al., 2002; Yoshida et al., 2008). These responses can be graded, meaning repeated stimuli in the presence of agonist can enhance the magnitude of persistent firing. Persistent firing does not require synaptic input but, rather, is intrinsic to the neurons themselves (Egorov et al., 2002). Selective inactivation of temporoammonic inputs to CA1 impairs temporal associations involved with fear conditioning (Suh et al., 2011). Co-administration of cholinergic and group I mGluR antagonists to the EC also impairs these associations, suggesting that persistent firing may enable the association between the tone and subsequent shock.

Finally, as part of the MTL, the EC plays a key role in semantic and episodic memory processes. Whereas semantic memory processes dependent on the LEC, episodic memory is dependent on the MEC (Eichenbaum et al., 2012). Episodic memory requires an ability to recognize environmental events or cues, organize them by their subjective temporal sequence, and to recall information via an internally driven reactivation process. Features of specialized cells within the MEC may equip this region to accomplish these tasks (Buzsaki and Moser, 2013; Sanders et al., 2015).

Pathological Conditions Related to the EC

The EC has been implicated in: neurodegenerative disorders, such as Alzheimer's Disease (AD) (Hyman et al., 1984; Gómez-Isla et al., 1996); neurological disorders, such as epilepsy (Du et al., 1993); and neuropsychiatric disorders, such as schizophrenia (Falkai et al., 1988; Prasad et al., 2004), depression (Watkins, 2008; Tu et al., 2012) and anxiety (Watkins, 2008; Hattingh et al., 2013). This section will examine more closely the relationship between the EC and some of these conditions.

Alzheimer's Disease

Cognitive decline is a naturally occurring process associated with aging. In a subset of the general population, the rate of decline is substantially larger and is considered pathological. Pathological forms of cognitive decline include mild cognitive impairment (MCI) and dementia. MCI involves a subtle loss in cognitive function and typically will convert to full dementia, including Alzheimer's disease (AD), in about half of MCI patients. Thus, MCI is considered as a transition period between normal function and dementia (Sanes and Jessell, 2013). Dementias are categorized into two broad classes: nondegenerative and degenerative. Nondegenerative dementias arise secondarily from factors including stroke, infections, or metabolic disorders. Degenerative dementias involve a primary loss of central function that is associated with histopathological markers and a degree of hereditary transmission (Kaufer and Dekosky, 1999). The most prevalent degenerative dementia is AD and the remainder of this subheading will focus on the relationship between the EC and AD.

AD is characterized by three pathological markers accompanying clinical signs of cognitive impairment. First, the extent of brain atrophy, neuron death, and enlargement of the ventricles correlates to progression of AD. Second, postmortem AD tissue exhibits large extracellular senile plaques consisting of 40 or 42 amino acid-length amyloid fragments ($A\beta_{40/42}$). $A\beta$ fragments are derived from proteolytic cleavage of amyloid precursor protein (APP) by β - or γ -secretases. Third, AD tissue exhibits neurofibrillary tangles (NFTs) resulting from aggregates of cytoskeletal elements consisting of hyperphosphorylated isoforms of the microtubule-associated protein, tau (Sanes and Jessell, 2013). However, the pathogenesis of AD remains poorly understood.

The EC, in particular layer II, is a region of interest in the pathogenesis of AD (Stranahan and Mattson, 2010). There is considerable cell death of superficial EC neurons reported in AD (Hyman et al., 1984; Gómez-Isla et al., 1996). No significant loss in cell number is seen between the sixth and ninth decade of life in healthy control persons, suggesting that AD is not simply an exacerbated condition of aging (Gómez-Isla et al., 1996). An accumulation of histopathological markers, such as NFTs and A β depositions, commences prior to clinical symptoms of AD (Braak and Braak, 1991). Plaque loads are variable at different stages in AD patients, whereas NFTs present in a more systematic fashion and are generally located near entorhinal regions at early stages (Braak and Braak, 1991). Both NFT density and neurite plaque density are negatively correlated in a significant fashion with cell number in AD (Gómez-Isla et al., 1996), although this does not imply causality. A loss of synapses is hypothesized to be the initial contributing factor to cognitive decline in AD and precedes the appearance of pathological markers (Selkoe, 2002). Consistent with this hypothesis, a reduction in synapse density, rather than the presence of NFTs or plaques, is the strongest physical correlate to cognitive impairment (Terry et al., 1991). Furthermore, significantly fewer synapses are found at the EC-DG synapse in patients at the transition stage of MCI (Scheff et al., 2006). Understanding what factors contribute to both the reduced synaptic density and development of pathological markers may lead to better treatments for AD.

Transgenic mice permit expression of mutant APP or tau in the EC to examine disease progression and potential causality of AD pathological markers. Harris et al (2010) asked whether expression of mutant APP in the EC would impair cognitive function (Harris et al., 2010). Crossing mice with restricted superficial layer II/III EC

expression of tetracycline transactivator (tTA-EC) (Yasuda and Mayford, 2006) with mice carrying the inducible expression of mutant APP, (tet-APP) (Jankowsky et al., 2005) yield EC-restricted mutant APP-producing mice (EC-APP). Plaques are primarily in the EC of younger EC-APP mice but begin to appear in the DG at older ages, suggesting AD-like pathology may spread between anatomically connected areas. Moreover, EC-APP mice display modest synaptic deficits at perforant pathway synapses and impaired acquisition and retrieval in Morris water maze at thirteen months (Harris et al., 2010). A similar study (Harris et al., 2012) crossed tTA-EC mice with TetO-TauP301L mice—an inducible model that produces prototypical NFTs (Terwel et al., 2005)—to evaluate EC-specific NFT contributions to cognitive decline. While significant NFTs were detected in an age-dependent fashion, no significant cognitive deficits in spatial memory recognition, or contextual fear learning were observed (Harris et al., 2012). Using the same EC-inducible tau expression system, Polydoro et al. (2014) asked whether soluble pathological tau that is expected to precede NFT formation and overt neurodegeneration may contribute to impaired synaptic function (Polydoro et al., 2014). They too found no substantial behavioral differences, however, there were significant reductions in Arc, an early inducible plasticity, with older mutant tau-expressing mice. Moreover, transgenic mice also displayed larger paired-pulse depression and reductions in long-term potentiation (LTP) (Polydoro et al., 2014), suggesting early changes in soluble tau may have a causal role in AD-related synaptic dysfunction. Finally, APP potentiates tau toxicity at younger ages in mice capable of EC-selective inducible expression of both mutant APP and tau (Khan et al., 2014), suggesting an interaction between tau and mutant APP-processing facilitates cognitive impairments, although

behavior was not assessed. *In vitro* studies show nanomolar concentrations of AB₄₂ oligimers impair EC layer II long-term potentiation LTP (Criscuolo et al., 2015). Taken together, an interaction likely exists between the pathological markers and their early expression in the EC may contribute to early impairments, like those seen in early stages of AD. Although either mutant APP or tau can impair synaptic function in this region, their underlying mechanism as it relates to AD remains unknown.

There is no cure for AD but there are strategies to manage symptoms. Two major pharmacological approaches currently employed target either cholinergic or glutamatergic transmission. The cholinergic strategy is emerged on the basis that brains of AD patients have reduced levels of the acetylcholine (ACh) synthesizing enzyme, choline acetyltransferase (Bowen et al., 1976; Davies and Maloney, 1976). ACh is an important neuromodulator for learning and memory (Hasselmo, 2006). The degradation of ACh is mediated by acetylcholinesterase (AChE) and inhibitors of AChE, e.g. rivastigmine or donepezil, result in elevated ACh levels and provide modest pro-cognitive effects in AD (Silvestrelli et al., 2006). The modulatory role of ACh in the MTL has been extensively studied, including in the MEC, where its actions likely contribute to the pro-cognitive effects. Cholinergic activation of layer II neurons increases their excitability (Klink and Alonso, 1997b) and elicits depolarization via a Ca²⁺-activated cationic conductance (Klink and Alonso, 1997c) with TRPC-like requirements (Zhang et al., 2011). Moreover, cholinergic activation enables persistent firing in layer II and V MEC neurons (Klink and Alonso, 1997b; Egorov et al., 2002) and inhibiting cholinergic signaling in the MEC impairs novel object working memory (McGaughy et al., 2005) grid cell firing patterns (Newman et al., 2014).

The second approach to managing AD symptoms targets the NMDAR, since excitotoxicity is implicated in AD (Silvestrelli et al., 2006). The EC is implicated in this approach since its superficial layers are especially vulnerable to excitotoxic insults (Schwarcz and Witter, 2002). Excitotoxic insults can be mediated by increased Ca^{2+} influx through excessive activation of NMDAR. Extrasynaptic NMDAR activation increases AD-like phenotypes, including $\text{A}\beta$ production (Bordji et al., 2010) and tauopathies (Xu et al., 2015). Memantine is a low affinity non-competitive antagonist of NMDARs and may impact the kinetics of channel function but not impair physiological glutamatergic transmission (Silvestrelli et al., 2006). In animals with lesions to the EC, infusions of memantine but not MK-801—another NMDAR antagonist—reversed lesion-induced memory impairments (Zajackowski et al., 1996), suggesting memantine's actions are distinct from simply blocking channel activity.

Both AChE inhibitors and memantine involve neuromodulatory approaches that manage symptoms and extend the end-of-life period before assisted care is necessary. However, neither of these treatments cure AD. The most promising treatment would be to target the underlying cause of AD.

Temporal Lobe Epilepsy

Seizures are temporary disruptions in the brain that result in abnormal, synchronous, and excessive neuronal activity. Epilepsy is a neurological disorder that consists of a chronic condition of repeated seizures (Westbrook, 2013). The etiology of most epilepsies is not well understood and may include aspects such as age, environmental factors (e.g. traumatic head injury, stress, diet), and genetics. Currently available pharmacological treatments for epilepsies include drugs that stabilize voltage-

gated Na⁺ channels in their inactive state, increase GABAergic tone, and inhibit voltage-gated Ca²⁺ channels (Nestler et al., 2009a). The most prevalent case of human epilepsy is temporal lobe epilepsy (TLE). TLE is characterized by hippocampal sclerosis—most often in CA1 and DG subfields—and is often resistant to anti-epileptic treatments (Engel, 2001). The MEC is uniquely situated upstream of both DG and CA1 and coordinates information input to and output from the hippocampus. Therefore, it is perhaps not surprising that the MEC is implicated in both seizures and TLE. Reductions in entorhinal volume (Jutila et al., 2001) and preferential loss of layer III principal neurons is reported in patients with pharmaco-resistant TLE (Du et al., 1993; Schwarcz et al., 2000). Surgical resection of the seizure focus typically involves removing portions of the hippocampus, parahippocampal regions (i.e. MEC), and amygdala. Surgery is an effective treatment for pharmaco-resistant TLE, however, there are considerable risks of cognitive impairment (Bonelli et al., 2013) and a possibility of relapse (Thom et al., 2010). A better understanding of the pathology of epilepsies may lead to better treatment strategies.

The intra- and inter-laminar connections in the MEC are extensive and provide a re-entry pathway between deep and superficial layers that closes the hippocampal circuit. Recurrent connections within layers III and V are more prevalent than other cortical regions (Dhillon and Jones, 2000) and connections between layer III and II (Winterer et al., 2017) and recurrent connections within layer II (Fuchs et al., 2016; Winterer et al., 2017) may facilitate synchronization of EC circuits that could lead to hyperexcitability. Additionally, GABAergic tone in deeper MEC layers is much lower than in superficial layers (Woodhall et al., 2005) and may enable layer V neurons to become hyperexcitable and readily propagate excitation to superficial layers.

Consistent with clinical observations, animal seizure models exhibit preferential loss in layer III using either local application of aminooxyacetic acid (Scharfman et al., 1998) or systemic administration of pilocarpine (Kumar and Buckmaster, 2006). In the pilocarpine model, an increase in excitability of layer II principal neurons concurrent with a reduction in GABAergic tone is also observed (Kumar and Buckmaster, 2006). One possible explanation for this observation could be due to reduced layer III excitatory drive onto intralaminar-spanning GABAergic interneurons. Such a possibility fits with a dormant GABAergic hypothesis (Du et al., 1995; Schwarcz et al., 2000). However, a loss of GABAergic interneurons and synapses is more likely the cause for reduced GABAergic tone seen in layer II (Kumar and Buckmaster, 2006; Kumar et al., 2007). Methods to increase GABAergic activity in superficial layers will likely dampen epileptic activity by restoring a lower excitability of layer II principal neurons.

Bathing parahippocampal-hippocampal slices in a recording solution lacking extracellular Mg^{2+} is a common method to study pharmacoresistant epileptic activity *in vitro* (Li Zhang et al., 1995). Under these conditions, increased excitability results from increased NMDAR activity and recurrent connections provide synchronization. Using this paradigm, a number of different modulators interacting with the GABAergic system reduce epileptic-like discharges, including serotonin (Deng and Lei, 2008), thyrotropin-releasing hormone (Deng et al., 2006) and bombesin (Zhang et al., 2014a). Targeting group II mGluR receptors using this *in vitro* approach also decreases epileptic-like discharges in layer III of the MEC (Zhang et al., 2015a). These receptor systems may be useful targets in the future of treatment for pharmacoresistant TLE.

Depression and Anxiety

Depression and anxiety are related but distinct neuropsychiatric mood disorders that involve negative emotional states. Different forms of depression include, but are not limited to, single episode depression, bipolar depression, and major depressive disorder (MDD). MDD is most common and may be characterized by several negative symptoms including feelings of hopelessness, irritability, fatigue, guilt, and thoughts of suicide. Like depression, there are different forms of anxiety including, but not limited to, social anxiety, post-traumatic stress disorder, panic disorders, and generalized anxiety disorder. Anxiety may be characterized by excessive self-consciousness, restlessness, fatigue, irritability, difficulty concentrating, and intense feelings of worry. The risk factors and diagnostic criteria associated with both disorders are distinct but there is often a high degree of co-morbidity (Kessler et al., 2008). Moreover, there is considerable overlap of involved limbic structures between both disorders (Krishnan and Nestler, 2008; Tovote et al., 2015) and there is emerging evidence for a role of the MEC.

The MEC is a component of the limbic system and thus involved in emotional processing (Papez, 1937; MacLean, 1949; Shah et al., 2012). The anterior cingulate cortex is consistently implicated in MDD (Hyman and Cohen, 2013) and this region forms reciprocal connections with the MEC (Insausti et al., 1997; Kerr et al., 2007). The amygdala is a key structure involved with anxiety (Hyman and Cohen, 2013) and provides input to the MEC (Sparta et al., 2014). In humans, thinning of EC and reduced EC volume are reported in MDD patients (Tu et al., 2012; Harel et al., 2016) and increased EC activation is triggered by emotional stimuli in patients diagnosed with an anxiety disorder. Both depression and anxiety involve a negative ruminating tendency

that concerns one's self or autobiographical memory (Watkins, 2008). Although rumination is not a negative behavior per se, for example rumination can facilitate adaptive preparedness and anticipatory planning, it can contribute to anxiety and depression when it involves worry, counterfactual thinking, and negative self-views (Watkins, 2008). Rumination is associated with increased EC activity (Piguet et al., 2014; Harel et al., 2016). Taken together, these findings support a role for EC activity in depression and anxiety disorders.

The involvement of the EC in anxiety has been demonstrated in rodent studies. Pavlovian fear conditioning involves a conditioned stimuli (CS), e.g. an audible tone, paired with an unconditioned stimulus (US), e.g. a foot shock. Through training, the procedure produces learned fear responses or a conditioned response (CR), e.g. freezing behaviors following the CS. Electrolytic lesions of the EC 1 week prior to Pavlovian fear conditioning results in anterograde impairments producing deficits in acquisition of the CR to US (Maren and Fanselow, 1997). Inactivation of ventral hippocampal structures, including MEC, also disrupt auditory fear conditioning (Maren and Holt, 2004). CRs are sensitive to conditioning contexts. Extinction of the CR in a new context can occur when the CS is not paired with the US over many trials but the CR will remain intact if the animal is subsequently returned to a third novel context, indicating that formation of new associations—learning—occurs regarding context interactions with the CS. Lesions to the EC impair maintenance of the CR in subsequent novel contexts following extinction procedures, whereas sham-treated animals continue to exhibit a CR (Ji and Maren, 2008). The basolateral amygdala (BLA) provides substantial glutamatergic input to the EC (Sparta et al., 2014). Using a fear conditioning paradigm, photoinhibition of BLA-EC

connections during the acquisition stages impaired contextual fear memories in mice (Sparta et al., 2014). A delay between the CS and US requires temporal associations to occur in order to elicit a CR. Inactivation of layer III MEC temporoammonic inputs prevents temporal associational memory in fear condition (Suh et al., 2011). These studies strongly support a role for EC function in anxiety.

Molecules linked to anxiety and depression are potent modulators of EC activity. The neuropeptide cortico-releasing factor (CRF) is found throughout limbic structures and CRF mRNA expression increases in the amygdala under periods of psychological stress (Makino et al., 1999). Whereas stress is a risk factor for both anxiety and depression (Belmaker and Agam, 2008), suggesting an increase in resultant CRF signaling may occur. Application of CRF significantly increases the activity of principal cells in the MEC (Kurada et al., 2014), suggesting psychological stress may increase EC activity. CCK is another neuropeptide expressed throughout the limbic structures. CCK exerts both anxiogenic actions (Bowers et al., 2012) and antagonism of CCK-receptors reduces depressive-like behaviors in rodents (Becker et al., 2008). In the EC, CCK transiently increases the excitability of the temporoammonic-projecting layer III pyramidal neurons (Wang et al., 2011) and facilitates glutamate release at the perforant synapse via a presynaptic mechanism (Deng et al., 2010a). Furthermore, infusion of CCK into the DG—downstream of MEC inputs—increases anxiety-like behavior in rats (Xiao et al., 2012).

Neuromodulation

General Overview

Neuromodulation adds depth to a relatively stable infrastructure of connections in the brain by modifying the cellular and network activity underlying an animal's internal state and behavior. Such cellular and network activity may be important for homeostatic or behavioral processes such as nociception, thermoregulation, metabolism, attention, mood, learning, and memory (Richerson et al., 2013; Marder et al., 2014). Small chemical mediators, neurotransmitters, peptides, and gases all have modulatory actions in the brain and these compounds can act at short-range (e.g. purines or endocannabinoids) or intermediate/long-range distances (e.g. glutamate, GABA, monoamines or peptides) to modify activity (Hille, 1992; Nestler et al., 2009b).

It is important to distinguish between neurotransmitter and neuromodulator. The former elicits a direct response on the target cell whereas the latter influences the former. Many of the molecules mentioned above can act as either neurotransmitters or neuromodulators. It is the receptor-function involved that generally defines whether a molecule acts as a modulator or transmitter (Nestler et al., 2009b). For example, glutamate, GABA, serotonin, and ACh interact with both ionotropic and metabotropic receptors. Ionotropic receptors are ligand-gated ion channels that, upon ligand-binding, provide a direct conduit for ion permeation and thereby directly influence excitability. Metabotropic receptors are most often G protein-coupled receptors (GPCRs) and engage different cell signal transduction and effector systems to elicit downstream changes in excitability.

G protein signaling involves the classic heterotrimeric complex of α , β , and γ subunits. The α subunit binds to the guanine nucleotides, guanosine triphosphate (GTP) and guanosine diphosphate (GDP). In the absence of ligand, the $G\alpha\beta\gamma$ complex exists in a GDP-bound state. Upon ligand binding, receptor conformational changes facilitate exchange of GDP for GTP, at which point the $G\alpha$ subunit can dissociate from $G\beta\gamma$ subunits. Both α and $\beta\gamma$ can interact with effector molecules and different types of $G\alpha$ subunits interact differently with effector systems. Three major $G\alpha$ proteins are commonly studied and include $G\alpha_s$, $G\alpha_{i/o}$, and $G\alpha_q$. Adenylate cyclase (AC) converts adenosine triphosphate (ATP) to cyclic adenosine monophosphate (cAMP) and is stimulated by $G\alpha_s$. cAMP is a secondary messenger molecule that leads to increased protein kinase A (PKA) activity. On the other hand, $G\alpha_{i/o}$ is negatively-coupled to AC and results in decreased production of cAMP and, in turn, reduced levels of PKA activity. $G\alpha_q$ increases phospholipase C β (PLC β) activity, which converts phosphoinositide bisphosphate (PIP₂) to diacylglycerol (DAG) and inositol trisphosphate (IP₃). These secondary messengers can in turn activate many downstream effectors. Ca²⁺ release and resultant elevations in cytoplasmic Ca²⁺ occurs via activation of IP₃ receptors located on the smooth endoplasmic reticulum. Ca²⁺ then interacts with many proteins but most commonly increases activity of protein kinases, such as protein kinase C or Ca²⁺/calmodulin-dependent protein kinase. Additionally, DAG increases PKC activation. Altered kinase activity resulting from G protein signaling will lead to phosphorylating events that directly or indirectly alter ion channel function. Such channels may include ligand binding receptors mediating fast synaptic events (e.g. AMPA, NMDA, GABA_A, etc.) or intrinsic ion channels (e.g. background K⁺, inwardly-rectifying K⁺ channels, non-

selective cation channels, voltage-gated Na⁺/Ca²⁺/K⁺ channels, for example) and consequences of changes may include changes in receptor kinetics, subunit composition, receptor density, action potential kinetics, subthreshold depolarization, or spike discharge rates. Once ligand is no longer present, endogenous GTPase activity of the G α subunit will result in hydrolysis of GTP to GDP, at which point the trimeric complex will re-associate, thus terminating the transduction events. Thus, these modulatory actions represent a complex sequence of cellular events that ultimately influence incoming ionotropic-mediated inputs and modify the integrating properties of the neuron, which will modify its output and the activity of the circuit.

Dissertation Research Objective

This dissertation is intended to continue our lab's mission to characterize neuromodulatory mechanisms within the MEC. Glutamate and GABA are the two primary neurotransmitters contributing to MEC activity. Our lab focuses on the modulatory aspects of both glutamatergic and GABAergic transmission to discern how different systems might regulate MEC activity. Our attention is primarily directed at the superficial layers because this layer mediates information entry into the hippocampal circuit. The MEC receives extensive subcortical modulatory input (ACh, DA, NE, 5-HT, and HA) and these molecules are expected to modulate MEC activity and performance. Moreover, the metabotropic receptors for glutamate and GABA will also influence MEC activity. The objective of this dissertation is to continue our lab's efforts in characterizing neuromodulatory mechanisms within this region. This dissertation is broken into three studies aimed at addressing the following questions:

1. Does dopamine modulate GABAergic transmission within the MEC?

2. Does HA modulate GABAergic transmission within the MEC?
3. How does group I activation modulate MEC excitability?

CHAPTER II

METHODS

Acute Slice Preparation

Animal protocols conformed to procedures approved by the University of North Dakota Animal Care and Use Committee. For Study 1, horizontal brain slices (400 μm) were prepared from 14- to 21-day-old Sprague-Dawley rats. For Study 2, horizontal brain slices (350 μm) from Sprague-Dawley rats were prepared. In this study, the age of the rats used were usually postnatal 14 to 22 days for most experiments. However, for some experiments involving recordings from interneurons, we extended the age of the rats to 30 days after birth because the number of interneurons in slices were low. Furthermore, it was difficult to find a specific type of interneuron required for experiments. We did not notice significant age-related differences for the effects of HA on spontaneous inhibitory postsynaptic currents (sIPSCs) or interneuron excitability. For Study 3, horizontal slices (350 μm) were prepared from 15- to 34-day old Sprague Dawley rats. TRPC1 knock-out (KO) and wild-type (WT) mice were provided by Dr. Brij Singh and animal ages used ~3 months old. In each study, a mix of female and male rats or mice were used and potential sex differences were not noticed.

Animals were deeply anesthetized in a bell jar using an isoflurane drop method. Brains were rapidly dissected into an ice-cold slurry of a cutting solution containing (in mM) 130 N-methyl-D-glucamine (NMDG)-Cl, 24 NaHCO₃, 3.5 KCl, 1.25 NaH₂PO₄,

0.5 CaCl₂, 5.0 MgCl₂, and 10 glucose and saturated with 95% O₂ and 5% CO₂. Slices were prepared using the same cutting solution and a vibratome (VT1000s or VT1200, Leica, Wetzlar, Germany). After cutting, slices were transferred to a holding chamber with the same solution, except NMDG was replaced with NaCl. For studies 2 and 3, the concentrations of CaCl₂ and MgCl₂ were modified to 2.5 mM and 1.5 mM, respectively. Slices recovered in these solutions for at least ~1 hr at 37°C, after which they held at room temperature until recordings.

Organotypic Slice Preparation

Horizontal sections were obtained from P8-P16 Sprague Dawley rats under aseptic conditions using a vibratome (VT1000s, Leica) and the above cutting solution (filter-sterilized). After isolating the MEC, slices were transferred to culture inserts and kept in petri dishes containing 1.1 mL of pre-warmed media comprised of 50% Hank's minimum essential medium without glutamine (Lonza cat#: 12-137F), 25% heat-inactivated horse serum (Hyclone cat #: SH30074.03HI), 25% Hank's buffered saline solution (Life technologies cat #: 24020), 2 mM glutamine (ThermoFisher cat#: 25030081), 5.95 mg/mL glucose, and 100 ug/mL penicillin and streptomycin (100x Pen/strep stock; Cellgro cat#: 30-002-CI). Culture media was changed on day-in-vitro (DIV) 1 and then every other day, thereafter. Experiments were conducted between DIV 4 and DIV 10.

Electrophysiological Recordings

For all studies, slices were transferred to a submersion recording chamber fitted on an Olympus BX51WI microscope equipped for both epifluorescence and differential interference contrast (DIC) imaging mounted on an air-table. Cells were identified using

video DIC microscopy with the use of top-mounted CCD cameras (Hitachi for DIC and Optimos CMOS for epifluorescence). Slices were continuously bathed using a gravity-driven perfusion system that had a constant flow-rate of ~1 mL/min. Whole-cell patch-clamp recordings were made using a Multiclamp 700B patch-clamp amplifier and signals were digitized using an Axon 1550 Digidata System (Axon Instruments). Recordings were filtered at 2 kHz, digitized at 10 kHz, and acquired using either Clampex versions 9.0 or 10.2 software versions. Patch electrodes had a tip resistance of 4-10 M Ω . A period of 10–15 min followed establishment of the whole-cell configuration and prior to recording stable responses. The extracellular solution, unless otherwise specified, was comprised of (in mM) 130 NaCl, 24 NaHCO₃, 3.5 KCl, 1.25 NaH₂PO₄, 1.5 MgCl₂, 2.5 CaCl₂, and 10 glucose, continuously saturated with 95% O₂ and 5% CO₂ (pH = 7.4). For experiments using NMDG, the extracellular NaCl was replaced with equimolar NMDG-Cl (pH = 7.4 with HCl). In experiments where extracellular Ca²⁺ was reduced, the extracellular CaCl₂ was replaced with equimolar MgCl₂ and ethylene glycol-bis-(2-aminoethylether)-N,N,N',N'-tetraacetic acid (EGTA, 0.1 to 1 mM) was added to chelate any potentially residual Ca²⁺. In experiments where extracellular Na⁺ was reduced and Ca²⁺ was replaced, equimolar MgCl₂ replaced the CaCl₂ used in the NMDG⁺ solution above. In Study 3, the 4-(2-hydroxyethyl)piperazine-1-ethanesulfonic acid (HEPES)-buffered extracellular solution was comprised of (mM) 147 NaCl, 3.5 KCl, 1.5 MgCl₂, 2.5 CaCl₂, 10 HEPES, and 10 glucose (pH = 7.4 with NaOH).

Recordings of GABA_A Receptor-Mediated sIPSCs, mIPSCs, and eIPSCs

GABAergic inhibitory postsynaptic currents (IPSCs) were recorded in studies 1 and 2. Spontaneous IPSCs (sIPSCs), miniature IPSCs (mIPSCs), and evoked IPSCs

(eIPSCs) were obtained using whole-cell patch-clamp recordings from principal cells located in layers II, III, and V of the MEC. Recording electrodes were filled with (in mM) 100 Cs⁺-gluconate, 0.6 EGTA, 5 MgCl₂, 8 NaCl, 2 ATPNa₂, 0.3 GTPNa, 40 HEPES and 1 QX-314 (pH 7.3 adjusted with CsOH). To record GABA_A receptor-mediated sIPSCs, cells were voltage-clamped at +30 mV and the external solution was supplemented with dl-2-amino-5-phosphonopentanoic acid (dl-APV; 50 μM) and 6,7-dinitroquinoxaline-2,3-dione (DNQX; 10 μM). Confirmation that sIPSCs were in fact GABAergic was determined by bath applying the GABA_A receptor antagonist bicuculline (10 μM) to a subset of slices. For recordings of mIPSCs, tetrodotoxin (TTX; 0.5 μM) was added to the dl-APV- and DNQX-supplemented extracellular solution. Both sIPSCs and mIPSCs were filtered during on-line acquisition with lowpass and highpass settings at 2kHz and 1Hz, respectively. eIPSCs were recorded from principal neurons using the same internal and external solution as sIPSCs and by placing a stimulation electrode (a patch-clamp recording pipette filled with extracellular solution) locally (~200 μm from the recorded neuron). Stimulations were delivered using an A360 stimulus isolator operated with pClamp. Data for both sIPSCs and mIPSCs were analyzed using Mini Analysis 6.0.1 (Synaptosoft Inc.) and recordings were visually inspected to exclude any obvious artifacts. Each detected event was inspected visually to exclude any obvious artifacts before analysis. The threshold for detection was set to 3 times the standard deviation of the noise as recorded in an event-free stretch of data. Mean amplitude, frequency, cumulative amplitude and frequency histograms were generated using this program. Because the basal frequency of sIPSCs and mIPSCs varied considerably among

cells, we normalized the frequency or amplitude of events to the averages recorded for 5 minutes prior to DA or HA application.

Recordings of Resting Membrane Potentials, Action Potentials,
Holding Currents, and Current-Voltage Relationships
from Layer III MEC Interneurons

For studies 1 and 2, recordings were made directly from local MEC interneurons. Resting membrane potentials (RMPs), action potentials (APs), holding currents (HCs), and current-voltage (I-V) relationships were recorded from interneurons in layer III of the MEC. Unless stated otherwise, the intracellular solution contained (in mM) 100 K⁺-gluconate, 0.6 EGTA, 5 MgCl₂, 8 NaCl, 2 ATPNa₂, 0.3 GTPNa, 7 phosphocreatine, and 33 HEPES (pH 7.3 adjusted with KOH). Interneurons were initially selected based on morphological criteria including a relatively small soma size as opposed to that of adjacent principal neurons and shapes that were unipolar, bipolar, spindle, irregular, or round. Following establishment of whole-cell configuration, interneurons were further identified based on electrophysiological properties including a putative fast-spiking narrow AP profile and steep afterhyperpolarization. The classification of interneurons was based on the presence or absence of a membrane potential sag-response to a hyperpolarizing current injection. Neurons exhibiting no sag were classified as Type I and those with a sag-response were classified as type II interneurons (Kumar and Buckmaster, 2006; Deng and Lei, 2008). The membrane capacitances of both interneurons were much smaller (~40-90 pF) compared to those of the principal neurons (~130-200 pF), as determined in pClamp.

Interneuron RMPs and HCs were recorded in the extracellular solution containing TTX (0.5 μM) to block AP generation and potential contaminations from DA- or HA-

dependent changes in synaptic inputs. Recordings of APs were made using the extracellular solution supplemented with (in μM) 50 dl-APV, 10 DNQX, 10 bicuculline, and 1 CGP55845 to exclude any possible DA- or HA-induced contributions of synaptic transmission on the firings of the recorded interneurons. Current was injected to the soma to raise the RMP to near threshold to elicit spontaneous AP firing. For the recordings of I-V relationships, the external solution contained (in μM) 0.5 TTX, 100 CdCl_2 , 200 NiCl_2 , 10 DNQX, 50 dl-APV, and 10 bicuculline. For voltage ramps, cells were clamped at -60 mV and a ramp protocol was applied at 0.05 Hz from -120 mV to 40 mV (velocity = 80 mVs⁻¹). For I-V relationships, because maximal DA- or HA-induced responses were typically seen around ~8 and ~5 min, respectively, an average of at least 3 ramp traces from these maximal time points were used for comparison to control ramps. For the recording of Kirs in Study 2, cells were clamped at -70 mV and 400 ms voltage steps from -150 mV to -60 mV were delivered every 10 seconds. The extracellular medium for K⁺-mediated I-V relationships contained NMDG, TTX (0.5 μM) and zero Ca²⁺. For the recording of the delayed rectifier K⁺ channels (I_K), cells were clamped at -60 mV before being briefly stepped to -50 mV for 50 ms, followed by 500 ms steps from -60 mV to +70 mV every 3 seconds. Access resistance was rigorously monitored before and after each protocol using the pClamp seal test. Cells with access resistance changes of greater than 15% were discarded.

Recordings of APs, RMPs, HCs, and I-Vs from Principal Neurons of the MEC

For Study 3, AP recordings were made from layers II, III, and V MEC principal neurons, whereas RMPs, HCs and I-Vs were made exclusively from layer III neurons. Intracellular recording electrodes were filled with, unless otherwise stated, either a K-

gluconate-containing or Cs-gluconate-containing internal solution. The K-gluconate internal solution was comprised of (mM) 100 K-gluconate, 0.6 EGTA, 5 MgCl₂, 8 NaCl, 2 ATPNa₂, 0.3 GTPNa, 7 phosphocreatine, and 33 HEPES (pH 7.3 adjusted with KOH). The Cs-gluconate internal solution was comprised of (mM) 100 Cs-gluconate, 0.6 EGTA, 5 MgCl₂, 8 NaCl, 2 ATPNa₂, 0.3 GTPNa, 40 HEPES and 1 QX-314 (pH 7.3 adjusted with CsOH). As done with interneuron AP recordings, blockers for glutamatergic and GABAergic synaptic transmission were included in the extracellular solution to isolate direct actions of (*S*)-3,5-dihydroxyphenylglycine (DHPG). Positive current was injected to elicit spontaneous AP firing and baseline AP firing frequencies for layer III pyramidal neurons were set to ~.5 Hz. Recordings of HCs were made by voltage-clamping the membrane to -60 mV. Both RMPs and HCs were recorded in the presence of TTX to block synaptic transmission and prevent AP generation. A Cs-containing intracellular solution was used for I-V relationships to isolate non-K⁺-mediated currents and the extracellular solution contained the same blockers as those described in interneuron I-V relationships. For layer III pyramidal ramps, the membrane potential was voltage-clamped at -60 mV and the ramp range was from -100 to +60 mV. The DHPG-induced net current was generated by subtracting from control ramp traces from responses following five minutes of application of DHPG. Intracellular dialysis of TRPC-targeting antibodies for HC experiments were performed using a Cs-based intracellular solution containing 4 ug/mL antibodies targeting TRPC1 (Alomone Labs, ACC-010), TRPC3 (Alomone Labs, ACC-016), TRPC4 (Alomone Labs, ACC-018), TRPC5 (Alomone Labs, ACC-020), or both TRPC4 and 5.

Western Blot

For Study 2, western blot analysis was performed on lysates prepared from MEC slices. Horizontal slices were prepared as described above and the MEC was isolated under a stereomicroscope from 3 rats. Tissue lysates and samples were processed as described previously (Deng et al., 2009; Ramanathan et al., 2012; Xiao et al., 2014). To each lane of a 12% polyacrylamide gel, 10 μ g of protein was added and run at 120 constant volts for 60 minutes. Samples were then transferred to PVDF membranes at 300 mA for 60 minutes. Membranes were rinsed and blocked in tris-buffered saline supplemented with 0.1% Tween 20 (TBS-T) and 3% bovine serum albumin (BSA) for 30 minutes. Membranes were then incubated with antibodies for either H1 (1:400; AHR-001, Alomone Labs) or H2 (1:400, SC-33974, Santa Cruz Biotechnology) receptors on a rocking platform overnight at 4°C. As a negative control, additional blots were processed in parallel using a primary antibody solution that had been pre-adsorbed with appropriate blocking peptide provided by the vendors (1 μ g blocking peptide: 1 μ g antibody, prepared 20 min prior to membrane application). Membranes were washed 2 times in TBS-T and then incubated for 1.5 hours with either anti-rabbit IgG-HRP for H1 (1:1000, SC-2357, Santa Cruz Biotechnology) or anti-goat IgG-HRP for H2 (1:1000, SC-2020, Santa Cruz Biotechnology) receptors. Following 3 rinses with TBS-T, membranes were then processed using SuperSignal West Pico Chemiluminescent Substrate kit (catalog No. 34080, Pierce) and developed using a UVP Imaging System and VisionWorks software.

Immunohistochemistry

Animals were deeply anesthetized using a xylazine/ketamine cocktail and transcardially perfused with saline (0.9% NaCl) followed by 4% paraformaldehyde (PFA) in saline. Brains were extracted and stored in 4% PFA overnight and subsequently transferred to a 30% sucrose solution for 3 days. Brains were then embedded in Tissue-Tek O.C.T compound and sectioned at 10 μ m using a cryostat (CM3050s, Leica) and fixed to frosted slides. After washes 3 times (2 min each) in 0.1 M phosphate buffered saline (PBS), slides were heated to 90°C in a 10 mM sodium citrate buffer containing 0.1% Tween 20 for 20 min. After cooling to room temperature, slides were again washed with PBS 3 times. Non-specific binding was blocked using a buffer (IHC buffer) comprised of PBS, 0.5% BSA, 0.1% Triton X-100, and 5% fetal bovine serum for 30 minutes. Slides were then individually incubated for 48 h at 4°C with either anti-H1 (1:500) or anti-H2 (1:200) receptors and mouse anti-GAD-67 (1:500, MAB5406, Millipore) to demonstrate co-localization of either HA receptor with GABAergic neurons. Slides were rinsed twice (3 min each) and then underwent a secondary incubation with fluorophore-conjugated donkey anti-rabbit IgG-TR (1:200, SC-2784, Santa Cruz Biotechnology) or donkey anti-goat IgG-TR (1:200, SC-2783, Santa Cruz Biotechnology) and bovine anti-mouse IgG-FITC (1:200, SC-2366, Santa Cruz Biotechnology) in IHC buffer for 2 hours at room temperature in the dark. After washes in PBS 6 times (5 min each), slides were coverslipped using Prolong mounting media (P36931, Life Technologies) and imaged using a Fluoview 300 confocal microscope (Olympus).

Knock-Down of TRPC4 and TRPC5

Unique shRNA constructs targeting either rat TRPC4 (rTRPC4) or TRPC5 (rTRPC5) in retroviral red fluorescent protein-(pRFP-C-RS) or green fluorescent protein-(pGFP-V-RS) containing vectors were purchased from Origene (Rockville, MD). Plasmids were amplified in *E. coli* and isolated using a mega prep kit purchased from Qiagen (cat#: 12181). DNA working solutions of 1 µg/µL in TE were prepared for HEK-293 and biolistic transfection. TRPC4 was targeted using the 29-mer sequence CAGCATTCCTGGTCTCAATGAACAGTGTG and TRPC5 was targeted using the 29-mer sequence AGCTTCTAACCTGCATGACCATTGGATTC. Knockdown efficiency was validated for each shRNA by co-transfecting HEK-293 with cDNAs for rTRPC4 (kindly provided by Dr. Brij Singh) or hTPRC5 (purchased from Origene (pCMV6-XL4, GenBank accession number NM_012471)), with their corresponding shRNA sequences. Concurrent scramble controls were performed using proprietary scramble sequences provided by Origene that were inserted into appropriate RFP-carrying or GFP-carrying vectors. After 48 hours of transfection, cells were lysed in RIPA buffer containing 1x protease and phosphatase inhibitors. Protein concentrations were determined with a Bradford assay and western blot analysis (using similar methods as those described above) was performed to determine expression levels using anti-TRPC5 (1:500, Alomone Labs cat #ACC-020) and anti-TPRC4 (1:500, NeuroMab N77/15).

Biolistic Transfection of Organotypic Slice Cultures

Transfection bullets were prepared by coating 12.5 mg of 1.6 µm gold pellets with 25 µg of each shRNAs for TRPC4 and TRPC5 or their corresponding scramble controls

using a tubing prep station (Biorad). Particles were delivered to MEC organotypic slices using a Helios Gene Gun (Biorad) on DIV 2 at 150 psi from a shooting distance of 1.25 inches above slice sections. Recordings were made on DIV 4-6 using methods described above.

Data Analysis

Data are presented as the mean \pm SEM. Throughout the text, *n* refers to the number of cells examined. The concentration-response curve for DA, HA, and DHPG was fit using the Hill equation: $I = I_{\max} \times \{1/[1+EC_{50}/(\text{ligand})^n]\}$, where I_{\max} is the maximum response, EC_{50} is the ligand concentration producing a half-maximal response, and *n* is the Hill coefficient. Student's paired or unpaired t-test, or analysis of variance was used for statistical analysis. Statistical analysis was performed using Origin 7 or GraphPad Prism 6. *P*-values are reported throughout the text and significance was set at $P < 0.05$. For sIPSC cumulative probability plots, events were pooled and used the same bin size across all cells (25 ms for frequency and 2 pA for amplitude) and only those recorded in the last minute of DA or HA application (maximal response) were compared to the average recorded in the control condition for 5 minutes.

Chemicals

SCH2339, LE300, SKF38393, SKF81297, sulpiride, corynanthine, mibefradil, ZD7288, 1,2-bis(2-aminophenoxy)ethane-*N,N,N',N'*-tetraacetic acid (BAPTA), thapsigargin, doxazosin, cetirizine, ranitidine, thioperamide, 2-pyridylethylamine, dimaprit, (R)-(-)- α -methylhistamine, DHPG, LY456236, MPEP, U73122, edelfosine, MDL 12330A, genistein, PP1, 2-APB, KB-R7943, ruthenium red, ML-204, dl-APV, DNQX, bicuculline, CGP55845, kynurenic acid, and TTX were purchased from Tocris

Cookson Inc. (Ellisville, MO, USA). GDP- β -S was purchased from Enzo Life Sciences. Other chemical reagents, including DA, HA, DMSO, FFA, LaCl₃ and NMDG, were purchased from Sigma-Aldrich.

All of the drugs were initially prepared as a stock solution that was frozen below -20°C until use. The stock solution was diluted in the extracellular solution to reach the final working concentrations applied to slices. When dimethyl sulfoxide (DMSO) or other vehicles were required to dissolve drugs, the final concentration of the vehicles was kept $< 0.1\%$. For experiments involving inhibitors, slices were usually pretreated with the extracellular solution containing the inhibitors for at least 20 min and the same concentration of the drugs were continuously applied, unless otherwise stated, in the bath to ensure a complete inhibition of the targets. For DA experiments, a stock DA solution at 100 mM was initially prepared, aliquoted, and frozen until use. To prevent oxidation of DA, 15 μL of the frozen DA stock solution was dissolved in 15 mL of the extracellular solution used for the experiment immediately prior to DA application. Using this method, we did not observe any changes in color of the solution during the experiment, suggesting oxidation was minimal.

CHAPTER III

RESULTS

Study 1 – Dopaminergic Modulation of MEC GABAergic Transmission

Introduction

Catecholamines including dopamine (DA) and norepinephrine are neurotransmitters or neuromodulators involved in the modulation of a variety of physiological functions such as working memory (Phillips et al., 2008; Sara, 2009) and neurological and psychiatric disorders, including Parkinson's disease, addiction, schizophrenia, bipolar disorder, Huntington's disease, attention deficit hyperactivity disorder, and Tourette's syndrome (Beaulieu and Gainetdinov, 2011; Kurian et al., 2011). DA activates 5 types of G protein-coupled receptors that can be classified as D1- (D1 and D5) and D2-like (D2, D3, and D4) receptors (Beaulieu and Gainetdinov, 2011), whereas norepinephrine interacts with $\alpha 1$, $\alpha 2$, $\beta 1$, $\beta 2$, and $\beta 3$ adrenergic receptors. However, evidence suggests that there are promiscuous interactions among dopaminergic and adrenergic receptors. For example, DA has been shown to activate $\alpha 1$ (Leedham and Pennefather, 1986; Rey et al., 2001; Cornil et al., 2002; Zhang et al., 2004; Lazou et al., 2006; Lin et al., 2008), $\alpha 2$ (Leedham and Pennefather, 1986; Cornil et al., 2002), and β (Rajfer et al., 1988; Anfossi et al., 1993; Lee et al., 1998; Ouedraogo et al., 1998) adrenergic receptors, whereas norepinephrine activates D2 dopaminergic receptors (Robbins et al., 1988). At least 4 major dopaminergic pathways have been identified in the mammalian brain; the nigrostriatal, mesolimbic, mesocortical, and tuberoinfundibular

tracts that originate from the dopaminergic neurons in the substantia nigra, ventral tegmental areas, arcuate nucleus, and periventricular area of the hypothalamus, respectively. Like other cortical regions, the EC receives profuse dopaminergic innervation mainly from the ventral tegmental areas in the midbrain (Akil and Lewis, 1993). Similarly, the EC also receives prominent noradrenergic projections from the locus coeruleus (Fallon et al., 1978; Palkovits et al., 1979; Wilcox and Unnerstall, 1990). Consistent with the anatomical dopaminergic and noradrenergic innervations of the EC, the EC also expresses dopaminergic receptors such as D1- (Savasta et al., 1986; Huang et al., 1992; Tarazi et al., 1999) and D2-like (Richfield et al., 1989; Weiner et al., 1991; Hemby et al., 2003; Rivera et al., 2008) receptors and adrenergic receptors including $\alpha 1$ (Wilcox and Unnerstall, 1990), $\alpha 2$ (Unnerstall et al., 1984, 1985; Boyajian et al., 1987), and β (Booze et al., 1993) receptors. Functionally, DA increases Na^+ channel currents (Rosenkranz and Johnston, 2007), inhibits the excitability of pyramidal neurons (Rosenkranz and Johnston, 2006; Mayne et al., 2013), and modulates excitatory synaptic transmission (Pralong and Jones, 1993; Stenkamp et al., 1998; Behr et al., 2000; Caruana et al., 2006; Caruana and Chapman, 2008) and plasticity (Caruana et al., 2007; Hamilton et al., 2010) in the EC. Application of norepinephrine in the EC inhibits glutamatergic transmission (Pralong and Magistretti, 1994, 1995) and neuronal excitability (Xiao et al., 2009a) via activation of $\alpha 2$ receptors and facilitates GABAergic transmission via the activation of $\alpha 1$ receptors (Lei et al., 2007). However, the effects of DA on inhibitory synaptic transmission and GABAergic interneurons are elusive, although DA slightly depresses evoked IPSPs in the EC (Pralong and Jones, 1993). In this study, we thoroughly examined the effects and the underlying mechanisms of DA in GABAergic

transmission in the EC. Our results showed that DA increased the frequencies of spontaneous IPSCs (sIPSCs) and miniature IPSCs (mIPSCs), but slightly depressed the amplitude of evoked IPSCs (eIPSCs). Further investigation revealed that DA augmented the frequencies of sIPSCs and mIPSCs not by DA receptors, but by the activation of $\alpha 1$ adrenergic receptors. Determination of the underlying ionic and signaling mechanisms indicated that functions of the inward rectifier K^+ channels (Kirs) and the T-type Ca^{2+} channels were required for DA-mediated facilitation of GABAergic transmission.

DA Increases the Frequency Not the Amplitude of sIPSCs Recorded from Entorhinal Neurons Via Activation of $\alpha 1$ Adrenergic Receptors

We examined the effects of DA on GABA_A receptor-mediated sIPSCs recorded from the principal neurons in each layer of the EC. Stellate and pyramidal neurons are the principal neurons in layer II, whereas pyramidal neurons are the major neuronal type in layers III and V. In layer II stellate neurons, application of DA (100 μ M) for 8 min significantly increased the frequency of sIPSCs to $198 \pm 18\%$ of control ($n = 13$, $P < 0.001$, Fig. 1A, B, and C) without altering the amplitude of sIPSCs significantly ($103 \pm 4\%$ of control, $n = 13$, $P = 0.97$, Fig. 1A and D). DA concentration dependently increased the frequency of sIPSCs (effective concentration range: 3–100 μ M) with an EC₅₀ value of 3.6 μ M (Fig. 1E). Similarly, application of DA significantly increased the frequency (F) with no effects on the amplitude (A) of sIPSCs recorded from the pyramidal neurons in layer II (F: $227 \pm 20\%$ of control, $n = 5$, $P = 0.003$; A: $114 \pm 13\%$ of control, $n = 5$, $P = 0.35$, Fig. 1F), layer III (F: $189 \pm 23\%$ of control, $n = 5$, $P = 0.02$; A: $113 \pm 12\%$ of control, $n = 5$, $P = 0.34$, Fig. 1F), and layer V (F: $229 \pm 20\%$ of control, $n = 5$, $P = 0.003$; A: $109 \pm 6\%$ of control, $n = 5$, $P = 0.22$, Fig. 1F). Whereas these results indicate that DA

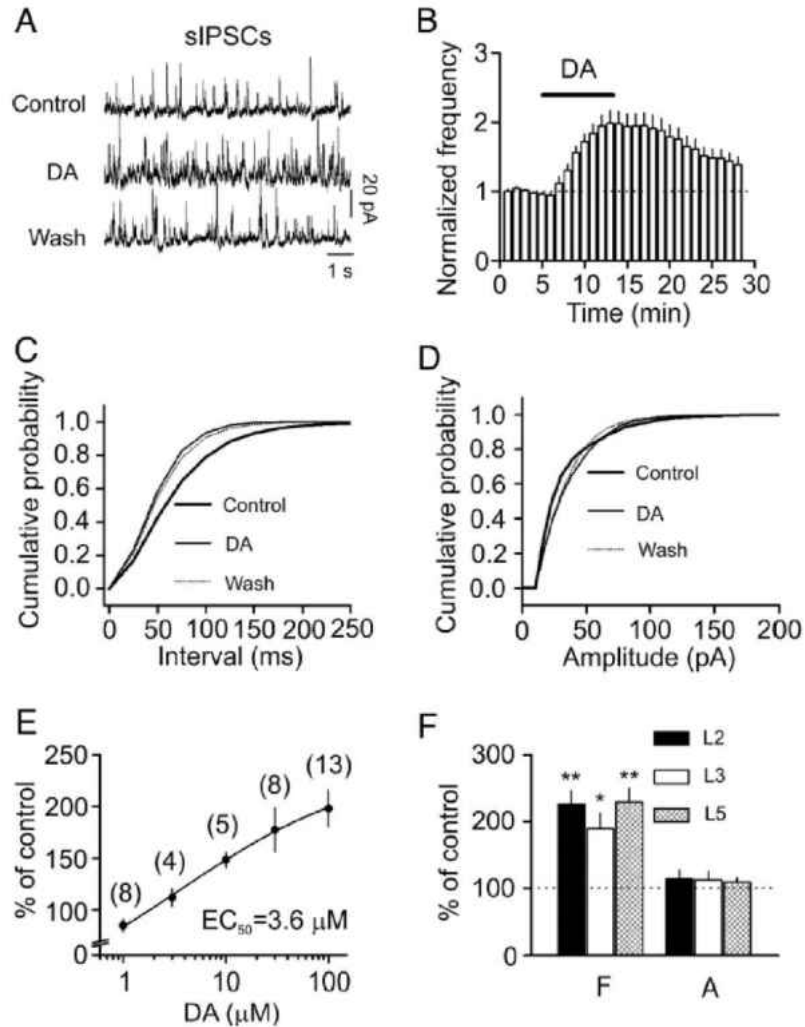
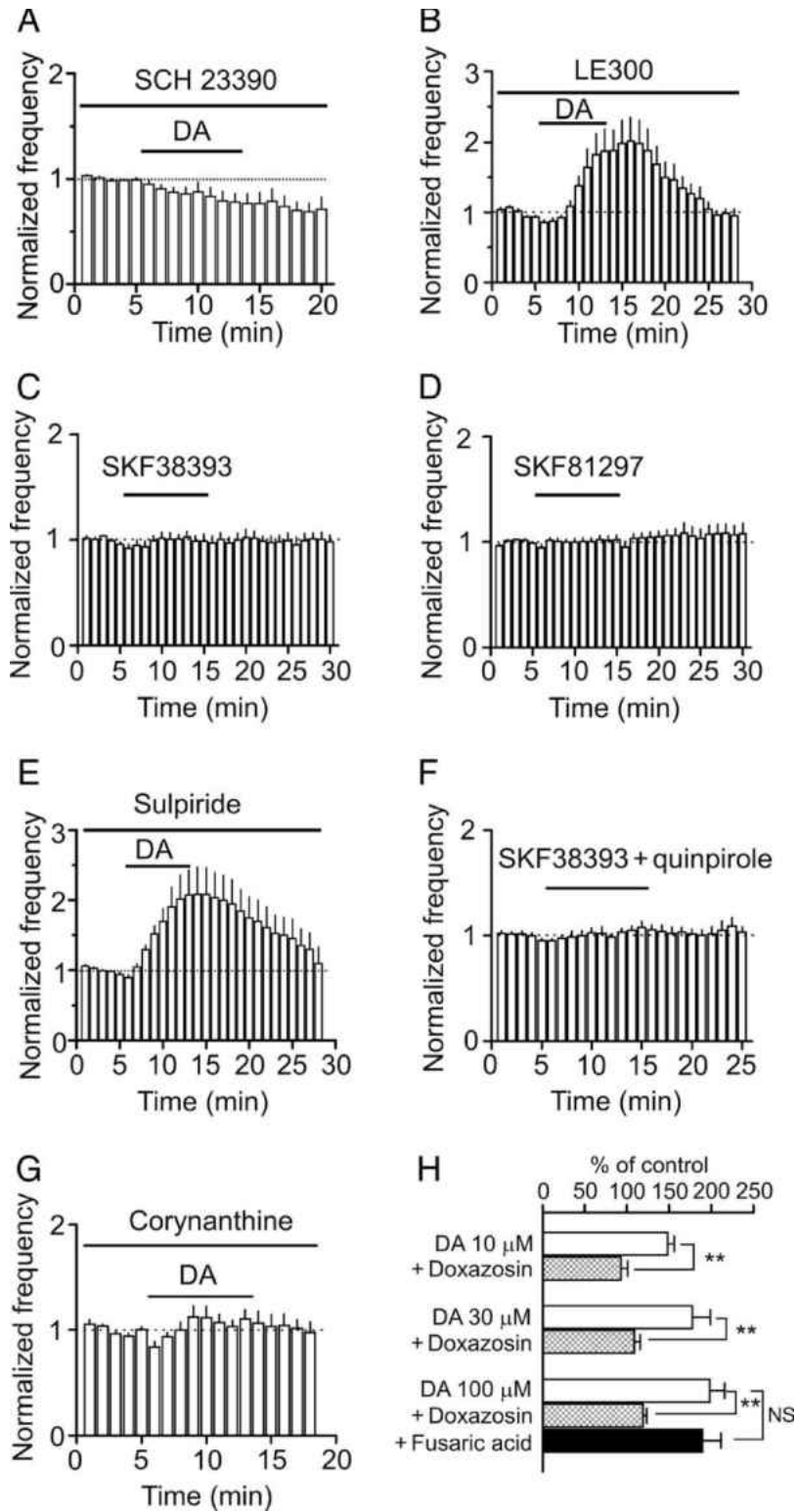


Figure 1. DA increases the frequency but not the amplitude of sIPSCs recorded from entorhinal neurons. (A) sIPSCs recorded from a layer II stellate neuron before, during, and after the application of DA (100 μM). (B) Time course of the sIPSC frequency averaged from 13 stellate neurons. (C) Cumulative frequency distribution from a layer II stellate neuron before, during, and after the application of DA. (D) Cumulative amplitude distribution from the same cell before, during, and after the application of DA. The flat line part of the curves was generated because zero events were detected at the amplitudes below threshold. (E) Concentration–response curve of DA. Numbers in the parenthesis are the numbers of cells recorded. (F) Bath application of DA (100 μM) significantly enhanced the frequency, F, with no effects on the amplitude, A, of sIPSCs recorded from the pyramidal neurons in layer II (L2), layer III (L3), and layer V (L5). * $P < 0.05$, ** $P < 0.01$.

facilitates the frequency of sIPSCs in all the principal neurons in the EC, we used layer II stellate neurons as an example to determine the underlying cellular and molecular mechanisms for the rest of the experiments.

We probed the involvement of DA receptors. Slices were pretreated with the selective D1-like receptor antagonist, SCH23390 (10 μ M), and the extracellular solution continued to contain the same concentration of SCH23390. Under these circumstances, bath application of DA for 8 min failed to increase, but slightly and significantly decreased the frequency ($80 \pm 6\%$ of control, $n = 8$, $P = 0.01$, Fig. 2A) and amplitude ($82 \pm 4\%$ of control, $n = 8$, $P = 0.004$, data not shown) of sIPSCs. We further tested the effects of another D1 antagonist of distinct structure and higher potency, LE300. Application of LE300 (100 nM, $K_i = 1.9$ nM for D1 receptors (Kassack et al., 2002)) failed to block DA-mediated augmentation of the frequency of sIPSCs ($187 \pm 32\%$ of control, $n = 9$, $P = 0.025$, Fig. 2B). Because of the distinct effects of these 2 D1 antagonists, we further tested the roles of D1-like receptors by using the agonists selective for D1-like receptors. Bath application of SKF38393 (20 μ M), a selective D1-like receptor agonist, failed to significantly alter the frequency ($99 \pm 6\%$ of control, $n = 5$, $P = 0.87$, Fig. 2C) and the amplitude ($88 \pm 5\%$ of control, $n = 5$, $P = 0.11$) of sIPSCs. Similarly, bath application of SKF81297 (20 μ M), another selective D1-like receptor agonist, did not significantly alter the frequency ($102 \pm 4\%$ of control, $n = 6$, $P = 0.64$, Fig. 2D) and the amplitude ($87 \pm 8\%$ of control, $n = 6$, $P = 0.14$) of sIPSCs. These results suggest that activation of D1-like receptors does not increase the frequency of sIPSCs. The effect of SCH23390 may thus not be mediated by blockade of D1-like receptors but due to its inhibition on Kirs, which were required for the effects of DA (see below)

Figure 2. DA facilitates sIPSC frequency via the activation of $\alpha 1$ adrenoreceptors, but not DA receptors. (A) Pretreatment of slices with and continuous bath application of the D1-like receptor antagonist, SCH23390 (10 μM), blocked DA-induced facilitation of sIPSC frequency. (B) Application of another D1-like receptor antagonist, LE300 (100 nM), in the same fashion failed to block DA-mediated enhancement of sIPSC frequency. (C) Bath application of the selective D1-like receptor agonist, SKF38393 (20 μM), did not increase sIPSC frequency. (D) Bath application of SKF81297 (20 μM), another selective D1-like receptor agonist, failed to facilitate the frequency of sIPSCs. (E) Application the D2-like receptor antagonist, sulpiride (100 μM), failed to alter DA-induced facilitation of sIPSC frequency significantly. (F) Bath application of the D1- and D2-like receptors agonists did not enhance the frequency of sIPSCs. (G) Application of the selective $\alpha 1$ antagonist, corynanthine (100 μM), blocked DA-induced enhancement of sIPSC frequency. (H) Application of another $\alpha 1$ antagonist, doxazosin (25 μM), failed to block DA-induced increases in sIPSC frequency at 10, 30, and 100 μM and in the presence of the dopamine- β -hydroxylase inhibitor, fusaric acid (100 μM), DA still increased sIPSC frequency. $**P < 0.01$, N.S., no significance.



because SCH23390 is also a blocker of Kirs (Kuzhikandathil and Oxford, 2002; Shankar et al., 2004; Sosulina et al., 2008; Chee et al., 2011). We then tested the roles of D2-like receptors by applying the selective D2-like receptor antagonist, sulpiride. In the presence of sulpiride (100 μ M), application of DA still significantly increased the frequency ($207 \pm 4\%$ of control, $n = 7$, $P = 0.02$, Fig. 2E) but failed to alter the amplitude ($96 \pm 7\%$ of control, $n = 7$, $P = 0.65$) of sIPSCs, suggesting that D2-like receptors are not involved. We further tested whether the facilitatory effect of DA on sIPSC frequency requires both D1- and D2-like receptors. Bath application of SKF38393 (20 μ M, D1-like agonist) and quinpirole (20 μ M, D2-like agonist) still failed to increase the frequency ($108 \pm 6\%$ of control, $n = 5$, $P = 0.27$, Fig. 2F) and amplitude of ($93 \pm 4\%$ of control, $n = 5$, $P = 0.19$) sIPSCs. These unexpected results suggest that DA receptors are not required for DA-induced enhancement of sIPSC frequency.

There is accumulating evidence indicating that DA can also act via the activation of $\alpha 1$ adrenergic receptors (Leedham and Pennefather, 1986; Rey et al., 2001; Cornil et al., 2002; Zhang et al., 2004; Lazou et al., 2006; Lin et al., 2008) and $\alpha 1$ adrenoreceptors enhance GABAergic transmission in the EC (Lei et al., 2007). We therefore tested the hypothesis that DA increases sIPSC frequency via the activation of $\alpha 1$ receptors in the EC. In the presence of the selective $\alpha 1$ receptor antagonist, corynanthine (100 μ M), application of DA (100 μ M) failed to increase either the frequency ($111 \pm 9\%$ of control, $n = 7$, $P = 0.26$, Fig. 2G) or the amplitude ($94 \pm 2\%$ of control, $n = 7$, $P = 0.311$) of sIPSCs. We also used another $\alpha 1$ receptor antagonist, doxazosin, which is distinct in structure compared with corynanthine. Pretreatment of slices with and continuous bath application of doxazosin (25 μ M) blocked the increase of sIPSC frequency induced by

DA at 10 ($93 \pm 8\%$ of control, $n = 5$, $P = 0.45$, Fig. 2H), 30 ($109 \pm 6\%$ of control, $n = 8$, $P = 0.21$, Fig. 2H), and 100 μM ($111 \pm 7\%$ of control, $n = 9$, $P = 0.16$, Fig. 2H). These results suggest that DA facilitates sIPSC frequency not by the activation of dopaminergic receptors, but instead by the activation of $\alpha 1$ adrenoreceptors.

DA could activate $\alpha 1$ adrenoreceptors directly or indirectly by transformation into norepinephrine within the slices via DA- β -hydroxylase. The generated norepinephrine could then bind to $\alpha 1$ adrenoreceptors to mediate the effects of DA. We therefore tested this possibility by applying fusaric acid, a DA- β -hydroxylase inhibitor (Nagatsu et al., 1970; Hidaka, 1971). Slices were pretreated with fusaric acid (100 μM) and the same concentration of fusaric acid was continuously applied in the bath. Under these circumstances, application of DA induced a comparable enhancement of sIPSC frequency ($190 \pm 22\%$ of control, $n = 4$, $P = 0.81$ vs. DA alone, Fig. 2H), suggesting that it is unlikely that the effects of DA were mediated by its conversion to norepinephrine.

*Endogenously Released DA Also Increases sIPSC Frequency
Via Activation of $\alpha 1$ Receptors*

We next probed the roles of endogenously released DA in modulating GABAergic transmission. Because the EC expresses DA transporter (DAT (Erickson et al., 1998)), we initially bath applied DAT inhibitor to elevate synaptic DA concentration. Bath application of the selective DAT inhibitor, GBR 12935 (5 μM), failed to significantly increase the frequency of sIPSCs ($91 \pm 2\%$ of control, $n = 8$), compared with vehicle application ($91 \pm 4\%$ of control, $n = 8$, $P = 0.95$, Fig. 3A,F). One possible explanation for the negative result is that there was no tonic spontaneous DA release at the dopaminergic terminals in the EC. We therefore used an alternative approach to

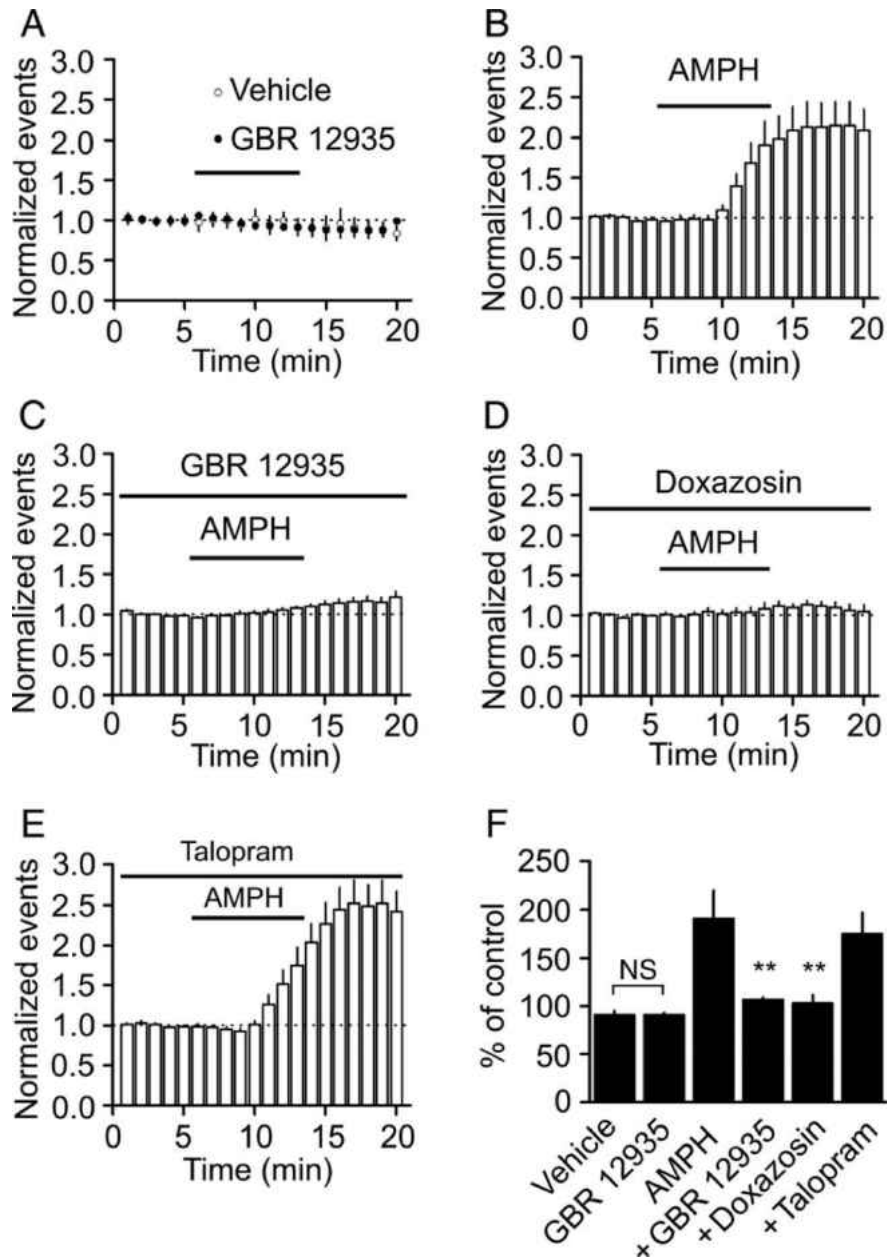


Figure 3. Endogenously released DA enhances sIPSC frequency via the activation of $\alpha 1$ receptors. (A) Bath application of the DAT inhibitor, GBR 12935 (5 μ M), had no significant effect on sIPSC frequency compared with that of vehicle (0.1% DMSO). (B) Bath application of AMPH (100 μ M) significantly increased the frequency of sIPSCs. (C) In the presence of GBR 12935, bath application of AMPH (100 μ M) induced a significantly smaller increase in sIPSC frequency. (D) AMPH-mediated increase in sIPSC frequency was blocked by $\alpha 1$ receptor antagonist, doxazosin (25 μ M). (E) Application of talopram (1 μ M) failed to alter AMPH-induced enhancement of sIPSC frequency. (F) Summary bar graph. n.s., no significant difference; ** $P < 0.01$ compared with AMPH alone.

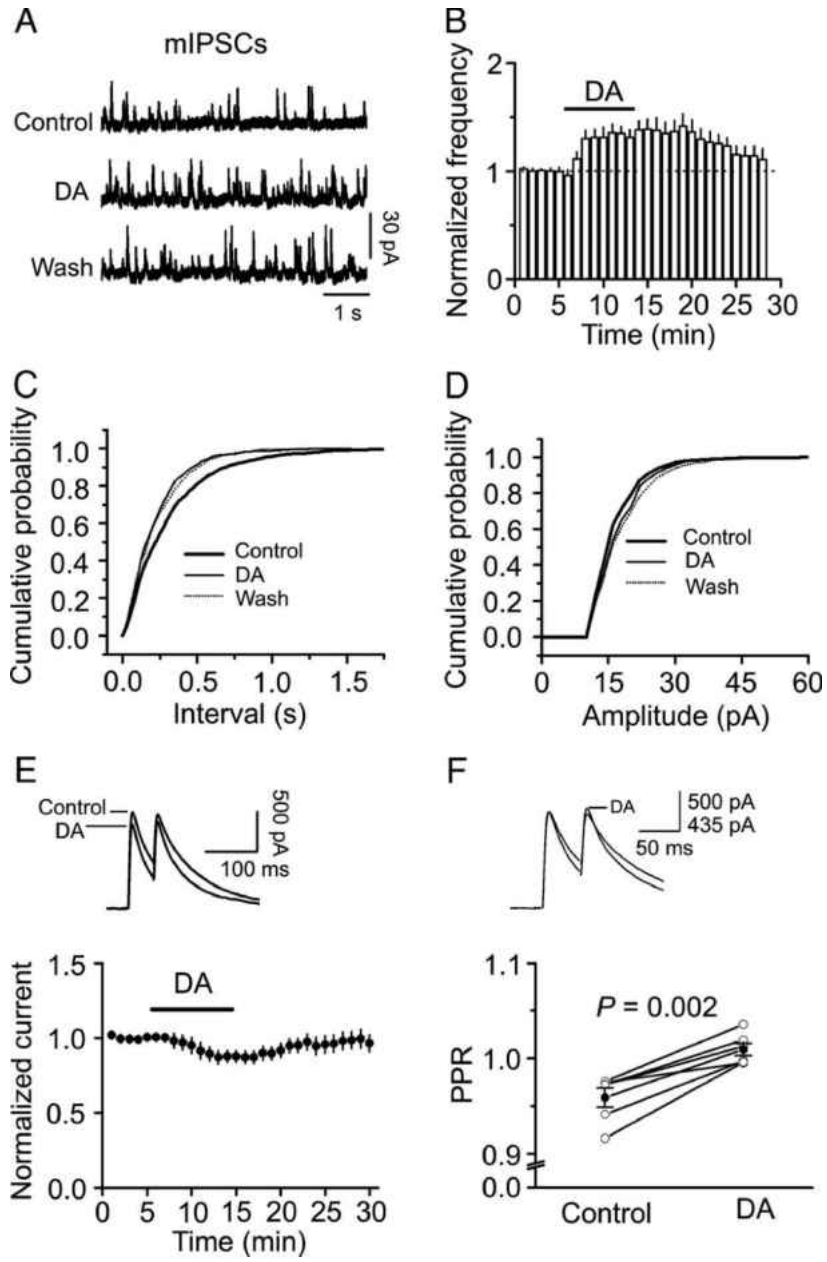
stimulate DA release. Amphetamine (AMPH) is a drug that increases transporter-mediated DA release (Leviel, 2011). Application of AMPH (100 μ M) for 8 min significantly increased the frequency of sIPSCs ($191 \pm 29\%$ of control, $n = 8$; $P = 0.02$, Fig. 3B and F). To test the involvement of DAT, we applied AMPH together with the DAT inhibitor. In the presence of GBR 12935 (5 μ M), application of AMPH induced a significantly smaller increase in the frequency of sIPSCs ($108 \pm 5\%$ of control, $n = 8$), compared with the effect of the application of AMPH alone ($P = 0.007$, Fig. 3C and F). We further validated the involvement of $\alpha 1$ receptors. Application of AMPH for 8 min in the presence of doxazosin (25 μ M) failed to increase sIPSC frequency significantly ($108 \pm 8\%$ of control, $n = 6$, $P = 0.35$, Fig. 3D). Because AMPH has been reported to increase the releases of both DA and norepinephrine (Rothman et al., 2001; Smith and Greene, 2012), we tested whether norepinephrine transporter was involved in AMPH-induced increases in sIPSC frequency. Application of talopram (1 μ M), a selective blocker for the norepinephrine transporter (McConathy et al., 2004), failed to alter AMPH-induced increases in sIPSC frequency ($175 \pm 22.3\%$ of control, $n = 10$, $P = 0.7$ vs. AMPH alone, Fig. 3E and F). These data together demonstrate that endogenously released DA also facilitates sIPSC frequency via the activation of $\alpha 1$ receptors in the EC.

*DA Enhances the Frequency of mIPSCs,
But Slightly Reduces the Amplitude of eIPSCs*

sIPSCs represent events caused by both AP-dependent and -independent release of GABA. In contrast, mIPSCs recorded in the presence of TTX, a voltage-gated Na^+ blocker, should be independent of APs. We therefore recorded mIPSCs in the presence of TTX (0.5 μ M). Application of DA significantly increased the frequency ($135 \pm 6\%$ of control, $n = 6$, $P = 0.003$, Fig. 4A, B, and C) without affecting the amplitude ($99 \pm 4\%$ of

control, $n = 6$, $P = 0.89$, Fig. 4A, B, and D) of mIPSCs. These results suggest that DA augments presynaptic GABA release without modulating postsynaptic GABA_A receptors. We also examined the effects of DA on the GABA_A receptor-mediated inhibitory postsynaptic current (IPSC) recorded from stellate neurons evoked by placing a stimulation electrode in a location of approximately 200 μm from the recorded neurons. We used a protocol of paired stimulation (interval: 50 ms and frequency: 0.1 Hz) to measure the paired-pulse ratio (PPR) simultaneously. Bath application of DA slightly but significantly reduced the amplitude of eIPSCs evoked by the first stimulation ($87 \pm 4\%$ of control, $n = 6$, $P = 0.023$, Fig. 4E). DA-induced depression of eIPSC amplitude was presynaptic in origin, because DA significantly increased the PPR ($n = 6$, $P = 0.002$, Fig. 4F). Two potential mechanisms could be proposed to explain the discrepancy of the results regarding sIPSCs and eIPSCs. The first explanation for DA-induced depression of eIPSCs is that DA-induced enhancement of spontaneous GABA release depletes the readily releasable vesicle pool that is subsequently available for eIPSCs as suggested for 5-HT₃ (Cui et al., 2012) and muscarinic (Xiao et al., 2009b) receptors. Alternatively, DA-mediated depression of eIPSCs could be due to its inhibitory effect on the AP amplitude of GABAergic interneurons, because DA-induced membrane depolarization could inactivate Na⁺ channels resulting in APs of lower amplitude (see below). Because sIPSCs, mIPSCs, and eIPSCs represent distinct modes of GABAergic transmission, the diverse effects of DA on these IPSCs suggest that DA exerts different actions depending on the status of the neural circuitry. The results that DA increased the frequency of sIPSCs and mIPSCs suggest that DA facilitates GABA release. We therefore further determined the mechanisms underlying DA-induced GABA release.

Figure 4. DA augments the frequency with no effects on the amplitude of mIPSCs recorded in the presence of TTX, but attenuates the amplitude of eIPSC. (A) mIPSC current traces recorded from a stellate neuron before, during, and after the application of DA. (B) Time course of mIPSC frequency summarized from 6 stellate neurons. (C) Cumulative frequency distribution of mIPSCs before, during, and after the application of DA. Note that DA reduced the interval of mIPSCs suggesting an increase in mIPSC frequency. (D) Cumulative amplitude distribution of mIPSCs before, during, and after the application of DA. Note that DA did not change the amplitude of mIPSCs. The flat line part of the curves was generated because zero events were detected at the amplitudes below threshold. (E) DA depressed the amplitude of eIPSCs recorded from layer II stellate neurons by application of a protocol comprising paired stimulation (50 ms interval at 0.1 Hz). The amplitudes of the eIPSCs evoked by the first stimulation were normalized to the average of the 5 min before application of DA. Upper panel shows the average of 6 eIPSCs before and during the application of DA. (F) DA increased the PPR. Upper panel shows the eIPSCs before and during the application of DA scaled to the amplitude evoked by the first stimulation. Note that the amplitude of the second eIPSC in the presence of DA is larger than control.



Because mIPSCs recorded in the presence of TTX are AP-independent, our results that DA facilitated the frequency of mIPSCs recorded in the presence of TTX suggest that there should be at least an AP-independent mechanism involved. We therefore tested whether extracellular Ca^{2+} was required for the effects of DA on GABAergic transmission by recording sIPSCs and mIPSCs from layer II stellate neurons in a Ca^{2+} -free extracellular solution. The extracellular Ca^{2+} was replaced by the same concentration of Mg^{2+} , and 1 mM of EGTA was included in the extracellular solution to chelate the ambient residual Ca^{2+} . Under these circumstances, bath application of DA failed to increase the frequencies of sIPSCs ($n = 11$, $P = 0.42$, Fig. 5A) and mIPSCs ($n = 6$, $P = 0.94$, Fig. 5B). These data together suggest that extracellular Ca^{2+} is required for the effects of DA on GABAergic transmission. Since extracellular Ca^{2+} is required for DA's presynaptic actions, we also tested whether Ca^{2+} influx via voltage-gated Ca^{2+} channels is necessary for DA-mediated increases in the frequencies of sIPSCs and mIPSCs. Inclusion of CdCl_2 (100 μM), a blocker for high-threshold voltage-dependent Ca^{2+} channels, in the extracellular solution, failed to block DA-induced increases in the frequency of sIPSCs ($n = 5$, $P = 0.67$ vs. control, Fig. 5C) and mIPSCs ($n = 5$, $P = 0.004$, Fig. 5D). However, addition of NiCl_2 (200 μM), a blocker for the low-threshold T-type Ca^{2+} channels, significantly reduced DA-induced increases in the frequency of sIPSCs ($n = 14$, $P = 0.033$ vs. control, Fig. 5E). DA-mediated augmentation of mIPSC frequency was blocked in the extracellular solution containing Ni^{2+} ($n = 5$, $P = 0.96$, Fig. 5F). We further examined the involvement of T-type Ca^{2+} channels with mibefradil, another T-type Ca^{2+} channels blocker. Bath application of mibefradil (15 μM) significantly reduced DA-induced increases in sIPSC frequency ($113 \pm 5\%$ of control, $n = 8$, $P = 0.04$ vs. DA

alone, Fig. 5G) but blocked completely DA-mediated facilitation of mIPSC frequency ($106 \pm 11\%$ of control, $n = 5$, $P = 0.64$ vs. baseline, Fig. 5H). These data together indicate that T-type Ca^{2+} channels are required for DA-induced facilitation of GABAergic transmission.

DA Depolarizes GABAergic Interneurons in the EC

Because our results point to a presynaptic mechanism underlying DA-induced facilitation of GABA release, we also examined the effects of DA on GABAergic interneurons by recording from the interneurons in layer III of the EC. As demonstrated previously (Deng and Lei, 2008), interneurons in the EC can be divided into 2 types according to their electrophysiological properties. Type I interneurons showed little voltage sag in response to hyperpolarizing current injection and no rebound burst firing (Fig. 6A₁), whereas Type II interneurons displayed prominent voltage sag in response to hyperpolarizing current injection and rebound burst firing (Fig. 6B₁). After having electrophysiologically identified the interneurons, we recorded the RMPs by washing with TTX ($0.5 \mu\text{M}$) in the extracellular solution. Because application of DA-induced depolarization in both types of interneurons (Fig. 6A₂ and B₂), the data recorded from Type I and Type II interneurons were pooled. Application of DA depolarized the interneurons recorded at the RMPs (Control: $-66.2 \pm 0.8 \text{ mV}$; DA: $-62.0 \pm 1.0 \text{ mV}$, $n = 9$, $P < 0.001$; Fig. 6C, *left*) and slightly but significantly increased the input resistance of the interneurons (Control: $304 \pm 54 \text{ M}\Omega$; DA: $330 \pm 55 \text{ M}\Omega$, $n = 9$, $P = 0.047$; Fig. 6C, *right*). Furthermore, application of DA induced a small inward HC recorded at -60 mV from interneurons ($-7.5 \pm 1.9 \text{ pA}$, $n = 5$, $P = 0.018$, Fig. 6D). We also probed the roles of DA in AP firing by including in the extracellular solution containing (in μM) 10 DNQX,

Figure 5. Ca^{2+} influx via T-type Ca^{2+} channels is required for DA-induced facilitation of GABAergic transmission. (A and B) Depletion of extracellular Ca^{2+} by replacing extracellular Ca^{2+} with Mg^{2+} and inclusion of 1 mM EGTA in the extracellular solution prevented DA-induced enhancement of sIPSC (A) and mIPSC (B) frequency. (C and D) Bath application of the high-threshold voltage-gated Ca^{2+} channel blocker, Cd^{2+} (100 μM), failed to block DA-induced enhancement of sIPSC (C) and mIPSC (D) frequency. (E and F) Bath application of the low-threshold T-type Ca^{2+} channel blocker, Ni^{2+} (200 μM), significantly reduced DA-induced augmentation of sIPSC frequency (E) and blocked DA-mediated increment of mIPSC frequency (F). (G and H) Bath application of the T-type Ca^{2+} channel blocker, mibefradil (15 μM), significantly reduced DA-induced increase of sIPSC frequency (G) and blocked DA-mediated enhancement of mIPSC frequency (H).

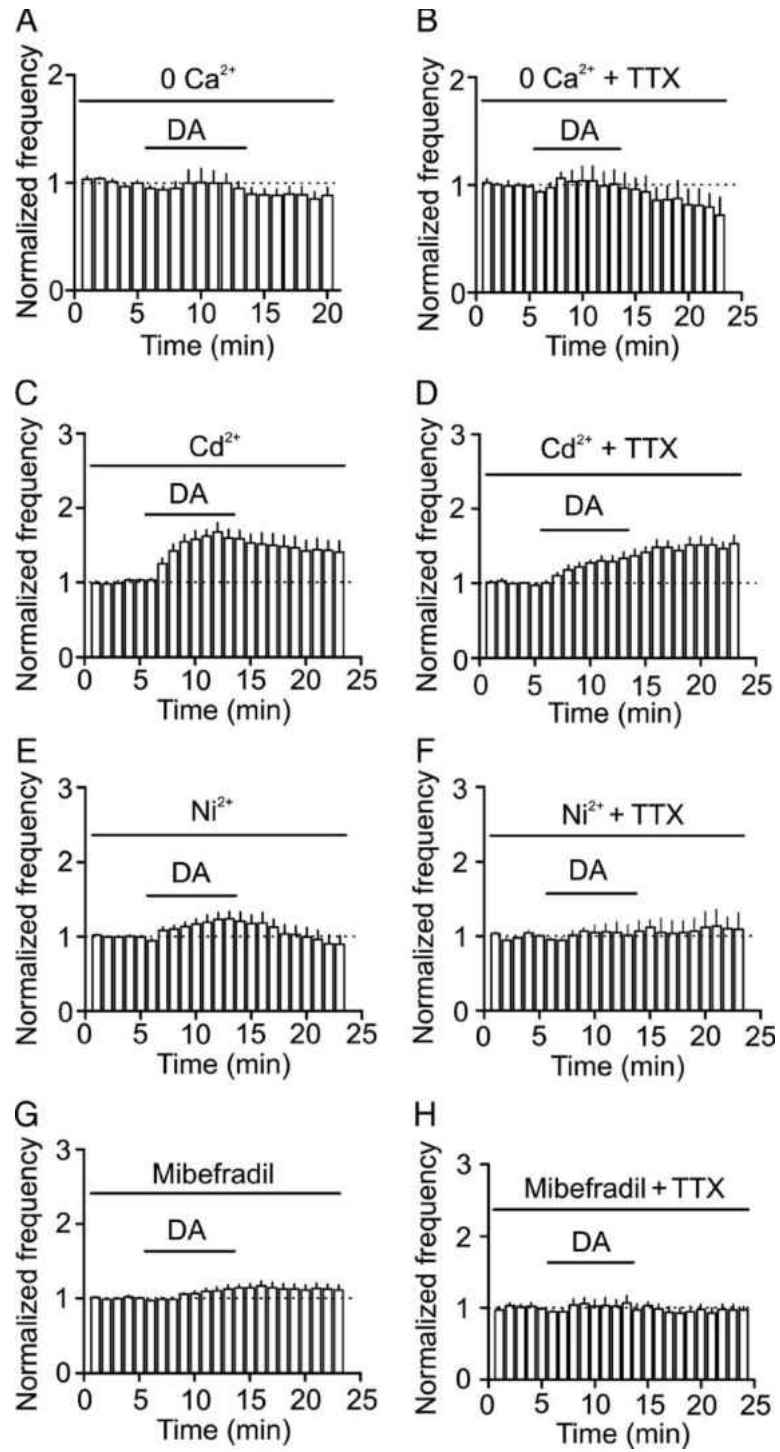
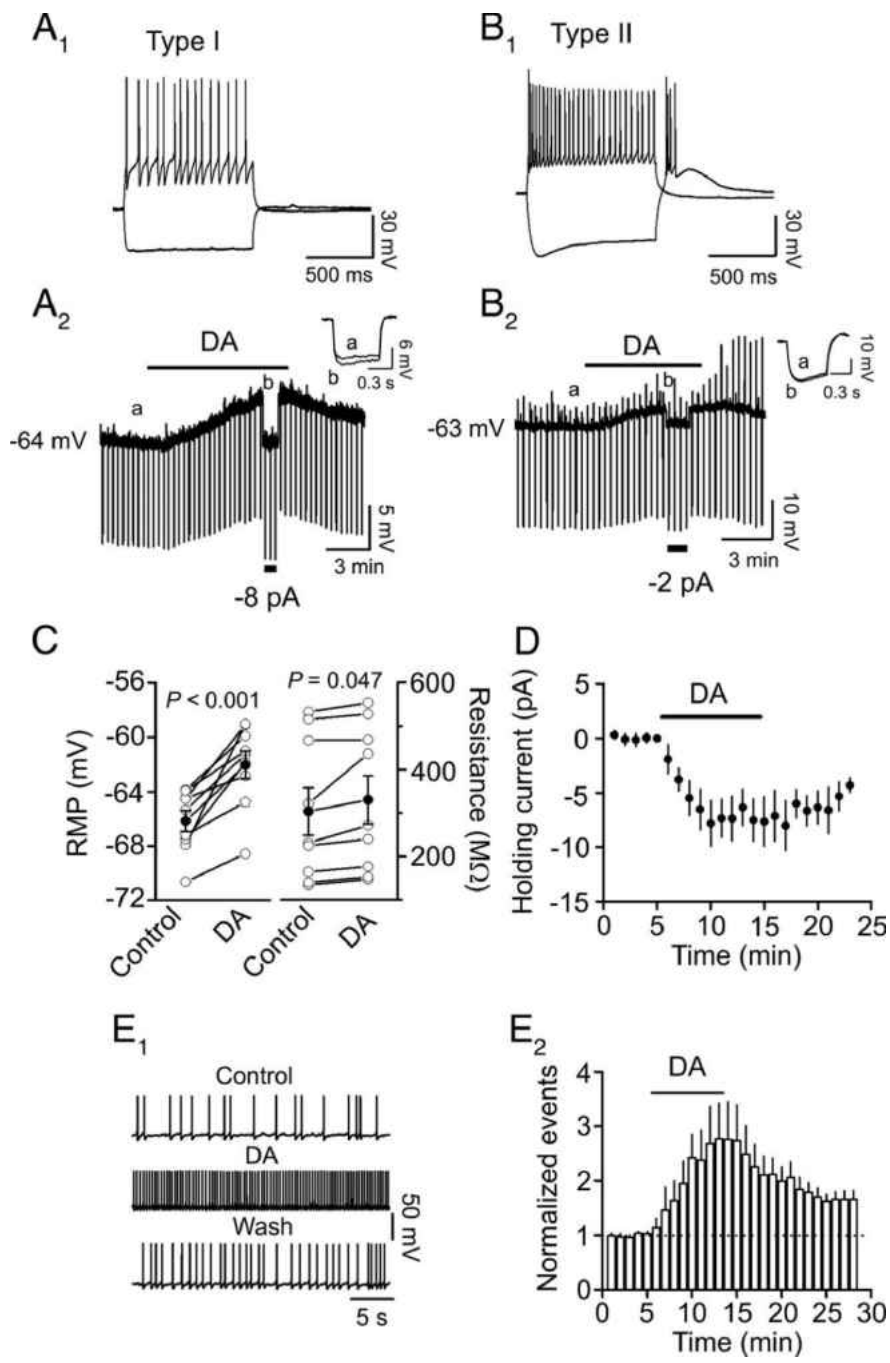


Figure 6. DA depolarizes GABAergic interneurons in the EC. (A₁ and A₂) Bath application of DA generated membrane depolarization and increased the input resistance of Type I interneurons in the EC. (A₁) Voltage changes in response to current injection (± 150 pA) in a Type I interneuron. (A₂) Application of DA (100 μ M) generated membrane depolarization and increased input resistance in the same interneuron. RMP was recorded in the current-clamp mode and a hyperpolarizing current (-50 pA, 500 ms) was injected every 20 s to measure the input resistance. Note that DA generated depolarization and increased the input resistance. To exclude the influence of DA-induced membrane depolarization on the input resistance, a negative current (-8 pA indicated by the horizontal bar) was injected briefly to bring the membrane potential back to the initial level. Under these conditions, the voltage responses induced by the injection of hyperpolarizing currents (-50 pA, 500 ms) were still larger compared with control, suggesting that DA-induced increases in input resistance are not secondary to its effect on membrane depolarization. Inset is the voltage traces taken before (a) and during (b) the application of DA when the negative current was injected. (B₁ and B₂) Bath application of DA generated membrane depolarization and increased the input resistance of Type II interneurons in the EC. The experiment was performed in the same fashion as Type I interneurons. (C) Pooled data for DA induced depolarization (left) and increase in input resistance (right). Empty circles represent values from individual cells and solid symbols denote the average values. (D) Application of DA induced an inward HC in interneurons ($n = 5$). (E₁ and E₂) Bath application of DA increased AP firing frequency in interneurons. APs were evoked by injecting a positive current to elevate the membrane potential just above the threshold for firing. (E₁) APs recorded from an interneuron before, during, and after the application of DA. (E₂) Pooled time course of AP firing ($n = 7$).



50 APV, 10 bicuculline, and 2 CGP55845 to block glutamatergic and GABAergic transmission. Because the RMPs of the interneurons were usually negative to -60 mV, interneurons did not show spontaneous firing at their RMPs. The depolarization generated by DA was not large enough to raise the RMPs to the threshold for AP firing. We therefore injected positive currents to elevate the membrane potential to just above the threshold to induce AP firing. Under these circumstances, application of DA significantly increased the firing frequency of APs ($n = 7$, $P = 0.036$, Fig. 6E1, E2), but slightly decreased the AP amplitude ($89 \pm 1\%$ of control, $n = 7$, $P < 0.001$, Fig. 6E1). DA-induced depression of AP amplitude might be due to its depolarizing effect resulting in inactivation of Na^+ channels.

*Ionic Mechanisms Underlying DA-Induced
Depolarization of Interneurons*

We recorded the RMPs of the interneurons to further determine the underlying ionic mechanisms. DA facilitates the hyperpolarization-activated channels (Ih channels) in layer V pyramidal neurons (Rosenkranz and Johnston, 2006). We therefore examined whether Ih channels are involved in DA-induced depolarization. Extracellular application of the selective Ih channel blocker, ZD7288 ($20 \mu\text{M}$), failed to block DA-induced depolarization ($n = 5$, $P = 0.7$ vs. DA alone, Fig. 7A and G), suggesting that DA-mediated membrane depolarization of interneurons is not dependent on Ih channels. If DA-induced membrane depolarization of interneurons is due to the opening of cation channels, the influx of extracellular Na^+ should be the major ions to mediate membrane depolarization. However, replacement of extracellular NaCl with the same concentration of NMDG-Cl failed to alter DA-induced depolarization ($n = 5$, $P = 0.47$ vs. DA alone, Fig. 7B and G). Because extracellular Ca^{2+} is required for

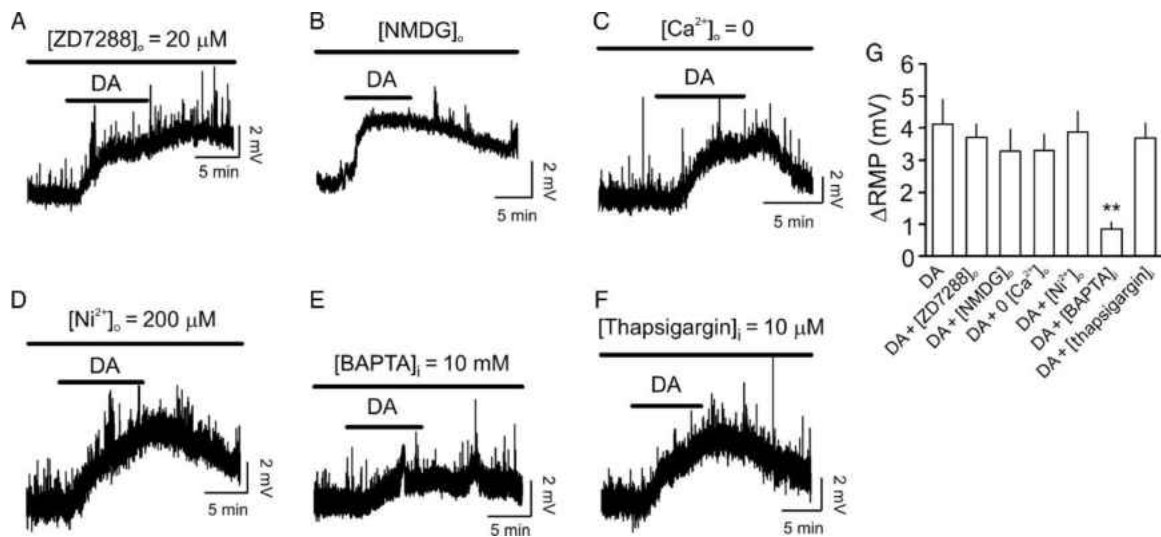


Figure 7. DA-induced depolarization of interneurons does not require the function of I_h channels and is independent of extracellular Na^+ and Ca^{2+} , but is affected by intracellular Ca^{2+} concentration. (A) Bath application of the I_h channel blocker, ZD7288 (20 μM), did not block DA-induced depolarization. (B) Replacement of extracellular NaCl with NMDG-Cl did not alter DA-induced depolarization. (C) Substitution of extracellular Ca^{2+} with Mg^{2+} and inclusion of EGTA (1 mM) in the extracellular solution failed to change DA-induced depolarization. (D) Inclusion of Ni^{2+} (200 μM) in the extracellular solution did not block DA-induced depolarization. (E) Inclusion of BAPTA (10 mM) in the recording pipettes reduced DA-induced depolarization, suggesting that intracellular Ca^{2+} concentration is related to DA-induced depolarization possibly by affecting Ca^{2+} -dependent intracellular signals. (F) Intracellular application of thapsigargin (10 μM) via the recording pipettes failed to modify DA-mediated depolarization, suggesting that intracellular Ca^{2+} release is not required for DA-mediated depolarization. (G) Pooled data. $**P < 0.01$

DA-induced increases in the frequencies of sIPSCs and mIPSCs, we also tested whether extracellular Ca^{2+} is required for DA-induced depolarization of interneurons.

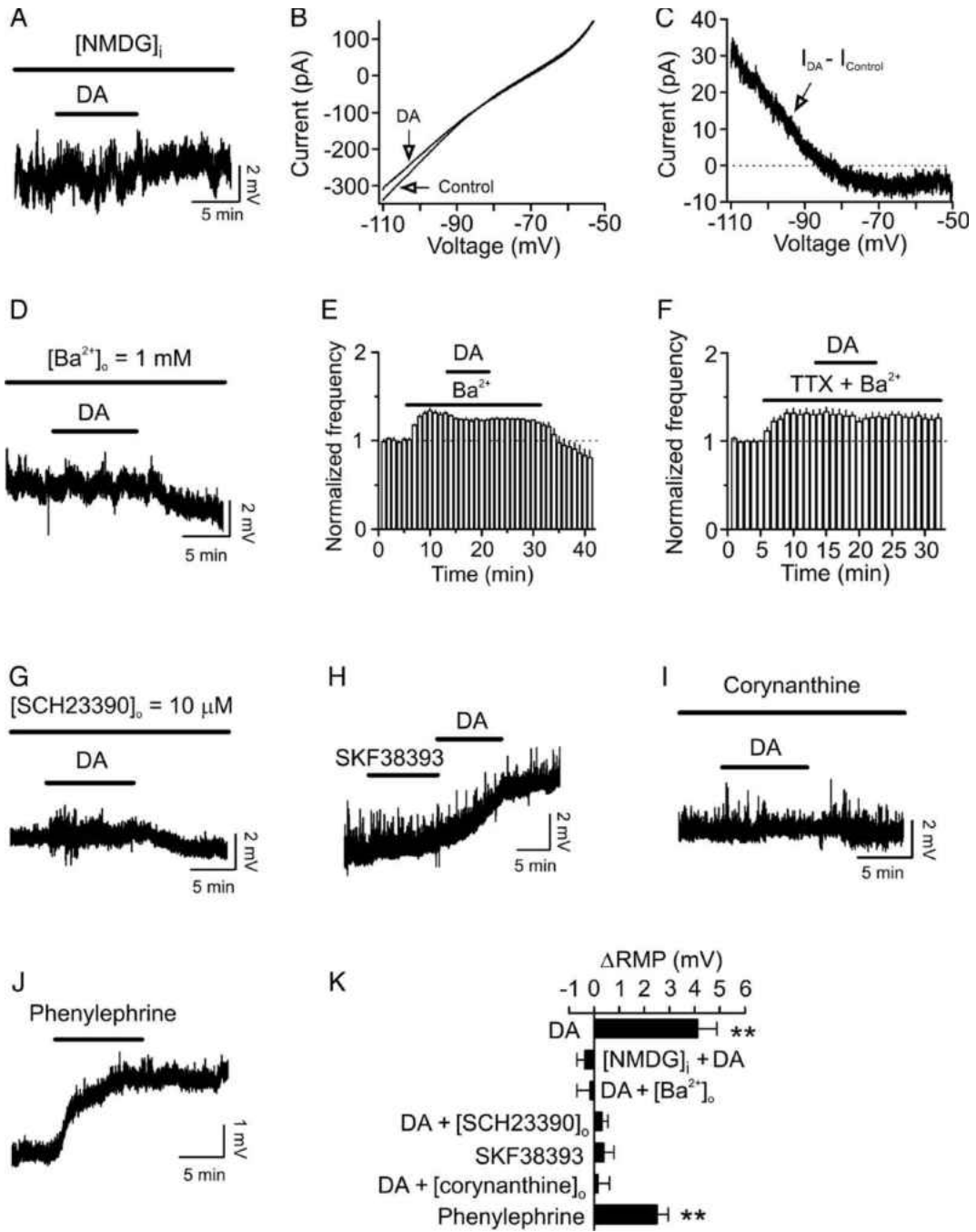
Replacement of extracellular Ca^{2+} with the same concentration of Mg^{2+} and simultaneous inclusion of 1 mM EGTA in the extracellular solution did not significantly change DA-induced depolarization ($n = 7$, $P = 0.41$ vs. DA alone, Fig. 7C and G). These data together suggest that DA does not depolarize interneurons by opening a cation channel. Furthermore, bath application of NiCl_2 (200 μM) failed to significantly change DA-

induced depolarization ($n = 6$, $P = 0.82$ vs. DA alone, Fig. 7D and G), suggesting that T-type Ca^{2+} channels are not involved in DA-mediated depolarization of the interneurons. Finally, we determined the requirement for intracellular Ca^{2+} in mediating the postsynaptic DA response. DA induced a smaller level of depolarization ($n = 6$, $P = 0.005$ vs. DA alone, Fig. 7E and G) when BAPTA (10 mM) was included in the recording pipettes. However, inclusion of thapsigargin (10 μM) in the pipettes failed to alter DA-induced depolarization significantly ($n = 5$, $P = 0.69$ vs. DA alone, Fig. 7F and G), suggesting that intracellular Ca^{2+} release is not required for DA-induced depolarization. One explanation for the result that intracellular application of BAPTA significantly reduced DA-induced depolarization is that the effects of DA may require the functions of some Ca^{2+} -dependent signals.

DA can inhibit background K^+ channels to generate membrane depolarization. Our result that DA increased the input resistance also supports the involvement of K^+ channels. To test the roles of K^+ channels, we first replaced the intracellular K^+ -gluconate with NMDG-gluconate and recorded the changes of membrane potentials in response to DA. Under these circumstances, bath application of DA failed to induce membrane depolarization ($n = 5$, $P = 0.31$, Fig. 8A and K). Secondly, we used a ramp protocol to measure the reversal potential of the current induced by DA. The DA-induced current had a reversal potential of -85.6 ± 6.5 mV ($n = 5$, Fig. 8B and C), which was close to the calculated K^+ reversal potential (-85.4 mV). These data indicate the involvement of K^+ channels. We also noticed that the current generated by DA showed an inward rectification (Fig. 8C), suggesting that DA inhibits K^+ channels. Consistent with this, inclusion of Ba^{2+} (1 mM) in the extracellular solution blocked DA-induced depolarization ($n = 6$, $P =$

0.78 vs. baseline, Fig. 8D and K), further supporting the involvement of Kirs. Moreover, bath application of Ba^{2+} alone significantly increased the frequency of sIPSCs ($n = 3$, $P = 0.004$, Fig. 8E). In the presence of Ba^{2+} , application of DA did not increase but slightly reduced the frequency of ($n = 3$, $P = 0.015$, Fig. 8E) sIPSC. Similarly, Ba^{2+} application blocked DA-induced increases in mIPSC frequency ($n = 6$, $P = 0.72$, Fig. 8F). We also tested the effects of SCH23390 on DA-induced depolarization. Slices were pretreated with SCH23390 (10 μ M) and the extracellular solution was continuously perfused with the same concentration of SCH23390. Application of SCH23390 prevented DA-induced depolarization ($n = 6$, $P = 0.97$, Fig. 8G and K). However, application of the selective D1-like agonist, SKF38393 (40 μ M), failed to depolarize interneurons ($n = 6$, $P = 0.27$ vs. baseline, Fig. 8H and K), but subsequent application of DA still induced depolarization in the same neurons (Fig. 8H). These results suggest that the blocking effect of SCH23390 was not mediated by antagonizing D1-like receptors, but by blockade of Kirs. We further tested the roles of $\alpha 1$ receptors in DA-induced depolarization of interneurons. Application of the $\alpha 1$ receptor antagonist, corynanthine (100 μ M), blocked DA-induced depolarization ($n = 5$, $P = 0.41$ vs. baseline, Fig. 8I and K) and application of the selective $\alpha 1$ receptor agonist, phenylephrine (100 μ M), induced depolarization of interneurons ($n = 6$, $P = 0.002$, Fig. 8J and K) demonstrating the involvement of $\alpha 1$ receptors.

Figure 8. DA-induced depolarization of interneurons is mediated by inhibition of Kirs. (A) DA did not induce conspicuous depolarization when the intracellular K^+ was replaced with NMDG. (B) Current–voltage relationship recorded by a ramp protocol (from -110 to -50 mV) in the extracellular solution containing 3.5 mM K^+ before and during the application of DA. Traces in the figure were averaged traces from 5 cells. (C) The DA-generated net current obtained by subtraction of the control from that in the presence of DA has a reversal potential at approximately -85.6 mV close to the calculated K^+ reversal potential (~ -85.4 mV). Note that the DA-sensitive current showed an inward rectification. (D) Bath application of Ba^{2+} blocked DA-induced depolarization. (E) Bath application of Ba^{2+} increased sIPSC frequency and subsequent application of DA slightly reduced sIPSC frequency. (F) Bath application of Ba^{2+} increased mIPSC frequency and blocked DA-induced increases in mIPSC frequency. (G) Pretreatment of slices with and continuous bath application of SCH23390 blocked DA-induced depolarization. (H) Bath application of SKF38393 (40 μ M) did not induce depolarization, but subsequent application of DA still induced depolarization in the same cell. (I) Pretreatment of slices with and continuous bath application of corynanthine (100 μ M) blocked DA-induced depolarization. (J) Bath application of the selective $\alpha 1$ receptor agonist, phenylephrine (100 μ M), induced depolarization of an interneuron. (K) Pooled data. $**P < 0.01$ versus baseline.



CHAPTER IV

RESULTS

Study 2 - Histaminergic Modulation of MEC GABAergic Transmission

Introduction

The tuberomammillary nucleus (TMN) of the hypothalamus produces several neurotransmitters, yet is unique in being the sole neuronal source of histamine (HA). The TMN projects extensively throughout the brain and HA signaling is important for wakefulness, thermoregulation, energy homeostasis, nociception and learning and memory (Haas and Panula, 2003; Haas et al., 2008a). Aberrant HA signaling is implicated in a variety of neurological disorders including narcolepsy, schizophrenia, Alzheimer's Disease (AD), Parkinson's Disease, epilepsy, and depression (Haas et al., 2008a). Understanding the neuromodulatory actions of HA in the brain is critical toward comprehending its intrinsic functions and informing potential therapeutic strategies involving the histaminergic system.

Receptors known to mediate HA signaling are G-protein-coupled and include H₁, H₂, H₃, and H₄. H₁, H₂, and H₃ are widely expressed throughout the brain, whereas H₄ is less abundant (Hill et al., 1997; Haas et al., 2008a). The H₁ is coupled to G α_q and its activation increases phosphatidylinositol turnover (Claro et al., 1986) and elevates intracellular Ca²⁺ (Leurs et al., 1994). H₂ activation increases cAMP production (Traiffort et al., 1992), consistent with G α_s -coupling. The H₃ is coupled to G α_i and regulates HA synthesis (Arrang et al., 1987; Moreno-Delgado et al., 2006), voltage-activated Ca²⁺

channels (Takeshita et al., 1998) and release of HA and several other neurotransmitters (Haas et al., 2008a). Atypical signaling has also been described for both H₁ and H₂ and colocalization of both receptors is consistent with functional overlap and synergism between H₁ and H₂ (Garbarg and Schwartz, 1988; Leopoldt et al., 1997; Maruko et al., 2005; Alonso et al., 2013). Neuromodulatory actions of HA typically involve enhancement of neuronal excitability via H₁ and/or H₂ and both receptors influence a variety of different ionic conductances. The H₁ is implicated in the inhibition of background K⁺ channels (McCormick and Williamson, 1991; Reiner and Kamondi, 1994; Whyment et al., 2006) and inward rectifier K⁺ channels (Kirs) (Gorelova and Reiner, 1996; He et al., 2016), activation of a TTX-insensitive Na⁺ channels (Gorelova and Reiner, 1996; Bell et al., 2000), nonselective cation channels (Hardwick et al., 2005) and Na⁺-Ca²⁺ exchanger (Zhang et al., 2013b). Activation of H₂ results in inhibition of K⁺ conductances (Munakata and Akaike, 1994; Starodub and Wood, 2000) including the voltage-gated (Atzori et al., 2000) and Ca²⁺-activated (Haas, 1984) K⁺ channels, and activation of hyperpolarization-activated cation channels (I_h) (McCormick and Williamson, 1991; Zhang et al., 2013b).

The medial entorhinal cortex (MEC) is positioned such that it gates the majority of cortical information into and out of the hippocampus (Steward and Scoville, 1976; Witter et al., 2006). The MEC is an important structure for spatial memory (Steffenach et al., 2005; Hales et al., 2014) and implicated in neurological disorders including AD (Hyman et al., 1984; Gómez-Isla et al., 1996), schizophrenia (Joyal et al., 2002; Baiano et al., 2008), and temporal lobe epilepsy (Du et al., 1993; Avoli et al., 2002). The MEC exhibits a moderate intensity of HA-immunoreactive fibers (Panula et al., 1989) and

receives projections from the TMN (Köhler et al., 1985; Staines et al., 1987). Consistent with the distribution of histaminergic fibers, the MEC also expresses HA receptors including the H₁, H₂, and H₃ as demonstrated by autoradiography studies (Bouthenet et al., 1988; Vizuite et al., 1997; Pillot et al., 2002). Collectively, these observations suggest the existence of a functional neuromodulatory action for HA on MEC circuitry and MEC-related behaviors and disorders, yet there are few studies examining the actions of HA in the MEC.

GABAergic transmission is critical for maintenance of network activity and its dysfunction is implicated in MEC-related disorders. Although HA has been reported to reduce the frequency of miniature inhibitory postsynaptic currents (mIPSCs) recorded in the presence of TTX via an H₃-dependent manner (He et al., 2016), it remains unknown whether HA modulates other forms of GABAergic transmission. We tested this possibility and observed that HA increased the frequency of spontaneous inhibitory postsynaptic currents (sIPSCs) via activation of H₁ or H₂ receptors. We also made direct recordings from MEC interneurons and found that both H₁ and H₂ are involved in HA-induced subthreshold membrane depolarization. Using immunohistochemical staining, we further showed that both H₁ and H₂ are expressed on GABAergic interneurons in the MEC. We propose that HA increases the excitability of GABAergic interneurons via a mixed ionic mechanism comprised of inhibition of the cesium(Cs⁺)-sensitive Kirs and activation of a TTX-insensitive, Na⁺-permeable cation channel. Some of these results were previously published in abstract form (Cilz and Lei, 2014).

HA Increases the Frequency without Significant Effects on the Amplitude of sIPSCs Recorded from Principal Neurons in the MEC

We examined the effects of HA on GABA_A receptor-mediated sIPSCs recorded from principal neurons in each layer of the MEC. Stellate and pyramidal neurons are the principal cells in layer II whereas pyramidal neurons are the predominant type in layer III and layer V. In layer II principal neurons, application of HA (30 μM) significantly increased the frequency (Control: 9.6 ± 1.2 Hz, HA: 15.1 ± 1.1 Hz, 196 ± 29% of control, n = 16, *P* < 0.001, Fig. 9A, B, C, and E) but not the amplitude (Control: 34.0 ± 2.8 pA, HA: 36.5 ± 4.1 pA, 107 ± 12% of control, n = 16, *P* = 0.33, Fig. 9D and F) of sIPSCs. Application of bicuculline (10 μM) completely blocked sIPSCs recorded in the presence of HA (data not shown), confirming that the recorded events were mediated by GABA_A receptors. The EC₅₀ value of HA was determined to be 1.3 μM (Fig. 9G). Similar to layer II principal neurons, application of HA (30 μM) significantly increased the frequency of sIPSCs recorded from layer III (Control: 6.7 ± 1.1 Hz, HA: 11.8 ± 1.3 Hz, 207 ± 36% of control, n = 7, *P* = 0.002, Fig. 9H) and layer V (Control: 1.2 ± 0.2 Hz, HA: 2.6 ± 0.6 Hz, 230 ± 57% of control, n = 10, *P* = 0.03, Fig. 9H) pyramidal neurons, but did not affect the amplitude of layer III (Control: 26.9 ± 2.3 pA, HA: 30.1 ± 4.8 pA, 114 ± 18% of control, n = 7, *P* = 0.52, Fig. 9H) or layer V (Control: 22.4 ± 1.5 pA, HA: 21.9 ± 1.3 pA, 100 ± 7% of control, n = 10, *P* = 0.72, Fig. 9H) pyramidal neurons. These results indicate that HA augments the frequency of sIPSCs in all layers of the MEC. Application of HA to slices prepared from weaned animals (ages p23-p26) increased the frequency of sIPSCs to 159 ± 22% of control (Control: 7.8 ± 6.6 Hz, HA: 12.3 ± 1.5 Hz, n = 5, *P* = 0.04 vs. baseline, Fig. 9I), which was not significantly different than slices prepared from pups (p14-p17, n = 16, *P* = 0.54). These results demonstrate that HA augments GABAergic

transmission in both younger and older animals used in this study. We used layer II principal neurons as an example to determine the underlying cellular and molecular mechanisms and applied HA at the concentration of 30 μM for the rest of the experiments.

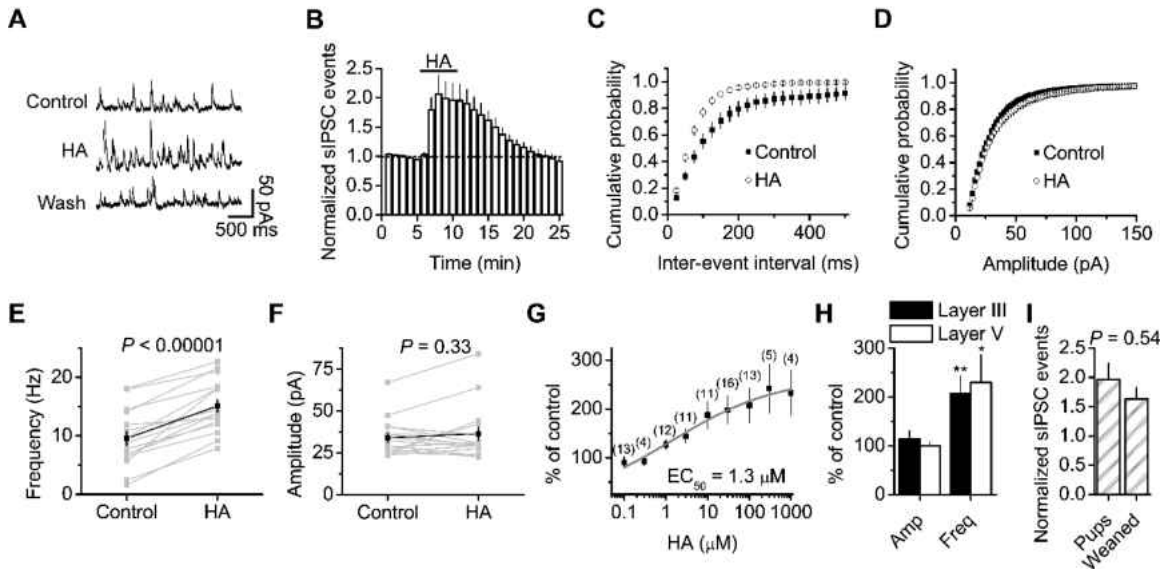
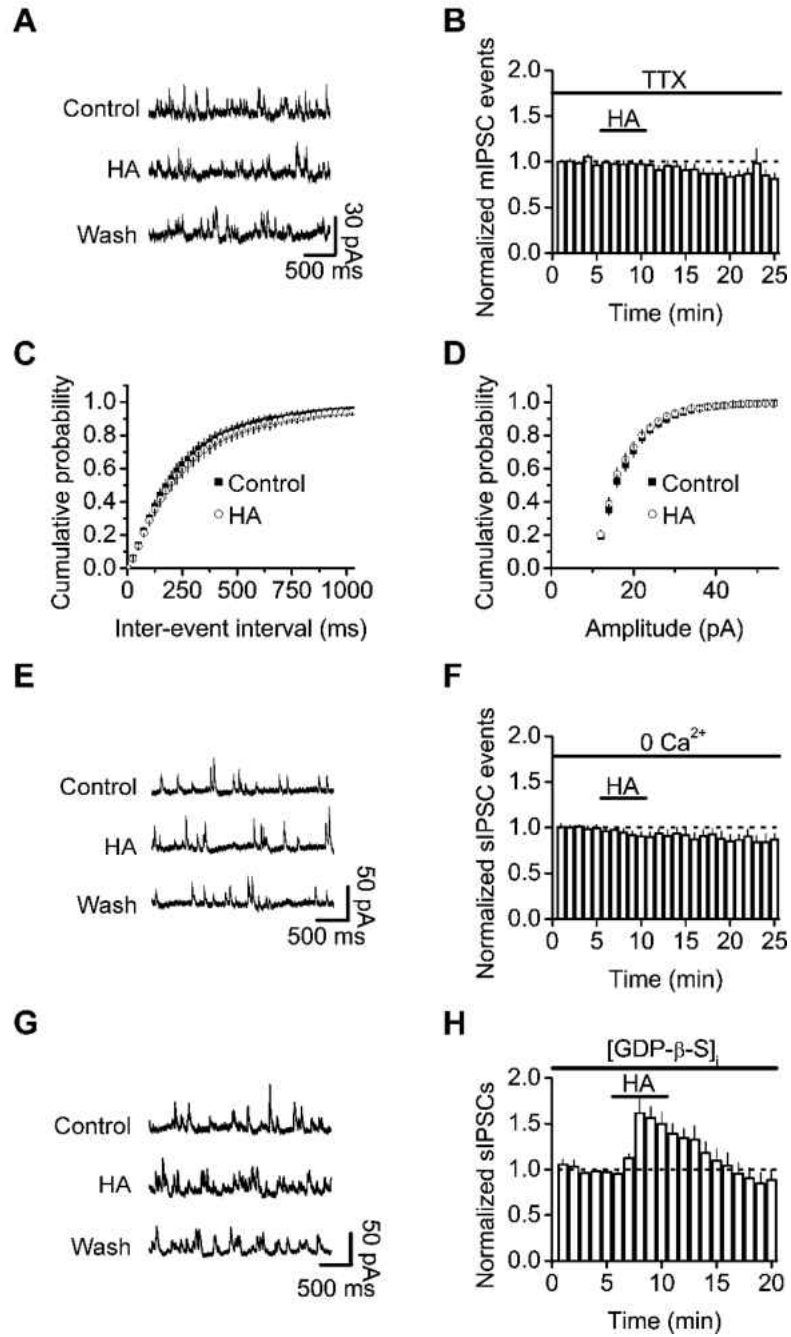


Figure 9. HA increases the frequency but not the amplitude of sIPSCs recorded from the principal neurons in the MEC. (A) Spontaneous IPSCs recorded from a layer II principal neuron before, during and after the application of HA (30 μM). (B) Time course of the sIPSC frequency averaged from 16 principal neurons. (C) Cumulative frequency distribution averaged from 16 layer II principal neurons before and during the application of HA. (D) Cumulative amplitude distribution averaged from 16 cells before and during the application of HA. (E) Frequency of sIPSCs pooled from 16 cells before and during the application of HA. Gray symbols are values from individual cells and black symbols are their averages. (F) Amplitude of sIPSCs pooled from 16 cells before and during the application of HA. (G) Concentration-response curve of HA. Numbers in the parenthesis are numbers of cells recorded. (H) Bath application of HA (30 μM) significantly enhanced the frequency with no effects on the amplitude of sIPSCs recorded from the pyramidal neurons in layer III and layer V. * $P < 0.05$, ** $P < 0.01$ vs baseline. (I) HA increased sIPSC frequency recorded from layer II principal neurons of both younger (p14-p17, $n = 16$ slices) and older (p23-p26, $n = 5$ slices) animals. HA increases spontaneous GABAergic transmission by facilitating presynaptic GABA release.

*HA Increases Spontaneous GABAergic Transmission
by Facilitating Presynaptic GABA Release*

Spontaneous IPSCs are the product of both AP-dependent and AP-independent release of GABA, whereas mIPSCs recorded in the presence of TTX should be independent of APs. We therefore recorded mIPSCs in the presence of TTX (0.5 μ M) to test whether the effects of HA on spontaneous GABAergic transmission are AP-dependent. Application of HA failed to alter either mIPSC frequency (Control: 4.3 ± 0.5 Hz, HA: 4.2 ± 0.6 Hz, $98 \pm 5\%$ of control, $n = 14$, $P = 0.64$, Fig. 10A, B and C) or amplitude (Control: 18.1 ± 0.8 pA, HA: 17.5 ± 0.7 pA, $97 \pm 2\%$ of control, $n = 14$, $P = 0.08$, Fig. 10D), indicating that generation of APs was necessary to augment spontaneous GABAergic transmission in the MEC. We further examined whether Ca^{2+} influx was required for HA-mediated increases in sIPSCs. Exclusion of extracellular Ca^{2+} blocked HA-induced increases in sIPSCs ($90 \pm 5\%$ of control, $n = 7$, $P = 0.12$, Fig. 10E and F). The requirement of both AP generation and Ca^{2+} influx supports a presynaptic mechanism for HA-induced increases in sIPSCs. To exclude a postsynaptic mechanism of action, sIPSCs were recorded with GDP- β -S (2 mM) in the pipette to block any direct receptor-mediated effects of HA on the recorded neurons. After waiting ~20 minutes for GDP- β -S to diffuse into the cells, application of HA continued to elicit a significant increase in the frequency of sIPSCs ($151 \pm 13\%$ of control, $n = 7$, $P = 0.007$, Fig. 10G and H). Collectively, these results suggest that HA acts presynaptically at a step upstream of action potential generation to increase GABAergic transmission in the MEC.

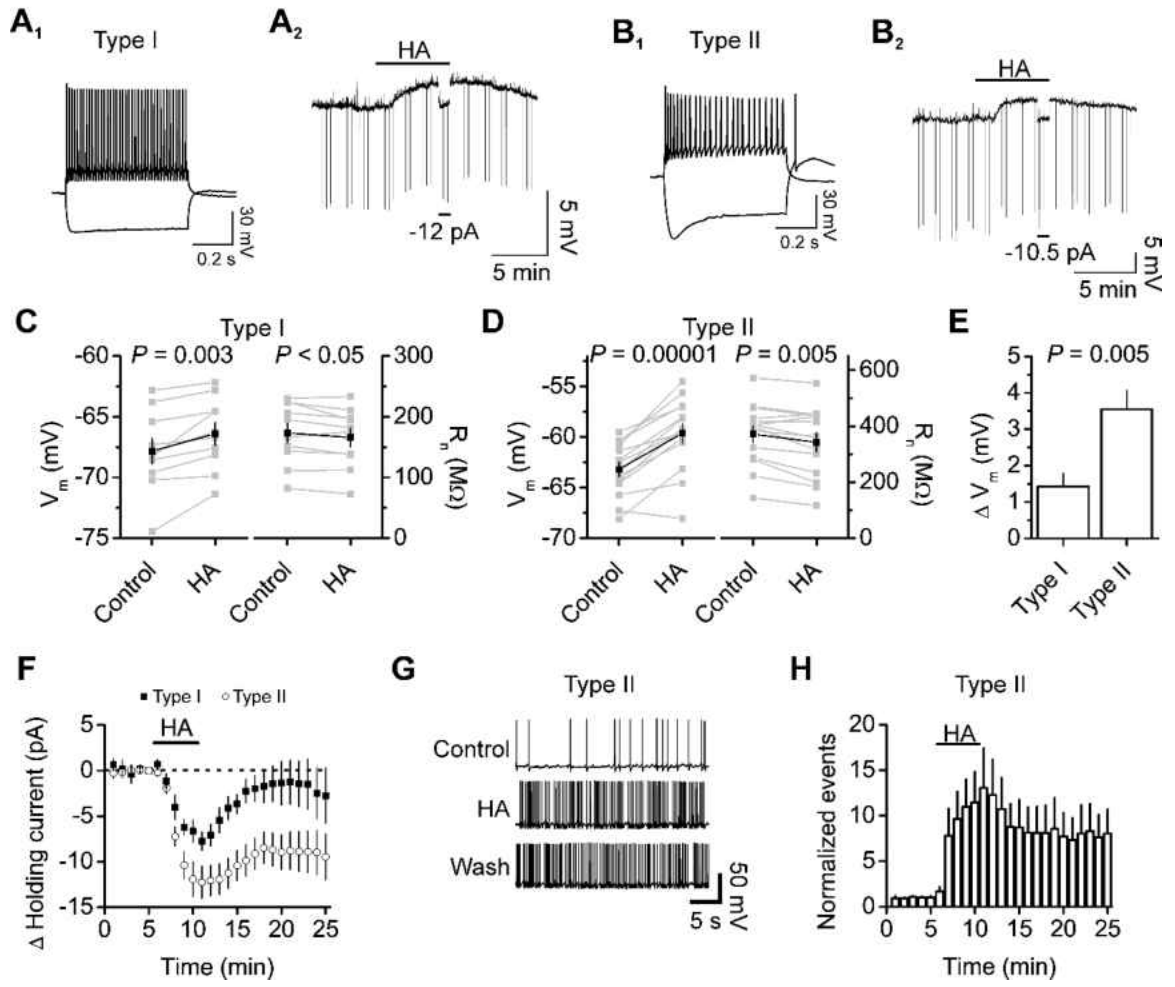
Figure 10. HA-induced augmentation of spontaneous GABAergic transmission is dependent on APs and extracellular Ca^{2+} , but does not involve postsynaptic HA receptors. (A) Example mIPSC current traces recorded from a principal neuron in layer II before, during and after the application of HA. (B) Time course of normalized mIPSC frequency summarized from 14 principal neurons. (C) Summary cumulative frequency distribution for mIPSCs averaged from 14 cells before and during the application of HA. (D) Summary cumulative amplitude distribution of mIPSCs averaged from 14 cells before and during the application of HA. (E) Spontaneous IPSCs recorded from a principal neuron in layer II before, during and after the application of HA in the extracellular solution containing zero Ca^{2+} . (F) Time course of normalized frequency for sIPSCs averaged from 7 cells recorded in the extracellular solution containing zero Ca^{2+} . (G) Spontaneous IPSCs recorded from a layer II principal neuron before, during and after the application of HA with GDP- β -S in the recording pipette. (H) Time course of normalized frequency for sIPSCs averaged from 7 cells recorded with the intracellular solution supplemented with GDP- β -S (2 mM).



HA Increases the Excitability of Local Interneurons in the MEC

We next tested the hypothesis that HA augments spontaneous GABAergic transmission by increasing the excitability of local MEC interneurons. We have shown previously that interneurons in layer III can be divided into two types according to their electrophysiological properties (Deng and Lei, 2008; Cilz et al., 2014). Type I interneurons showed little voltage sag in response to a hyperpolarizing current injection and no rebound burst firing (Fig. 11A₁) whereas Type II interneurons displayed prominent voltage sag and rebound burst firing in response to a hyperpolarizing current injection (Fig. 11B₁). After having electrophysiologically identified interneurons, we recorded the RMPs by washing in TTX (0.5 μ M) in the extracellular solution. Current injections (50 pA, 500 ms) were delivered at 0.05 Hz to monitor changes in input resistance. Application of HA caused significant depolarization in both Type I (Control: -67.8 ± 1.1 mV, HA: -66.4 ± 0.9 mV, $n = 10$, $P = 0.003$, Fig. 11A₂ and C, *left*) and Type II (Control: -63.2 ± 0.7 mV, HA: -59.6 ± 1.0 mV, $n = 14$, $P = 0.00001$, Fig. 11B₂ and D, *left*) interneurons and was accompanied by a significant reduction in the input resistance for both Type I (Control: 174 ± 16 M Ω , HA: 166 ± 16 M Ω , $n = 10$, $P < 0.05$, Fig. 11A₂ and C, *right*) and Type II (Control: 371 ± 30 M Ω , HA: 342 ± 41 M Ω , $n = 14$, $P = 0.005$, Fig. 11B₂ and D, *right*) interneurons. The magnitude of the average HA-induced depolarization was significantly different between Type I and Type II interneurons (Type I: 1.4 ± 0.4 mV, Type II: 3.6 ± 0.5 mV, $P = 0.005$, Fig. 11E). When interneurons were voltage-clamped at -65 mV, application of HA induced a small inward holding current in both Type I (-7.8 ± 1.0 pA, $n = 6$, $P = 0.0005$, Fig. 11F) and Type II (-11.9 ± 1.9 pA, $n = 9$, $P = 0.0003$, Fig. 11F) interneurons and HA-induced inward currents were significantly

Figure 11. HA depolarizes GABAergic interneurons in the MEC. (A₁-A₂) Bath application of HA generated membrane depolarization in Type I interneurons in the EC. (A₁) Voltage changes in response to current injection (± 200 pA) in a Type I interneuron. (A₂) Application of HA (30 μ M) generated membrane depolarization. RMP was recorded in current-clamp mode and a hyperpolarizing current (-50 pA, 500 ms) was injected every 20 s to measure the input resistance. Note that HA generated depolarization and slightly decreased the input resistance. To exclude the influence of HA-induced membrane depolarization on the input resistance, a negative current (-12 pA indicated by the horizontal bar) was injected briefly to bring the membrane potential back to the initial level. Under these conditions, the voltage responses induced by the injection of hyperpolarizing currents (-50 pA, 500 ms) were slightly smaller compared with control, suggesting that the HA-induced reduction in input resistance is not secondary to its effect on membrane depolarization. (B₁-B₂) Bath application of HA generated membrane depolarization and decreased the input resistance of Type II interneurons in the EC. The experiment was performed in the same fashion as Type I interneurons. (C) Data for Type I interneurons (n = 10) depicting HA-induced depolarization (*left*) and decrease in input resistance (*right*). Gray squares represent values from individual cells and black symbols denote the average values. (D) Data for Type II interneurons (n = 14) depicting HA-induced depolarization (*left*) and decrease in input resistance (*right*). (E) Average HA-induced change in membrane potential (ΔV_m) for Type I and Type II interneurons from C and D, respectively. (F) Application of HA induced a significant inward holding current in both Type I (filled squares, n = 6) and Type II (open circles, n = 9) interneurons. $P = 0.02$, two-way ANOVA. (G) APs recorded from a Type II interneuron before, during and after the application of HA. Bath application of HA increased AP firing frequency in interneurons. APs were evoked by injecting a positive current to elevate the membrane potential to just above the threshold for firing. (H) Average time course of normalized AP firing for Type II interneurons (n = 6).

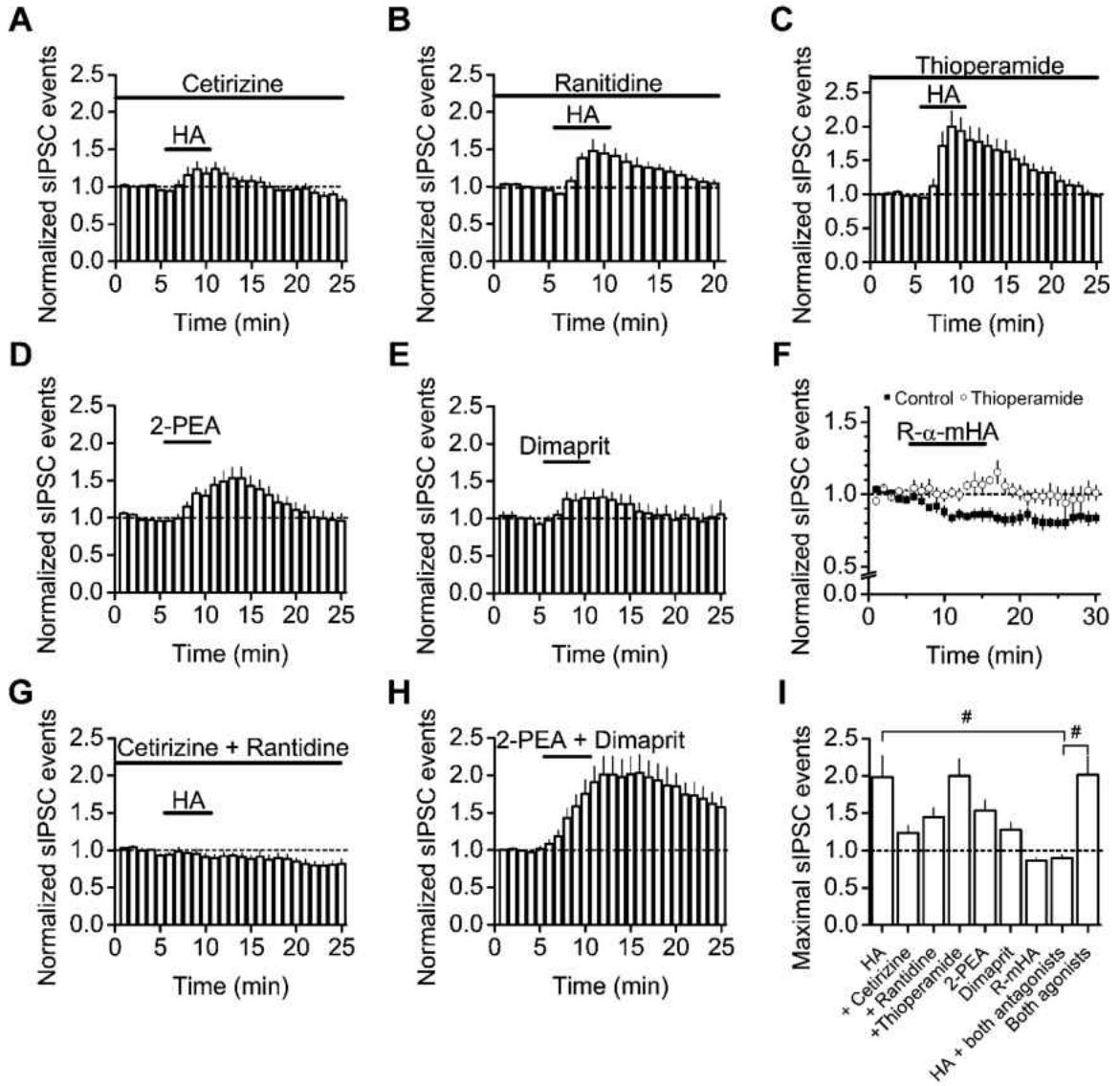


different between the two classifications ($P = 0.02$, two-way ANOVA). Because AP generation was required for HA-induced increases in sIPSCs, we also tested whether HA increased AP firing frequency. The extracellular solution contained blockers for both glutamatergic and GABAergic receptors to exclude any HA-mediated changes in synaptic input. Because interneurons typically did not exhibit spontaneous firing at their RMPs, we injected a positive current to elevate the membrane potential to just above threshold in order to induce spontaneous AP firing. We only tested Type II interneurons because Type I cells usually stopped firing APs after long periods of sustained current injection. Application of HA significantly increased the firing frequency of Type II interneurons ($1143 \pm 337\%$ of control, $n = 6$, $P = 0.03$, Fig. 11G and H) but slightly decreased the amplitude of APs ($90 \pm 2\%$ of control, $n = 6$, $P = 0.003$, Fig. 11G). HA-induced depression of AP amplitude might be due to its depolarizing effect resulting in inactivation of voltage-gated Na^+ channels.

Both H_1 and H_2 Receptors are Involved in HA-Induced Enhancement of Spontaneous GABAergic Transmission

Activation of H_1 , H_2 , and H_3 can modulate neuronal excitability in various regions of the brain. We next probed the involvement of each of these receptors in HA-mediated enhancement of spontaneous GABAergic transmission by recording sIPSCs from layer II principal neurons. Slices were pretreated with the selective H_1 receptor antagonist, cetirizine ($10 \mu\text{M}$), for at least 10 minutes and the same concentration was continuously bath-applied. Under these circumstances, application of HA continued to increase sIPSC frequency ($124 \pm 10\%$ of control, $n = 11$, $P = 0.04$ vs. baseline, Fig. 12A and I) but did not affect sIPSC amplitude ($95 \pm 10\%$ of control, $n = 11$, $P = 0.38$ vs. baseline, data not shown). The average maximal effect elicited in the presence of cetirizine was not

Figure 12. HA facilitates sIPSC frequency via activation of H₁ and H₂ but not H₃. (A) Pretreatment of slices with and continuous bath application of the H₁ antagonist, cetirizine (10 μM, n = 11), did not completely block HA-induced facilitation of sIPSC frequency. (B) Application of H₂ antagonist, ranitidine (10 μM, n = 8), in the same fashion also failed to block HA-mediated enhancement of sIPSC frequency. (C) Application of H₃ antagonist, thioperamide (10 μM, n = 8), in the same fashion also failed to block HA-mediated enhancement of sIPSC frequency. (D) Bath application of the selective H₁ agonist, 2-pyridylethylamine (2PEA, 300 μM, n = 12), facilitated sIPSC frequency. (E) Application the H₂ agonist, dimaprit (100 μM, n = 7), significantly increased sIPSC frequency. (F) Bath application of the selective H₃ agonist R-α-methylhistamine (R-α-mHA, 10μM) significantly reduced sIPSC frequency. The effect of R-α-mHA was blocked when slices were pretreated with and continuously exposed to the H₃ antagonist, thioperamide (10 μM). Filled boxes indicate average time course of sIPSC events for R-α-mHA alone (n = 6) whereas open circles indicate average time course of sIPSC events for R-α-mHA in presence of the H₃ antagonist (n = 6). *P* = 0.006, two-way ANOVA. (G) Pretreatment with and continuous bath co-application of both H₁ and H₂ antagonists (10 μM each, n = 8) blocked HA-induced facilitation of sIPSC frequency. (H) Bath co-application of H₁ (300 μM) and H₂ (100 μM, n = 6) agonists significantly increased sIPSC frequency to a maximal level reached at 13 minutes. (I) Summary data for A-H. # *P* < 0.05 one-way ANOVA with Tukey posthoc.



significantly different from control ($P > 0.05$ vs. HA, one-way ANOVA with Tukey). The presence of a selective H₂ antagonist, ranitidine (10 μM), did not prevent HA-induced augmentation of sIPSC frequency ($145 \pm 12\%$ of control, $n = 8$, $P = 0.008$ vs. baseline, Fig. 12B and I) and no changes in amplitude were observed ($107 \pm 16\%$ of control, $n = 8$, $P = 0.48$ vs. baseline, data not shown). The average maximal effect elicited in the presence of ranitidine was also not significantly different from control ($P > 0.05$ vs. HA, one-way ANOVA with Tukey). Thioperamide (10 μM), a selective H₃ antagonist, also did not prevent HA-induced increases in sIPSC frequency ($200 \pm 23\%$ of control, $n = 8$, $P = 0.003$ vs. baseline, Fig. 12C and I), nor did it alter sIPSC amplitude ($126 \pm 14\%$ of control, $n = 8$, $P = 0.12$ vs. baseline, data not shown). Application of thioperamide did not significantly alter the maximal HA-induced effect compared with control ($P > 0.05$ vs. HA, one-way ANOVA with Tukey). One explanation for these data is that multiple HA receptors are involved in HA-elicited augmentation of sIPSC frequency and blockade of single subtype of HA receptors is unable to annul the effect of HA.

We next tested whether HA receptor agonists mimic the effects of HA on sIPSCs. Bath application of the selective H₁ agonist, 2-pyridylethylamine (2-PEA, 300 μM, $pK_i = 3.7$ (Ratnala et al., 2004)), significantly increased the sIPSC frequency to a maximal level of $153 \pm 14\%$ of control ($n = 12$, $P = 0.003$ vs. baseline, Fig. 12D and I) but did not significantly alter the amplitude ($101 \pm 7\%$ of control, $n = 12$, $P = 0.82$ vs. baseline, data not shown). Similarly, application of the selective H₂ agonist, dimaprit (100 μM, $pK_i = 4.6$ (Lim et al., 2005)), significantly increased the maximal sIPSC frequency ($127 \pm 10\%$ of control, $n = 7$, $P = 0.04$ vs. baseline, Fig. 12E and I) but did not alter the amplitude

($88 \pm 8\%$ of control, $n = 7$, $P = 0.18$, data not shown) of sIPSCs. Application of the selective H₃ agonist, R- α -methylhistamine (R- α -mHA, 10 μ M) for 10 min, failed to increase but rather significantly decreased sIPSC frequency ($86 \pm 5\%$ of control, $n = 6$, $P = 0.03$ vs. baseline, Fig. 12F and I). The amplitude of sIPSCs was also significantly reduced by R- α -mHA ($87 \pm 6\%$ of control, $n = 6$, $P = 0.005$ vs. baseline, data not shown). Application of thioperamide (10 μ M) blocked R- α -mHA-mediated inhibition of sIPSC frequency ($107 \pm 5\%$ of control, $n = 6$, $P = 0.26$ vs. baseline, Fig. 12F) and amplitude ($104 \pm 5\%$ of control vs. baseline, $n = 6$, $P = 0.52$, data not shown), confirming the involvement of H₃ receptors. Collectively, these results indicate that activation of either H₁ or H₂ receptors increases sIPSC frequency, whereas activation of H₃ receptors reduces sIPSC frequency and amplitude.

Since activation of either H₁ or H₂ increased sIPSC frequency, we tested the roles of both receptors in augmenting GABAergic transmission by combining both H₁ and H₂ antagonists. In the presence of both H₁ antagonist (Cetirizine, 10 μ M) and H₂ antagonist (Rantidine, 10 μ M), application of HA significantly reduced, instead of increased, sIPSC frequency ($90 \pm 4\%$ of control, $n = 8$, $P = 0.04$ vs. baseline, $P < 0.05$ vs. HA, one-way ANOVA with Tukey, Fig. 12G and I) and amplitude ($87 \pm 5\%$ of control, $n = 8$, $P = 0.002$ vs. baseline, data not shown). One possible explanation for this result is that the facilitatory effect of H₁ and H₂ overwhelmed the inhibitory effect of H₃ on sIPSCs and blockade of both H₁ and H₂ uncovered the inhibitory effect of H₃ in response to HA. Moreover, co-application of both H₁ and H₂ agonists induced a maximal increase in sIPSC frequency at 13 min ($201 \pm 24\%$ of control, $n = 6$, $P = 0.009$ vs. baseline, Fig. 12H and I) with no significant effect on amplitude ($127 \pm 20\%$ of control, $n = 6$, $P = 0.16$ vs.

baseline, data not shown). There was no significant difference for the facilitation of sIPSC frequency in response to HA or the co-application of H₁ and H₂ agonists ($P > 0.05$, one-way ANOVA with Tukey). These results demonstrate that both H₁ and H₂ contribute to HA-induced increases in sIPSC frequency in the MEC.

Because our results indicate a direct modulatory action of HA on interneurons and that both H₁ and H₂ mediate HA-induced increases in sIPSCs, we next examined the expression of H₁ and H₂ in the MEC. Western blot analysis from MEC lysates of 3 rats displayed intense bands slightly below 72 kDa for H₁ receptors (Fig. 13B, *Top*) and near 52 kDa for H₂ (Fig. 13C, *Top*). Based on the amino acid sequence, the predicted molecular weight is ~56 kDa for H₁ and ~40 kDa for H₂. Our observations for both receptors are consistent with previous reports demonstrating higher molecular weights for these two receptors, possibly due to post-translational modifications such as receptor glycosylation (Mitsuhashi and Payan, 1989; Fukushima et al., 1995). Pre-incubation of the antibodies to H₁ or H₂ for 15 minutes with their corresponding blocking peptides eliminated the detection of the bands (Fig. 13B and C, *Bottom*), confirming the specificity of the antibodies. Because our data demonstrate that HA facilitates GABA release via activation of H₁ and H₂ on interneurons, we performed co-immunofluorescence staining for either H₁ or H₂ and the GABA synthesizing enzyme, GAD-67. Our results validated that both receptors are clearly found on the soma of GABAergic interneurons in layer III of the MEC, as well as on the adjacent principal neurons (Fig. 13D and E), which is consistent with the electrophysiological data showing that both H₁ and H₂ are involved in HA-induced increases in spontaneous GABAergic transmission.

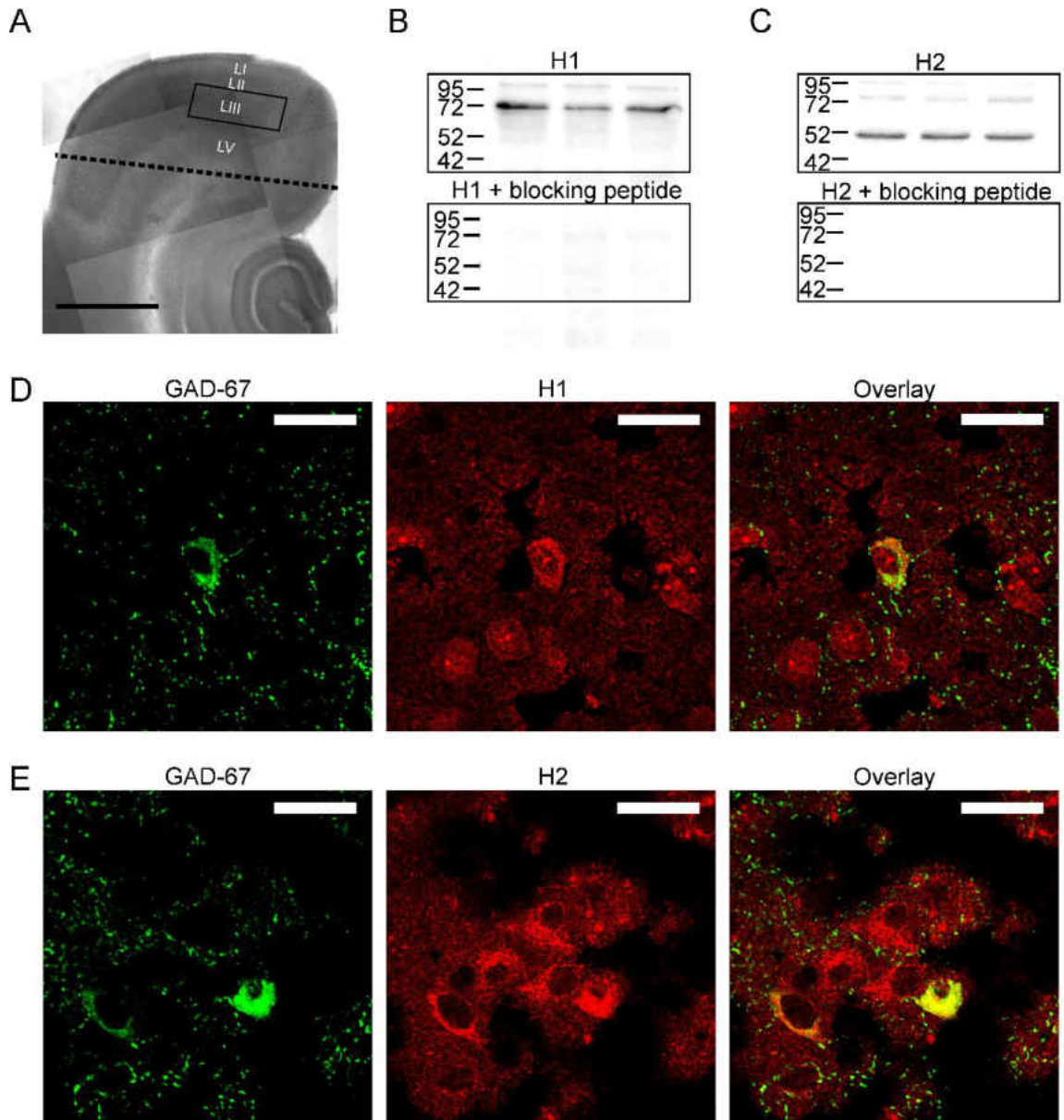


Figure 13. Both H₁ and H₂ are expressed in MEC and co-localize to GABAergic interneurons. (A) Example of a differential interference contrast image of a horizontal acute slice provided for reader orientation. Dashed line indicates region cut to isolate EC from the rest of slice for lysate preparation. Box indicates layer III region where images from D and E were acquired. Scale bar: 1 mm. (B-C) Western blot demonstrated the expression of H₁ (B) and H₂ (C) in the MEC and pre-incubation of H₁ or H₂ antibody with their corresponding blocking peptides blocked the detection of the bands. (D-E) Immunostaining demonstrated the co-expression of GAD-67 and H₁ (D) or H₂ (E) on the interneurons of the MEC. Note presence of H₁ and H₂ on surrounding principal neurons in addition to GAD-67⁺ cells. Scale bar: 25 μm.

Having confirmed the presence of H₁ and H₂ on GABAergic neurons within the EC, we next verified their functions in modulating interneuron excitability. Because the magnitude of HA-induced depolarization was larger and more distinguishable for Type II interneurons, we focused primarily on these neurons. Bath application of HA resulted in a significant depolarization of > 1 mV in 25 of 26 Type II interneurons tested, with an average of 3.6 ± 0.3 mV (Control: -64.1 ± 0.5 mV, HA: -60.5 ± 0.6 mV, $n = 26$, $P < 0.001$ vs. baseline, Fig. 14A and F). Application of HA in the presence of cetirizine failed to block HA-induced depolarization (Control: -65.1 ± 0.7 mV, HA: -62.3 ± 1.0 mV, $n = 6$, $P = 0.003$ vs. baseline, $P > 0.05$ vs. HA, Fig. 14B and F). Similarly, application of ranitidine failed to block HA-induced depolarization (Control: -64.9 ± 1.0 mV, HA: -62.3 ± 1.3 mV, $n = 8$, $P = 0.01$ vs. baseline, $P > 0.05$ vs. HA, Fig. 14C and F). Consistent with our sIPSC data, application of HA in the presence of both antagonists completely blocked HA-induced depolarization (Control: -65.9 ± 1.0 mV, HA: -65.8 ± 1.0 mV, $n = 4$, $P = 0.42$ vs. baseline, $P < 0.05$ vs. HA, Fig. 14D and F). Furthermore, co-application of both H₁ and H₂ agonists induced a significant depolarization (Control: -65.3 ± 0.8 mV, both agonists: -62.6 ± 1.0 mV, $n = 6$, $P = 0.0004$ vs. baseline, Fig. 14E and F), which was comparable to control ($P > 0.05$ vs. HA, $P < 0.05$ vs. both antagonists, Fig. 14F). HA also significantly depolarized Type I interneurons with an average of 1.4 ± 0.3 mV (Control: -67.3 ± 0.8 , HA: -65.9 ± 0.8 , $n = 17$, $P < 0.001$ vs. baseline, Fig. 14G). Due to the small magnitude of HA-induced depolarization in Type I interneurons and variability of individual neurons, resolving the roles of either H₁ or H₂ with their respective antagonists was challenging. However, application of both H₁ and H₂ antagonists completely blocked

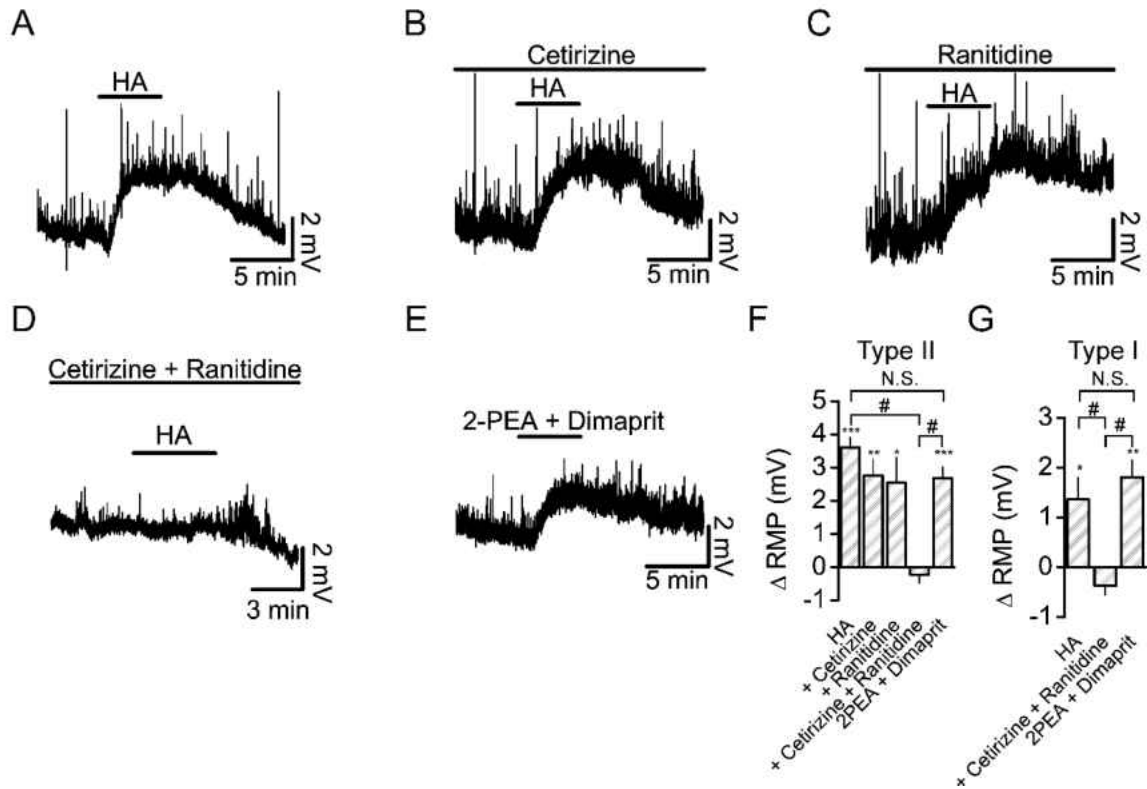


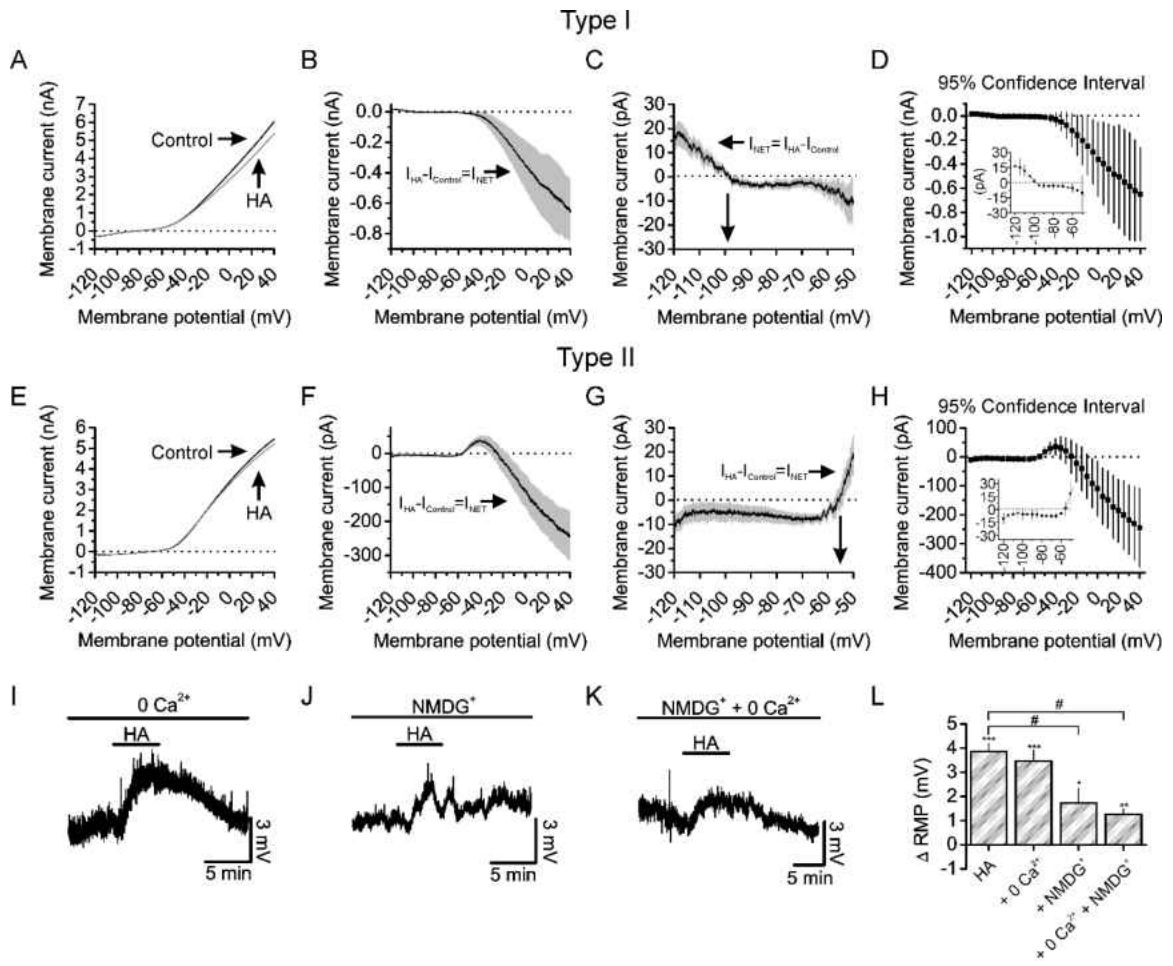
Figure 14. HA depolarizes MEC interneurons via both H₁ and H₂. (A) Representative trace showing HA-induced depolarization of Type II interneurons. (B) Representative trace demonstrating that the H₁ antagonist, cetirizine (10 μM), failed to block HA-induced depolarization of Type II interneurons. (C), Representative trace demonstrating the H₂ antagonist, ranitidine (10 μM), also failed to block HA-induced depolarization of Type II interneurons. (D) Representative trace demonstrating that the presence of both H₁ and H₂ antagonists completely blocked HA-induced depolarization of Type II interneurons. (E) Representative trace illustrating that co-application of H₁ and H₂ agonists, 2-PEA (300 μM) and dimaprit (100 μM), induced significant depolarization of Type II interneurons (n = 6). (F) Summary data from Type II interneurons for HA (n = 26), cetirizine (n = 6), ranitidine (n = 8), both antagonists (n = 4), and both agonists (n = 6). * *P* < 0.05, ** *P* < 0.01, ***, *P* < 0.001 vs baseline. # *P* < 0.05, One-way ANOVA with Tukey. (G) Summary data from Type I interneurons for HA (n = 17), both antagonists (n = 4), and both agonists (n = 5). * *P* < 0.05, ** *P* < 0.01 vs baseline. # *P* < 0.05 One-way ANOVA with Tukey.

HA-induced depolarization (Control: -73.7 ± 0.9 mV, HA: -74.1 ± 1.1 mV, $n = 4$, $P = 0.14$ vs. baseline, $P < 0.05$ vs. HA, Fig. 14G). Furthermore, co-application of both H₁ and H₂ agonists significantly depolarized Type I interneurons, mimicking the effect of HA (Control: -67.8 ± 1.9 mV, HA: -66.0 ± 2.0 mV, $n = 5$, $P = 0.006$ vs. baseline, $P > 0.05$ vs. HA, $P < 0.05$ vs. both antagonists, Fig. 14G). These results indicate that both H₁ and H₂ are involved in HA-induced depolarization of MEC interneurons.

*Partial Involvement of a Na⁺-Permeable Cation Channel in
HA-Induced Depolarization of Interneurons*

To investigate the underlying ionic mechanisms mediating HA-induced augmentation of interneuron excitability, we first constructed the voltage-current relationships before and during HA application using a voltage-ramp protocol for both Type I and Type II interneurons. Figure 15A and 15E show the average traces of voltage-current relationship from Type I ($n = 7$) and Type II ($n = 10$) interneurons, respectively, before and during the application of HA. HA-induced net currents were obtained through subtraction (Fig. 15B, C, D, F, G, and H). The averaged reversal potential for HA-induced net current in Type I interneurons was -99.1 ± 2.1 mV, which is negative to the expected K⁺ reversal potential (~ -86 mV). In Type II interneurons, HA-elicited current did not fully reverse but rather exhibited a small outward bump between -55.0 ± 1.6 mV and -24.7 ± 5.7 mV. Because the net current was largely inward for majority of the ramp in both Type I and Type II interneurons, a mixed ionic mechanism is implicated. The transient bump for the Type II interneurons may reflect a range in which a non-selective cation channel conductance predominates but becomes occluded at more depolarized potentials, possibly due to inhibition of a larger K⁺ current (see below). As indicated by the standard (Fig. 15B, C, F, and G) and margin (Fig. 15D and H) of error presented for

Figure 15. HA-induced depolarization is mediated by a mixed ionic mechanism including activation of a TTX-insensitive Na⁺ permeable channel. (A-D) Voltage-current relationship of HA-elicited currents in Type I interneurons. (A) Voltage-current relationship averaged from 7 Type I interneurons before and during the application of HA. (B) Average voltage-current relationship of the net currents obtained by subtraction for individual cells in A. The gray shaded region represents the standard errors. (C) Average voltage-current relationship of the net currents from B was enlarged to highlight HA-induced inward currents within the subthreshold voltage range. Arrow indicates the reversal potential of the net currents. (D) Average net currents with margin of error based on a 95% confidence interval. Inset shows expanded subthreshold region. (E-H) Voltage-current relationship of HA-induced currents in Type II interneurons. The graphs were arranged in the same fashion. (I) Typical RMP trace demonstrating that removal of extracellular Ca²⁺ failed to block HA-induced depolarization of Type II interneurons. (J) Example RMP trace demonstrating that replacement of extracellular NaCl with NMDG-Cl did not completely block HA-induced depolarization of Type II interneurons. (K) Representative trace illustrating that substitution of extracellular NaCl with NMDG-Cl and removal of extracellular Ca²⁺ still did not completely block HA-induced depolarization. (L) Summary data for HA-induced depolarization of Type II interneurons from I-K. * $P < 0.05$, ** $P < 0.01$, *** $P < 0.001$ vs. baseline. # $P < 0.05$, one-way ANOVA with Tukey.



average traces, both Type I and Type II net currents were very consistent, especially for subthreshold regions near the RMP.

We then recorded the RMPs under various ion substituting conditions to identify the contribution of cation influx in HA-induced facilitation of interneuron excitability. Type II interneurons were again used because HA induced a relatively larger depolarization in these neurons. Extracellular Ca^{2+} was replaced with the same concentration of Mg^{2+} and 0.1 mM EGTA was added to the extracellular solution to chelate trace amounts of Ca^{2+} . Under these circumstances, HA depolarized interneurons by 3.5 ± 0.5 mV (Control: -63.1 ± 1.5 mV, HA: -59.6 ± 1.2 mV, $n = 6$, $P = 0.0006$ vs. baseline, Fig. 15I and L), which was insignificantly different from control ($P > 0.05$ vs. HA), suggesting that extracellular Ca^{2+} is not required for HA-induced depolarization of interneurons. Reduction of extracellular Na^+ by replacing NaCl with equimolar NMDG-Cl did not prevent HA-induced depolarization (Control: -63.0 ± 1.0 mV, HA: -61.2 ± 1.3 mV, $n = 7$, $P = 0.03$ vs. baseline, Fig. 15J and L) but significantly reduced the magnitude of depolarization compared with control ($P < 0.05$ vs. HA), indicating that HA-induced depolarization is partially but not exclusively mediated by cation influx. Substitution of extracellular NaCl with NMDG-Cl and Ca^{2+} with Mg^{2+} should largely abolish cation influx. In this situation, application of HA still induced an average depolarization of 1.3 ± 0.2 mV (Control: -64.7 ± 1.0 mV, HA: -63.5 ± 1.0 mV, $n = 11$, $P = 0.002$ vs. baseline, Fig. 15K and L), which was significantly smaller than control ($P < 0.05$ vs HA). It is possible that the residual depolarization may be due to inhibition of a K^+ current. Attempts were made to block HA-induced depolarization of Type II interneurons using different cation channel blockers. HA-induced depolarization was not sensitive to the

non-selective cation channel blockers, gadolinium (Gd^{3+} , 100 μ M, Control: -63.3 ± 0.7 mV, HA: -60.2 ± 1.2 mV, $n = 5$, $P = 0.03$ vs. baseline, data not shown) or lanthanum (La^{3+} , 100 μ M, Control: -66.9 ± 1.2 mV, HA: -64.1 ± 1.3 mV, $n = 5$, $P = 0.005$ vs. baseline, data not shown). Intracellular delivery of Ih channel blocker ZD7288 (20 μ M) also failed to block HA-elicited depolarization of Type II interneurons (Control: -67.6 ± 0.8 mV, HA: -63.0 ± 1.4 mV, $n = 4$, $P = 0.04$ vs. baseline, data not shown). These results indicate that HA-induced depolarization of interneurons was partially dependent on the function of a TTX-insensitive Na^+ -permeable channel.

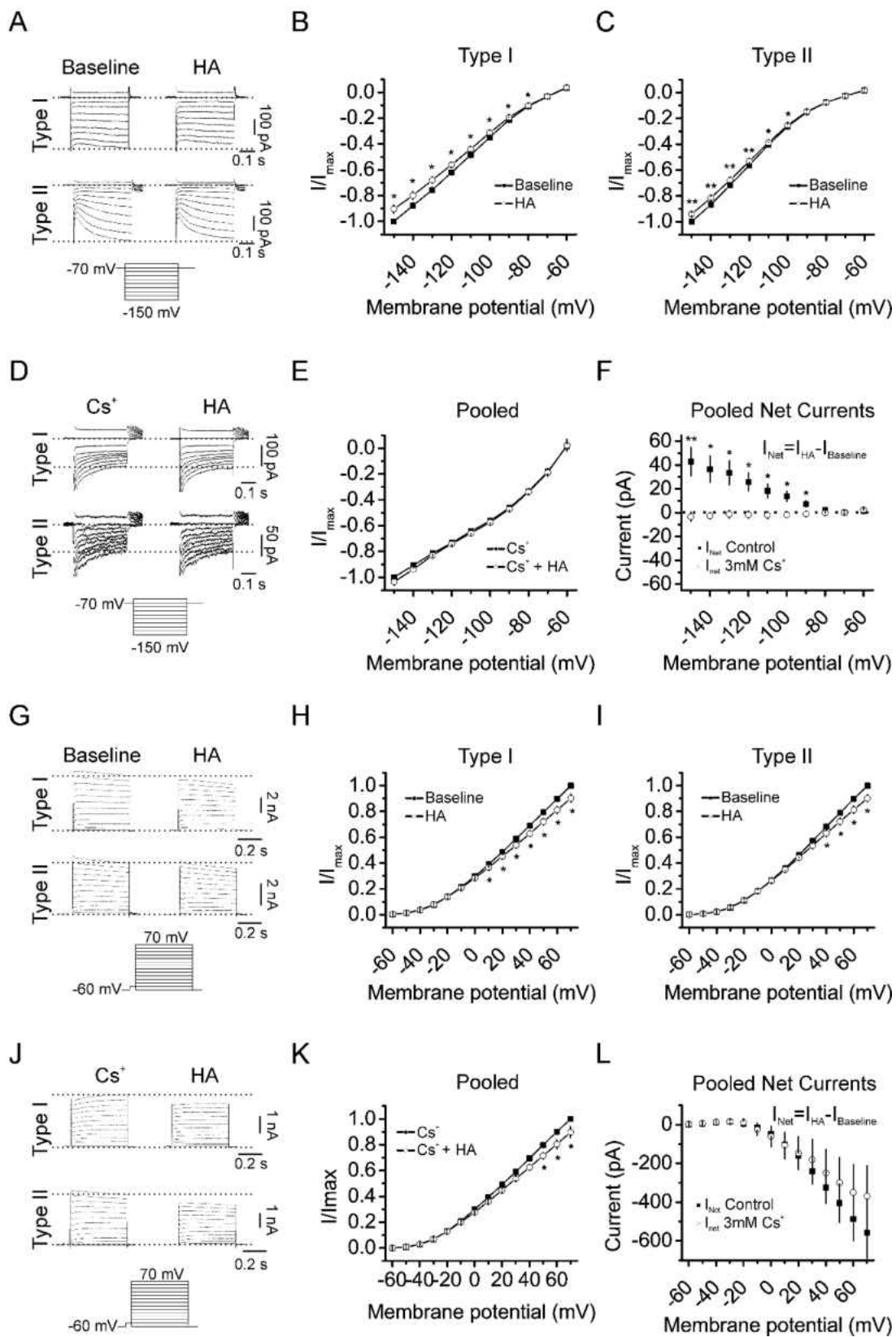
HA Inhibits I_{Ks} and I_K in MEC Interneurons

Stimulation of H_1 and H_2 leads to inhibition of K^+ currents in many brain regions (Reiner and Kamondi, 1994; Whyment et al., 2006; Zhou et al., 2006). Because HA-induced net currents were largely inward across the range of the voltages tested in our ramp experiments and preventing cation influx failed to completely block HA-induced depolarization, we reasoned that HA-induced facilitation of interneuron excitability may involve a mixed ionic mechanism including activation of cation channels and inhibition of K^+ channels. Such a mixed ionic mechanism has been observed elsewhere in the brain (Gorelova and Reiner, 1996). We tested this possibility by making voltage-clamp recordings from interneurons. Because cation influx is a mechanism responsible for HA-elicited depolarization, we isolated K^+ currents by using a K^+ -containing intracellular solution and replacing extracellular Na^+ and Ca^{2+} with the same concentration of NMDG⁺ and Mg^{2+} , respectively. Following electrophysiological identification of interneurons, the normal extracellular solution was changed to the modified solution for at least 15 min before the experiment started. After application of HA for 5 minutes, 8 of 11 Type I

(n = 8, Fig. 16A and B) and 7 of 9 Type II (n = 7, Fig. 16A and C) interneurons showed inhibition of K⁺ currents. A total of 5 cells across both groups were not included in our analysis because they displayed atypical and unexplainable inward currents. Because Cs⁺ blocks Kirs, we used Cs⁺ (3 mM) to further identify the properties of the K⁺ channels. Since HA inhibited K⁺ currents in both Type I and Type II interneurons, we pooled the data together for our Cs⁺ experiments (Type I: n = 4, Type II: n = 6). Under these conditions, application of HA in the presence of Cs⁺ failed to further inhibit any currents in interneurons (n = 10, Fig. 16D and E) and Cs⁺ completely abolished HA-induced net currents (Fig. 16F). These results indicate that HA inhibited Kirs in both Type I and Type II MEC interneurons.

Because HA has been reported to block I_K in hippocampal interneurons (Atzori et al., 2000), we also explored the effects of HA on I_K in MEC interneurons using the same recording conditions to isolate K⁺ currents as performed above. HA significantly reduced I_K in Type I (n = 6, Fig. 16G and H) and Type II (n = 9, Fig. 16G and I) interneurons. We next tested whether HA-induced inhibition of I_K was also sensitive to Cs⁺. Because inhibition of I_K was seen in both types of interneurons, we again pooled data from both types of interneurons (Type I: n = 3, Type II: n = 6). Extracellular Cs⁺ was unable to prevent further HA-induced inhibition of the I_K currents (Fig. 16J and K) and the pooled HA-induced net currents were not significantly different (Fig. 16L). Together, these results suggest that HA inhibited both Kirs and I_K in entorhinal interneurons although only the HA-induced inhibition of Kirs was sensitive to Cs⁺.

Figure 16. HA inhibits both I_{Kirs} and I_K recorded from Type I and Type II interneurons of the MEC. (A) I_{Kirs} recorded from a Type I (*Upper*) and a Type II (*Lower*) interneuron in the MEC before (*Left*) and during (*Right*) the application of HA using the extracellular solution containing NMDG⁺ and zero Ca²⁺ and intracellular solution containing K⁺-gluconate. The voltage protocol is shown at the bottom. (B) Voltage-current relationship of I_{Kirs} before and during the application of HA for Type I interneurons (n = 8). For each cell, the steady-state currents were measured just before the end of the voltage step and were normalized to the current evoked at -150 mV in control condition. (C) Voltage-current relationship of I_{Kirs} before and during the application of HA for Type II interneurons (n = 7). (D) K⁺ currents recorded from a Type I (*Upper*) and a Type II (*Lower*) interneuron in the above-mentioned extracellular solution containing Cs⁺ (3 mM) before (*Left*) and during (*Right*) the application of HA using the same voltage protocol (*bottom*) as in A. (E) Voltage-current relationship of K⁺ currents in the presence of Cs⁺ (3 mM) for pooled MEC interneurons (Type I: n = 4, Type II: n = 6). (F) Net currents obtained by subtraction in control condition (pooled from B and C) and in the extracellular solution containing Cs⁺ (from E). Note that the HA-elicited net currents in control condition showed inward rectification and application of Cs⁺ blocked HA-induced net currents. (G) I_K recorded from a Type I (*Upper*) and a Type II (*Lower*) interneuron in the MEC before (*Left*) and during (*Right*) the application HA using the extracellular solution in which NaCl and Ca²⁺ were replaced with NMDG⁺ and Mg²⁺, respectively, and the K⁺-gluconate-containing intracellular solution. The voltage protocol is shown at the bottom. (H) Voltage-current relationship of I_K before and during the application of HA for Type I interneurons (n = 6). For each cell, the steady-state currents were measured just before the end of voltage steps and were normalized to the current evoked by +70 mV in control condition. (I) Voltage-current relationship of I_K before and during the application of HA for Type II interneurons (n = 9). (J) I_K recorded from a Type I (*Upper*) and a Type II (*Lower*) interneuron in the presence of Cs⁺ (3 mM) before (*Left*) and during (*Right*) the application of HA using the same recording conditions as in G. (K) Voltage-current relationship of I_K in the presence of Cs⁺ (3 mM) for pooled interneurons (Type I: n = 3, Type II: n = 6) before and during application of HA. (L) Net currents generated by subtraction pooled in control condition (from H and I) and in the extracellular solution supplemented with Cs⁺ (from K). * $P < 0.05$, ** $P < 0.01$.



Extracellular Cs⁺ Reduces HA-Induced Depolarization and Prevents HA-Elicited Increases in sIPSCs Independent of Changes to I_h

Because HA inhibited K⁺ currents of interneurons, including Cs⁺-sensitive Kirs, we next tested whether Cs⁺ reduced HA-induced depolarization of interneurons. In Type II interneurons, application of HA in the presence of Cs⁺ did not result in significant depolarization (Control: -66.2 ± 0.8 mV, HA: -64.9 ± 1.8 mV, $n = 9$, $P = 0.21$ vs. baseline, Fig. 17A and B) and was significantly different from HA alone ($P = 0.005$, Fig. 17B). Similar results were also obtained in Type I interneurons (Control: -67.7 ± 1.6 mV, HA: -67.3 ± 1.3 mV, $n = 6$, $P = 0.44$ vs. baseline, data not shown). Because Cs⁺ blocked Kirs and inhibited HA-induced depolarization, we tested whether HA-induced augmentation of sIPSCs was sensitive to extracellular Cs⁺. Because application of Cs⁺ (3 mM) alone significantly increased the basal sIPSC frequency (data not shown) and the resulting elevated basal frequency may have narrowed the window for detection of HA-dependent increases in sIPSCs, we reduced the extracellular Ca²⁺ concentration to 0.75 mM and elevated Mg²⁺ concentration to 3.25 mM to reduce the basal frequency of sIPSCs in the presence of Cs⁺. Under these conditions, application of HA still significantly increased sIPSC frequency in the absence of Cs⁺ ($155 \pm 29\%$ of control, $n = 4$, $P = 0.01$ vs. baseline, Fig. 17D). However, in the extracellular solution containing 0.75 mM Ca²⁺ and 3 mM Cs⁺, application of HA failed to significantly increase sIPSC frequency ($94 \pm 10\%$ of control, $n = 7$, $P = 0.56$, Fig. 17C and D). In addition to Kirs and other K⁺ channels, Cs⁺ also blocks I_h. To test whether the effect of Cs⁺ may have been due to blockade of I_h, we tested whether selectively blocking I_h using ZD7288 prevented HA-induced increases in sIPSCs. Slices were pretreated with ZD7288 (20 μM) and the same concentration of ZD7288 was continuously bath applied. Under these

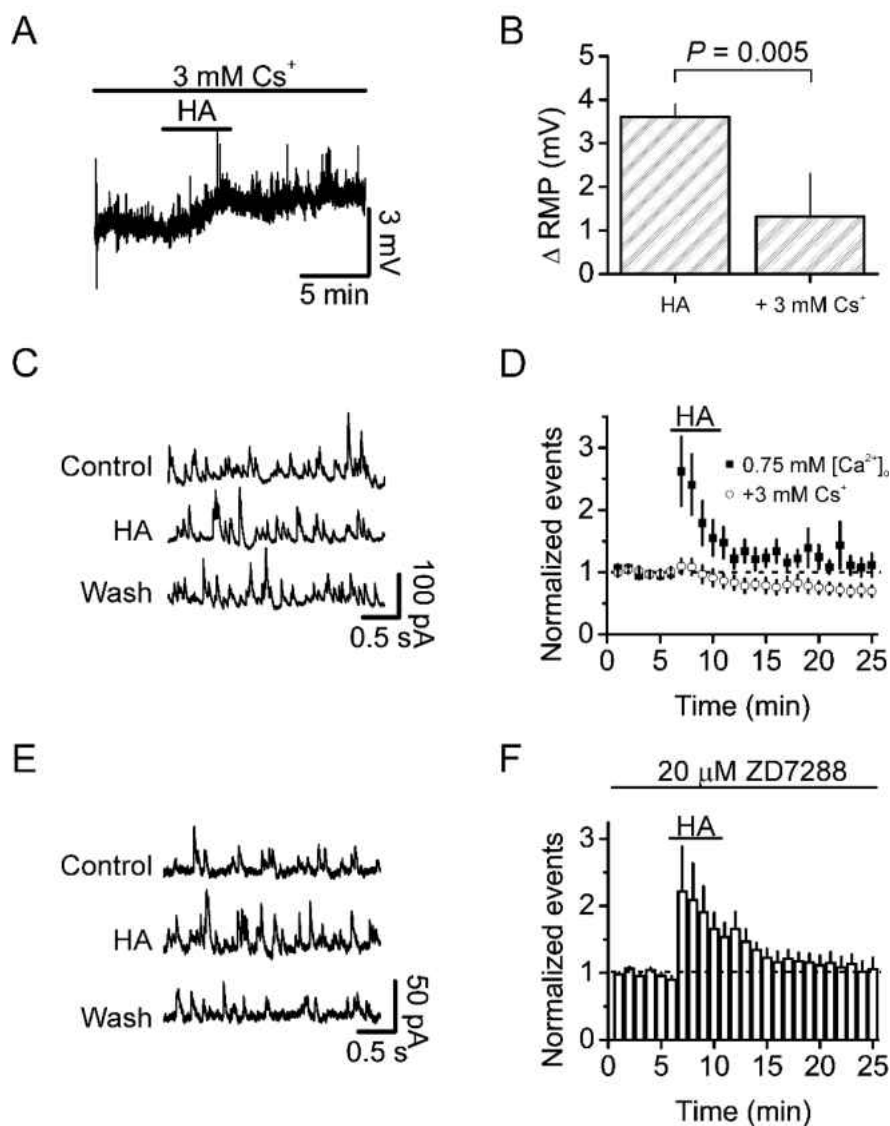


Figure 17. Extracellular Cs^+ inhibits the depolarization of interneurons and blocks the facilitation of sIPSC frequency in response to HA. (A) Example RMP trace from a Type II interneuron demonstrating that HA-induced depolarization is significantly inhibited in the presence of 3 mM Cs^+ . (B) Summary data comparing the depolarization of Type II interneurons in the absence and presence of 3 mM Cs^+ . (C) Representative traces of sIPSCs recorded before, during and after the application of HA in the extracellular solution containing 0.75 mM CaCl_2 with Cs^+ (3 mM). (D) Time course of HA-induced increases in sIPSC frequency in the extracellular solution containing 0.75 mM CaCl_2 with or without Cs^+ (3 mM). (E) Example traces of sIPSCs recorded in the presence of ZD7288 before, during and after the application of HA. (F) Time course of HA-mediated increases in sIPSC frequency in the presence of ZD7288.

circumstances, HA still increased the frequency of sIPSCs ($165 \pm 25\%$ of control, $n = 7$, $P = 0.04$ vs. baseline, Fig. 17E and F), which was comparable to the control ($P = 0.52$).

These results suggest that blockade of I_h channels is not sufficient to prevent HA-induced increases in sIPSCs and the inhibitory effect of extracellular Cs^+ may be mediated by inhibition of interneuron Kirs.

CHAPTER V

RESULTS

Study 3 - Group I mGluR Modulation within the Entorhinal Cortex

Introduction

Glutamate interacts with two types of receptors: the ionotropic (iGluR) and metabotropic (mGluR) glutamate receptors (Niswender and Conn, 2010; Traynelis et al., 2010). The iGluRs are divided into three subtypes based on sequence homology and pharmacology. The three iGluR types are kainate, AMPA, and NMDA receptors. The mGluRs are GPCRs that engage in several different signal transduction mechanisms upon ligand binding. There are eight known subtypes (mGluR1-8) of mGluRs. The mGluRs are distributed across three broad groups that are defined by sequence homology, pharmacology, and coupled signaling systems. Group I receptors consist of mGluR1 and 5; group II consist of mGluR2 and 3; and, group III consist of mGluR4, 6, 7, and 8 (Niswender and Conn, 2010). Classically, group I receptors are coupled to $G_{q/11}$ signaling pathways and their activation results in PLC activity, IP_3 production, and Ca^{2+} signaling (Sladeczek et al., 1985; Nicoletti et al., 1986; Houamed et al., 1991; Masu et al., 1991; Abe et al., 1992). On the other hand, group II and III receptors are coupled to G_i signaling pathways and their activation leads to reductions in cAMP production (Tanabe et al., 1992, 1993). Other than mGluR6 (Nakajima et al., 1993), members of each group are abundantly expressed throughout the central nervous system (Niswender and Conn,

2010). Functionally, mGluRs modulate cellular excitability and many aspects of synaptic plasticity (Conn and Pin, 1997; Anwyl, 1999; Niswender and Conn, 2010).

Members of group I, II, and III mGluRs are present in the EC. In the rat, *in situ* hybridization studies for group I mGluRs indicate high levels of mGluR5 transcripts, whereas mGluR1 levels are present but at comparatively lower levels relative to other hippocampal areas (Shigemoto et al., 1992; Fotuhi et al., 1994). Similar studies for group II and III mGluRs also indicate the presence of mGluR2 (Ohishi et al., 1993a; Fotuhi et al., 1994), mGluR3 (Ohishi et al., 1993b; Fotuhi et al., 1994), mGluR4 (Fotuhi et al., 1994; Ohishi et al., 1995), and mGluR7 (Ohishi et al., 1995). Although the EC is not mentioned, mGluR8 mRNA is also moderately present in the hippocampus and cortex (Saugstad et al., 1997). mGluR6 is absent from the hippocampus (Nakajima et al., 1993; Schools and Kimelberg, 1999) as these receptors are primarily localized to the “ON” bipolar cells of the retina (Nakajima et al., 1993). Moreover, immunostaining indicates the presence of both group II mGluRs (Zhang et al., 2015a) as well as mGluR7a, and mGluR8 (Shigemoto et al., 1997), however, group I mGluRs have not been examined. The existence of members from each group of mGluRs in the MEC suggests a functional role for these receptors in modulating MEC activity.

Functional evidence indicates group I mGluRs modulate both GABAergic and glutamatergic transmission within the MEC. In layer III, either the glutamate transporter inhibitor TBOA—used to elevate extracellular glutamate levels—or application of the non-selective group I/II mGluR agonist tACPD (Schoepp et al., 1999) reduces the amplitude of both AMPA and NMDA eEPSCs (Iserhot et al., 2004), suggesting a presynaptic site of action. The tACPD-induced depression is sensitive to a non-selective

mGluR antagonist and a selective group I antagonist blocks the TBOA-induced depression (Iserhot et al., 2004), specifically implicating group I mGluRs. Selective activation of group I mGluRs with DHPG (Schoepp et al., 1999) enhances persistent firing in layer III (Yoshida et al., 2008), although the underlying mechanism remains unexplored. Regarding GABAergic transmission, group I activation elicits differential effects whereby DHPG significantly increases sIPSCs but reduces eIPSCs in the superficial MEC (Deng et al., 2010b). The DHPG-induced increase in sIPSCs involves a direct modulatory action on MEC interneurons via mGluR5, but not mGluR1, resulting in the inhibition of a background K^+ channel (Deng et al., 2010b).

Group II receptors are both pre- and postsynaptically functional in the MEC. Presynaptic activation of mGluR2/3 using the selective mGluR2/3 agonist LY354740 (Schoepp et al., 1999) reduces AMPA-mediated eEPSCs but exerts no effect on GABA_A-mediated eIPSCs (Wang et al., 2012). This depression of eEPSCs involves the inhibition of presynaptic P/Q voltage-gated Ca^{2+} channels (Wang et al., 2012). Postsynaptically, group II activation transiently hyperpolarizes principal neurons throughout the MEC but this hyperpolarization is most pronounced and long-lasting in layer III pyramidal neurons (Zhang et al., 2015a). Mechanistically, this group II-induced hyperpolarization involves both the inhibition of a cation conductance and activation of a K^+ conductance (Zhang et al., 2015a).

Group III receptors modulate both excitatory and inhibitory transmission in the MEC. Group III mGluRs are tonically activated with each stimulation and constrain eEPSC amplitudes in layer V (Woodhall et al., 2007). Moreover, application of the selective mGluR4 agonist ACPT-1 (Schoepp et al., 1999) depresses eEPSCs in layer V

(Woodhall et al., 2007). However, spontaneous glutamate release in layer V is unexpectedly increased in response to either ACPT-1 or the group III selective agonist L-AP4 applied at a concentration selective for mGluR4/8, but not mGluR7 (Evans et al., 2000, 2001; Woodhall et al., 2007). This group III-induced facilitatory action on spontaneous glutamate release is unique to layer V, since group III mGluR activation reduces glutamate release in layer II (Evans et al., 2000). Thus, group III mGluRs exert distinct modulatory actions on glutamatergic transmission depending on both network activity and the MEC cortical layer. With respect to GABAergic transmission, ACPT-1 significantly reduces the frequency of spontaneous GABA release in layer V but not layer II (Woodhall et al., 2001) and no constitutive regulation of eIPSCs is seen in layer V (Woodhall et al., 2001), unlike what is seen with eEPSCs.

Overall, mGluR members of all 3 groups are present in the MEC and these functional studies indicate an important modulatory role on both excitatory and inhibitory synaptic transmission, as well as MEC intrinsic excitability.

Study 3 Rationale

Group I mGluRs are commonly regarded as postsynaptic receptors and their activation generally leads to increased excitability in various brain regions. Group I mGluRs can increase excitability by inhibiting K⁺ channels, including Ca²⁺-activated K⁺ channels (Charpak et al., 1990), M-current K⁺ channels (Chuang et al., 2002), or background-leak K⁺ channels (Mannaioni et al., 2001). Alternatively, group I mGluRs may increase excitability by activating a cation channel, including voltage-gated Ca²⁺ channels (Park et al., 2010), Ca²⁺-dependent cation channels (Congar et al., 1997; Gee et al., 2003; Kim et al., 2003), Ca²⁺-independent cation channels (Guerineau et al., 1995),

persistent Na⁺ channels (D'Ascenzo et al., 2009), or activation of the Na⁺-Ca²⁺ exchanger (NCX) (Keele et al., 1997). As stated above, group I mGluR activation enhances persistent firing of layer III pyramidal neurons (Yoshida et al., 2008), however, the underlying mechanism mediating this increase in excitability remains unknown. We wanted to examine this mechanism because our lab is interested in modulation of hippocampal inputs derived from the MEC at the cellular level and because persistent firing is proposed to be a cellular model for working memory (Hasselmo and Stern, 2006). Although persistent firing is a phenomenon seen throughout the MEC (Klink and Alonso, 1997b; Egorov et al., 2002; Yoshida et al., 2008), we chose to focus primarily on layer III because the axons of this cell layer make up the temporoammonic pathway, which is important for temporal associational memory processes (Suh et al., 2011). We therefore set out to examine the underlying ionic mechanisms mediating group I mGluR-induced increases in layer III excitability.

*Activation of Group I mGluRs Increases the Excitability of
MEC Principal Neurons and Requires Both mGluR1 and mGluR5*

We recorded APs from layer III pyramidal neurons within the MEC in the presence of synaptic blockers to examine any potential direct modulatory effect of group I mGluR activation. Constant direct current was injected to the soma to simulate synaptic input and drive spontaneous action potential firing. After recording at least five minutes of stable baseline, we applied the group I selective agonist (S)-3,5-dihydroxyphenylglycine (DHPG, 10 μ M) for 5 minutes. DHPG significantly increased the AP firing frequency to 350 ± 96 % of control (Control: 0.51 ± 0.03 Hz, DHPG: 1.97 ± 0.38 Hz, $n = 11$, $P < 0.005$ vs. baseline, Fig. 18A, B, and J). This increase gradually returned to near-baseline levels by 20 minutes into washout (Washout: $0.68 \pm$

0.12 Hz, Fig. 18A and B). Similar increases were seen for layer II (Control: 0.75 ± 0.01 Hz, DHPG: 4.34 ± 0.50 Hz, $n = 9$, $P < 0.0001$ vs. baseline, data not shown) and layer V (Control: 0.20 ± 0.004 Hz, DHPG: 0.85 ± 0.09 Hz, $n = 5$, $P < 0.005$ vs. baseline, data not shown) principal neurons, indicating that DHPG increased excitability throughout all layers of the MEC. We chose to focus on layer III neurons for the remainder of this study to examine underlying molecular mechanisms mediating DHPG's effect in the MEC. The effect of DHPG-induced increased AP firing had a dose-dependent response with a calculated EC_{50} value of $1.76 \mu\text{M}$ (Fig. 18C). We used a concentration of $10 \mu\text{M}$ for the remainder of all experiments.

The group I mGluR subtypes underlying DHPG-dependent increased AP firing were examined using selective antagonists for mGluR1 and mGluR5. Pretreatment and continuous bath application of slices with the selective mGluR1 antagonist LY456236 ($5 \mu\text{M}$) prevented any significant DHPG-induced increases in AP firing frequency (Control: 0.51 ± 0.06 Hz, DHPG: 1.01 ± 0.27 Hz, $n = 8$, $P = 0.13$ vs. baseline, Fig. 18D, E, and J), however, LY456236 alone did not significantly reduce DHPG-induced increased AP firing compared to control ($P > 0.05$ vs. control, One-Way ANOVA with Tukey, Fig. 18E and J). In a similar fashion, DHPG failed to significantly increase the frequency of APs in the presence of $5 \mu\text{M}$ MPEP (Control: 0.45 ± 0.04 Hz, DHPG: 1.11 ± 0.35 Hz, $n = 7$, $P = 0.09$ vs. baseline, Fig. 18F, G, and J), although MPEP did not significantly reduce DHPG-induced increased AP firing compared to control ($P > 0.05$ vs. control, One-Way ANOVA with Tukey, Fig. 18G and J). However, when slices were exposed to both MPEP and LY456236, DHPG failed to increase AP firing frequency (Control: 0.55 ± 0.03 Hz, DHPG: 0.60 ± 0.09 Hz, $n = 7$, $P = 0.66$ vs. baseline, Fig. 18H,

I, and J) and DHPG's effect was completely blocked compared to control conditions ($P < 0.05$ vs. control, One-Way ANOVA with Tukey, Fig. 18I and J). No significant difference in baseline AP firing frequency was observed between conditions, mitigating any concerns about experimental conditions influencing these results ($P = 0.44$, One-Way ANOVA with Tukey, Fig. 18J).

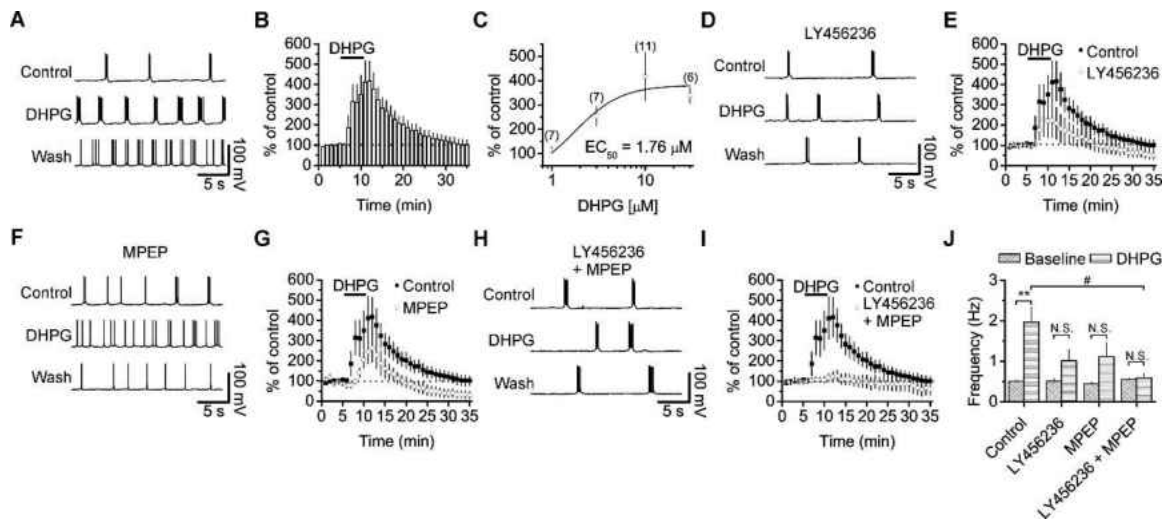


Figure 18. DHPG significantly increased the AP firing frequency of a layer III pyramidal neurons. (A) Example of AP trace from a layer III pyramidal neuron before, during, and after application of 10 μM DHPG. (B) Summary data for 11 cells. (C) Concentration-response curve for DHPG-induced increases in normalized AP firing. (D) Example AP trace from a layer III pyramidal neuron before, during and after application of DHPG in the presence of 5 μM LY456236, an mGluR1-selective antagonist. (E) Summary data showing 8 cells in the presence of LY456236 alongside control. (F) Example AP trace from a layer III pyramidal neuron before, during, and after application of DHPG in the presence of 5 μM MPEP, a selective mGluR5 antagonist. (G) Summary data showing 7 cells in the presence of MPEP alongside control. (H) Example AP trace from a layer III pyramidal neuron before, during, and after application of DHPG in the presence of both LY456236 and MPEP. (I) Summary data showing 7 cells in the presence of both group I antagonists alongside control cells. (J) Summary figure for DHPG receptor pharmacology in layer III MEC. * $P < 0.01$ vs. baseline; # $P < 0.05$, one-way ANOVA with Tukey; N.S., Not Significant.

DHPG Induces Subthreshold Changes in Principal Cell Excitability

Subthreshold modulatory actions that destabilize the RMP can increase excitability and AP generation. To examine potential DHPG-induced changes in subthreshold excitability, we made RMP recordings in the presence of TTX (0.5 μ M). Changes in the input resistance were monitored by applying brief current injections (-100 pA, 100 ms) every 20 seconds. After a five-minute stable baseline recording, application of DHPG induced a significant maximal depolarization of 6.2 ± 1.8 mV (Control: -62.8 ± 0.5 mV, DHPG: -56.6 ± 2.1 mV, $n = 12$, $P = 0.005$ vs. baseline, Fig. 19A, B *left*). To offset any voltage-dependent changes in the input resistance resulting secondarily from DHPG-induced depolarization, we injected negative current to briefly return the RMP to baseline levels and calculated DHPG-induced changes in input resistance. DHPG did not significantly change the input resistance (Control: 277 ± 17 M Ω , DHPG: 284 ± 17 M Ω , $n = 12$, $P = 0.08$ vs. baseline, Fig. 19A, B *right*). Application of DHPG to layer III neurons voltage-clamped at -60 mV induced a maximal inward current of -16.8 ± 1.7 pA ($n = 22$, $P < 0.00001$ vs. baseline, Fig. 19C). The magnitude of this current was not significantly different compared to the baseline-returning current we injected in RMP current-clamp experiments above (-11.3 ± 2.6 pA, $n = 12$, $P = 0.08$ vs. voltage-clamp experiments, data not shown). Plotting maximal DHPG-induced inward currents versus animal ages used in this study did not reveal a strong correlation (Pearson's $r = 0.261$, Fig. 19D), suggesting that age did not influence DHPG-induced currents for our experiments. These data demonstrate that DHPG-induced increases in excitability are due, at least in part, to changes in subthreshold excitability.

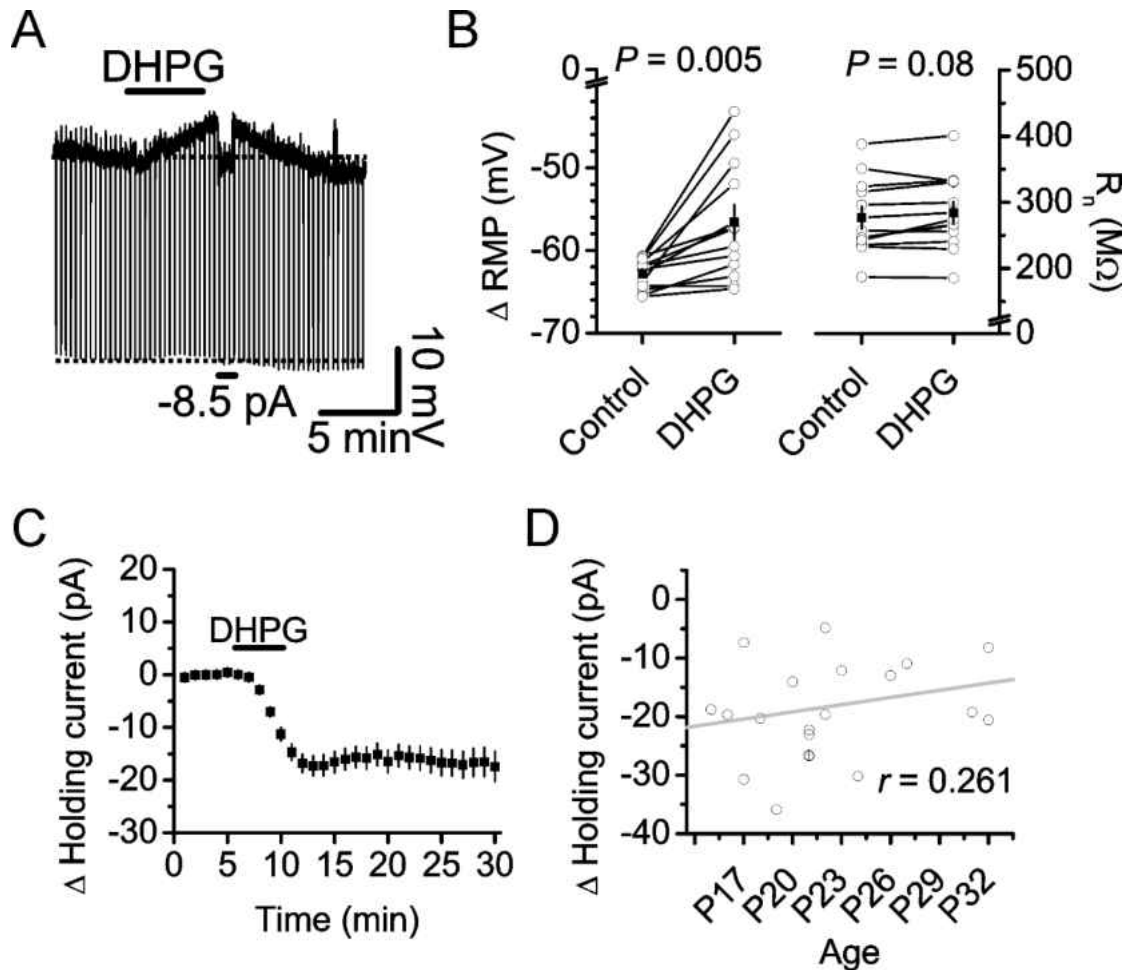


Figure 19. DHPG induced a significant RMP depolarization. (A) Example illustrating DHPG-induced depolarization with minimal effects on input resistance. A hyperpolarizing current (-100 pA , 100 ms) was injected every 20 s to measure the input resistance. Note that DHPG generated a clear depolarization. A negative current (-8.5 pA) was injected to briefly return the RMP to baseline levels. (indicated by the horizontal bar). (B) Summary data for DHPG-induced changes in RMP and input resistance (R_n). (C) Voltage-clamp experiments at -60 mV reveal DHPG-induced a significant inward current. (D) DHPG-induced inward currents across animal age-ranges tested in this study do not indicate a strong relationship.

Potential Signaling Mechanisms Underlying DHPG-Induced Changes in Subthreshold Excitability

Both G protein-dependent (Congar et al., 1997; Gee et al., 2003; Kubota et al., 2014) and -independent (Heuss et al., 1999; Gee et al., 2003; Kubota et al., 2014)

signaling is implicated in group I mGluR signaling. We therefore sought to determine whether G proteins are involved in DHPG-induced changes in subthreshold excitability using voltage-clamp experiments. Because DHPG-induced changes in excitability for both RMP and HC typically appeared to be maximal around 7-8 minutes after start of application, this time point was chosen for comparisons across different conditions. The G protein inactivator GDP- β -S (2 mM) was included inside the K-gluconate-containing internal solution. DHPG was applied after waiting ~30 minutes to allow for complete exchange between the recording pipette and cell. Under these conditions, DHPG induced a significant maximal inward current of -7.7 ± 1.0 pA ($n = 9$, $P = 0.00006$ vs. baseline, Fig. 20A and G), which was significantly reduced compared to control alone ($P = 0.003$ vs. control alone). Because group I mGluRs are G_q -coupled, we next determined whether PLC was involved in DHPG-induced inward currents. Pretreatment of slices for 30 minutes and continuous bath application of the PLC inhibitor U73122 (10 μ M), did not prevent DHPG-induced currents (-15.8 ± 4.2 pA, $n = 8$, $P = 0.007$ vs. baseline, $P = 0.79$ vs. control alone, Fig. 20B and G). A 2-hour pretreatment of slices and continuous bath application of another structurally distinct PLC inhibitor edelfosine (10 μ M) also failed to prevent DHPG-induced inward currents (-15.0 ± 2.9 pA, $n = 11$, $P = 0.0004$ vs. baseline, $P = 0.58$ vs. control alone, Fig. 20C and G). These results indicate that PLC is not involved, which might suggest downstream PLC-dependent signaling pathways are also not likely involved. Group I mGluRs can increase cAMP and it is possible DHPG-induced changes may be due to G_s -coupling to AC. We therefore tested whether AC is involved by pretreating, but not continuously bath applying, slices with the selective AC

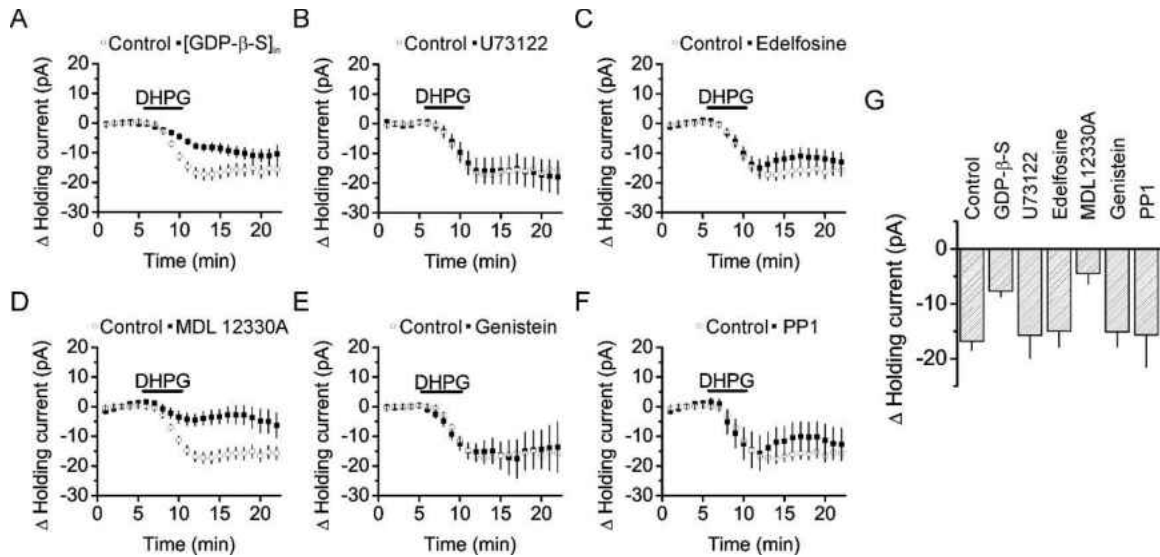


Figure 20. DHPG-induced inward currents may require G proteins and AC but not PLC or Src. (A) DHPG continued to induce a smaller but significant current while G proteins were inhibited ($n = 9$). (B) Inhibition of PLC with 10 μM U73122 did not affect DHPG-induced currents ($n = 8$). (C) Another PLC inhibitor, 10 μM edelfosine, also failed to block DHPG-induced currents ($n = 11$). (D) Inhibition of AC by pretreatment with 30 μM MDL 12330A prevented DHPG-induced currents ($n = 7$) (E) Inhibition of Src with 30 μM genistein failed to affect DHPG-induced currents ($n = 6$). (F) Another Src inhibitor, 20 μM PP1, also failed to affect DHPG-induced currents ($n = 8$) (G) Summary data for A-F.

inhibitor MDL 12330A (30 μM). MDL 12330A pretreatment prevented DHPG-induced currents (-4.5 ± 2.0 , $n = 7$, $P = 0.06$ vs. baseline, $P = 0.0009$ vs control alone, Fig. 20D and G), suggesting involvement of AC. Because DHPG can also modulate excitability independent of G proteins and because inhibiting G proteins did not completely prevent DHPG-induced currents, we also tested for a G protein-independent signaling pathway mediating DHPG's effect. Pretreatment and continuous bath application of slices with the Src inhibitor genistein (30 μM) did affect DHPG-induced currents (-15.1 ± 2.7 pA, $n = 6$, $P = 0.002$ vs. baseline, $P = 0.65$ vs. control alone, Fig. 20E and G). Pretreatment and continuous bath application of another inhibitor of Src, PP1 (20 μM), also did affect DHPG-induced currents (-15.7 ± 5.9 pA, $n = 8$, $P = 0.03$ vs. baseline, $P = 0.81$ vs. control

alone, Fig. 20F and G). Taken together these results suggest that G proteins and AC may be involved, but more experiments are necessary to support this conclusion.

*DHPG-Induced Changes in Subthreshold Excitability Involve
Activation of a Non-Selective Cationic Current*

To examine a role for Ca^{2+} influx in DHPG-induced inward currents, we replaced extracellular Ca^{2+} with Mg^{2+} and supplemented the external solution with TTX (0.5 μM) to block voltage-gated Na^+ channels and EGTA (100 μM) to chelate any residual Ca^{2+} ions. Under these conditions DHPG continued to induce a significant inward current (-12.7 ± 5.1 pA, $n = 8$, $P = 0.04$ vs. baseline, $P = 0.34$ vs. control alone, Fig. 21A and E). We next tested a role for Na^+ influx by replacing extracellular NaCl with equimolar NMDG-Cl. Under these conditions, DHPG continued to induce a significant inward current (-5.5 ± 1.8 pA, $n = 9$, $P = 0.02$ vs. baseline, Fig. 21B and E) but this current was reduced compared to control ($P = 0.0007$ vs. control alone). To determine whether changes in K^+ flux contributed to DHPG-induced inward currents, we replaced intracellular K^+ with Cs^+ . With Cs^+ inside the pipette, DHPG continued to induce a significant inward current (-22.2 ± 3.7 pA, $n = 23$, $P < 0.00001$ vs. baseline, $P = 0.2$ vs. control alone, Fig. 21C and E). When both NaCl and extracellular Ca^{2+} were replaced, DHPG no longer induced a significant inward current (7.9 ± 5.4 pA, $n = 8$, $P = 0.19$ vs. baseline, $P < 0.00001$ vs. control alone, Fig. 21D and E). Together, these experiments suggest DHPG-induced inward currents occur via activation of a predominantly Na^+ -permeant non-selective cation channel.

We next recorded I-V relationships from layer III pyramidal neurons prior to and following application of DHPG (Fig. 21F). The DHPG-induced net current (I_{Net} , Fig. 21G) was obtained by subtracting control traces from current recorded in the

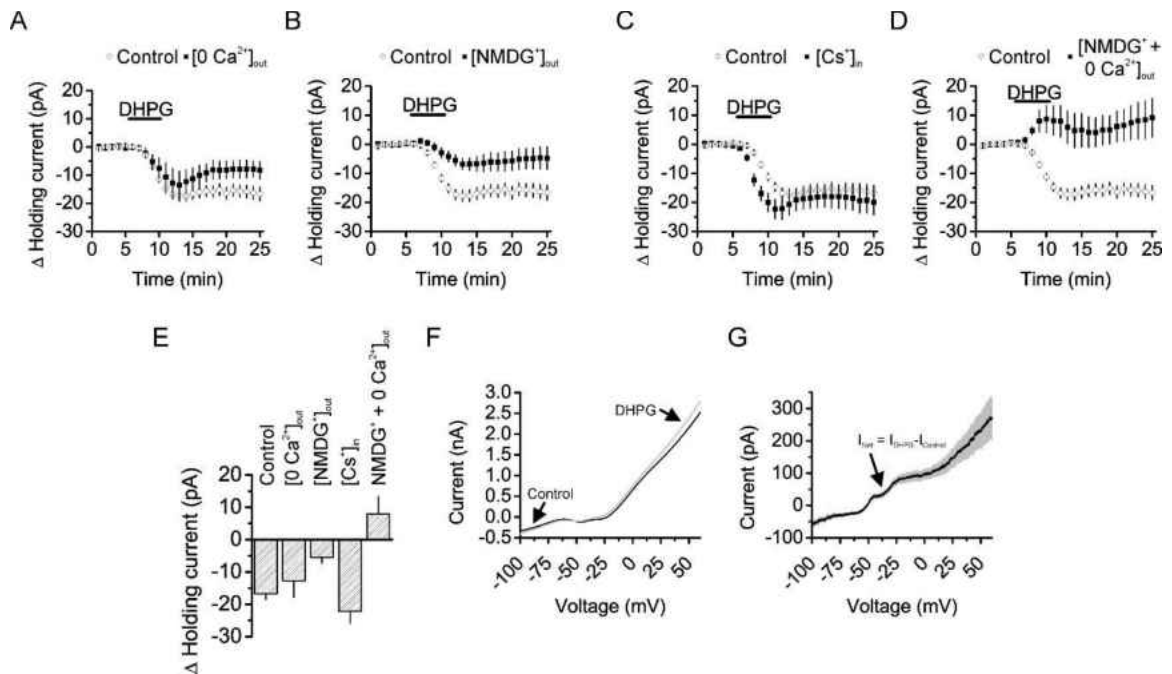


Figure 21. DHPG activated a non-selective cationic conductance. (A) Removal of extracellular Ca^{2+} failed to block DHPG-induced currents ($n = 8$). (B) Removal of extracellular Na^+ reduced DHPG-induced currents ($n = 9$). (C) Replacement of intracellular K^+ with Cs^+ failed to block DHPG-induced currents ($n = 23$). (D) Removal of both extracellular Na^+ and Ca^{2+} prevented DHPG-induced inward currents ($n = 8$). (E) Summary data for A-D. (F) Voltage-ramps before and after application of DHPG ($n = 12$). (G) Average DHPG-induced net current obtained from subtracting control from DHPG currents in F. Shaded region indicates S.E.M.

presence of DHPG. I_{Net} had experimental reversal potential of $-48.7 \pm 2.0 \text{ mV}$ ($n = 12$).

This reversal potential is not near an expected potential for any one ion species and supports a role for a non-selective cation channel (NSCC) in DHPG-induced inward currents.

To further establish the involvement of a NSCC in DHPG-induced currents, we made voltage-clamp recordings using various pharmacological inhibitors. We used a Cs^+ -containing internal solution to isolate only cation influx. Pretreatment and bath application of slices with the NSCC blocker flufenamic acid (FFA, $100 \mu\text{M}$) prevented

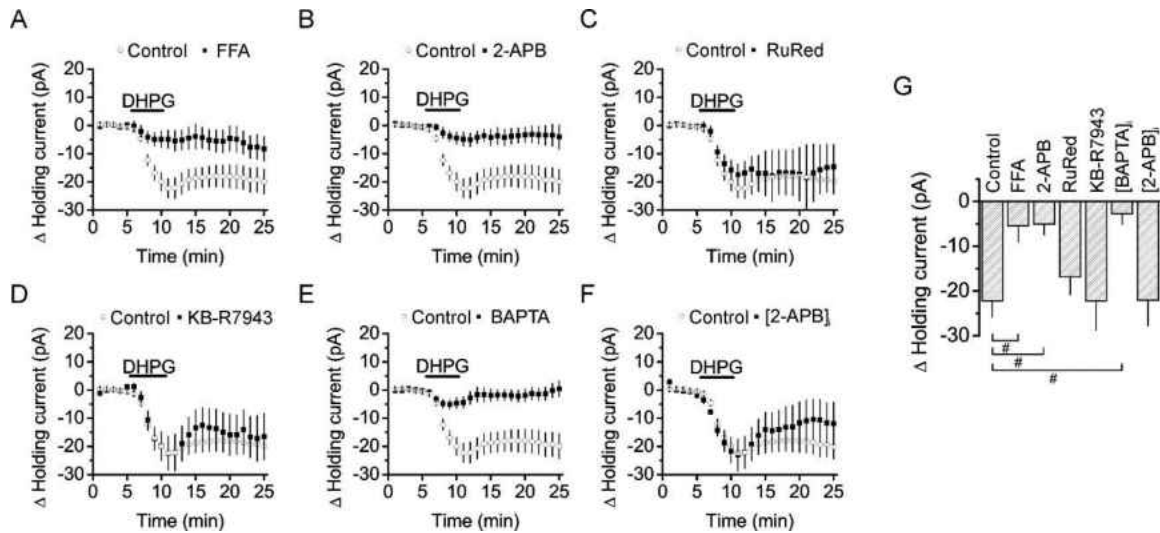


Figure 22. DHPG-induced currents require Ca^{2+} signaling but not Ca^{2+} release and are sensitive to NSCC blockers. (A) The NSCC blocker FFA (100 μM) prevented DHPG-induced currents ($n = 9$). (B) Another NSCC blocker 2-APB (100 μM) prevented DHPG-induced currents ($n = 11$). (C) The selective TRPV blocker did not affect DHPG-induced currents ($n = 8$). (D) Blockade of NCX did not prevent DHPG-induced currents ($n = 7$). (E) Intracellular BAPTA prevented DHPG-induced currents, indicating a role for Ca^{2+} signaling ($n = 7$). (F) Intracellular application of 2-APB (100 μM) did not prevent DHPG-induced currents, suggesting Ca^{2+} release is not involved ($n = 5$). (G) Summary figure for A-F. # $P < 0.05$ vs. Control, One-Way ANOVA with Tukey

DHPG-induced currents (-5.4 ± 3.6 pA, $n = 9$, $P = 0.17$ vs. baseline, $P < 0.05$ vs. control, Fig. 22A and G). Pretreatment with and continuous bath application of another NSCC blocker 2-aminoethoxydiphenylborane (2-APB, 100 μM) prevented DHPG-induced inward currents (-5.1 ± 2.4 pA, $n = 11$, $P = 0.06$ vs. baseline, $P < 0.05$ vs. control, Fig. 22B and G). Application of DHPG to slices pretreated and continuously exposed to the selective TRPV cation channel inhibitor ruthenium red (RuRed, 20 μM) continued to induce a significant inward current (-16.8 ± 4.0 pA, $n = 8$, $P = 0.004$ vs. baseline, $P > 0.05$ vs. control, Fig. 22C and G), suggesting TRPV channels are not the involved NSCC. Because group I mGluRs increase activation of the electrogenic NCX (Keele et al., 1997;

Huang and van den Pol, 2007) which would be affected by removal of extracellular Na^+ , we next tested whether NCX may be involved in DHPG-induced currents. When slices were pretreated with and continuously exposed to the selective NCX inhibitor KB-R7943 (20 μM), DHPG continued to elicit a significant inward current (-22.2 ± 6.5 pA, $n = 7$, $P = 0.01$ vs. baseline, $P > 0.05$ vs. control, Fig. 22D and G). Because NSCCs can be Ca^{2+} -dependent, we tested a role for intracellular Ca^{2+} . Inclusion of BAPTA (25 mM) inside the pipette blocked DHPG-induced currents (-2.8 ± 2.3 pA, $n = 7$, $P = 0.28$ vs. baseline, $P < 0.05$ vs. control, Fig. 22E and G). To test if intracellular Ca^{2+} release via IP_3 receptors was involved, we patched cells with 2-APB (100 μM) inside the pipette. Under these conditions, DHPG continued to induce a significant inward current (-22.1 ± 5.7 pA, $n = 5$, $P = 0.02$ vs. baseline, $P > 0.05$ vs. control, Fig. 22F and G). These results suggest that DHPG-induced inward currents are mediated by non-TRPV-containing NSCCs that requires intracellular Ca^{2+} signaling.

Group I mGluRs Activate a TRPC-Like Conductance That May Involve TRPC1, TRPC4, and TRPC5

A candidate group of NSCCs for DHPG-induced currents are TRPC channels because these channels are sensitive to FFA, 2-APB, and require intracellular Ca^{2+} signaling. Trivalent lanthanides are NSCC blockers but augment currents of some TRPC channels (TRPC4/5), making them a useful tool to probe for certain TRPCs. We therefore tested the sensitivity of DHPG-induced currents to La^{3+} (100 μM). After obtaining a stable baseline, DHPG was applied for 10 minutes to ensure the maximal effect had been achieved. DHPG induced a significant inward current of -25.8 ± 3.8 pA ($n = 13$, $P = 0.00001$ vs. baseline, Fig. 23A). We subsequently applied La^{3+} in the presence of DHPG for an additional 10 minutes. At 8 minutes into application, the inward current

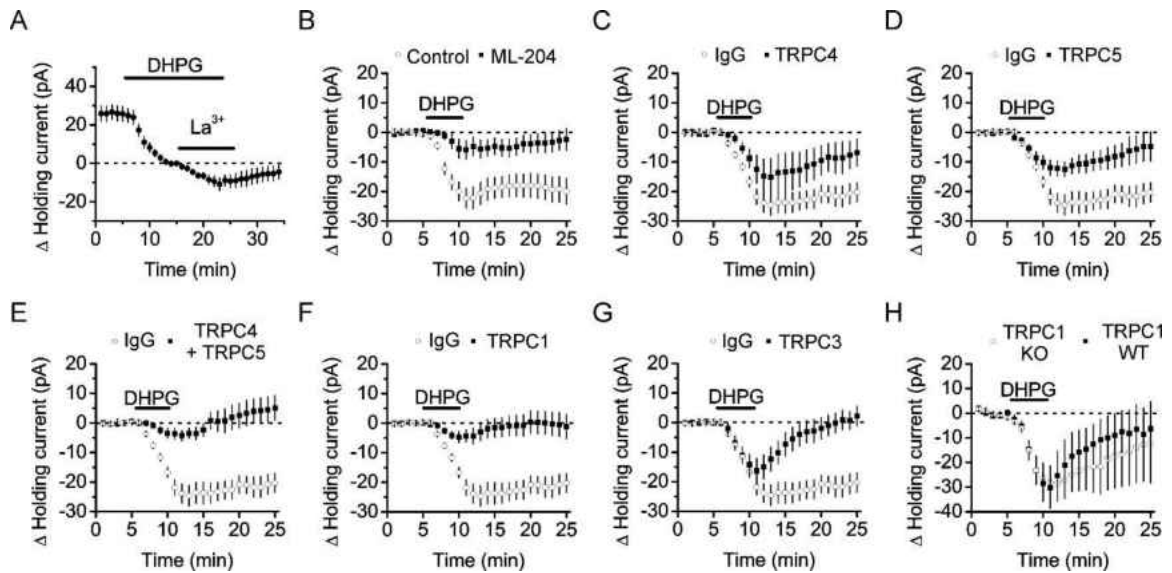


Figure 23. DHPG-induced currents involve a TRPC-like conductance that involves TRPC4 and TRPC5. (A) Following 10 min of DHPG application, subsequent application of La^{3+} (100 μM) potentiated DHPG-induced currents. ($n = 13$). (B) The selective TRPC4/5 channel blocker ML-204 (50 μM) prevented DHPG-induced currents ($n = 10$). (C) Intracellular application of antibodies targeting an intracellular TRPC4 epitope did not prevent DHPG-induced currents compared to control IgG ($n = 7$). (D) Intracellular application of antibodies targeting an intracellular TRPC5 epitope did not prevent DHPG-induced currents compared to control IgG ($n = 9$). (E) Co-administration of both TRPC4 and TRPC5 antibodies significantly reduced DHPG-induced currents compared to control IgG ($n = 9$). (F) Intracellular application of antibodies targeting an intracellular TRPC1 epitope significantly reduced DHPG-induced currents compared to control IgG ($n = 11$). (G) Intracellular application of antibodies targeting an intracellular TRPC3 epitope did not prevent DHPG-induced currents compared to control IgG ($n = 7$). (H) DHPG continued to induce a significant inward current in both TRPC1 KO ($n = 6$) and WT ($n = 7$) mice.

was potentiated to a maximal value of -10.9 ± 3.8 pA ($n = 13$, $P = 0.004$ vs. DHPG, Fig. 23A). These experiments were carried out using a HEPES-based extracellular solution to prevent the precipitation of La^{3+} . Because La^{3+} potentiated rather than blocked DHPG-induced currents, we suspected a role for TRPC4/5 subunits. To test this hypothesis, we used an antagonist selective for TRPC4 and, to lesser extent, TRPC5

channels (Miller et al., 2011). In the presence of ML-204 (50 μ M), DHPG failed to induce a significant inward current (-5.5 ± 3.2 pA, $n = 10$, $P = 0.12$ vs. baseline, Fig. 23B). We next applied antibodies (4 μ g/ μ L) targeting intracellular epitopes of TRPC channels to probe their involvement in DHPG-induced currents. We waited 20-30 minutes after patching the cells to allow for dialysis of antibodies into the cell. Application of DHPG to cells patched with control IgG antibodies in the pipette continued to elicit a significant inward current of -23.9 ± 3.2 pA ($n = 10$, $P = 0.00004$ vs. baseline, Fig. 23C-G). DHPG continued to induce a significant inward current in cells patched with antibodies directed at TRPC4 (-14.8 ± 5.7 pA, $n = 7$, $P = 0.04$ vs. baseline, $P > 0.05$ vs. IgG, Fig. 23C), TRPC5 (-12.2 ± 2.6 pA, $n = 9$, $P = 0.002$ vs. baseline, $P > 0.05$ vs. IgG, Fig. 23D), and TRPC4 and TRPC5 together (-4.3 ± 1.7 pA, $n = 9$, $P = 0.04$ vs. baseline, Fig. 23E). DHPG-induced current was reduced compared to control only when both TRPC4 and TRPC5 antibodies were administered ($P < 0.05$ vs. IgG, Fig. 23E), implicating the involvement of both subunits. Because TRPC4 and TRPC5 can form heteromeric channels with TRPC1, we also looked at a role for TRPC1. Application of DHPG to cells patched with TRPC1 antibodies failed to elicit a significant inward current (-4.4 ± 2.6 pA, $n = 11$, $P = 0.13$ vs. baseline, $P < 0.05$ vs. IgG, Fig. 23F), indicating TRPC1 is also involved. We also considered a role for TRPC3 because this subunit can also interact with TRPC1. DHPG continued to elicit a significant inward current in cells patched with antibodies targeting TRPC3 (-15.0 ± 4.0 pA, $n = 7$, $P = 0.01$ vs. baseline, $P > 0.05$ vs. IgG, Fig. 23G), suggesting these channels alone are not significantly involved. Taken together, these results strongly indicate a role for TRPC 1/4/5-containing heteromeric channels in DHPG-induced currents.

Because antibodies targeting TRPC1 were sufficient to block DHPG-induced currents, we next used a knock-out mouse to further test the involvement of TRPC1. Application of DHPG induced a significant inward current in cells of slices prepared from either wild-type (WT, -25.3 ± 9.9 pA, $n = 7$, $P = 0.04$ vs. baseline, Fig. 23H) or knock-out mice (KO, -28.5 ± 7.2 pA, $n = 6$, $P = 0.01$ vs. baseline, $P = 0.80$ vs. WT, Fig. 23H). These results might suggest that either TRPC1 is not involved in DHPG-induced currents or some compensatory change has occurred during development that enables DHPG-currents to persist.

Because the pharmacological and antibody dialysis evidence supported a role for both TRPC4 and TRPC5 channels in DHPG-induced currents, we employed an shRNA knock-down strategy using an organotypic slice model of the MEC. Transfection of MEC cultured slices with shRNAs against TRPC4 (indicated by a RFP marker) or TRPC5 (indicated by a GFP marker) demonstrate a high degree of co-transfection of layer III principal neurons (Fig. 24A). We validated both shRNAs in HEK-239 cells co-transfected with appropriate TRPC channel (Fig. 24B). Application of DHPG for 7 minutes to slices co-transfected with scramble shRNA controls carrying either RFP or GFP markers induced a significant inward current of -22.4 ± 3.2 pA ($n = 10$, $P = 0.00006$ vs. baseline, Fig. 24C). Application of DHPG to co-transfected slices with shRNAs targeting both TRPC4 (RFP marker) or TRPC5 (GFP marker) still induced a significant inward current (-14.2 ± 3.7 pA, $n = 10$, $P = 0.004$ vs. baseline, Fig. 24C). Although no significant difference in maximal DHPG-induced current was seen ($P = 0.11$ vs. scramble), there was a significant difference in the time course of DHPG-induced current in knock-down slices ($P < 0.05$, two-way ANOVA, Fig. 24C). When slices were co-

transfected with rTRPC5 + GFP (Fig. 24D), DHPG elicited a significantly larger inward current (-29.7 ± 5.2 pA, $n = 5$, $P = 0.005$ vs. baseline, $P = 0.01$ vs. non-transfected, Fig. 24E) compared to non-transfected cells (-10.7 ± 3.1 pA, $n = 5$, $P = 0.03$ vs. baseline, Fig. 24E). These results confirm that endogenous activation of group I mGluRs in layer III of the MEC couple to TRPC5.

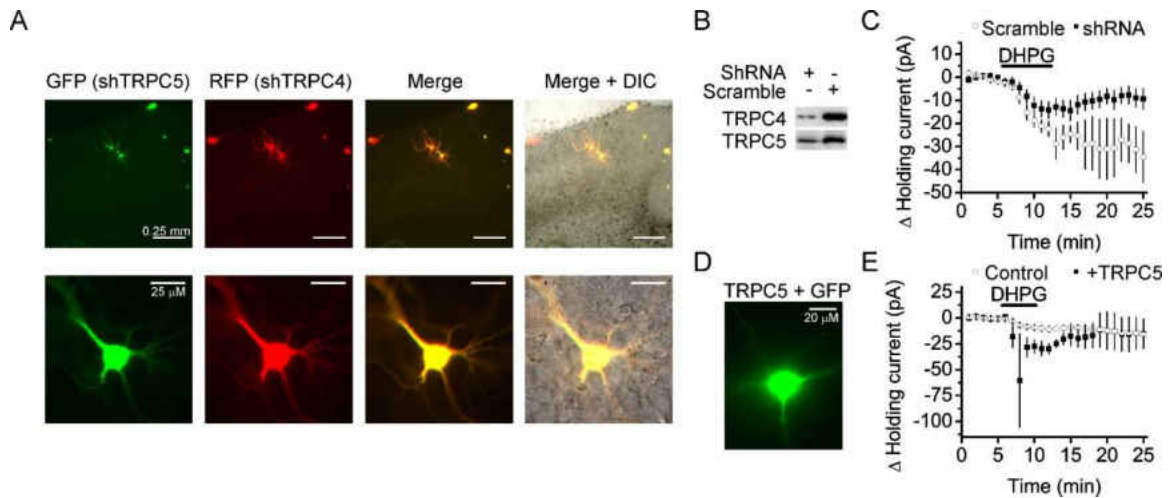


Figure 24. Knock-down of TRPC4 and TRPC5 did not reduce maximal DHPG-induced currents and endogenous group I mGluRs couple to TRPC5. (A) Representative example of a cultured MEC slice that was transfected with shRNAs for TRPC5 (GFP) and TRPC4 (RFP). (B) Western blot analysis of TRPC4 and TRPC5 from HEK-293 lysates that were co-transfected with TRPC4 or TRPC5 and either the appropriate shRNA or scramble shRNA corresponding to the respective channel. (C) Summary data of DHPG-induced currents from both scramble-transfected and shRNA-transfected MEC slices. ($n = 10$, each). (D) Representative MEC layer III cell transfected with both GFP and TRPC5. (E) Summary data of DHPG-induced currents from either control non-transfected slices or slices over-expressing TRPC5 ($n = 5$, each).

CHAPTER VI

DISCUSSION

Study 1 – Dopaminergic Modulation of MEC GABAergic Transmission

Our results demonstrate that DA increases the frequency without affecting the amplitude of sIPSCs and mIPSCs in the MEC. The effects of DA are not mediated by DA receptors, but by α_1 adrenoreceptors. Endogenously released DA exerts the same effects on GABAergic transmission. DA-induced increases in the frequencies of sIPSCs and mIPSCs are due to DA-mediated depolarization of GABAergic interneurons resulting in the facilitation of AP firing frequency and the activation of T-type Ca^{2+} channels. DA-mediated depolarization of interneurons is caused by the inhibition of Kirs (Fig. 25).

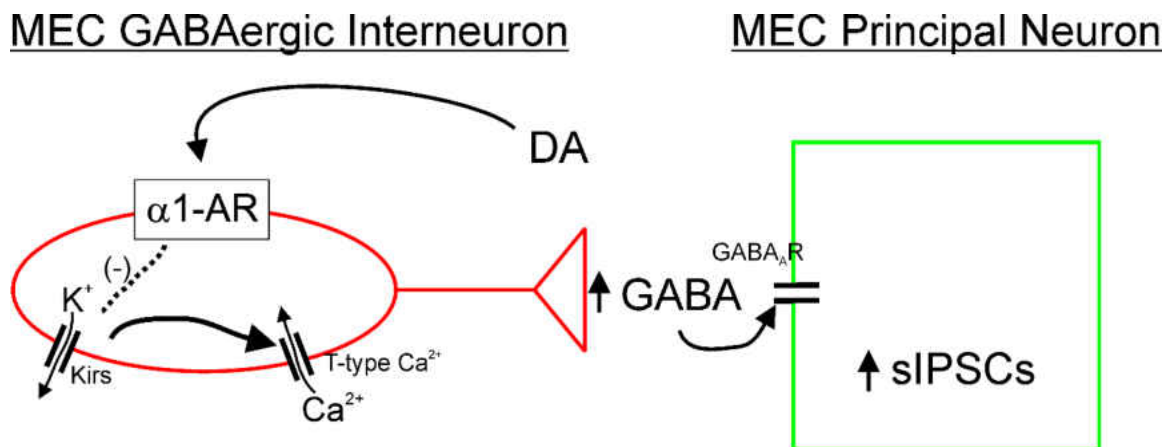


Figure 25. Summary figure for Study 1. Dopamine activates α_1 adrenoreceptors (α_1 -AR) on MEC local interneurons. This activation results in the inhibition of Kirs, via an unknown mechanism. Inhibition of Kirs results in membrane depolarization that enables activation of t-type Ca^{2+} channels, which facilitates GABAergic transmission secondarily to inhibition of Kirs-induced increases in interneuron excitability. The net result is an increase in GABAergic transmission onto the superficial principal MEC cells.

DA-Induced Facilitation of Transmitter Release Involves T-Type Ca²⁺ Channels Secondary to RMP Depolarization

DA increases the frequencies of sIPSCs and mIPSCs with no effects on their amplitudes in the MEC. These results indicate that DA increases presynaptic GABA release with no effects on postsynaptic GABA_A receptors. Because sIPSCs are usually considered to be AP-dependent, whereas mIPSCs recorded in the presence of TTX are not, our results suggest that DA facilitates GABA release at least in part by an AP-independent mechanism. Because DA-mediated increases in the frequencies of sIPSCs and mIPSCs are dependent on extracellular Ca²⁺, we examined the involvement of voltage-gated Ca²⁺ channels. Bath application of Cd²⁺, a blocker of high-threshold voltage-gated Ca²⁺ channels, failed to block DA-mediated increases in the frequencies of sIPSC and mIPSC, whereas application of Ni²⁺ and mibefradil—two blockers of T-type Ca²⁺ channels—significantly reduced DA-induced facilitation of the frequency of sIPSCs and mIPSCs, indicating the involvement of T-type Ca²⁺ channels. Furthermore, whereas DA depolarizes GABAergic interneurons, T-type Ca²⁺ channels are not required for DA-induced depolarization of interneurons because bath application of Ni²⁺ did not alter DA-mediated depolarization. Our results therefore suggest that DA depolarizes interneurons, which in turn facilitates the activity of T-type Ca²⁺ channels. Increased influx of Ca²⁺ through T-type Ca²⁺ channels leads to increases in GABA release.

T-type Ca²⁺ channels are low-voltage-activated Ca²⁺ channels that control Ca²⁺ entry in excitable cells during small depolarization above resting potentials. For example, sustained depolarization generated by elevation of extracellular K⁺ concentration (Barish, 1991; Varnai et al., 1995; Bao et al., 1998; Boyer et al., 1998; Jensen et al., 2004) or direct neuronal depolarization (Varnai et al., 1995; Lu et al., 1997; Kawai and Miyachi,

2001; Pan et al., 2001; Bessaih et al., 2008) activates T-type Ca^{2+} channels. Although bath application of DA increases the firing frequency of APs when the membrane potential of the interneurons is raised above threshold by injection of positive current, application of DA is incapable of inducing APs when interneurons are at rest. Under our recording conditions, interneurons rest negative to -60 mV and the average depolarization generated by DA is approximately 3–4 mV. The threshold for AP firing in the interneurons is at least positive to -50 mV. Therefore, DA makes little contribution to increasing the firing rate of the interneurons at rest. However, DA-induced, small subthreshold depolarization would likely shift the activation curve of T-type Ca^{2+} channels to the direction of negative potentials (Varnai et al., 1995) thereby increasing Ca^{2+} influx. Ca^{2+} influx via T-type Ca^{2+} channels has been shown to facilitate the release of neurotransmitters including GABA (Carbone et al., 2006).

Our results do not support a role of nonselective cation channel activation in DA-induced depolarization of interneurons. If opening of a nonselective cationic conductance is responsible for DA-induced facilitation of GABA release, the influxes of extracellular Na^+ and Ca^{2+} should be the major cations to mediate the depolarization of interneurons. The result that substitution of extracellular NaCl with NMDG-Cl failed to alter DA-induced depolarization does not support a role for Na^+ in DA-induced depolarization of interneurons. However, our results suggest a role for extracellular Ca^{2+} influx in DA-mediated enhancement of GABA release, because depletion of extracellular Ca^{2+} blocked DA-induced increases in the frequencies of sIPSCs and mIPSCs. Because exclusion of extracellular Ca^{2+} does not alter the DA-induced depolarization of interneurons, the effects of Ca^{2+} are likely secondary to DA-induced depolarization. Our results that

blocking T-type Ca^{2+} channels reduces DA-induced increases in the frequencies of sIPSCs and mIPSCs, but does not alter DA-mediated depolarization of interneurons, indicate that the required Ca^{2+} is through T-type Ca^{2+} channels secondary to membrane depolarization.

Activation of D_1 -like receptors in the pyramidal neurons of the EC generates membrane hyperpolarization via the activation of I_h channels (Rosenkranz and Johnston, 2006). Our results do not support a role of I_h channels in DA-induced facilitation of GABA release based on the following lines of evidence. First, at the RMP (~ -60 mV) of the interneurons, I_h channels should be open. If I_h channels are involved, DA should increase the function of I_h channels to generate membrane depolarization. Bath application of the I_h channel blocker, ZD7288, should block DA-induced depolarization. However, bath application of DA still induced a comparable depolarization in the presence of ZD7288. Secondly, if I_h channels are involved, influx of Na^+ should be responsible for depolarization. However, replacing extracellular Na^+ with NMDG did not alter DA-induced depolarization. Thirdly, whereas Type II interneurons exhibit a sag response that is generated by the activation of I_h channels, Type I do not show noticeable sag, suggesting that Type I interneurons do not express I_h channels. However, DA depolarizes both Type I and Type II interneurons, suggesting that I_h channels are not responsible for DA-induced depolarization. Fourthly, if I_h channels are involved, DA-mediated activation of I_h channels should reduce the input resistance. Nevertheless, application of DA increases the input resistance further excluding the contribution of I_h channels. Therefore, we conclude that the depolarization of interneurons is largely independent of cation influx.

Promiscuous Activity of DA Linked to Inhibition of Kirs

Our results support a role of Kirs in DA-induced depolarization of interneurons based on the following pieces of evidence. First, the reversal potential of DA-generated currents is close to the K^+ reversal potential. Secondly, replacement of intracellular K^+ with NMDG blocked DA-induced depolarization. These two lines of evidence buttress the involvement of K^+ channels. Thirdly, the I-V relationship of the DA-induced current exhibits an inward rectification. Fourthly, bath application of Ba^{2+} , a Kir blocker, annuls the DA-induced depolarization of interneurons and the facilitatory effects of DA on sIPSCs and mIPSCs, further supporting the participation of Kirs. Whereas the results that application of SCH23390 blocks both DA-mediated increases in sIPSC frequency and DA-mediated depolarization of interneurons could be explained either by the involvement of D_1 -like receptors or by SCH23390-mediated blockade of Kirs, our results support the latter. If the blocking effects of SCH23390 are mediated by blockade of D_1 -like receptors, application of the selective D_1 -like receptor agonists should also exert the same actions as DA. However, our results showed that application of D_1 -like receptor agonists or co-application of the agonists for D_1 - and D_2 -like receptors failed to have any effects on sIPSCs and the RMPs of the interneurons, suggesting that the blocking effects of SCH23390 are not mediated by interaction with D_1 -like receptors. Coincidentally, we found that DA generates membrane depolarization in the MEC interneurons via inhibition of Kirs, which can be blocked by SCH23390 (Kuzhikandathil and Oxford, 2002; Shankar et al., 2004; Sosulina et al., 2008; Chee et al., 2011). Further evidence to support the idea that the effects of SCH23390 were mediated by blocking Kirs instead of D_1 -like receptors is that application of a structurally distinct D_1 receptor antagonist,

LE300, failed to prevent DA-induced facilitation of sIPSC frequency. Moreover, the results that DA-induced facilitation of sIPSCs and mIPSCs and depolarization of interneurons are blocked by application of α_1 adrenoreceptor antagonists suggest that D₁-like receptors are not involved. Our results demonstrate that DA depolarizes GABAergic interneurons via α_1 receptor-mediated inhibition of Kirs. Consistent with our findings, DA has been shown to inhibit Kirs (Gorelova et al., 2002; Dong et al., 2004; Witkowski et al., 2008; Govindaiah et al., 2010; Podda et al., 2010). Different from our results is that application of the D₁-like receptor agonists in these studies exerts the same actions as DA, suggesting the involvement of D₁-like receptors.

Whereas our results demonstrate that DA facilitates GABAergic transmission via activation of α_1 adrenoreceptors, there are still differences between the effects of DA and norepinephrine, which also facilitates GABAergic transmission in the MEC. First, DA increases only the frequency of sIPSCs, whereas norepinephrine facilitates both the frequency and amplitude of sIPSCs. Secondly, extracellular Ca²⁺ is required for DA-induced increases in the frequency of sIPSCs and mIPSCs, but not required for the effects of norepinephrine on GABA release. Thirdly, DA transiently increases the action potential firing frequency in interneurons, whereas norepinephrine has no obvious effects on the firing frequency of action potentials and holding currents recorded from the interneurons. Several mechanisms can be proposed to explain the discrepancy between the effects of DA and those of norepinephrine on GABAergic transmission. First, norepinephrine interacts with many different types of receptors including α_1 , α_2 , and β adrenoreceptors as well as D₂ DA receptors (Robbins et al., 1988), whereas DA activates α_1 , α_2 , and β adrenoreceptors (Rajfer et al., 1988; Anfossi et al., 1993; Lee et al., 1998;

Ouedraogo et al., 1998; Ooi and Colucci, 2001; Cornil et al., 2002) in addition to activating DA receptors. Activation of these receptors likely produces distinct or even opposite effects. Whereas our previous results demonstrate a role for α_1 receptors in norepinephrine-induced facilitation of GABAergic transmission in the MEC, the permissive or shrouded roles of other receptors activated by norepinephrine are unknown. Secondly, there are several different subtypes of α_1 adrenoreceptors. As demonstrated previously (Rey et al., 2001), norepinephrine and DA may activate distinct subtypes of α_1 receptors. Thirdly, whereas DA and norepinephrine exert promiscuous effects on different receptors, there are significant differences with regard to the affinities of the receptors activated by DA and norepinephrine. For example, DA has only 1 of 50 the affinity of norepinephrine for α_1 receptors (Leedham and Pennefather, 1986). Receptors activated by distinct agonists of different affinities likely generate distinguishable intracellular signaling events resulting in dissimilar actions. Lastly, although our results do not support a role for D₁- and D₂-like receptors in the effects of DA on GABAergic transmission, it is still possible that DA modulates GABAergic transmission by a cooperative effects on α_1 , D₁, and D₂ receptors because there is strong evidence demonstrating an interaction of α_1 , D₁, and D₂ receptors (Gioanni et al., 1998; Wadenberg et al., 2000; Stuchlik et al., 2008).

Synaptic DA concentrations can reach approximately 100 μ M (Ford et al., 2009). At this concentration, DA or DA receptor agonists have been reported to increase sIPSC frequency in the lateral amygdala (Lorétan et al., 2004), cerebral cortex (Zhou and Hablitz, 1999; Seamans et al., 2001), and thalamus (Munsch et al., 2005). In the MEC, the effect of DA on GABAergic transmission was reliably observed when DA was

applied at a concentration range of 3–100 μ M. In the present study, we performed a series of experiments to test the role of endogenously released DA in modulating GABAergic transmission. We initially tried to elevate synaptic DA concentration by bath application of the DAT inhibitor, GBR 12935. However, bath application of the DAT inhibitor failed to increase the frequency of sIPSCs significantly. One explanation is that there is no tonic DA release at the dopaminergic projections in the EC possibly due to the severing of the terminals from their somas in our slice preparation. We also used AMPH, a drug that promotes DA efflux via interaction with the DAT (Leviel, 2011). Bath application of AMPH increases the sIPSC frequency and the effect of AMPH is almost completely abolished by application of GBR 12935, suggesting that the effect of AMPH is mediated by increasing endogenous DA efflux. We further demonstrate that bath application of α_1 receptor antagonist block AMPH-induced increases in the frequency of sIPSCs, whereas application of the inhibitor for the norepinephrine transporter failed to affect the effect of AMPH. These results together indicate that endogenously released DA is capable of facilitating GABA release in the EC.

DA and MEC GABAergic System: Functional Implications

In the MEC, DA usually exerts an overall inhibitory effect. For example, DA has been shown to inhibit the excitability of pyramidal neurons (Rosenkranz and Johnston, 2006; Mayne et al., 2013), excitatory synaptic transmission (Pralong and Jones, 1993; Stenkamp et al., 1998; Behr et al., 2000; Caruana and Chapman, 2008), and synaptic plasticity (Caruana et al., 2007). DA has bidirectional effects on excitatory synaptic transmission with low concentrations enhancing, and high concentrations depressing it (Caruana et al., 2006). Consistent with the generally inhibitory roles of DA in the MEC,

our results indicate that DA facilitates GABA release. GABAergic transmission in the MEC synchronizes neural network activities and serves as the precision clockwork for gamma and theta oscillations (Cutsuridis and Hasselmo, 2012). Neural oscillatory events are thought to be crucially involved in various cognitive processes. Because the functions of the EC are closely related to the processes of learning and memory (Steffenach et al., 2005), Alzheimer's disease (Hyman et al., 1984) and schizophrenia (Prasad et al., 2004), DA-mediated modulation of GABAergic transmission would likely play a role in the modification of these physiological functions and neurological diseases.

In conclusion, our results demonstrate that DA facilitates the frequency of sIPSCs and mIPSCs, indicating that DA increases GABA release in the MEC. The facilitatory effects of DA are not mediated by DA receptors but via the activation of α_1 adrenergic receptors. DA inhibits Kirs to generate a small depolarization of GABAergic interneurons resulting in facilitation of T-type Ca^{2+} channels. Our results have revealed a collaborative role of α_1 adrenoreceptors, Kirs, and T-type Ca^{2+} channels in DA-induced augmentation of GABA release in the MEC.

Study 2 – Histaminergic Modulation of MEC GABAergic Transmission

We demonstrate that HA increased the frequency but not the amplitude of sIPSCs recorded from principal neurons in each layer of the MEC. HA-mediated facilitation of spontaneous GABAergic transmission was AP-dependent and required the influx of extracellular Ca^{2+} . Application of HA decreased the input resistance and induced significant subthreshold depolarization in both Type I and Type II interneurons. Activation of H_1 or H_2 was sufficient to significantly augment sIPSCs and combination of both H_1 and H_2 antagonists blocked the effect of HA. Conversely, activation of H_3

slightly, but significantly, reduced sIPSCs whereas application of the H₃ antagonist did not significantly affect HA-elicited augmentation of sIPSCs. Both H₁ and H₂ were expressed on GABAergic interneurons, as well as on principal neurons, of the MEC and HA-induced increases in the excitability of interneurons involved both H₁ and H₂. Because HA-induced net currents in both Type I and Type II interneurons were largely inward and did not reverse near an expected reversal potential for one ion, we concluded that a mixed ionic mechanism is responsible for HA-elicited increases in interneuron excitability. Accordingly, we found that HA-induced depolarization of Type II interneurons was due partially to the opening of a TTX-insensitive Na⁺ permeable cation channel and HA inhibited both I_K and Cs⁺-sensitive Kirs in Type I and Type II interneurons. Finally, extracellular Cs⁺ inhibited interneuron depolarization and blocked HA-induced increases in sIPSC frequency, whereas HA-induced increases in sIPSCs were not sensitive to Ih blocker ZD7288, suggesting that the effect of extracellular Cs⁺ is on Kirs and not on Ih channels. Taken together, our results strongly indicate that both H₁ and H₂ mediate HA-induced increases in GABAergic transmission in the MEC via excitation of local interneurons and HA-induced inhibition of Cs⁺-sensitive Kirs in GABAergic interneurons contributes to the facilitatory action of HA on sIPSCs (Fig. 26).

Modulation of synaptic transmission can occur by changes in presynaptic transmitter release and/or the functions or numbers of postsynaptic receptors. Our results demonstrate that HA-dependent increases in spontaneous GABAergic transmission in the MEC are mediated by increased excitability of GABAergic interneurons based on the following lines of evidence. First, changes in frequency, but not amplitude, of

MEC GABAergic Interneuron

MEC Principal Neuron

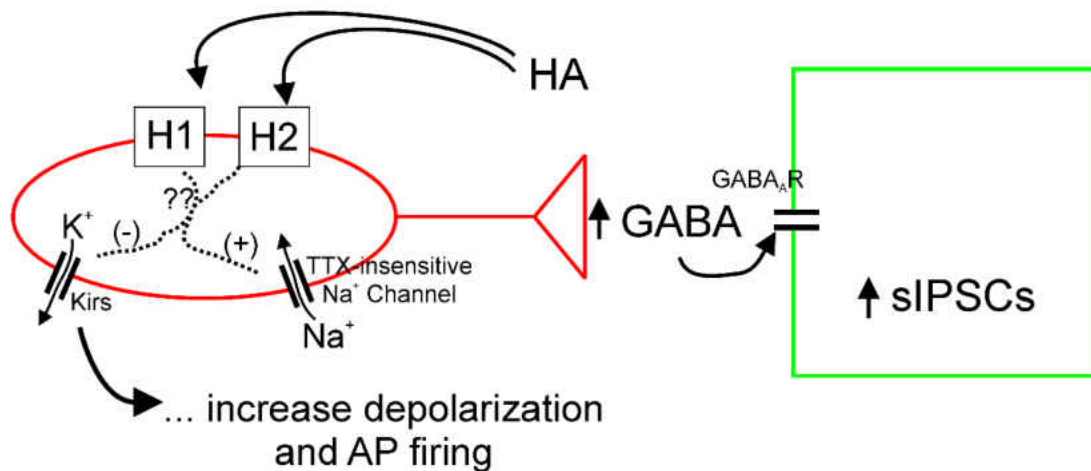


Figure 26. Summary figure for Study 2. Application of HA results in activation of both interneuron expressing H1 and H2 to induce increased interneuron excitability. Increases in excitability occur via activation of a TTX-insensitive Na⁺ channel and inhibition of Cs⁺-sensitive Kirs, although the precise signaling mechanism downstream of receptor activation remains unknown. This increased excitability increases action potential generation and results in elevated GABAergic transmission onto superficial principal neurons.

spontaneous synaptic events typically connote a presynaptic locus of action (Yang and Calakos, 2013). Our experiments showed a consistent increase in the frequency of sIPSCs whereas changes in amplitude were varied and insignificant. Second, application of HA in the presence of TTX to block AP generation did not produce any changes in the frequency or amplitude of mIPSCs. This indicates that HA-induced increases in spontaneous GABAergic transmission are dependent on the generation of presynaptic APs. Consistent with a role for AP generation, removal of extracellular Ca²⁺ also blocked HA-dependent increases in sIPSCs, suggesting that the action of HA lies upstream of Ca²⁺ influx, possibly at the level of AP initiation. Third, if HA increases GABAergic transmission by increasing interneuron excitability, recordings from local interneurons should reveal elevations of intrinsic excitability following HA application. Direct

recordings from interneurons in the presence of TTX showed HA-dependent increases in excitability as illustrated by HA-induced depolarization and generation of an inward holding current in both Type I and Type II interneurons, as well as increased AP firing of Type II interneurons in the presence of synaptic blockers. Fourth, HA-induced increases in GABAergic transmission via facilitation of interneuron excitability would require that HA receptors be expressed on GABAergic interneurons. Our immunostaining demonstrated a clear somatic co-localization of H₁ or H₂ with GAD-67, a marker of GABAergic interneurons. Furthermore, our recordings demonstrated that HA directly increased the excitability of local interneurons via activation of H₁ and H₂ receptors. Finally, if HA enhances spontaneous GABAergic transmission in the MEC via a postsynaptic mechanism, postsynaptic HA receptors, which are G protein-coupled, should be involved. However, inclusion of GDP- β -S in the recording pipettes did not prevent HA-induced increases in sIPSCs, suggesting that it is unlikely that HA increased GABAergic transmission by interacting with postsynaptic GABA_A receptors. In the medium septum, HA facilitates GABAergic neurons indirectly by increasing acetylcholine release (Xu et al., 2004). However, such an indirect mechanism is unlikely in the MEC because application of HA in the presence of TTX, which non-discriminately blocks synaptic transmission, still induced remarkable interneuron depolarization. We therefore conclude that HA directly facilitates the excitability of GABAergic interneurons in the MEC to increase action potential firing and GABAergic output.

HA increases interneuron excitability and GABAergic transmission via activation of both H₁ and H₂, whereas application of a H₃-selective agonist reduced GABAergic transmission. Consistent with our results, HA has been shown to increase neuronal

excitability by activation of either H₁ or H₂ or both H₁ and H₂ receptors in a variety of brain regions including the thalamus (McCormick and Williamson, 1991), neostriatum (Munakata and Akaike, 1994), ventrolateral preoptic nucleus (Liu et al., 2010), and vestibular nucleus (Zhang et al., 2013b). Evidence supporting the involvement of both H₁ and H₂ receptors in the MEC is provided by our immunohistochemical staining and the requirement of both H₁ and H₂ antagonists to block HA-induced interneuron depolarization and facilitation of sIPSCs. It is difficult to conclude whether H₁ and H₂ receptors are colocalized to the same MEC interneurons because sIPSCs reflect inputs presumably from many GABAergic interneurons. Our data may hint at such a possibility but more evidence is necessary to unequivocally reach this conclusion.

*Ionic Mechanisms Mediating HA-Induced
Increased Excitability of Interneurons*

The ionic mechanisms underlying HA-induced increases in interneuron excitability in the MEC appear to involve both the activation of a TTX-insensitive Na⁺ channel and the inhibition of a K⁺ conductance. This conclusion is based on the following lines of evidence. First, the HA-induced net current in both Type I and Type II interneurons was predominantly inward across the range of the voltage ramp protocol and the reversal potentials for the net current did not conform to one permeating ion species. Second, the opening of cation channels is consistent with the significantly reduced input resistance observed in both types of interneurons following application of HA. Third, replacement of extracellular NaCl with NMDG-Cl or the same solution containing no extracellular Ca²⁺ significantly reduced HA-induced depolarization, confirming a partial role for cation influx. However, a significant depolarization in response to HA was still detected in both solutions, suggesting the contribution of K⁺ channel inhibition. Fourth,

recording K^+ currents demonstrated that HA inhibited both I_K and Cs^+ -sensitive $Kirs$. Lastly, our results that HA-induced depolarization of interneurons was sensitive to extracellular Cs^+ , which blocks several K^+ channels and I_h , but was insensitive to the selective I_h channel blocker, ZD7288, implicate the inhibition of Cs^+ -sensitive K^+ channels in HA-induced depolarization. Because inclusion of Cs^+ in the extracellular solution blocked HA-induced inhibition of $Kirs$ but had no effects on HA-mediated depression of I_K , these results further suggest that inhibition of $Kirs$ may underlie HA-induced depolarization of MEC interneurons. In line with our results, $Kirs$ are involved in controlling RMPs whereas I_K are largely responsible for the AP shapes. Consistent with our study, a mixed ionic mechanism including activation of a TTX-insensitive Na^+ channel and inhibition of $Kirs$ has been identified to explain HA-induced depolarization of cholinergic neurons in the medial septum (Gorelova and Reiner, 1996).

Our results demonstrate a partial role for Na^+ -permeable cation channels in HA-mediated depolarization of entorhinal interneurons but the identity of the involved cation channels have not been determined. Whereas HA has been reported to modulate neuronal excitability via changes in Na^+ -conducting I_h channels (McCormick and Williamson, 1991; Zhang et al., 2013b) and I_h channels are found in cortical interneurons similar to Type I and II interneurons described in this study (Williams and Hablitz, 2015), our results do not support a role for I_h channels because ZD7288, a selective I_h channel blocker, was unable to block either HA-induced interneuron depolarization or increases in sIPSCs. Several alternative mechanisms for cation influx are worth consideration. First, the Na^+ -permeable TRPC4/5 channels have been proposed in H_1 -mediated regulation of neuronal excitability (Hardwick et al., 2005). Because TRPC4/5 channels

are potentiated by Gd^{3+} or La^{3+} (Strübing et al., 2001), our results that application of Gd^{3+} and La^{3+} did not alter HA-mediated depolarization suggest that TRPC4/5 channels are not targeted in MEC interneurons. Furthermore, because HA-induced depolarization was not sensitive to either Gd^{3+} or La^{3+} , several other TRP channels may be excluded.

Experiments using several more non-selective cation channel blockers would help to identify any potential involvement of other TRP members. Second, HA directly interacts with and potentiates NMDA receptor function (Burban et al., 2010), which could increase cation influx and excitability of interneurons. However, this mechanism is unlikely to be responsible for HA-induced facilitation of GABAergic transmission because, firstly, the extracellular solution used to record sIPSCs contained dl-APV to block NMDA receptors and, secondly, direct NMDA receptor interactions with HA would not be blocked by HA receptor antagonists but our results demonstrate that both H_1 and H_2 are involved. Lastly, because activation of H_1 receptors has been reported to increase the activity of the electrogenic Na^+ - Ca^{2+} exchanger (Zhang et al., 2013b) and replacement of extracellular Na^+ with NMDG⁺ would annul the currents generated by the Na^+ - Ca^{2+} exchanger, our results showing that replacement of extracellular NaCl with NMDG-Cl significantly reduced HA-mediated depolarization of interneurons can also be explained by this mechanism. Further research is required to identify the exact cationic mechanism involved in HA-mediated facilitation of GABAergic transmission in the MEC.

Whereas HA has been demonstrated to inhibit the background “leak” K^+ channels (McCormick and Williamson, 1991; Munakata and Akaike, 1994; Reiner and Kamondi, 1994; Whyment et al., 2006), it seems that this mechanism is not applicable to the interneurons in the MEC because the background K^+ channels belong to the family of

two-pore domain K^+ channels and most members of the two-pore domain K^+ channels are insensitive to Cs^+ . Our results that HA-induced net currents displayed an inward rectification and are Cs^+ -sensitive suggest that Kirs are involved. Similar to the leak K^+ channels, Kirs are also involved in the controlling of RMPs (Hibino et al., 2010) and are targets for HA-induced increases in neuronal excitability (Gorelova and Reiner, 1996; He et al., 2016).

It remains unknown to what extent, if any, either synergistic or differential actions of H_1 or H_2 may mediate HA's effects on cation influx and inhibition of Kirs/ I_K in MEC interneurons. The reductions seen in interneuron I_K are likely due to the activation of H_2 (Atzori et al., 2000), whereas H_1 -mediated depolarization is linked to inhibition of Kirs (He et al., 2016). The activation of a TTX-insensitive Na^+ permeable channel is also likely due to H_1 activity (Gorelova and Reiner, 1996; Bell et al., 2000); however, H_2 may also increase Na^+ influx via a non-selective cation channel, as seen is in promyelocytes (Suh et al., 2001). Future work using selective receptor agonists and methods to isolate particular ionic mechanisms will be helpful in clarifying the roles of H_1 and H_2 in HA-induced activation of TTX-insensitive Na^+ currents and inhibition of Kirs/ I_K .

HA and GABAergic Systems

The effects of HA on GABAergic transmission vary in different brain regions. HA facilitates the excitability and transmission of GABAergic neurons in substantia nigra (Zhou et al., 2006), ventral tegmental area (Korotkova et al., 2002), medial septum (Xu et al., 2004), and the ventrolateral preoptic nuclei (Liu et al., 2010; Williams et al., 2014), but depresses GABAergic neuronal excitability and transmission in ventromedial nucleus of the hypothalamus (Jang et al., 2001), thalamic perigeniculate nuclei (Lee et al., 2004),

anterior hypothalamus (Lundius et al., 2010), and the striatum (Ellender et al., 2011). In the MEC, HA has been reported to reduce mIPSCs recorded in the presence of TTX via an H₃-dependent mechanism (He et al., 2016), whereas we did not observe a significant change in mIPSCs in response to HA application. Because the analysis of frequency for spontaneous activity and its modulation are very sensitive to exact experimental conditions (Ascoli et al., 2008), differences in experimental procedures and conditions could be proposed to explain the discrepancy. However, we indeed observed that activation of H₃ receptors slightly but significantly reduced sIPSCs. One explanation for this result is that the facilitatory action of H₁ and H₂ receptors on sIPSCs overwhelmed the inhibitory effect of H₃ receptors in response to HA application.

HA and Disease

HA is involved in the modulation of a variety of physiological functions including wakefulness, thermoregulation, energy homeostasis, nociception and learning and memory (Haas and Panula, 2003; Haas et al., 2008b). Aberrant HA signaling is implicated in a plethora of neurological disorders including narcolepsy, schizophrenia, AD, Parkinson's Disease, epilepsy, and depression (Haas et al., 2008b). Many of the physiological functions and neurological diseases are closely associated with the MEC. For instance, stimulation of H₁ receptors suppresses seizures in experimental studies, while antagonizing either H₁ or H₂ receptors can occasionally induce convulsions in children, epileptic or critically ill patients (Yokoyama and Inuma, 1996). Knockout of H₁ (Dai et al., 2007; Dere et al., 2008; Zlomuzica et al., 2009) or H₂ (Dai et al., 2007) receptors impairs spatial memory in rodents. Furthermore, antagonizing H₁ or H₃ but not H₂ in the superficial MEC impairs spatial learning in rats (He et al., 2016). In humans,

reduced H₁ binding has been reported in AD patients (Higuchi et al., 2000). Our results that HA facilitates GABA release in the MEC via activation of H₁ and H₂ receptors likely provide a cellular mechanism to explain some of the physiological functions and neurological diseases.

Study 3 – Group I mGluR Modulation within the Entorhinal Cortex

We demonstrate that DHPG increases the AP firing frequency of layer III pyramidal neurons via both mGluR1 and mGluR5. Application of DHPG causes a subthreshold RMP depolarization and generation of inward currents that may contribute to increases in AP firing. The precise signaling mechanism mediating DHPG's effect remain unclear at this point. DHPG induces inward currents that are sensitive to extracellular Na⁺ substitution and removal of both extracellular Na⁺ and Ca²⁺ prevents DHPG-induced currents. Accordingly, DHPG activates a NSCC with TRPC4- and TRPC5-like pharmacology and endogenous group I receptors couple to at least TRPC5 (Fig. 27).

Both mGluR 1 and mGluR5 are Functionally Present in the MEC

DHPG-induced increases in AP firing involve both mGluR1 and mGluR5. The inability of either MPEP or LY456236 alone to significantly reduce DHPG-induced increases in AP firing support this conclusion and suggest that both mGluR1 and mGluR5 subtypes are present within the MEC. Although immunostaining for both receptors would strengthen this conclusion, these results are in-line with previous reports suggesting that both group I mGluRs are found in the EC (Fotuhi et al., 1994; Luján et al., 1996; Shigemoto et al., 1997).

MEC Layer III Pyramidal Neuron

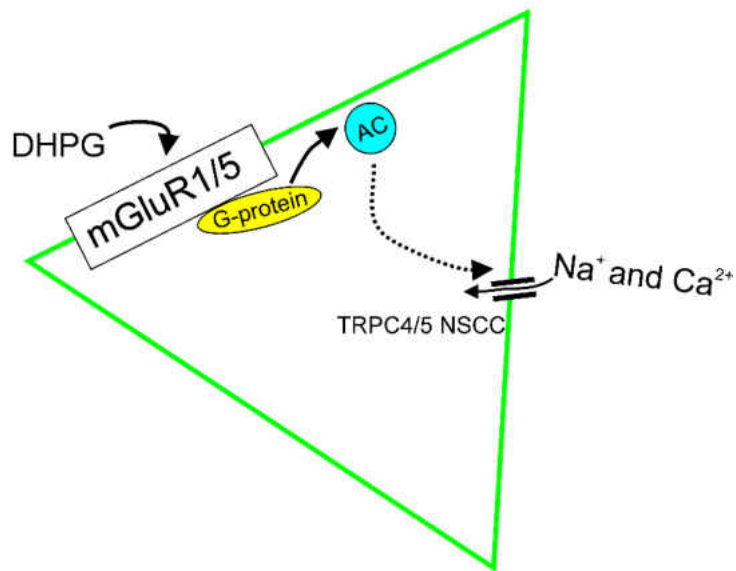


Figure 27. Summary figure for Study 3. DHPG activates both mGluR1 and mGluR5 and results in an increase in layer III pyramidal cell excitability. These increases in excitability require G proteins and AC. The ionic mechanism of DHPG-induced increases in excitability involves activation of a TRPC4/5-containing non-selective cation channel.

Although both receptors are involved in DHPG-induced increases in AP firing, it remains unknown to what extent either group I mGluR subtype contributes to DHPG-induced subthreshold currents. One possibility is that the two receptors participate in a redundant form of signaling. Alternatively, one subtype may be primarily responsible for the DHPG-induced subthreshold current. In CA3, group I mGluRs induce slow EPSCs and inhibit afterhyperpolarizations (AHPs) in a mGluR1-dependent manner (Heuss et al., 1999), whereas in CA1, DHPG-induced depolarization and inhibition of AHPs is dependent on mGluR1 and mGluR5, respectively (Mannaioni et al., 2001). Comparing DHPG-induced depolarization of pyramidal neurons in both CA1 and CA3 of mGluR1 KO and WT mice indicate a primary role for mGluR1 in DHPG-induced depolarization of both populations (Chuang et al., 2002); however, in CA1 interneurons, DHPG-induced

depolarization requires mGluR5, not mGluR1 (Gee and Lacaille, 2004). On the other hand, pharmacological functional evidence in both CA3 (Gee et al., 2003) and CA1 (Rae and Irving, 2004; Park et al., 2010) suggest a dual-role for both subtypes in group I-induced changes in excitability. Future studies may address the group I subtype involvement in DHPG-induced inward currents in the MEC using the above selective mGluR1 and mGluR5 antagonists and/or a knock-down approach in cultured slices. Selective agonists could also be employed, however, such agonists are limited in availability for group I mGluRs and results with the available mGluR5-specific agonist (CHPG) should be interpreted with caution (Kammermeier, 2012). These future studies in the MEC would be useful toward addressing any potential convergent or independent receptor involvement in DHPG-induced currents.

DHPG-Induced Currents are Mediated by TRPC-Like NSCCs

Whereas activation of group I mGluRs inhibits K⁺ channels (Charpak et al., 1990; Guérineau et al., 1994) and the group I selective agonist DHPG inhibits a variety of K⁺ channels (Mannaioni et al., 2001; Chuang et al., 2002; Sohn et al., 2007; Deng et al., 2010b); our results do not support the involvement of a DHPG-modulated K⁺-conductance based on the following pieces of evidence. First, using a K-gluconate-based intracellular solution, we did not observe any significant increase in the input resistance following application of DHPG, which would be expected if the closure of a K⁺ channel was exclusively involved in mediating DHPG-induced depolarization. Second, replacement of intracellular K⁺ with Cs⁺ failed to prevent DHPG-induced currents whereas changes to extracellular cation composition did annul DHPG's effect. Third, a clear DHPG I_{NET} typical of a non-selective cationic conductance continued to be elicited

in the presence of intracellular Cs^+ . Together, these results suggest that DHPG-induced currents were not mediated by the inhibition of a K^+ channel.

Our study supports a role for a NSCCs in mediating DHPG-induced currents based on the following lines of experimental evidence. First, replacement of extracellular Na^+ significantly reduced DHPG-induced inward currents compared to control conditions, indicating a Na^+ permeable channel is involved. Second, whereas substitution of extracellular Na^+ reduced but did not block DHPG-induced currents, substitution of extracellular Ca^{2+} with Mg^{2+} and reducing extracellular Na^+ did prevent DHPG-induced currents, consistent with a NSCC. Third, the DHPG I_{NET} is reflective of a non-selective cationic conductance. Lastly, the NSCC blockers FFA and 2-APB were effective in reducing DHPG-induced currents. Although a decrease in the input resistance would be expected if the opening of a cation channel were involved, the lack of a significant change in either direction is not necessarily inconsistent with a role for cation influx. One possible explanation may be due to a non-detectable change in a K^+ conductance that obfuscates the opening of a cation channel. Because our experiments for measuring RMP depolarization and input resistance used a K^+ -based intracellular solution, we cannot rule out this possibility. An experiment designed to monitor DHPG-induced changes in input resistance using a Cs^+ -based intracellular solution may address this apparent discrepancy.

In line with a NSCC being involved in DHPG-induced currents, we provide further evidence indicating that a TRPC-like channel is involved. This conclusion is supported by the following lines of evidence. First, the NSCC blockers FFA and 2-APB reduced DHPG-induced currents and both are blockers of TRPC-like channels (Clapham et al., 2005; Guinamard et al., 2013). Second, elevations in intracellular Ca^{2+} lead to

activation of TRPC channels (Birnbaumer, 2009). Inclusion of BAPTA in the pipette blocked DHPG-induced currents, indicating a requirement for intracellular Ca^{2+} signaling. Third, unlike many NSCCs which are inhibited by La^{3+} , TRPC4 and TRPC5 are unique in that they are potentiated by La^{3+} (Schaefer et al., 2000; Strübing et al., 2001). DHPG-induced currents were potentiated by La^{3+} , suggesting that TRPC4 and/or TRPC5 are involved. Fourth, the selective TRPC4/TRPC5 blocker ML-204 (Miller et al., 2011) prevented DHPG-induced currents. Fifth, intracellular dialysis of antibodies targeting TRPC1 or co-administration of TRPC4 and TRPC5 targeting antibodies reduced DHPG-induced currents. Sixth, although shRNA knock-down of TRPC4 and TRPC5 did not significantly reduce maximal DHPG-induced currents, it did significantly alter the time course of DHPG-induced currents. Finally, overexpression of rTRPC5 in MEC neurons significantly increased DHPG-induced inward currents compared to non-transfected cells, indicating that activation of endogenous mGluRs couples to, at least, TRPC5-containing channels.

Whereas DHPG is known to facilitate NCX activity (Keele et al., 1997), this mechanism is not involved in DHPG-induced currents since they were insensitive to KB-R7943. Agonists for the NSCC TRPV1 can modulate DHPG-induced LTD in the CA1 (Bennion et al., 2011) and TRPV1 is functionally present in the MEC (Banke, 2016). Because DHPG-induced inward currents were insensitive to the TRPV blocker ruthenium red, these channels were not involved.

The fact that intracellular dialysis of antibodies targeting either TRPC1 or both TRPC4 and TRPC5 reduced DHPG-induced currents is consistent with these channels forming heteromultimeric ion channels in the MEC (Birnbaumer, 2009). This possibility

might explain why targeting either TRPC4 or TRPC5 alone was ineffective in reducing DHPG-induced currents. For example, if TRPC4 is targeted, functional TRPC1:TRPC5 heteromultimers may still be functional and permit DHPG-induced currents. The fact that DHPG continued to induce a significant inward current in TRPC1 KO mice suggests that either TRPC1 is not involved in DHPG-induced currents or that some compensatory change has occurred during development in the KO mice to preserve DHPG-induced currents. In support of the latter, TRPC6 is upregulated in response to silencing of TRPC1 in the rat aorta (Selli et al., 2009; Erac et al., 2010). Consistent with a role for TRPC1, TRPC4, and TRPC5 channels in DHPG-induced currents, all three TRPC subunits are present in the MEC (von Bohlen und Halbach et al., 2005; Fowler et al., 2007). Additionally, in the MEC both cholecystokinin (Wang et al., 2011) and muscarinic (Zhang et al., 2011) receptors are linked to TRPC4 and TRPC 5. Although knock-down of TRPC4 and TRPC5 in MEC slice cultures failed to reduce DHPG-induced currents, these results do not necessarily exclude their involvement. One possibility is that a compensatory change has occurred during the transfection period. Future experiments utilizing dominant negative-forms of TRPC4 and TRPC5 will be more useful in evaluating their involvement. Taken together, these results support a role for TRPC1/4/5 in DHPG-induced currents.

At present, the source of Ca^{2+} involved in DHPG-induced activation of TRPC1/4/5 currents remains unknown. DHPG-induced inward currents were sensitive to BAPTA, indicating that Ca^{2+} must be involved. However, we demonstrate that neither extracellular Ca^{2+} influx nor intracellular Ca^{2+} release is involved. It may be possible that both sources of Ca^{2+} are involved and are able to compensate for the other when one

source is inhibited. Alternatively, a baseline level of intracellular Ca^{2+} might be required for DHPG-induced currents and our BAPTA experiments resulted in a level below such a baseline.

Signaling Mechanism Involved in DHPG-Induced Currents

Our results indicate that a G protein-dependent mechanism contributes to DHPG-induced inward currents, although the involved downstream effectors remain unclear. Because group I receptors are generally regarded as G_q -coupled and because TRPC4 and TRPC5 channels are receptor-activated most often via G_q /PLC-dependent pathways (Schaefer et al., 2000), it is somewhat surprising that we were unable to inhibit DHPG-induced currents with two different PLC inhibitors. However, the mechanisms of TRPC activation is still controversial and other pathways have been described.

Because group I activation increases cAMP production (Aramori and Nakanishi, 1992; Joly et al., 1995; Reid et al., 1996), we tested a hypothesis involving adenylate cyclase, which would be downstream of a DHPG-induced G_s -dependent pathway. Our finding that pretreatment with the AC inhibitor MDL 12330A reduced DHPG's effect is intriguing. It is worth noting that MDL 12330A has previously been used to inhibit DHPG-induced TRPC-like currents in area CA3, however its inhibitory action was attributed to a direct interaction with SOCE channels. The effects of MDL 12330A on AC are reported as irreversible (Guellaen et al., 1977) but its effects on SOCE channels are rapidly reversible (van Rossum et al., 2000). For our experiments, slices were pretreated with MDL 12330A for 30 minutes and then bathed in external solution for ~20-30 minutes prior to DHPG application. Thus, under our conditions, the inhibition of DHPG-induced inward currents with MDL 12330A being absent from the recording

solution might suggest its inhibitory action is due to inhibition of AC. It is worth highlighting that Gee et al. (2003) report that the DHPG-induced current reduced by MDL 12330A in area CA3 washed out in only 1 of 6 cells treated, which is not convincing evidence of MDL 12330A's effect being reversible. Consistent with an AC-dependent mechanism, activation of the G_s cascade in HEK cells activates TRPC5 and this effect is mimicked by the AC activator, forskolin (Sung et al., 2011; Hong et al., 2012). Because intracellular ATP inhibits TRPC5 activity (Dattilo et al., 2008), AC-dependent depletion of ATP may result in TRPC5 activation. An analogous mechanism would be PLC-dependent depletions of PIP_2 , which gates TRPC5 activity, however the precise relationship to PIP_2 -TRPC5 activity is unclear (Trebak et al., 2009). On the contrary, cAMP also negatively modulates TRPC5 activity through PKA-mediated phosphorylation of TRPC5 (Sung et al., 2011), which provides a negative feedback mechanism for G_s -mediated TRPC5 activation. These studies support a role for AC in DHPG-induced TRPC-mediated currents in the MEC, and this pathway will be the subject of future research.

Group I mGluR activation results in production of IP_3 (Masu et al., 1991; Aramori and Nakanishi, 1992) and modulation of voltage-gated calcium channels (McCool et al., 1998) in a pertussis toxin-sensitive manner—indicating a role for G_i signaling in group I mGluR activation. Because G_i is an activator of TRPC4 (Jeon et al., 2012; Thakur et al., 2016) and TRPC5 (Jeon et al., 2012) and because mGluR1 couples to TRPC4 by this mechanism (Kang et al., 2014), a role for G_i in DHPG-induced currents in the MEC should be considered. To test this possibility, experiments using pertussis toxin,

intracellular antibodies directed at G_i , and dominant-negative over-expression of G_i in MEC cultures will be useful.

With G proteins blocked, DHPG continued to induce a significant inward current, suggesting the involvement of a G protein-independent mechanism. Such mechanisms downstream of group I mGluR activation are well established with regard to modulation of excitability and synaptic transmission and may involve β -arrestins, Src, and MAPK members (Heuss et al., 1999; Kubota et al., 2014; Eng et al., 2016). Although Src-dependent tyrosine phosphorylation is implicated in function of different TRPC members (Hisatsune et al., 2004; Vazquez et al., 2004; Odell et al., 2005; Kawasaki et al., 2006; Gervásio et al., 2008), such a mechanism may not be involved in the MEC. Because two different Src inhibitors failed to block DHPG-induced inward currents, we conclude that Src is not involved. However, additional experiments are required to examine other modes of mGluR G protein-independent signaling.

The precise mechanism of TRPC activation continues to be unclear and this study in the MEC does not clarify the mechanism involved in TRPC4 and TRPC5 activation. Clearly, a multitude of possibilities exist for signaling between group I mGluRs and activation of TRPC channels. Future work using molecular biological approaches in EC slice cultures will be useful in systematically addressing MEC group I coupling to these channels.

Group I mGluRs and Neuropsychiatric Disorders

Dysfunctional glutamatergic signaling is implicated in several neuropsychiatric disorders including schizophrenia (Conn et al., 2009), depression (Sanacora et al., 2012), and anxiety (Bergink et al., 2004).

Schizophrenia is a neuropsychiatric disorder characterized by both positive (hallucinations and delusions) and negative (social withdrawal and poor working memory) symptoms. The etiology of schizophrenia is unclear but a strong genetic component is implicated. One hypothesis of schizophrenia states that low levels glutamatergic transmission are an underlying cause. This hypothesis is based on observations that administration of ketamine or phencyclidine (PCP), both of which antagonize NMDA receptors, produce psychotic-like episodes in humans that resemble the positive symptoms of schizophrenia (Nestler et al., 2009c). Consistent with this hypothesis, targeting group I mGluRs has emerged as a promising target for treatment of schizophrenia. Impaired sensorimotor gating describes a process by which an individual is unable to effectively filter irrelevant external or internal information and is a symptom of schizophrenia. This process is measured in rodents using prepulse inhibition of startle responses (PPI). In mGluR5 KO mice, the ability to suppress startle responses is significantly reduced, suggesting mGluR5 is necessary for effective sensorimotor gating (Brody et al., 2004). In another way, positive allosteric modulators of mGluR5 reverse amphetamine-induced PPI deficits, which is a model that also responds to antipsychotic treatments (Kinney et al., 2005). The impaired working memory seen in schizophrenia may be due to impaired glutamatergic transmission in the MEC. Although the prefrontal cortex is most often implicated in working memory tasks, the MEC is important for working memory of novel information (McGaughy et al., 2005; Hasselmo and Stern, 2006). The results of this study, in conjunction with previous reports, support a role for targeting mGluRs to enhance MEC activity. This preclinical evidence supports a

therapeutic potential for group I mGluRs as a candidate for the treatment of schizophrenia.

Whereas hypoglutamatergic conditions are implicated in schizophrenia, hyperglutamatergic conditions may underlie anxiety. In support of this view, antagonists for group I receptors produce anxiolytic actions (Brodkin et al., 2002; Mikulecká and Mareš, 2009). Our study indicates that TRPC4 and TRPC5 are effector channels mediating increases in MEC excitability following group I activation. Because KO mice for TRPC4 (Riccio et al., 2014) or TRPC5 (Riccio et al., 2009) display decreased anxiety-like behaviors, it is possible that enhanced MEC group I mGluR activity may contribute to anxiety. This study may provide some cellular and molecular insights into the mechanisms of action involved for these disorders.

Limitations of the Work Presented in this Dissertation

This dissertation provide insights into some of the mechanisms of action for three different modulatory systems within the MEC. Presented below are some of the limitations associated with these projects and proposed improvements for future studies.

Direct recordings from MEC interneurons are made in Study 1 and Study 2 with an assumption that they are GABAergic. This assumption is based on both visual morphology of the soma at the time of patching and subsequent electrophysiological validation that is consistent with previous reports (Kumar and Buckmaster, 2006; Ascoli et al., 2008; Deng and Lei, 2008; Canto and Witter, 2012b). However, this classification scheme, while effective in producing a population to test, may be rather simplistic given the rich diversity of interneurons within the cortex (Ascoli et al., 2008) and, specifically, the MEC (Ferrante et al., 2017). With our classifying system, Type I and Type II

interneurons likely correspond to PV-positive and SOM-positive interneurons (Yekhlief et al., 2015). However, SOM-positive interneurons are about half as prevalent as 5HT3Ra interneurons, meaning we might be missing out on understanding the modulatory consequences of a sizable pool of MEC interneurons. Alternatively, 5HT3Ra-positive interneurons might possess a mild sag response (Ferrante et al., 2017), in which case our type II classification might include both SOM and 5HT3Ra interneurons. Thus, these studies would benefit from clarification of from which interneuron sub-populations are being recorded. One approach to address this issue is the technically-demanding procedure of post-hoc immunohistochemical validation to confirm that recorded neurons are in fact GABAergic and co-stain for a marker of interest (e.g. PV). A better high-throughput approach to address these questions would be to make use of transgenic mice carrying a fluorescent marker controlled by a unique promoter for an interneuron of interest. Study 2 found a significant difference between the two interneuron classes analyzed with respect to HA-induced changes in excitability. This difference might suggest weighted modulatory control of HA over MEC interneurons that favors one population over another. Such interneuron-specific modulation may not be trivial as discrete interneuron populations might preferentially influence different projecting neuron populations, as might be the case for 5HT3Ra+CCK-positive interneurons that appear to preferentially target island cells of the MEC (Varga et al., 2010).

Study 1 and 2 focus specifically on postsynaptic changes in GABAergic activity of layer II. Whereas this cell layer contains at least two distinct cell types (Alonso and Klink, 1993; Canto et al., 2008; Fuchs et al., 2016) that differentially project to specific hippocampal subfields (Kitamura et al., 2014, 2015), changes in the magnitude of

modulator-induced enhancement of GABAergic transmission between cell populations, if any exist, would likely be functionally relevant to hippocampal dependent processes. For instance, although not significant, it appears that some cells display very robust increases in GABA_A-mediated amplitudes following HA application, suggesting a post-synaptic action of HA (N.C. unpublished observation). Posthoc analysis for stellate vs pyramidal classes with regard to modulation of sIPSC might provide novel findings of cell-specific changes in GABAergic transmission. Posthoc analysis would be necessary because the reliable electrophysiological marker of a sag response that distinguishes between stellate and pyramidal neurons is not available when using a Cs-gluconate-based intracellular solution for IPSC recordings.

Each of these studies is limited by the fact that the work is all conducted *in situ* and involves exogenous introduction of compounds, which may raise questions about the physiological significance of the observations reported. We do demonstrate an endogenous action of DA in Study 1 but this is with the use of another compound at a high concentration to stimulate DA release. In Study 2, we do not provide any evidence of endogenous actions. In Study 3, we use a selective agonist to trigger the receptor activation whereas as attempts to endogenously activate these receptors with electrical stimulation were not successful (N.C. unpublished observation).

The potential anxiogenic contribution of group I receptor activation in the MEC hypothesized above is based on the involvement of TRPC4 and TRPC5 channels contributing to increased DHPG-induced excitability, as these channels contribute to anxious behavior (Riccio et al., 2009, 2014). Intracranial injections of DHPG directly to the MEC and behavioral assays for anxiety could test this proposed mechanism.

Behavioral assays involving temporal (e.g. trace fear-conditioning) or contextual (e.g. conditional place preference) association processes might be effective in testing this hypothesis. The elevated-plus maze is commonly used to screen anxiolytic compounds; however, this test may not be useful for MEC-dependent activity related to anxiety because injections of anxiolytic group II agonists failed to produce change in behavior (N.C. and S.L. unpublished observations). However, the plus maze does not involve associational processes which are hippocampal dependent. Thus, a role for mGluRs in the MEC contributing to anxiety awaits more investigation.

APPENDICES

List of Abbreviations

2-APB; 2-Aminoethoxydiphenyl borate
5-HT; Serotonin
5HTR3a; Serotonin receptor 3a
A β ; Amyloid beta
AC; Adenylate cyclase
ACh; Acetylcholine
AChE; Acetylcholinesterase
AD; Alzheimer's disease
AMPA; α -amino-3-hydroxy-5-methyl-4-isoxazolpropionic acid
AP; Action potential
ATP; Adenosine triphosphate
BAPTA; 1,2-bis(2-aminophenoxy)ethane-N,N,N',N'-tetraacetic acid
BLA; Basolateral Amygdala
BSA; Bovine serum albumin
CA; Cornu ammonis
cAMP; Cyclic Adenosine monophosphate
CCK; Cholecystokinin
CR; Conditioned response
CRF; Cortico-releasing factor
CS; Conditioned stimulus
DA; Dopamine
DAG; Diacylglycerol
DG; Dentate gyrus
DHPG; (S)-3,5-Dihydroxyphenylglycine
DIV; Day-in-vitro
dl-APV; DL-2-Amino-5-phosphonopentanoic acid

DNQX; 6,7-Dinitroquinoxaline-2,3-dione
EC; Entorhinal Cortex
eEPSCs; Evoked excitatory postsynaptic currents
EGTA; ethylene glycol-bis-(2-aminoethylether)-N,N,N',N'-tetraacetic acid;
eIPSCs; Evoked inhibitory postsynaptic currents
FFA; Flufenamic Acid
FS; Fast-spiking
GABA; γ -aminobutric acid
GAD; Glutamic acid decarboxylase
GDP; Guanosine diphosphate
GFP; Green fluorescent protein
GTP; Guanosine triphosphate
HA; Histamine
HC; Holding current
HEK-293; Human embryonic kidney-293 cell line
HEPES; 4-(2-hydroxyethyl)piperazine-1-ethanesulfonic acid
iGluR; Ionotropic glutamate receptor
I_h; Hyperpolarization-activated cation current
I_{Net}; A drug-induced current (e.g. DA-, HA-, DHPG- induced)
IP₃; Inositol trisphosphate
IPSCs; Inhibitory postsynaptic currents
I-V; Current-voltage relationship
KO; Knock-out
LEC; Lateral entorhinal cortex
LTP; Long-term potentiation
MCI; Mild cognitive impairment
MDD; Major depressive disorder
MEC; Medial entorhinal cortex
mGluR; Metabotropic glutamate receptor
mIPSCs; miniature inhibitory postsynaptic currents
MPO; Membrane potential oscillations

MTL; Medial temporal lobe
NE; Norepinephrine
NCX; Na⁺-Ca²⁺ Exchanger
NFT; Neurofibrillary tangle
NGF; Neurogliaform
NMDA; N-methyl-D-aspartate
NMDG; N-Methyl-D-glucamine
NPY; neuropeptide Y
NSCC; Non-selective cation channel
NT; Neurotensin
pA; Picoamp
PBS; Phosphate buffered saline
PCP4; Purkinje cell protein 4
PER; Perirhinal cortex
PFA; Paraformaldehyde
PIP₂; phosphoinositide biphosphate
PKA; Protein kinase A
PKC; Protein kinase C
PLC(β); Phospholipase C
POR; Postrhinal cortex
PPR; Paired-pulse ratio
PV; Parvalbumin
RCan2; regulator of calcineurin 2
RFP; Red fluorescent protein
RMP; Resting membrane potential
R_n; Input resistance
RuRed; Ruthenium red
sIPSCs; Spontaneous inhibitory postsynaptic currents
SOCE; Store-operated Ca²⁺ entry
SOM; Somatostatin
TLE; Temporal lobe epilepsy

TRPC; Transient receptor potential canonical cation channel

TRPV; Transient receptor potential vanilloid cation channel

TTX; Tetrodotoxin

US; Unconditioned stimulus

VIP; Vasoactive intestinal peptide

V_m ; Membrane potential

WT; Wild-type

Copyright Clearance

Study 1 and Study 2 of this dissertation are derived almost entirely from publications where Nicholas Cilz is listed as the primary author. Copyright clearance was obtained from the publishers of Oxford University Press for Study 1 and Wiley of John Wiley and Sons for Study 2 to reproduce text, figures, and legends for this dissertation. The published manuscripts for both studies are listed below.

- Cilz NI, Kurada L, Hu B, Lei S. 2014. Dopaminergic Modulation of GABAergic Transmission in the Entorhinal Cortex: Concerted Roles of $\alpha 1$ Adrenoreceptors, Inward Rectifier K^+ , and T-Type Ca^{2+} Channels. *Cereb Cortex* 24:3195–3208.
- Cilz NI, Lei S. 2017. Histamine facilitates GABAergic transmission in the rat entorhinal cortex: Roles of H1 and H2 receptors, Na^+ -permeable cation channels, and inward rectifier K^+ channels. *Hippocampus* 27:613-631.

REFERENCES

- Abe T, Sugihara H, Nawa H, Shigemoto R, Mizuno N, Nakanishi S. 1992. Molecular characterization of a novel metabotropic glutamate receptor mGluR5 coupled to inositol phosphate/Ca²⁺ signal transduction. *J Biol Chem* 267:13361–13368.
- Akil M, Lewis DA. 1993. The Dopaminergic Innervation of Monkey Entorhinal Cortex. *Cereb Cortex* 3:533–550.
- Alonso A, Klink R. 1993. Differential electroresponsiveness of stellate and pyramidal-like cells of medial entorhinal cortex layer II. *J Neurophysiol* 70:128 LP-143.
- Alonso N, Fernandez N, Notcovich C, Monczor F, Simaan M, Baldi A, Gutkind JS, Davio C, Shayo C. 2013. Cross-Desensitization and Cointernalization of H1 and H2 Histamine Receptors Reveal New Insights into Histamine Signal Integration. *Mol Pharmacol* 83:1087–1098.
- Andersen P, Bliss T V, Skrede KK. 1971. Lamellar organization of hippocampal pathways. *Exp brain Res* 13:222–238.
- Anfossi G, Massucco P, Mularoni E, Mattiello L, Cavalot F, Burzacca S, Trovati M. 1993. Effect of dopamine on adenosine 3',5'-cyclic monophosphate levels in human platelets. *Gen Pharmacol* 24:435–438.
- Anwyl R. 1999. Metabotropic glutamate receptors: electrophysiological properties and role in plasticity. *Brain Res Rev* 29:83–120.
- Aramori I, Nakanishi S. 1992. Signal transduction and pharmacological characteristics of a metabotropic glutamate receptor, mGluR1, in transfected CHO cells. *Neuron* 8:757–765.
- Arrang J-M, Garbarg M, Schwartz J-C. 1987. Autoinhibition of histamine synthesis mediated by presynaptic H3-receptors. *Neuroscience* 23:149–157.

- Ascoli GA, Alonso-Nanclares L, Anderson SA, Barrionuevo G, Benavides-Piccione R, Burkhalter A, Buzsáki G, Cauli B, DeFelipe J, Fairén A, Feldmeyer D, Fishell G, Fregnac Y, Freund TF, Gardner D, Gardner EP, Goldberg JH, Helmstaedter M, Hestrin S, Karube F, Kisvárdy ZF, Lambolez B, Lewis DA, Marin O, Markram H, Muñoz A, Packer A, Petersen CCH, Rockland KS, Rossier J, Rudy B, Somogyi P, Staiger JF, Tamas G, Thomson AM, Toledo-Rodriguez M, Wang Y, West DC, Yuste R. 2008. Petilla terminology: nomenclature of features of GABAergic interneurons of the cerebral cortex. *Nat Rev Neurosci* 9:557–568.
- Atzori M, Lau D, Tansey EP, Chow A, Ozaita A, Rudy B, McBain CJ. 2000. H2 histamine receptor-phosphorylation of Kv3.2 modulates interneuron fast spiking. *Nat Neurosci* 3:791–798.
- Avoli M, D’Antuono M, Louvel J, Köhling R, Biagini G, Pumain R, D’Arcangelo G, Tancredi V. 2002. Network and pharmacological mechanisms leading to epileptiform synchronization in the limbic system in vitro. *Prog Neurobiol* 68:167–207.
- Baiano M, Perlino C, Rambaldelli G, Cerini R, Dusi N, Bellani M, Spezzapria G, Versace A, Balestrieri M, Mucelli RP, Tansella M, Brambilla P. 2008. Decreased entorhinal cortex volumes in schizophrenia. *Schizophr Res* 102:171–180.
- Banke T. 2016. Inhibition of TRPV1 channels enables long-term potentiation in the entorhinal cortex. *Pflügers Arch - Eur J Physiol* 1–10.
- Bao J, Li JJ, Perl ER. 1998. Differences in Ca²⁺ Channels Governing Generation of Miniature and Evoked Excitatory Synaptic Currents in Spinal Laminae I and II. *J Neurosci* 18:8740–8750.
- Barish ME. 1991. Increases in intracellular calcium ion concentration during depolarization of cultured embryonic *Xenopus* spinal neurones. *J Physiol* 444:545–565.
- Beaulieu J-M, Gainetdinov RR. 2011. The Physiology, Signaling, and Pharmacology of Dopamine Receptors. *Pharmacol Rev* 63:182–217.
- Becker C, Zeau B, Rivat C, Blugeot A, Hamon M, Benoliel J-J. 2008. Repeated social defeat-induced depression-like behavioral and biological alterations in rats: involvement of cholecystokinin. *Mol Psychiatry* 13:1079–1092.
- Becker JT, Walker JA, Olton DS. 1980. Neuroanatomical bases of spatial memory. *Brain Res* 200:307–320.
- Beed P, Bendels MHK, Wiegand HF, Leibold C, Jochenning FW, Schmitz D. 2010. Analysis of Excitatory Microcircuitry in the Medial Entorhinal Cortex Reveals Cell-Type-Specific Differences. *Neuron* 68:1059–1066.

- Behr J, Gloveli T, Schmitz D, Heinemann U. 2000. Dopamine Depresses Excitatory Synaptic Transmission Onto Rat Subicular Neurons Via Presynaptic D1-Like Dopamine Receptors. *J Neurophysiol* 84:112–119.
- Bell MI, Richardson PJ, Lee K. 2000. Histamine depolarizes cholinergic interneurons in the rat striatum via a H1-receptor mediated action. *Br J Pharmacol* 131:1135–1142.
- Belmaker RH, Agam G. 2008. Major Depressive Disorder. *N Engl J Med* 358:55–68.
- Bennion D, Jensen T, Walther C, Hamblin J, Wallmann A, Couch J, Blickenstaff J, Castle M, Dean L, Beckstead S, Merrill C, Muir C, St. Pierre T, Williams B, Daniel S, Edwards JG. 2011. Transient receptor potential vanilloid 1 agonists modulate hippocampal CA1 LTP via the GABAergic system. *Neuropharmacology* 61:730–738.
- Bergink V, van Megen and HJGM, Westenberg HGM. 2004. Glutamate and anxiety. *Eur Neuropsychopharmacol* 14:175–183.
- Bessaih T, Leresche N, Lambert RC. 2008. T current potentiation increases the occurrence and temporal fidelity of synaptically evoked burst firing in sensory thalamic neurons. *Proc Natl Acad Sci* 105:11376–11381.
- Birnbaumer L. 2009. The TRPC Class of Ion Channels: A Critical Review of Their Roles in Slow, Sustained Increases in Intracellular Ca²⁺ Concentrations*. *Annu Rev Pharmacol Toxicol* 49:395–426.
- Bliss TVP, Lømo T. 1973. Long-lasting potentiation of synaptic transmission in the dentate area of the anaesthetized rabbit following stimulation of the perforant path. *J Physiol* 232:331–356.
- von Bohlen und Halbach O, Hinz U, Unsicker K, Egorov A V. 2005. Distribution of TRPC1 and TRPC5 in medial temporal lobe structures of mice. *Cell Tissue Res* 322:201–206.
- Bonelli SB, Thompson PJ, Yogarajah M, Powell RHW, Samson RS, McEvoy AW, Symms MR, Koepp MJ, Duncan JS. 2013. Memory reorganization following anterior temporal lobe resection: a longitudinal functional MRI study. *Brain* 136:1889–1900.
- Booze RM, Crisostomo EA, Davis JN. 1993. Beta-adrenergic receptors in the hippocampal and retrohippocampal regions of rats and guinea pigs: Autoradiographic and immunohistochemical studies. *Synapse* 13:206–214.
- Bordji K, Becerril-Ortega J, Nicole O, Buisson A. 2010. Activation of extrasynaptic, but not synaptic, NMDA receptors modifies amyloid precursor protein expression pattern and increases amyloid-ss production. *J Neurosci* 30:15927–15942.

- Bouthenet ML, Ruat M, Sales N, Garbarg M, Schwartz JC. 1988. A detailed mapping of histamine H₁-receptors in guinea-pig central nervous system established by autoradiography with [¹²⁵I]iodobolpyramine. *Neuroscience* 26:553–600.
- Bowen DM, Smith CB, White P, Davison AN. 1976. Neurotransmitter-related enzymes and indices of hypoxia in senile dementia and other abiotrophies. *Brain* 99:459–496.
- Bowers ME, Choi DC, Ressler KJ. 2012. Neuropeptide regulation of fear and anxiety: Implications of cholecystokinin, endogenous opioids, and neuropeptide Y. *Physiol Behav* 107:699–710.
- Boyajian CL, Loughlin SE, Leslie FM. 1987. Anatomical evidence for alpha-2 adrenoceptor heterogeneity: differential autoradiographic distributions of [³H]rauwolscine and [³H]idazoxan in rat brain. *J Pharmacol Exp Ther* 241:1079 LP-1091.
- Boyer C, Lehouelleur J, Sans A. 1998. Potassium depolarization of mammalian vestibular sensory cells increases [Ca^{2+}]_i through voltage-sensitive calcium channels. *Eur J Neurosci* 10:971–975.
- Braak H, Braak E. 1991. Neuropathological staging of Alzheimer-related changes. *Acta Neuropathol* 82:239–259.
- Brodkin J, Busse C, Sukoff SJ, Varney MA. 2002. Anxiolytic-like activity of the mGluR5 antagonist MPEP: A comparison with diazepam and buspirone. *Pharmacol Biochem Behav* 73:359–366.
- Brody SA, Dulawa SC, Conquet F, Geyer MA. 2004. Assessment of a prepulse inhibition deficit in a mutant mouse lacking mGlu5 receptors. *Mol Psychiatry* 9:35–41.
- Burban A, Faucard R, Armand V, Bayard C, Vorobjev V, Arrang J-M. 2010. Histamine Potentiates N-Methyl-d-aspartate Receptors by Interacting with an Allosteric Site Distinct from the Polyamine Binding Site. *J Pharmacol Exp Ther* 332:912–921.
- Burwell RD, Amaral DG. 1998a. Perirhinal and postrhinal cortices of the rat: Interconnectivity and connections with the entorhinal cortex. *J Comp Neurol* 391:293–321.
- Burwell RD, Amaral DG. 1998b. Cortical afferents of the perirhinal, postrhinal, and entorhinal cortices of the rat. *J Comp Neurol* 398:179–205.
- Buzsaki G, Moser EI. 2013. Memory, navigation and theta rhythm in the hippocampal-entorhinal system. *Nat Neurosci* 16:130–138.

- Caballero-Bleda M, Witter MP. 1993. Regional and laminar organization of projections from the presubiculum and parasubiculum to the entorhinal cortex: An anterograde tracing study in the rat. *J Comp Neurol* 328:115–129.
- Canto CB, Witter MP. 2012a. Cellular properties of principal neurons in the rat entorhinal cortex. II. The medial entorhinal cortex. *Hippocampus* 22:1277–1299.
- Canto CB, Witter MP. 2012b. Cellular properties of principal neurons in the rat entorhinal cortex. I. The lateral entorhinal cortex. *Hippocampus* 22:1256–1276.
- Canto CB, Wouterlood FG, Witter MP. 2008. What does the anatomical organization of the entorhinal cortex tell us? *Neural Plast* 2008:381243.
- Carbone E, Marcantoni A, Giaccipoli A, Guido D, Carabelli V. 2006. T-type channels-secretion coupling: evidence for a fast low-threshold exocytosis. *Pflugers Arch* 453:373–383.
- Caruana DA, Chapman CA. 2008. Dopaminergic Suppression of Synaptic Transmission in the Lateral Entorhinal Cortex. *Neural Plast* 2008.
- Caruana DA, Reed SJ, Sliz DJ, Chapman CA. 2007. Inhibiting dopamine reuptake blocks the induction of long-term potentiation and depression in the lateral entorhinal cortex of awake rats. *Neurosci Lett* 426:6–11.
- Caruana DA, Sorge RE, Stewart J, Chapman CA. 2006. Dopamine Has Bidirectional Effects on Synaptic Responses to Cortical Inputs in Layer II of the Lateral Entorhinal Cortex. *J Neurophysiol* 96:3006–3015.
- Cenquizca LA, Swanson LW. 2007. Spatial organization of direct hippocampal field CA1 axonal projections to the rest of the cerebral cortex. *Brain Res Rev* 56:1–26.
- Charpak S, Gahwiler BH, Do KQ, Knopfel T. 1990. Potassium conductances in hippocampal neurons blocked by excitatory amino-acid transmitters. *Nature* 347:765–767.
- Chee MJ, Price CJ, Statnick MA, Colmers WF. 2011. Nociceptin/orphanin FQ suppresses the excitability of neurons in the ventromedial nucleus of the hypothalamus. *J Physiol* 589:3103–3114.
- Chin J, Massaro CM, Palop JJ, Thwin MT, Yu G-Q, Bien-Ly N, Bender A, Mucke L. 2007. Reelin Depletion in the Entorhinal Cortex of Human Amyloid Precursor Protein Transgenic Mice and Humans with Alzheimer's Disease. *J Neurosci* 27:2727 LP-2733.

- Chuang S-C, Zhao W, Young SR, Conquet F, Bianchi R, Wong RKS. 2002. Activation of group I mGluRs elicits different responses in murine CA1 and CA3 pyramidal cells. *J Physiol* 541:113–121.
- Cilz N, Lei S. 2014. Both H1 and H2 receptors are involved in histamine-dependent enhancement of GABAergic transmission in the entorhinal cortex. In: Society for Neuroscience Annual Meeting.
- Cilz NI, Kurada L, Hu B, Lei S. 2014. Dopaminergic Modulation of GABAergic Transmission in the Entorhinal Cortex: Concerted Roles of $\alpha 1$ Adrenoreceptors, Inward Rectifier K^+ , and T-Type Ca^{2+} Channels. *Cereb Cortex* 24:3195–3208.
- Cilz NI, Lei S. 2017. Histamine facilitates GABAergic transmission in the rat entorhinal cortex: Roles of H1 and H2 receptors, Na^+ -permeable cation channels, and inward rectifier K^+ channels. *Hippocampus* 27:613-631.
- Clapham DE, Julius D, Montell C, Schultz G. 2005. International Union of Pharmacology. XLIX. Nomenclature and Structure-Function Relationships of Transient Receptor Potential Channels. *Pharmacol Rev* 57:427 LP-450.
- Claro E, Arbonés L, García A, Picatoste F. 1986. Phosphoinositide hydrolysis mediated by histamine H1-receptors in rat brain cortex. *Eur J Pharmacol* 123:187–196.
- Congar P, Leinekugel X, Ben-Ari Y, Crépel V. 1997. A Long-Lasting Calcium-Activated Nonselective Cationic Current Is Generated by Synaptic Stimulation or Exogenous Activation of Group I Metabotropic Glutamate Receptors in CA1 Pyramidal Neurons. *J Neurosci* 17:5366 LP-5379.
- Conn PJ, Lindsley CW, Jones CK. 2009. Activation of metabotropic glutamate receptors as a novel approach for the treatment of schizophrenia. *Trends Pharmacol Sci* 30:25–31.
- Conn PJ, Pin JP. 1997. Pharmacology and functions of metabotropic glutamate receptors. *Annu Rev Pharmacol Toxicol* 37:205–237.
- Corkin S, Amaral DG, González RG, Johnson KA, Hyman BT. 1997. H. M.'s Medial Temporal Lobe Lesion: Findings from Magnetic Resonance Imaging. *J Neurosci* 17:3964–3979.
- Cornil CA, Balthazart J, Motte P, Massotte L, Seutin V. 2002. Dopamine Activates Noradrenergic Receptors in the Preoptic Area. *J Neurosci* 22:9320–9330.
- Couey JJ, Witoelar A, Zhang S-J, Zheng K, Ye J, Dunn B, Czajkowski R, Moser M-B, Moser EI, Roudi Y, Witter MP. 2013. Recurrent inhibitory circuitry as a mechanism for grid formation. *Nat Neurosci* 16:318–324.

- Criscuolo C, Fabiani C, Bonadonna C, Origlia N, Domenici L. 2015. BDNF prevents amyloid-dependent impairment of LTP in the entorhinal cortex by attenuating p38 MAPK phosphorylation. *Neurobiol Aging* 36:1303–1309.
- Cui RJ, Roberts BL, Zhao H, Zhu M, Appleyard SM. 2012. Serotonin Activates Catecholamine Neurons in the Solitary Tract Nucleus by Increasing Spontaneous Glutamate Inputs. *J Neurosci* 32:16530–16538.
- Cutsuridis V, Hasselmo M. 2012. GABAergic contributions to gating, timing, and phase precession of hippocampal neuronal activity during theta oscillations. *Hippocampus* 22:1597–1621.
- D'Ascenzo M, Podda MV, Fellin T, Azzena GB, Haydon P, Grassi C. 2009. Activation of mGluR5 induces spike afterdepolarization and enhanced excitability in medium spiny neurons of the nucleus accumbens by modulating persistent Na⁺ currents. *J Physiol* 587:3233–3250.
- Dai H, Kaneko K, Kato H, Fujii S, Jing Y, Xu A, Sakurai E, Kato M, Okamura N, Kuramasu A, Yanai K. 2007. Selective cognitive dysfunction in mice lacking histamine H1 and H2 receptors. *Neurosci Res* 57:306–313.
- Dattilo M, Penington NJ, Williams K. 2008. Inhibition of TRPC5 Channels by Intracellular ATP. *Mol Pharmacol* 73:42–49.
- Davies P, Maloney AJ. 1976. Selective loss of central cholinergic neurons in Alzheimer's disease. *Lancet (London, England)* 2:1403.
- Deng P-Y, Lei S. 2008. Serotonin increases GABA release in rat entorhinal cortex by inhibiting interneuron TASK-3 K⁺ channels. *Mol Cell Neurosci* 39:273–284.
- Deng P-Y, Porter JE, Shin H-S, Lei S. 2006. Thyrotropin-releasing hormone increases GABA release in rat hippocampus. *J Physiol* 577:497–511.
- Deng P-Y, Xiao Z, Jha A, Ramonet D, Matsui T, Leitges M, Shin H-S, Porter JE, Geiger JD, Lei S. 2010a. Cholecystinin Facilitates Glutamate Release by Increasing the Number of Readily Releasable Vesicles and Releasing Probability. *J Neurosci* 30:5136–5148.
- Deng P-Y, Xiao Z, Lei S. 2010b. Distinct modes of modulation of GABAergic transmission by Group I metabotropic glutamate receptors in rat entorhinal cortex. *Hippocampus* 20:980–993.
- Deng P-Y, Xiao Z, Yang C, Rojanathammanee L, Grisanti L, Watt J, Geiger JD, Liu R, Porter JE, Lei S. 2009. GABAB Receptor Activation Inhibits Neuronal Excitability and Spatial Learning in the Entorhinal Cortex by Activating TREK-2 K⁺ Channels. *Neuron* 63:230–243.

- Dere E, Zlomuzica A, Viggiano D, Ruocco LA, Watanabe T, Sadile AG, Huston JP, De Souza-Silva MA. 2008. Episodic-like and procedural memory impairments in histamine H1 Receptor knockout mice coincide with changes in acetylcholine esterase activity in the hippocampus and dopamine turnover in the cerebellum. *Neuroscience* 157:532–541.
- Dhillon A, Jones RSG. 2000. Laminar differences in recurrent excitatory transmission in the rat entorhinal cortex in vitro. *Neuroscience* 99:413–422.
- Dickson CT, Alonso A. 1997. Muscarinic Induction of Synchronous Population Activity in the Entorhinal Cortex. *J Neurosci* 17:6729 LP-6744.
- Dickson CT, Mena AR, Alonso A. 1997. Electroresponsiveness of medial entorhinal cortex layer III neurons in vitro. *Neuroscience* 81:937–950.
- Dong Y, Cooper D, Nasif F, Hu X-T, White FJ. 2004. Dopamine Modulates Inwardly Rectifying Potassium Currents in Medial Prefrontal Cortex Pyramidal Neurons. *J Neurosci* 24:3077–3085.
- Du F, Eid T, Lothman EW, Kohler C, Schwarcz R. 1995. Preferential neuronal loss in layer III of the medial entorhinal cortex in rat models of temporal lobe epilepsy. *J Neurosci* 15:6301–6313.
- Du F, Whetsell Jr. WO, Abou-Khalil B, Blumenkopf B, Lothman EW, Schwarcz R. 1993. Preferential neuronal loss in layer III of the entorhinal cortex in patients with temporal lobe epilepsy. *Epilepsy Res* 16:223–233.
- Durstewitz D, Seamans JK, Sejnowski TJ. 2000. Neurocomputational models of working memory. *Nat Neurosci* 3:1184–1191.
- Egorov A V, Hamam BN, Franssen E, Hasselmo ME, Alonso AA. 2002. Graded persistent activity in entorhinal cortex neurons. *Nature* 420:173–178.
- Eichenbaum H, Sauvage M, Fortin N, Komorowski R, Lipton P. 2012. Towards a functional organization of episodic memory in the medial temporal lobe. *Neurosci Biobehav Rev* 36:1597–1608.
- Ellender TJ, Huerta-Ocampo I, Deisseroth K, Capogna M, Bolam JP. 2011. Differential Modulation of Excitatory and Inhibitory Striatal Synaptic Transmission by Histamine. *J Neurosci* 31:15340–15351.
- Eng AG, Kelder DA, Hedrick TP, Swanson GT. 2016. Transduction of group I mGluR-mediated synaptic plasticity by β -arrestin2 signalling. *Nat Commun* 7:13571.
- Engel JJ. 2001. Mesial temporal lobe epilepsy: what have we learned? *Neuroscientist* 7:340–352.

- Erac Y, Selli C, Kosova B, Akcali KC, Tosun M. 2010. Expression levels of TRPC1 and TRPC6 ion channels are reciprocally altered in aging rat aorta: implications for age-related vasospastic disorders. *Age (Dordr)* 32:223–230.
- Erickson SL, Akil M, Levey AI, Lewis DA. 1998. Postnatal development of tyrosine hydroxylase- and dopamine transporter-immunoreactive axons in monkey rostral entorhinal cortex. *Cereb Cortex* 8:415–427.
- Evans DI, Jones RSG, Woodhall G. 2000. Activation of Presynaptic Group III Metabotropic Receptors Enhances Glutamate Release in Rat Entorhinal Cortex. *J Neurophysiol* 83:2519–2525.
- Evans DI, Jones RSG, Woodhall G. 2001. Differential Actions of PKA and PKC in the Regulation of Glutamate Release by Group III mGluRs in the Entorhinal Cortex. *J Neurophysiol* 85:571–579.
- Falkai P, Bogerts B, Rozumek M. 1988. Limbic pathology in schizophrenia: The entorhinal region—a morphometric study. *Biol Psychiatry* 24:515–521.
- Fallon JH, Koziell DA, Moore RY. 1978. Catecholamine innervation of the basal forebrain II. Amygdala, suprarhinal cortex and entorhinal cortex. *J Comp Neurol* 180:509–531.
- Ferrante M, Tahvildari B, Duque A, Hadzipasic M, Salkoff D, Zaghera EW, Hasselmo ME, McCormick DA. 2017. Distinct Functional Groups Emerge from the Intrinsic Properties of Molecularly Identified Entorhinal Interneurons and Principal Cells. *Cereb Cortex* 27:3186–3207.
- Ford CP, Phillips PEM, Williams JT. 2009. The Time Course of Dopamine Transmission in the Ventral Tegmental Area. *J Neurosci* 29:13344–13352.
- Fotuhi M, Standaert DG, Testa CM, Penney Jr. JB, Young AB. 1994. Differential expression of metabotropic glutamate receptors in the hippocampus and entorhinal cortex of the rat. *Mol Brain Res* 21:283–292.
- Fowler MA, Sidiropoulou K, Ozkan ED, Phillips CW, Cooper DC. 2007. Corticolimbic Expression of TRPC4 and TRPC5 Channels in the Rodent Brain. *PLoS One* 2:e573.
- Fuchs EC, Neitz A, Pinna R, Melzer S, Caputi A, Monyer H. 2016. Local and Distant Input Controlling Excitation in Layer II of the Medial Entorhinal Cortex. *Neuron* 89:194–208.
- Fukushima Y, Oka Y, Saitoh T, Katagiri H, Asano T, Matsushashi N, Takata K, van Breda E, Yazaki Y, Sugano K. 1995. Structural and functional analysis of the canine histamine H₂ receptor by site-directed mutagenesis: N-glycosylation is not vital for its action. *Biochem J* 310:553–558.

- Furtak SC, Wei S-M, Agster KL, Burwell RD. 2007. Functional neuroanatomy of the parahippocampal region in the rat: The perirhinal and postrhinal cortices. *Hippocampus* 17:709–722.
- Fyhn M, Molden S, Witter MP, Moser EI, Moser M-B. 2004. Spatial Representation in the Entorhinal Cortex. *Science* (80-) 305:1258 LP-1264.
- Garbarg M, Schwartz JC. 1988. Synergism between histamine H1- and H2-receptors in the cAMP response in guinea pig brain slices: effects of phorbol esters and calcium. *Mol Pharmacol* 33:38–43.
- Gee CE, Benquet P, Gerber U. 2003. Group I metabotropic glutamate receptors activate a calcium-sensitive transient receptor potential-like conductance in rat hippocampus. *J Physiol* 546:655–664.
- Gee CE, Lacaille J-C. 2004. Group I metabotropic glutamate receptor actions in oriens/alveus interneurons of rat hippocampal CA1 region. *Brain Res* 1000:92–101.
- Germroth P, Schwerdtfeger WK, Buhl EH. 1989. GABAergic neurons in the entorhinal cortex project to the hippocampus. *Brain Res* 494:187–192.
- Gervásio OL, Whitehead NP, Yeung EW, Phillips WD, Allen DG. 2008. TRPC1 binds to caveolin-3 and is regulated by Src kinase – role in Duchenne muscular dystrophy. *J Cell Sci* 121:2246 LP-2255.
- Gioanni Y, Thierry A-M, Glowinski J, Tassin J-P. 1998. α 1-adrenergic, D1, and D2 receptors interactions in the prefrontal cortex: Implications for the modality of action of different types of neuroleptics. *Synapse* 30:362–370.
- Giocomo LM, Hasselmo ME. 2008. Time Constants of h Current in Layer II Stellate Cells Differ along the Dorsal to Ventral Axis of Medial Entorhinal Cortex. *J Neurosci* 28:9414 LP-9425.
- Gloveli T, Schmitz D, Empson RM, Dugladze T, Heinemann U. 1997. Morphological and electrophysiological characterization of layer III cells of the medial entorhinal cortex of the rat. *Neuroscience* 77:629–648.
- Gómez-Isla T, Price JL, McKeel Jr. DW, Morris JC, Growdon JH, Hyman BT. 1996. Profound Loss of Layer II Entorhinal Cortex Neurons Occurs in Very Mild Alzheimer's Disease. *J Neurosci* 16:4491–4500.
- Gorelova N, Reiner PB. 1996. Histamine depolarizes cholinergic septal neurons. *J Neurophysiol* 75:707–714.

- Gorelova N, Seamans JK, Yang CR. 2002. Mechanisms of Dopamine Activation of Fast-Spiking Interneurons That Exert Inhibition in Rat Prefrontal Cortex. *J Neurophysiol* 88:3150–3166.
- Govindaiah G, Wang Y, Cox CL. 2010. Dopamine enhances the excitability of somatosensory thalamocortical neurons. *Neuroscience* 170:981–991.
- Guellaen G, Mahu JL, Mavier P, Berthelot P, Hanoune J. 1977. RMI 12330 A, an inhibitor of adenylate cyclase in rat liver. *Biochim Biophys Acta* 484:465–475.
- Guerineau NC, Bossu JL, Gähwiler BH, Gerber U. 1995. Activation of a nonselective cationic conductance by metabotropic glutamatergic and muscarinic agonists in CA3 pyramidal neurons of the rat hippocampus. *J Neurosci* 15:4395–4407.
- Guérineau NC, Gähwiler BH, Gerber U. 1994. Reduction of resting K⁺ current by metabotropic glutamate and muscarinic receptors in rat CA3 cells: mediation by G-proteins. *J Physiol* 474:27–33.
- Guinamard R, Simard C, Del Negro C. 2013. Flufenamic acid as an ion channel modulator. *Pharmacol Ther* 138:272–284.
- Haas H, Panula P. 2003. The role of histamine and the tuberomammillary nucleus in the nervous system. *Nat Rev Neurosci* 4:121–130.
- Haas HL. 1984. Histamine potentiates neuronal excitation by blocking a calcium-dependent potassium conductance. *Agents Actions* 14:534–7.
- Haas HL, Sergeeva OA, Selbach O. 2008a. Histamine in the Nervous System. *Physiol Rev* 88:1183–1241.
- Haas HL, Sergeeva OA, Selbach O. 2008b. Histamine in the Nervous System. *Physiol Rev* 88:1183–1241.
- van Haeften T, Baks-te-Bulte L, Goede PH, Wouterlood FG, Witter MP. 2003. Morphological and numerical analysis of synaptic interactions between neurons in deep and superficial layers of the entorhinal cortex of the rat. *Hippocampus* 13:943–952.
- van Haeften T, Wouterlood FG, Jorritsma-Byham B, P. Witter M. 1997. GABAergic Presubicular Projections to the Medial Entorhinal Cortex of the Rat. *J Neurosci* 17:862 LP-874.
- Hafting T, Fyhn M, Molden S, Moser M-B, Moser EI. 2005. Microstructure of a spatial map in the entorhinal cortex. *Nature* 436:801–806.

- Hales JB, Schlesiger MI, Leutgeb JK, Squire LR, Leutgeb S, Clark RE. 2014. Medial Entorhinal Cortex Lesions Only Partially Disrupt Hippocampal Place Cells and Hippocampus-Dependent Place Memory. *Cell Rep* 9:893–901.
- Hamam BN, Kennedy TE, Alonso A, Amaral DG. 2000. Morphological and electrophysiological characteristics of layer V neurons of the rat medial entorhinal cortex. *J Comp Neurol* 418:457–472.
- Hamilton TJ, Wheatley BM, Sinclair DB, Bachmann M, Larkum ME, Colmers WF. 2010. Dopamine modulates synaptic plasticity in dendrites of rat and human dentate granule cells. *Proc Natl Acad Sci* 107:18185–18190.
- Hardwick JC, Kotarski AF, Powers MJ. 2005. Ionic mechanisms of histamine-induced responses in guinea pig intracardiac neurons. 290:R241–R250.
- Harel EV, Tennyson RL, Fava M, Bar M. 2016. Linking major depression and the neural substrates of associative processing. *Cogn Affect Behav Neurosci* 16:1017–1026.
- Harris JA, Devidze N, Verret L, Ho K, Halabisky B, Thwin MT, Kim D, Hamto P, Lo I, Yu G-Q, Palop JJ, Masliah E, Mucke L. 2010. Transsynaptic Progression of Amyloid- β -Induced Neuronal Dysfunction within the Entorhinal-Hippocampal Network. *Neuron* 68:428–441.
- Harris JA, Koyama A, Maeda S, Ho K, Devidze N, Dubal DB, Yu G-Q, Masliah E, Mucke L. 2012. Human P301L-Mutant Tau Expression in Mouse Entorhinal-Hippocampal Network Causes Tau Aggregation and Presynaptic Pathology but No Cognitive Deficits. *PLoS One* 7:e45881.
- Hasselmo ME. 2006. The role of acetylcholine in learning and memory. *Curr Opin Neurobiol* 16:710–715.
- Hasselmo ME, Stern CE. 2006. Mechanisms underlying working memory for novel information. *Trends Cogn Sci* 10:487–493.
- Hattingh C, Ipser J, Tromp S, Syal S, Lochner C, Brooks S, Stein D. 2013. Functional magnetic resonance imaging during emotion recognition in social anxiety disorder: an activation likelihood meta-analysis. *Front Hum Neurosci* 6:347.
- He C, Luo F, Chen X, Chen F, Li C, Ren S, Qiao Q, Zhang J, de Lecea L, Gao D, Hu Z. 2016. Superficial Layer-Specific Histaminergic Modulation of Medial Entorhinal Cortex Required for Spatial Learning. *Cereb Cortex* 26:1590–1608.
- Hemby SE, Trojanowski JQ, Ginsberg SD. 2003. Neuron-specific age-related decreases in dopamine receptor subtype mRNAs. *J Comp Neurol* 456:176–183.

- Heuss C, Scanziani M, Gahwiler BH, Gerber U. 1999. G-protein-independent signaling mediated by metabotropic glutamate receptors . *Nat Neurosci* 2:1070–1077.
- Hibino H, Inanobe A, Furutani K, Murakami S, Findlay I, Kurachi Y. 2010. Inwardly Rectifying Potassium Channels: Their Structure, Function, and Physiological Roles. *Physiol Rev* 90:291–366.
- Hidaka H. 1971. Fusaric (5-butylpicolinic) acid, an inhibitor of dopamine beta-hydroxylase, affects serotonin and noradrenaline. *Nature* 231:54–55.
- Higuchi M, Yanai K, Okamura N, Meguro K, Arai H, Itoh M, Iwata R, Ido T, Watanabe T, Sasaki H. 2000. Histamine H1 receptors in patients with Alzheimer's disease assessed by positron emission tomography. *Neuroscience* 99:721–729.
- Hill SJ, Ganellin CR, Timmerman H, Schwartz JC, Shankley NP, Young JM, Schunack W, Levi R, Haas HL. 1997. International Union of Pharmacology. XIII. Classification of Histamine Receptors. *Pharmacol Rev* 49:253–278.
- Hille B. 1992. G protein-coupled mechanisms and nervous signaling. *Neuron* 9:187–195.
- Hisatsune C, Kuroda Y, Nakamura K, Inoue T, Nakamura T, Michikawa T, Mizutani A, Mikoshiba K. 2004. Regulation of TRPC6 Channel Activity by Tyrosine Phosphorylation. *J Biol Chem* 279:18887–18894.
- van Hoesen GW, Pandya DN, Butters N. 1972. Cortical Afferents to the Entorhinal Cortex of the Rhesus Monkey. *Science* (80-) 175:1471–1473.
- Hong C, Kim J, Jeon J-P, Wie J, Kwak M, Ha K, Kim H, Myeong J, Kim SY, Jeon J-H, So I. 2012. Gs cascade regulates canonical transient receptor potential 5 (TRPC5) through cAMP mediated intracellular Ca²⁺ release and ion channel trafficking. *Biochem Biophys Res Commun* 421:105–111.
- Houamed KM, Kuijper JL, Gilbert TL, Haldeman BA, O'Hara PJ, Mulvihill ER, Almers W, Hagen FS. 1991. Cloning, expression, and gene structure of a G protein-coupled glutamate receptor from rat brain. *Science* (80-) 252:1318 LP-1321.
- Huang H, van den Pol AN. 2007. Rapid Direct Excitation and Long-Lasting Enhancement of NMDA Response by Group I Metabotropic Glutamate Receptor Activation of Hypothalamic Melanin-Concentrating Hormone Neurons. *J Neurosci* 27:11560 LP-11572.
- Huang Q, Zhou D, Chase K, Gusella JF, Aronin N, DiFiglia M. 1992. Immunohistochemical localization of the D1 dopamine receptor in rat brain reveals its axonal transport, pre- and postsynaptic localization, and prevalence in the basal ganglia, limbic system, and thalamic reticular nucleus. *Proc Natl Acad Sci U S A* 89:11988–11992.

- Hyman BT, Hoesen GW Van, Damasio AR, Barnes CL. 1984. Alzheimer's Disease: Cell-Specific Pathology Isolates the Hippocampal Formation. *Science* 225:1168–1170.
- Hyman SE, Cohen J. 2013. Disorders of Mood and Anxiety. In: Kandel ER, Schwartz JH, Jessell T, Siegelbaum S, Hudspeth A, editors. *Principles of Neural Science*. 5th ed. The McGraw-Hill Companies. p 1402–1424.
- Insausti R, Herrero MT, Witter MP. 1997. Entorhinal cortex of the rat: Cytoarchitectonic subdivisions and the origin and distribution of cortical efferents. *Hippocampus* 7:146–183.
- Iserhot C, Gebhardt C, Schmitz D, Heinemann U. 2004. Glutamate transporters and metabotropic receptors regulate excitatory neurotransmission in the medial entorhinal cortex of the rat. *Brain Res* 1027:151–160.
- Jang I-S, Rhee J-S, Watanabe T, Akaike N, Akaike N. 2001. Histaminergic modulation of GABAergic transmission in rat ventromedial hypothalamic neurones. *J Physiol* 534:791–803.
- Jankowsky JL, Slunt HH, Gonzales V, Savonenko A V, Wen JC, Jenkins NA, Copeland NG, Younkin LH, Lester HA, Younkin SG, Borchelt DR. 2005. Persistent Amyloidosis following Suppression of A β Production in a Transgenic Model of Alzheimer Disease. *PLOS Med* 2:e355.
- Jensen LJ, Salomonsson M, Jensen BL, Holstein-Rathlou N-H. 2004. Depolarization-induced calcium influx in rat mesenteric small arterioles is mediated exclusively via mibefradil-sensitive calcium channels. *Br J Pharmacol* 142:709–718.
- Jeon J-P, Hong C, Park EJ, Jeon J-H, Cho N-H, Kim I-G, Choe H, Muallem S, Kim HJ, So I. 2012. Selective G α i Subunits as Novel Direct Activators of Transient Receptor Potential Canonical (TRPC)4 and TRPC5 Channels. *J Biol Chem* 287:17029–17039.
- Ji J, Maren S. 2008. Lesions of the entorhinal cortex or fornix disrupt the context-dependence of fear extinction in rats. *Behav Brain Res* 194:201–206.
- Joly C, Gomeza J, Brabet I, Curry K, Bockaert J, Pin JP. 1995. Molecular, functional, and pharmacological characterization of the metabotropic glutamate receptor type 5 splice variants: comparison with mGluR1. *J Neurosci* 15:3970 LP-3981.
- Joyal CC, Laakso MP, Tiihonen J, Syvälahti E, Vilkmann H, Laakso A, Alakare B, Rääköläinen V, Salokangas RKR, Hietala J. 2002. A volumetric MRI study of the entorhinal cortex in first episode neuroleptic-naive schizophrenia. *Biol Psychiatry* 51:1005–1007.

- Jutila L, Ylinen A, Partanen K, Alafuzoff I, Mervaala E, Partanen J, Vapalahti M, Vainio P, Pitkänen A. 2001. MR Volumetry of the Entorhinal, Perirhinal, and Temporopolar Cortices in Drug-Refractory Temporal Lobe Epilepsy. *Am J Neuroradiol* 22:1490 LP-1501.
- Kammermeier PJ. 2012. The orthosteric agonist 2-chloro-5-hydroxyphenylglycine activates mGluR5 and mGluR1 with similar efficacy and potency. *BMC Pharmacol* 12:6.
- Kang HJ, Menlove K, Ma J, Wilkins A, Lichtarge O, Wensel TG. 2014. Selectivity and Evolutionary Divergence of Metabotropic Glutamate Receptors for Endogenous Ligands and G Proteins Coupled to Phospholipase C or TRP Channels. *J Biol Chem* 289:29961–29974.
- Kassack MU, Höfgen B, Decker M, Eckstein N, Lehmann J. 2002. Pharmacological characterization of the benz[d]indolo[2,3-g]azecine LE300, a novel type of a nanomolar dopamine receptor antagonist. *Naunyn Schmiedebergs Arch Pharmacol* 366:543–550.
- Kaufers DI, Dekosky ST. 1999. Diagnostic classifications: relationship to the neurobiology of dementia. In: Charney DS, Nestler EJ, Bunney BS, editors. *Neurobiology of Mental Illness*. 1st ed. Oxford University Press. p 641–649.
- Kawai F, Miyachi E. 2001. Enhancement by T-Type Ca^{2+} Currents of Odor Sensitivity in Olfactory Receptor Cells. *J Neurosci* 21:RC144.
- Kawasaki BT, Liao Y, Birnbaumer L. 2006. Role of Src in C3 transient receptor potential channel function and evidence for a heterogeneous makeup of receptor- and store-operated Ca^{2+} entry channels. *Proc Natl Acad Sci United States Am* 103:335–340.
- Keele NB, Arvanov VL, Shinnick-Gallagher P. 1997. Quisqualate-preferring metabotropic glutamate receptor activates Na^{+} - Ca^{2+} exchange in rat basolateral amygdala neurones. *J Physiol* 499:87–104.
- Kerr KM, Agster KL, Furtak SC, Burwell RD. 2007. Functional neuroanatomy of the parahippocampal region: The lateral and medial entorhinal areas. *Hippocampus* 17:697–708.
- Kessler RC, Gruber M, Hettema JM, Hwang I, Sampson N, Yonkers KA. 2008. Comorbid major depression and generalized anxiety disorders in the National Comorbidity Survey follow-up. *Psychol Med* 38:365–374.
- Khan UA, Liu L, Provenzano FA, Berman DE, Profaci CP, Sloan R, Mayeux R, Duff KE, Small SA. 2014. Molecular drivers and cortical spread of lateral entorhinal cortex dysfunction in preclinical Alzheimer's disease. *Nat Neurosci* 17:304–311.

- Kim SJ, Kim YS, Yuan JP, Petralia RS, Worley PF, Linden DJ. 2003. Activation of the TRPC1 cation channel by metabotropic glutamate receptor mGluR1. *Nature* 426:285–291.
- Kim Y, Spruston N. 2012. Target-specific output patterns are predicted by the distribution of regular-spiking and bursting pyramidal neurons in the subiculum. *Hippocampus* 22:693–706.
- Kinney GG, O'Brien JA, Lemaire W, Burno M, Bickel DJ, Clements MK, Chen T-B, Wisnoski DD, Lindsley CW, Tiller PR, Smith S, Jacobson MA, Sur C, Duggan ME, Pettibone DJ, Conn PJ, Williams DL. 2005. A Novel Selective Positive Allosteric Modulator of Metabotropic Glutamate Receptor Subtype 5 Has in Vivo Activity and Antipsychotic-Like Effects in Rat Behavioral Models. *J Pharmacol Exp Ther* 313:199 LP-206.
- Kitamura T, Pignatelli M, Suh J, Kohara K, Yoshiki A, Abe K, Tonegawa S. 2014. Island Cells Control Temporal Association Memory. *Science* 343:896 LP-901.
- Kitamura T, Sun C, Martin J, Kitch LJ, Schnitzer MJ, Tonegawa S. 2015. Entorhinal Cortical Ocean Cells Encode Specific Contexts and Drive Context-Specific Fear Memory. *Neuron* 87:1317–1331.
- Klink R, Alonso A. 1997a. Morphological characteristics of layer II projection neurons in the rat medial entorhinal cortex. *Hippocampus* 7:571–583.
- Klink R, Alonso A. 1997b. Muscarinic Modulation of the Oscillatory and Repetitive Firing Properties of Entorhinal Cortex Layer II Neurons. *J Neurophysiol* 77:1813 LP-1828.
- Klink R, Alonso A. 1997c. Ionic Mechanisms of Muscarinic Depolarization in Entorhinal Cortex Layer II Neurons. *J Neurophysiol* 77:1829 LP-1843.
- Kloosterman F, Van Haeften T, Witter MP, Lopes da Silva FH. 2003. Electrophysiological characterization of interlaminar entorhinal connections: an essential link for re-entrance in the hippocampal–entorhinal system. *Eur J Neurosci* 18:3037–3052.
- Köhler C, Swanson LW, Haglund L, J-Yen W. 1985. The cytoarchitecture, histochemistry and projections of the tuberomammillary nucleus in the rat. *Neuroscience* 16:85–110.
- Korotkova TM, Haas HL, Brown RE. 2002. Histamine excites GABAergic cells in the rat substantia nigra and ventral tegmental area in vitro. *Neurosci Lett* 320:133–136.
- Krishnan V, Nestler EJ. 2008. The molecular neurobiology of depression. *Nature* 455:894–902.

- Kubota H, Nagao S, Obata K, Hirono M. 2014. mGluR1-Mediated Excitation of Cerebellar GABAergic Interneurons Requires Both G Protein-Dependent and Src-ERK1/2-Dependent Signaling Pathways. *PLoS One* 9:e106316.
- Kumar SS, Buckmaster PS. 2006. Hyperexcitability, Interneurons, and Loss of GABAergic Synapses in Entorhinal Cortex in a Model of Temporal Lobe Epilepsy. *J Neurosci* 26:4613 LP-4623.
- Kumar SS, Jin X, Buckmaster PS, Huguenard JR. 2007. Recurrent Circuits in Layer II of Medial Entorhinal Cortex in a Model of Temporal Lobe Epilepsy. *J Neurosci* 27:1239–1246.
- Kurada L, Yang C, Lei S. 2014. Corticotropin-Releasing Factor Facilitates Epileptiform Activity in the Entorhinal Cortex: Roles of CRF2 Receptors and PKA Pathway. *PLoS One* 9:e88109.
- Kurian MA, Gissen P, Smith M, Heales SJR, Clayton PT. 2011. The monoamine neurotransmitter disorders: an expanding range of neurological syndromes. *Lancet Neurol* 10:721–733.
- Kuzhikandathil E V, Oxford GS. 2002. Classic D1 Dopamine Receptor Antagonist R-(+)-7-Chloro-8-hydroxy-3-methyl-1-phenyl-2,3,4,5-tetrahydro-1H-3-benzazepine hydrochloride (SCH23390) Directly Inhibits G Protein-Coupled Inwardly Rectifying Potassium Channels. *Mol Pharmacol* 62:119–126.
- Lazou A, Markou T, Zioga M, Vasara E, Efstathiou A, Gaitanaki C. 2006. Dopamine mimics the cardioprotective effect of ischemic preconditioning via activation of alpha1-adrenoceptors in the isolated rat heart. *Physiol res* 55:1–8.
- Lee KH, Broberger C, Kim U, McCormick DA. 2004. Histamine modulates thalamocortical activity by activating a chloride conductance in ferret perigeniculate neurons. *Proc Natl Acad Sci U S A* 101:6716–6721.
- Lee T-L, Hsu C-T, Yen S-T, Lai C-W, Cheng J-T. 1998. Activation of β_3 -adrenoceptors by exogenous dopamine to lower glucose uptake into rat adipocytes. *J Auton Nerv Syst* 74:86–90.
- Leedham JA, Pennefather JN. 1986. Selectivities of some agonists acting at alpha 1- and alpha 2-adrenoreceptors in the rat vas deferens. *J Aut Pharmacol* 6:39–46.
- Lei S, Deng P-Y, Porter JE, Shin H-S. 2007. Adrenergic Facilitation of GABAergic Transmission in Rat Entorhinal Cortex. *J Neurophysiol* 98:2868–2877.

- Lein ES, Hawrylycz MJ, Ao N, Ayres M, Bensinger A, Bernard A, Boe AF, Boguski MS, Brockway KS, Byrnes EJ, Chen L, Chen L, Chen T-M, Chi Chin M, Chong J, Crook BE, Czaplinska A, Dang CN, Datta S, Dee NR, Desaki AL, Desta T, Diep E, Dolbeare TA, Donelan MJ, Dong H-W, Dougherty JG, Duncan BJ, Ebbert AJ, Eichele G, Estin LK, Faber C, Facer BA, Fields R, Fischer SR, Fliss TP, Frensley C, Gates SN, Glattfelder KJ, Halverson KR, Hart MR, Hohmann JG, Howell MP, Jeung DP, Johnson RA, Karr PT, Kawal R, Kidney JM, Knapik RH, Kuan CL, Lake JH, Laramée AR, Larsen KD, Lau C, Lemon TA, Liang AJ, Liu Y, Luong LT, Michaels J, Morgan JJ, Morgan RJ, Mortrud MT, Mosqueda NF, Ng LL, Ng R, Orta GJ, Overly CC, Pak TH, Parry SE, Pathak SD, Pearson OC, Puchalski RB, Riley ZL, Rockett HR, Rowland SA, Royall JJ, Ruiz MJ, Sarno NR, Schaffnit K, Shapovalova N V, Svisay T, Slaughterbeck CR, Smith SC, Smith KA, Smith BI, Sodt AJ, Stewart NN, Stumpf K-R, Sunkin SM, Sutram M, Tam A, Teemer CD, Thaller C, Thompson CL, Varnam LR, Visel A, Whitlock RM, Wohnoutka PE, et al. 2007. Genome-wide atlas of gene expression in the adult mouse brain. *Nature* 445:168–176.
- Leopoldt D, Harteneck C, Nürnberg B. 1997. G Proteins endogenously expressed in Sf 9 cells: interactions with mammalian histamine receptors. *Naunyn Schmiedeberg's Arch Pharmacol* 356:216–224.
- Leurs R, Traiffort E, Arrang JM, Tardivel-Lacombe J, Ruat M, Schwartz J-C. 1994. Guinea Pig Histamine H1 Receptor. II. Stable Expression in Chinese Hamster Ovary Cells Reveals the Interaction with Three Major Signal Transduction Pathways. *J Neurochem* 62:519–527.
- Leutgeb JK, Leutgeb S, Moser M-B, Moser EI. 2007. Pattern Separation in the Dentate Gyrus and CA3 of the Hippocampus. *Science* 315:961 LP-966.
- Leviel V. 2011. Dopamine release mediated by the dopamine transporter, facts and consequences. *J Neurochem* 118:475–489.
- Li Zhang C, Dreier JP, Heinemann U. 1995. Paroxysmal epileptiform discharges in temporal lobe slices after prolonged exposure to low magnesium are resistant to clinically used anticonvulsants. *Epilepsy Res* 20:105–111.
- Lim HD, van Rijn RM, Ling P, Bakker RA, Thurmond RL, Leurs R. 2005. Evaluation of Histamine H1-, H2-, and H3-Receptor Ligands at the Human Histamine H4 Receptor: Identification of 4-Methylhistamine as the First Potent and Selective. *J Pharmacol Exp Ther* 314:1310 LP-1321.
- Lin Y, Quartermain D, Dunn AJ, Weinshenker D, Stone EA. 2008. Possible dopaminergic stimulation of locus coeruleus α 1-adrenoceptors involved in behavioral activation. *Synapse* 62:516–523.

- Lingenhohl K, Finch DM. 1991. Morphological characterization of rat entorhinal neurons in vivo: soma-dendritic structure and axonal domains. *Exp Brain Res* 84:57–74.
- Liu Y-W, Li J, Ye J-H. 2010. Histamine regulates activities of neurons in the ventrolateral preoptic nucleus. *J Physiol* 588:4103–4116.
- Lorente de No R. 1933. Studies on the Structure of the Cerebral Cortex. *J fur Psychol und Neurol* 45:381–438.
- Lorétan K, Bissière S, Lüthi A. 2004. Dopaminergic modulation of spontaneous inhibitory network activity in the lateral amygdala. *Neuropharmacology* 47:631–639.
- Lu J, Dalton JF, Stokes DR, Calabrese RL. 1997. Functional Role of Ca²⁺ Currents in Graded and Spike-Mediated Synaptic Transmission Between Leech Heart Interneurons. *J Neurophysiol* 77:1779–1794.
- Luján R, Nusser Z, Roberts JDB, Shigemoto R, Somogyi P. 1996. Perisynaptic Location of Metabotropic Glutamate Receptors mGluR1 and mGluR5 on Dendrites and Dendritic Spines in the Rat Hippocampus. *Eur J Neurosci* 8:1488–1500.
- Lundius EG, Sanchez-Alavez M, Ghochani Y, Klaus J, Tabarean I V. 2010. Histamine Influences Body Temperature by Acting at H1 and H3 Receptors on Distinct Populations of Preoptic Neurons. *J Neurosci* 30:4369–4381.
- MacLean PD. 1949. Psychosomatic disease and the visceral brain; recent developments bearing on the Papez theory of emotion. *Psychosom Med* 11:338–353.
- Mahut H, Zola-Morgan S, Moss M. 1982. Hippocampal Resection Impair Associative Learning and Recognition Memory in the Monkey. *J Neurosci* 2:1214–1229.
- Makino S, Shibasaki T, Yamauchi N, Nishioka T, Mimoto T, Wakabayashi I, Gold PW, Hashimoto K. 1999. Psychological stress increased corticotropin-releasing hormone mRNA and content in the central nucleus of the amygdala but not in the hypothalamic paraventricular nucleus in the rat. *Brain Res* 850:136–143.
- Mannaioni G, Marino MJ, Valenti O, Traynelis SF, Conn PJ. 2001. Metabotropic Glutamate Receptors 1 and 5 Differentially Regulate CA1 Pyramidal Cell Function. *J Neurosci* 21:5925 LP-5934.
- Marder E, O’Leary T, Shruti S. 2014. Neuromodulation of circuits with variable parameters: single neurons and small circuits reveal principles of state-dependent and robust neuromodulation. *Annu Rev Neurosci* 37:329–346.

- Maren S, Fanselow MS. 1997. Electrolytic Lesions of the Fimbria/Fornix, Dorsal Hippocampus, or Entorhinal Cortex Produce Anterograde Deficits in Contextual Fear Conditioning in Rats. *Neurobiol Learn Mem* 67:142–149.
- Maren S, Holt WG. 2004. Hippocampus and Pavlovian Fear Conditioning in Rats: Muscimol Infusions Into the Ventral, but Not Dorsal, Hippocampus Impair the Acquisition of Conditional Freezing to an Auditory Conditional Stimulus. *Behav Neurosci* 118:97–110.
- Maruko T, Nakahara T, Sakamoto K, Saito M, Sugimoto N, Takawa Y, Ishii K. 2005. Involvement of the $\beta\gamma$ subunits of G proteins in the cAMP response induced by stimulation of the histamine H1 receptor. *Naunyn Schmiedebergs Arch Pharmacol* 372:153–159.
- Masu M, Tanabe Y, Tsuchida K, Shigemoto R, Nakanishi S. 1991. Sequence and expression of a metabotropic glutamate receptor. *Nature* 349:760–765.
- Mayne EW, Craig MT, McBain CJ, Paulsen O. 2013. Dopamine suppresses persistent network activity via D1-like dopamine receptors in rat medial entorhinal cortex. *Eur J Neurosci* 37:1242–1247.
- McConathy J, Owens MJ, Kilts CD, Malveaux EJ, Camp VM, Votaw JR, Nemeroff CB, Goodman MM. 2004. Synthesis and biological evaluation of [¹¹C]talopram and [¹¹C]talsupram: candidate PET ligands for the norepinephrine transporter. *Nucl Med Biol* 31:705–718.
- McCool BA, Pin J-P, Harpold MM, Brust PF, Stauderman KA, Lovinger DM. 1998. Rat group I Metabotropic Glutamate Receptors Inhibit Neuronal Ca²⁺ Channels via Multiple Signal Transduction Pathways in HEK 293 Cells. *J Neurophysiol* 79:379 LP-391.
- McCormick DA, Williamson A. 1991. Modulation of neuronal firing mode in cat and guinea pig LGNd by histamine: possible cellular mechanisms of histaminergic control of arousal. *J Neurosci* 11:3188–3199.
- McGaughy J, Koene RA, Eichenbaum H, Hasselmo ME. 2005. Cholinergic Deafferentation of the Entorhinal Cortex in Rats Impairs Encoding of Novel But Not Familiar Stimuli in a Delayed Nonmatch-to-Sample Task. *J Neurosci* 25:10273 LP-10281.
- Melzer S, Michael M, Caputi A, Eliava M, Fuchs EC, Whittington MA, Monyer H. 2012. Long-Range-Projecting GABAergic Neurons Modulate Inhibition in Hippocampus and Entorhinal Cortex. *Science* 335:1506 LP-1510.

- Miettinen M, Koivisto E, Riekkinen Sr. P, Miettinen R. 1996. Coexistence of parvalbumin and GABA in nonpyramidal neurons of the rat entorhinal cortex. *Brain Res* 706:113–122.
- Mikulecká A, Mareš P. 2009. Effects of mGluR5 and mGluR1 antagonists on anxiety-like behavior and learning in developing rats. *Behav Brain Res* 204:133–139.
- Miller M, Shi J, Zhu Y, Kustov M, Tian J, Stevens A, Wu M, Xu J, Long S, Yang P, Zholos A V, Salovich JM, Weaver CD, Hopkins CR, Lindsley CW, McManus O, Li M, Zhu MX. 2011. Identification of ML204, a Novel Potent Antagonist That Selectively Modulates Native TRPC4/C5 Ion Channels. *J Biol Chem* 286:33436–33446.
- Milner B. 1962. *Physiologie de l'hippocampe*. (Passouat P, editor.). Paris: Centre National de la Recherche Scientifique.
- Mishkin M. 1978. Memory in monkeys severely impaired by combined but not separate removal of amygdala and hippocampus. *Nature* 273:297–8.
- Mitsuhashi M, Payan DG. 1989. Receptor glycosylation regulates the affinity of histamine H1 receptors during smooth muscle cell differentiation. *Mol Pharmacol* 35:311–318.
- Morales M, Bloom FE. 1997. The 5-HT₃ Receptor Is Present in Different Subpopulations of GABAergic Neurons in the Rat Telencephalon. *J Neurosci* 17:3157 LP-3167.
- Moreno-Delgado D, Torrent A, Gómez-Ramírez J, de Esch I, Blanco I, Ortiz J. 2006. Constitutive activity of H3 autoreceptors modulates histamine synthesis in rat brain through the cAMP/PKA pathway. *Neuropharmacology* 51:517–523.
- Munakata M, Akaike N. 1994. Regulation of K⁺ conductance by histamine H1 and H2 receptors in neurones dissociated from rat neostriatum. *J Physiol* 480:233–245.
- Munsch T, Yanagawa Y, Obata K, Pape H-C. 2005. Dopaminergic control of local interneuron activity in the thalamus. *Eur J Neurosci* 21:290–294.
- Nagatsu T, Hidaka H, Kuzuya H, Takeya K, Umezawa H. 1970. Inhibition of dopamine beta-hydroxylase by fusaric acid (5-butylpicolinic acid) in vitro and in vivo. *Biochem Pharmacol* 19:35–44.
- Nakajima Y, Iwakabe H, Akazawa C, Nawa H, Shigemoto R, Mizuno N, Nakanishi S. 1993. Molecular characterization of a novel retinal metabotropic glutamate receptor mGluR6 with a high agonist selectivity for L-2-amino-4-phosphonobutyrate. *J Biol Chem* 268:11868–11873.

- Nestler EJ, Hyman SE, Malenka RC. 2009a. Seizure Disorders. In: *Molecular Neuropharmacology: A Foundation for Clinical Neuroscience* 2. 2nd ed. The McGraw-Hill Companies. p 443–456.
- Nestler EJ, Hyman SE, Malenka RC. 2009b. Widely Projecting Systems: Monoamines, Acetylcholine, and Orexin. In: *Molecular Neuropharmacology: A Foundation for Clinical Neuroscience*. Second. The McGraw-Hill Companies. p 145–180.
- Nestler EJ, Hyman SE, Malenka RC. 2009c. Schizophrenia and Other Psychoses. In: *Molecular Neuropharmacology: A Foundation for Clinical Neuroscience*. 2nd ed. The McGraw-Hill Companies. p 389–408.
- Newman EL, Climer JR, Hasselmo ME. 2014. Grid cell spatial tuning reduced following systemic muscarinic receptor blockade. *Hippocampus* 24:643–655.
- Nicoletti F, Meek JL, Iadarola MJ, Chuang DM, Roth BL, Costa E. 1986. Coupling of Inositol Phospholipid Metabolism with Excitatory Amino Acid Recognition Sites in Rat Hippocampus. *J Neurochem* 46:40–46.
- Niswender CM, Conn PJ. 2010. Metabotropic glutamate receptors: physiology, pharmacology, and disease. *Annu Rev Pharmacol Toxicol* 50:295–322.
- O’Keefe J, Dostrovsky J. 1971. The hippocampus as a spatial map. Preliminary evidence from unit activity in the freely-moving rat. *Brain Res* 34:171–175.
- Odell AF, Scott JL, Van Helden DF. 2005. Epidermal Growth Factor Induces Tyrosine Phosphorylation, Membrane Insertion, and Activation of Transient Receptor Potential Channel 4. *J Biol Chem* 280:37974–37987.
- Ohishi H, Akazawa C, Shigemoto R, Nakanishi S, Mizuno N. 1995. Distributions of the mRNAs for L-2-amino-4-phosphonobutyrate-sensitive metabotropic glutamate receptors, mGluR4 and mGluR7, in the rat brain. *J Comp Neurol* 360:555–570.
- Ohishi H, Shigemoto R, Nakanishi S, Mizuno N. 1993a. Distribution of the messenger RNA for a metabotropic glutamate receptor, mGluR2, in the central nervous system of the rat. *Neuroscience* 53:1009–1018.
- Ohishi H, Shigemoto R, Nakanishi S, Mizuno N. 1993b. Distribution of the mRNA for a metabotropic glutamate receptor (mGluR3) in the rat brain: An in situ hybridization study. *J Comp Neurol* 335:252–266.
- Olton DS, Walker JA, Gage FH. 1978. Hippocampal connections and spatial discrimination. *Brain Res* 139:295–308.
- Ooi H, Colucci W. 2001. Pharmacological treatment of heart failure. In: Hardman J, Limbird L, Gilman A, editors. *The pharmacological basis of therapeutics*. . p 901.

- Ouedraogo L, Magnon M, Sawadogo L, Tricoche R. 1998. Receptors involved in the positive inotropic action induced by dopamine on the ventricle of a 7-day-old chick embryo heart. *Fundam Clin Pharmacol* 12:133–142.
- Palkovits M, Záborszky L, Brownstein MJ, Fekete MIK, Herman JP, Kanyicska B. 1979. Distribution of norepinephrine and dopamine in cerebral cortical areas of the rat. *Brain Res Bull* 4:593–601.
- Pan Z-H, Hu H-J, Perring P, Andrade R. 2001. T-Type Ca^{2+} Channels Mediate Neurotransmitter Release in Retinal Bipolar Cells. *Neuron* 32:89–98.
- Panula P, Pirvola U, Auvinen S, Airaksinen MS. 1989. Histamine-immunoreactive nerve fibers in the rat brain. *Neuroscience* 28:585–610.
- Papez JW. 1937. A proposed mechanism of emotion. *Arch Neurol Psychiatry* 38:725–743.
- Park J-Y, Remy S, Varela J, Cooper DC, Chung S, Kang H-W, Lee J-H, Spruston N. 2010. A Post-Burst Afterdepolarization Is Mediated by Group I Metabotropic Glutamate Receptor-Dependent Upregulation of Cav2.3 R-Type Calcium Channels in CA1 Pyramidal Neurons. *PLOS Biol* 8:e1000534.
- Pastoll H, Solanka L, van Rossum MCW, Nolan MF. 2013. Feedback Inhibition Enables Theta-Nested Gamma Oscillations and Grid Firing Fields. *Neuron* 77:141–154.
- Phillips AG, Vacca G, Ahn S. 2008. A top-down perspective on dopamine, motivation and memory. *Pharmacol Biochem Behav* 90:236–249.
- Piguet C, Desseilles M, Sterpenich V, Cojan Y, Bertschy G, Vuilleumier P. 2014. Neural substrates of rumination tendency in non-depressed individuals. *Biol Psychol* 103:195–202.
- Pillot C, Heron A, Cochois V, Tardivel-Lacombe J, Ligneau X, Schwartz J-C, Arrang J-M. 2002. A detailed mapping of the histamine H3 receptor and its gene transcripts in rat brain. *Neuroscience* 114:173–193.
- Podda M V, Riccardi E, D'Ascenzo M, Azzena GB, Grassi C. 2010. Dopamine D1-like receptor activation depolarizes medium spiny neurons of the mouse nucleus accumbens by inhibiting inwardly rectifying K^+ currents through a cAMP-dependent protein kinase A-independent mechanism. *Neuroscience* 167:678–690.
- Polydoro M, Dzhala VI, Pooler AM, Nicholls SB, McKinney AP, Sanchez L, Pitstick R, Carlson GA, Staley KJ, Spires-Jones TL, Hyman BT. 2014. Soluble pathological tau in the entorhinal cortex leads to presynaptic deficits in an early Alzheimer's disease model. *Acta Neuropathol* 127:257–270.

- Pralong E, Jones RSG. 1993. Interactions of Dopamine with Glutamate- and GABA-mediated Synaptic Transmission in the Rat Entorhinal Cortex In Vitro. *Eur J Neurosci* 5:760–767.
- Pralong E, Magistretti PJ. 1994. Noradrenaline reduces synaptic responses in normal and tottering mouse entorhinal cortex via $\alpha 2$ receptors. *Neurosci Lett* 179:145–148.
- Pralong E, Magistretti PJ. 1995. Noradrenaline Increases K-conductance and Reduces Glutamatergic Transmission in the Mouse Entorhinal Cortex by Activation of $\alpha 2$ -Adrenoreceptors. *Eur J Neurosci* 7:2370–2378.
- Prasad KMR, Patel AR, Muddasani S, Sweeney J, Keshavan MS. 2004. The Entorhinal Cortex in First-Episode Psychotic Disorders: A Structural Magnetic Resonance Imaging Study. *Am J Psychiatry* 161:1612–1619.
- Quilichini P, Sirota A, Buzsáki G. 2010. Intrinsic Circuit Organization and Theta–Gamma Oscillation Dynamics in the Entorhinal Cortex of the Rat. *J Neurosci* 30:11128–11142.
- Rae MG, Irving AJ. 2004. Both mGluR1 and mGluR5 mediate Ca^{2+} release and inward currents in hippocampal CA1 pyramidal neurons. *Neuropharmacology* 46:1057–1069.
- Rajfer SI, Borow KM, Lang RM, Neumann A, Carroll JD. 1988. Effects of dopamine on left ventricular afterload and contractile state in heart failure: Relation to the activation of beta1-adrenoceptors and dopamine receptors. *J Am Coll Cardiol* 12:498–506.
- Ramon y Cajal S. 1902. *Trabajos del Laboratorio de Investigaciones Biológicas de la Universidad de Madrid*.
- Ratnala VRP, Swarts HGP, VanOostrum J, Leurs R, DeGroot HJM, Bakker RA, DeGrip WJ. 2004. Large-scale overproduction, functional purification and ligand affinities of the His-tagged human histamine H1 receptor. *Eur J Biochem* 271:2636–2646.
- Ray S, Burgalossi A, Brecht M, Naumann RK. 2017. Complementary Modular Microcircuits of the Rat Medial Entorhinal Cortex. *Front Syst Neurosci* 11:20.
- Ray S, Naumann R, Burgalossi A, Tang Q, Schmidt H, Brecht M. 2014. Grid-Layout and Theta-Modulation of Layer 2 Pyramidal Neurons in Medial Entorhinal Cortex. *Science* 343:891 LP-896.
- Reid SNM, Daw NW, Gregory DS, Flavin H. 1996. cAMP Levels Increased by Activation of Metabotropic Glutamate Receptors Correlate with Visual Plasticity. *J Neurosci* 16:7619 LP-7626.

- Reiner PB, Kamondi A. 1994. Mechanisms of antihistamine-induced sedation in the human brain: H1 receptor activation reduces a background leakage potassium current. *Neuroscience* 59:579–588.
- Rey E, Hernandez D, Abreu P, Alonso R, Tabares L. 2001. Dopamine induces intracellular Ca^{2+} signals mediated by $\alpha 1B$ -adrenoceptors in rat pineal cells. *Eur J Pharmacol* 430:9–17.
- Riccio A, Li Y, Moon J, Kim K-S, Smith KS, Rudolph U, Gapon S, Yao GL, Tsvetkov E, Rodig SJ, Van't Veer A, Meloni EG, Carlezon Jr. WA, Bolshakov VY, Clapham DE. 2009. Essential Role for TRPC5 in Amygdala Function and Fear-Related Behavior. *Cell* 137:761–772.
- Riccio A, Li Y, Tsvetkov E, Gapon S, Yao GL, Smith KS, Engin E, Rudolph U, Bolshakov VY, Clapham DE. 2014. Decreased Anxiety-Like Behavior and $Gaq/11$ -Dependent Responses in the Amygdala of Mice Lacking TRPC4 Channels. *J Neurosci* 34:3653–3667.
- Richerson GB, Aston-Jones G, Saper CB. 2013. The Modulatory Systems of the Brain Stem. In: Nestler EJ, Schwartz JH, Jessell T, Siegelbaum S, Hudspeth A, editors. *Principles of Neural Science*. 5th ed. The McGraw-Hill Companies. p 1038–1055.
- Richfield EK, Young AB, Penney JB. 1989. Comparative distributions of dopamine D-1 and D-2 receptors in the cerebral cortex of rats, cats, and monkeys. *J Comp Neurol* 286:409–426.
- Rivera A, Peñafiel A, Megías M, Agnati LF, López-Téllez JF, Gago B, Gutiérrez A, de la Calle A, Fuxe K. 2008. Cellular localization and distribution of dopamine D4 receptors in the rat cerebral cortex and their relationship with the cortical dopaminergic and noradrenergic nerve terminal networks. *Neuroscience* 155:997–1010.
- Robbins J, Wakakuwa K, Ikeda H. 1988. Noradrenaline action on cat retinal ganglion cells is mediated by dopamine (D2) receptors. *Brain Res* 438:52–60.
- Rosenkranz JA, Johnston D. 2006. Dopaminergic Regulation of Neuronal Excitability through Modulation of I_h in Layer V Entorhinal Cortex. *J Neurosci* 26:3229–3244.
- Rosenkranz JA, Johnston D. 2007. State-Dependent Modulation of Amygdala Inputs by Dopamine-Induced Enhancement of Sodium Currents in Layer V Entorhinal Cortex. *J Neurosci* 27:7054–7069.
- van Rossum DB, Patterson RL, Ma H-T, Gill DL. 2000. Ca^{2+} Entry Mediated by Store Depletion, S-Nitrosylation, and TRP3 Channels: comparison of coupling and function. *J Biol Chem* 275:28562–28568.

- Rothman RB, Baumann MH, Dersch CM, Romero D V, Rice KC, Carroll FI, Partilla JS. 2001. Amphetamine-type central nervous system stimulants release norepinephrine more potently than they release dopamine and serotonin. *Synapse* 39:32–41.
- Sanacora G, Treccani G, Popoli M. 2012. Towards a glutamate hypothesis of depression: An emerging frontier of neuropsychopharmacology for mood disorders. *Neuropharmacology* 62:63–77.
- Sanders H, Rennó-Costa C, Idiart M, Lisman J. 2015. Grid Cells and Place Cells: An Integrated View of their Navigational and Memory Function. *Trends Neurosci* 38:763–775.
- Sanes J, Jessell T. 2013. The Aging Brain. In: Kandel ER, Schwartz JH, Jessell TM, Siegelbaum SA, Hudspeth AJ, editors. *Principles of Neural Science*. 5th ed. The McGraw-Hill Companies. p 1328–1346.
- Sara SJ. 2009. The locus coeruleus and noradrenergic modulation of cognition. *Nat Rev Neurosci* 10:211–223.
- Sargolini F, Fyhn M, Hafting T, McNaughton BL, Witter MP, Moser M-B, Moser EI. 2006. Conjunctive Representation of Position, Direction, and Velocity in Entorhinal Cortex. *Science* 312:758 LP-762.
- Saugstad JA, Kinzie JM, Shinohara MM, Segerson TP, Westbrook GL. 1997. Cloning and Expression of Rat Metabotropic Glutamate Receptor 8 Reveals a Distinct Pharmacological Profile. *Mol Pharmacol* 51:119 LP-125.
- Savasta M, Dubois A, Scatton B. 1986. Autoradiographic localization of D1 dopamine receptors in the rat brain with [3H]SCH 23390. *Brain Res* 375:291–301.
- Schaefer M, Plant TD, Obukhov AG, Hofmann T, Gudermann T, Schultz G. 2000. Receptor-mediated Regulation of the Nonselective Cation Channels TRPC4 and TRPC5. *J Biol Chem* 275:17517–17526.
- Scharfman HE, Goodman JH, Du F, Schwarcz R. 1998. Chronic Changes in Synaptic Responses of Entorhinal and Hippocampal Neurons After Amino-Oxyacetic Acid (AOAA)–Induced Entorhinal Cortical Neuron Loss. *J Neurophysiol* 80:3031 LP-3046.
- Scheff SW, Price DA, Schmitt FA, Mufson EJ. 2006. Hippocampal synaptic loss in early Alzheimer’s disease and mild cognitive impairment. *Neurobiol Aging* 27:1372–1384.
- Schmitz D, Gloveli T, Behr J, Dugladze T, Heinemann U. 1998. Subthreshold membrane potential oscillations in neurons of deep layers of the entorhinal cortex. *Neuroscience* 85:999–1004.

- Schoepp DD, Jane DE, Monn JA. 1999. Pharmacological agents acting at subtypes of metabotropic glutamate receptors. *Neuropharmacology* 38:1431–1476.
- Schools GP, Kimelberg HK. 1999. mGluR3 and mGluR5 are the predominant metabotropic glutamate receptor mRNAs expressed in hippocampal astrocytes acutely isolated from young rats. *J Neurosci Res* 58:533–543.
- Schwarcz R, Eid T, Du FU. 2000. Neurons in Layer III of the Entorhinal Cortex: A Role in Epileptogenesis and Epilepsy? *Ann N Y Acad Sci* 911:328–342.
- Schwarcz R, Witter MP. 2002. Memory impairment in temporal lobe epilepsy: the role of entorhinal lesions. *Epilepsy Res* 50:161–177.
- Scoville WB, Milner B. 1957. Loss of Recent Memory After Bilateral Hippocampal Lesions. *J Neurol Neurosurg Psychiatry* 20:11–21.
- Seamans JK, Gorelova N, Durstewitz D, Yang CR. 2001. Bidirectional Dopamine Modulation of GABAergic Inhibition in Prefrontal Cortical Pyramidal Neurons. *J Neurosci* 21:3628–3638.
- Selkoe DJ. 2002. Alzheimer's Disease Is a Synaptic Failure. *Science* 298:789 LP-791.
- Selli C, Erac Y, Kosova B, Tosun M. 2009. Post-transcriptional silencing of TRPC1 ion channel gene by RNA interference upregulates TRPC6 expression and store-operated Ca²⁺ entry in A7r5 vascular smooth muscle cells. *Vascul Pharmacol* 51:96–100.
- Shah A, Jhavar SS, Goel A. 2012. Analysis of the anatomy of the Papez circuit and adjoining limbic system by fiber dissection techniques. *J Clin Neurosci* 19:289–298.
- Shankar H, Murugappan S, Kim S, Jin J, Ding Z, Wickman K, Kunapuli SP. 2004. Role of G protein-gated inwardly rectifying potassium channels in P2Y2 receptor-mediated platelet functional responses. *Blood*;1104:1335 LP-1343.
- Shigemoto R, Kinoshita A, Wada E, Nomura S, Ohishi H, Takada M, Flor PJ, Neki A, Abe T, Nakanishi S, Mizuno N. 1997. Differential Presynaptic Localization of Metabotropic Glutamate Receptor Subtypes in the Rat Hippocampus. *J Neurosci* 17:7503 LP-7522.
- Shigemoto R, Nakanishi S, Mizuno N. 1992. Distribution of the mRNA for a metabotropic glutamate receptor (mGluR1) in the central nervous system: An in situ hybridization study in adult and developing rat. *J Comp Neurol* 322:121–135.
- Silvestrelli G, Lanari A, Parnetti L, Tomassoni D, Amenta F. 2006. Treatment of Alzheimer's disease: From pharmacology to a better understanding of disease pathophysiology. *Mech Ageing Dev* 127:148–157.

- Sladeczek F, Pin JP, Recasens M, Bockaert J, Weiss S. 1985. Glutamate stimulates inositol phosphate formation in striatal neurones. *Nature* 317:717–719.
- Smith CC, Greene RW. 2012. CNS Dopamine Transmission Mediated by Noradrenergic Innervation. *J Neurosci* 32:6072 LP-6080.
- Sohn J-W, Lee D, Cho H, Lim W, Shin H-S, Lee S-H, Ho W-K. 2007. Receptor-specific inhibition of GABAB-activated K⁺ currents by muscarinic and metabotropic glutamate receptors in immature rat hippocampus. *J Physiol* 580:411–422.
- Solstad T, Boccara CN, Kropff E, Moser M-B, Moser EI. 2008. Representation of Geometric Borders in the Entorhinal Cortex. *Science* 322:1865 LP-1868.
- Sosulina L, Schwesig G, Seifert G, Pape H-C. 2008. Neuropeptide Y activates a G-protein-coupled inwardly rectifying potassium current and dampens excitability in the lateral amygdala. *Mol Cell Neurosci* 39:491–498.
- Sparta DR, Smithuis J, Stamatakis AM, Jennings JH, Kantak PA, Ung RL, Stuber GD. 2014. Inhibition of projections from the basolateral amygdala to the entorhinal cortex disrupts the acquisition of contextual fear. *Front Behav Neurosci* 8:129.
- Staines WA, Daddona PE, Nagy JJ. 1987. The organization and hypothalamic projections of the tuberomammillary nucleus in the rat: An immunohistochemical study of adenosine deaminase-positive neurons and fibers. *Neuroscience* 23:571–596.
- Starodub AM, Wood JD. 2000. Histamine Suppresses A-Type Potassium Current in Myenteric Neurons from Guinea Pig Small Intestine. *J Pharmacol Exp Ther* 294:555–561.
- Steffenach H-A, Witter M, Moser M-B, Moser EI. 2005. Spatial Memory in the Rat Requires the Dorsolateral Band of the Entorhinal Cortex. 45:301–313.
- Stenkamp K, Heinemann U, Schmitz D. 1998. Dopamine suppresses stimulus-induced field potentials in layer III of rat medial entorhinal cortex. *Neurosci Lett* 255:119–121.
- Steward O. 1976. Topographic organization of the projections from the entorhinal area to the hippocampal formation of the rat. *J Comp Neurol* 167:285–314.
- Steward O, Scoville SA. 1976. Cells of origin of entorhinal cortical afferents to the hippocampus and fascia dentata of the rat. *J Comp Neurol* 169:347–370.
- Stranahan AM, Mattson MP. 2010. Selective vulnerability of neurons in layer II of the entorhinal cortex during aging and Alzheimer’s disease. *Neural Plast* 2010:108190.

- van Strien NM, Cappaert NLM, Witter MP. 2009. The anatomy of memory: an interactive overview of the parahippocampal-hippocampal network. *Nat Rev Neurosci* 10:272–282.
- Strübing C, Krapivinsky G, Krapivinsky L, Clapham DE. 2001. TRPC1 and TRPC5 Form a Novel Cation Channel in Mammalian Brain. *Neuron* 29:645–655.
- Stuchlik A, Petrasek T, Vales K. 2008. Dopamine D2 receptors and alpha1-adrenoceptors synergistically modulate locomotion and behavior of rats in a place avoidance task. *Behav Brain Res* 189:139–144.
- Suh B-C, Lee H, Jun D-J, Chun J-S, Lee J-H, Kim K-T. 2001. Inhibition of H2 Histamine Receptor-Mediated Cation Channel Opening by Protein Kinase C in Human Promyelocytic Cells. *J Immunol* 167:1663 LP-1671.
- Suh J, Rivest AJ, Nakashiba T, Tominaga T, Tonegawa S. 2011. Entorhinal Cortex Layer III Input to the Hippocampus Is Crucial for Temporal Association Memory. *Science* 334:1415 LP-1420.
- Sun C, Kitamura T, Yamamoto J, Martin J, Pignatelli M, Kitch LJ, Schnitzer MJ, Tonegawa S. 2015. Distinct speed dependence of entorhinal island and ocean cells, including respective grid cells. *Proc Natl Acad Sci* 112:9466–9471.
- Sung TS, Jeon JP, Kim BJ, Hong C, Kim SY, Kim J, Jeon JH, Kim HJ, Suh CK, Kim SJ, So I. 2011. Molecular determinants of PKA-dependent inhibition of TRPC5 channel. *Am J Physiol - Cell Physiol* 301:C823 LP-C832.
- Swanson LW, Kohler C. 1986. Anatomical evidence for direct projections from the entorhinal area to the entire cortical mantle in the rat. *J Neurosci* 6:3010–3023.
- Takeshita Y, Watanabe T, Sakata T, Munakata M, Ishibashi H, Akaike N. 1998. Histamine modulates high-voltage-activated calcium channels in neurons dissociated from the rat tuberomammillary nucleus. *Neuroscience* 87:797–805.
- Tanabe Y, Masu M, Ishii T, Shigemoto R, Nakanishi S. 1992. A family of metabotropic glutamate receptors. *Neuron* 8:169–179.
- Tanabe Y, Nomura A, Masu M, Shigemoto R, Mizuno N, Nakanishi S. 1993. Signal transduction, pharmacological properties, and expression patterns of two rat metabotropic glutamate receptors, mGluR3 and mGluR4. *J Neurosci* 13:1372 LP-1378.
- Tang Q, Ebbesen CL, Sanguinetti-Scheck JI, Preston-Ferrer P, Gundlfinger A, Winterer J, Beed P, Ray S, Naumann R, Schmitz D, Brecht M, Burgalossi A. 2015. Anatomical Organization and Spatiotemporal Firing Patterns of Layer 3 Neurons in the Rat Medial Entorhinal Cortex. *J Neurosci* 35:12346 LP-12354.

- Tarazi FI, Tomasini EC, Baldessarini RJ. 1999. Postnatal development of dopamine D1-like receptors in rat cortical and striatolimbic brain regions: An autoradiographic study. *Dev Neurosci* 21:43–49.
- Terry RD, Masliah E, Salmon DP, Butters N, DeTeresa R, Hill R, Hansen LA, Katzman R. 1991. Physical basis of cognitive alterations in Alzheimer's disease: synapse loss is the major correlate of cognitive impairment. *Ann Neurol* 30:572–580.
- Terwel D, Lasrado R, Snauwaert J, Vandeweert E, Van Haesendonck C, Borghgraef P, Van Leuven F. 2005. Changed Conformation of Mutant Tau-P301L Underlies the Moribund Tauopathy, Absent in Progressive, Nonlethal Axonopathy of Tau-4R/2N Transgenic Mice. *J Biol Chem* 280:3963–3973.
- Thakur DP, Tian J, Jeon J, Xiong J, Huang Y, Flockerzi V, Zhu MX. 2016. Critical roles of Gi/o proteins and phospholipase C- δ 1 in the activation of receptor-operated TRPC4 channels. *Proc Natl Acad Sci* 113:1092–1097.
- Thom M, Mathern GW, Cross JH, Bertram EH. 2010. Mesial temporal lobe epilepsy: How do we improve surgical outcome? *Ann Neurol* 68:424–434.
- Tovote P, Fadok JP, Luthi A. 2015. Neuronal circuits for fear and anxiety. *Nat Rev Neurosci* 16:317–331.
- Traiffort E, Ruat M, Arrang JM, Leurs R, Piomelli D, Schwartz JC. 1992. Expression of a cloned rat histamine H2 receptor mediating inhibition of arachidonate release and activation of cAMP accumulation. *Proc Natl Acad Sci* 89:2649–2653.
- Traynelis SF, Wollmuth LP, McBain CJ, Menniti FS, Vance KM, Ogden KK, Hansen KB, Yuan H, Myers SJ, Dingledine R. 2010. Glutamate Receptor Ion Channels: Structure, Regulation, and Function. *Pharmacol Rev* 62:405 LP-496.
- Trebak M, Lemonnier L, DeHaven WI, Wedel BJ, Bird GS, Putney JW. 2009. Complex functions of phosphatidylinositol 4,5-bisphosphate in regulation of TRPC5 cation channels. *Pflügers Arch - Eur J Physiol* 457:757–769.
- Tu P-C, Chen L-F, Hsieh J-C, Bai Y-M, Li C-T, Su T-P. 2012. Regional cortical thinning in patients with major depressive disorder: A surface-based morphometry study. *Psychiatry Res Neuroimaging* 202:206–213.
- Unnerstall JR, Fernandez I, Orensanz LM. 1985. The alpha-adrenergic receptor: Radiohistochemical analysis of functional characteristics and biochemical differences. *Pharmacol Biochem Behav* 22:859–874.

- Unnerstall JR, Kopajtic TA, Kuhar MJ. 1984. Distribution of α_2 agonist binding sites in the rat and human central nervous system: Analysis of some functional, anatomic correlates of the pharmacologic effects of clonidine and related adrenergic agents. *Brain Res Rev* 7:69–101.
- Varga C, Lee SY, Soltesz I. 2010. Target-selective GABAergic control of entorhinal cortex output. *Nat Neurosci* 13:822–824.
- Varnai P, Osipenko ON, Vizi ES, Spat A. 1995. Activation of calcium current in voltage-clamped rat glomerulosa cells by potassium ions. *J Physiol* 483:67–78.
- Vazquez G, Wedel BJ, Kawasaki BT, Bird GSJ, Putney JW. 2004. Obligatory Role of Src Kinase in the Signaling Mechanism for TRPC3 Cation Channels. *J Biol Chem* 279:40521–40528.
- Vizuete ML, Traffort E, Bouthenet ML, Ruat M, Souil E, Tardivel-Lacombe J, Schwartz J-C. 1997. Detailed mapping of the histamine H₂ receptor and its gene transcripts in guinea-pig brain. *Neuroscience* 80:321–343.
- Wadenberg ML, Hertel P, Fernholm R, Hygge Blakeman K, Ahlenius S, Svensson TH. 2000. Enhancement of antipsychotic-like effects by combined treatment with the α_1 -adrenoceptor antagonist prazosin and the dopamine D₂ receptor antagonist raclopride in rats. *J Neural Transm* 107:1229–1238.
- Wang S, Chen X, Kurada L, Huang Z, Lei S. 2012. Activation of Group II Metabotropic Glutamate Receptors Inhibits Glutamatergic Transmission in the Rat Entorhinal Cortex via Reduction of Glutamate Release Probability. *Cereb Cortex* 22:584–594.
- Wang S, Zhang A-P, Kurada L, Matsui T, Lei S. 2011. Cholecystokinin facilitates neuronal excitability in the entorhinal cortex via activation of TRPC-like channels. *J Neurophysiol* 106:1515–1524.
- Watkins ER. 2008. Constructive and unconstructive repetitive thought. *Psychol Bull* 134:163–206.
- Weiner DM, Levey AI, Sunahara RK, Niznik HB, O'Dowd BF, Seeman P, Brann MR. 1991. D₁ and D₂ dopamine receptor mRNA in rat brain. *Proc Natl Acad Sci U S A* 88:1859–1863.
- Westbrook GL. 2013. Seizures and Epilepsy. In: Kandel ER, Schwartz JH, Jessell T, Siegelbaum S, Hudspeth A, editors. *Principles of Neural Science*. 5th ed. The McGraw-Hill Companies. p 1116–1139.
- Whyment AD, Blanks AM, Lee K, Renaud LP, Spanswick D. 2006. Histamine Excites Neonatal Rat Sympathetic Preganglionic Neurons In Vitro Via Activation of H₁ Receptors. *J Neurophysiol* 95:2492–2500.

- Wilcox BJ, Unnerstall JR. 1990. Identification of a subpopulation of neuropeptide Y-containing locus coeruleus neurons that project to the entorhinal cortex. *Synapse* 6:284–291.
- Williams RH, Chee MJS, Kroeger D, Ferrari LL, Maratos-Flier E, Scammell TE, Arrigoni E. 2014. Optogenetic-Mediated Release of Histamine Reveals Distal and Autoregulatory Mechanisms for Controlling Arousal. *J Neurosci* 34:6023–6029.
- Williams SB, Hablitz JJ. 2015. Differential modulation of repetitive firing and synchronous network activity in neocortical interneurons by inhibition of A-type K(+) channels and I(h). *Front Cell Neurosci* 9:89.
- Winterer J, Maier N, Wozny C, Beed P, Breustedt J, Evangelista R, Peng Y, D’Albis T, Kempter R, Schmitz D. 2017. Excitatory Microcircuits within Superficial Layers of the Medial Entorhinal Cortex. *Cell Rep* 19:1110–1116.
- Witkowski G, Szulczyk B, Rola R, Szulczyk P. 2008. D1 dopaminergic control of G protein-dependent inward rectifier K⁺ (GIRK)-like channel current in pyramidal neurons of the medial prefrontal cortex. *Neuroscience* 155:53–63.
- Witter MP, Naber PA, van Haeften T, Machielsen WCM, Rombouts SARB, Barkhof F, Scheltens P, Lopes da Silva FH. 2000. Cortico-hippocampal communication by way of parallel parahippocampal-subicular pathways. *Hippocampus* 10:398–410.
- Witter MP, Wouterlood FG, Naber PA, Van Haeften T. 2006. Anatomical Organization of the Parahippocampal-Hippocampal Network. *Ann N Y Acad Sci* 911:1–24.
- Woodhall G, Evans DIP, Jones RSG. 2001. Activation of presynaptic group III metabotropic glutamate receptors depresses spontaneous inhibition in layer V of the rat entorhinal cortex. *Neuroscience* 105:71–78.
- Woodhall GL, Ayman G, Jones RSG. 2007. Differential control of two forms of glutamate release by group III metabotropic glutamate receptors at rat entorhinal synapses. *Neuroscience* 148:7–21.
- Woodhall GL, Bailey SJ, Thompson SE, Evans DIP, Jones RSG. 2005. Fundamental differences in spontaneous synaptic inhibition between deep and superficial layers of the rat entorhinal cortex. *Hippocampus* 15:232–245.
- Wouterlood FG, Pothuizen H. 2000. Sparse colocalization of somatostatin- and GABA-immunoreactivity in the entorhinal cortex of the rat. *Hippocampus* 10:77–86.
- Xiao Z, Cilz NI, Kurada L, Hu B, Yang C, Wada E, Combs CK, Porter JE, Lesage F, Lei S. 2014. Activation of neurotensin receptor 1 facilitates neuronal excitability and spatial learning and memory in the entorhinal cortex: Beneficial actions in an Alzheimer’s disease model. *J Neurosci* 34.

- Xiao Z, Deng P-Y, Rojanathammanee L, Yang C, Grisanti L, Permpoonputtana K, Weinschenker D, Doze VA, Porter JE, Lei S. 2009a. Noradrenergic Depression of Neuronal Excitability in the Entorhinal Cortex via Activation of TREK-2 K⁺ Channels. *J Biol Chem* 284:10980–10991.
- Xiao Z, Deng P-Y, Yang C, Lei S. 2009b. Modulation of GABAergic Transmission by Muscarinic Receptors in the Entorhinal Cortex of Juvenile Rats. *J Neurophysiol* 102:659–669.
- Xiao Z, Jaiswal MK, Deng P-Y, Matsui T, Shin H-S, Porter JE, Lei S. 2012. Requirement of phospholipase C and protein kinase C in cholecystinin-mediated facilitation of NMDA channel function and anxiety-like behavior. *Hippocampus* 22:1438–1450.
- Xu C-S, Liu A-C, Chen J, Pan Z-Y, Wan Q, Li Z-Q, Wang Z-F. 2015. Overactivation of NR2B-containing NMDA receptors through entorhinal–hippocampal connection initiates accumulation of hyperphosphorylated tau in rat hippocampus after transient middle cerebral artery occlusion. *J Neurochem* 134:566–577.
- Xu C, Michelsen KA, Wu M, Morozova E, Panula P, Alreja M. 2004. Histamine innervation and activation of septohippocampal GABAergic neurones: involvement of local ACh release. *J Physiol* 561:657–670.
- Yang X, Yao C, Tian T, Li X, Yan H, Wu J, Li H, Pei L, Liu D, Tian Q, Zhu L-Q, Lu Y. 2016. A novel mechanism of memory loss in Alzheimer's disease mice via the degeneration of entorhinal-CA1 synapses. *Mol Psychiatry*.
- Yang Y, Calakos N. 2013. Presynaptic long-term plasticity. *Front Synaptic Neurosci* 5.
- Yasuda M, Mayford MR. 2006. CaMKII Activation in the Entorhinal Cortex Disrupts Previously Encoded Spatial Memory. *Neuron* 50:309–318.
- Yekhlief L, Breschi GL, Lagostena L, Russo G, Taverna S. 2015. Selective activation of parvalbumin- or somatostatin-expressing interneurons triggers epileptic seizurelike activity in mouse medial entorhinal cortex. *J Neurophysiol* 113:1616–1630.
- Yokoyama H, Iinuma K. 1996. Histamine and Seizures. *CNS Drugs* 5:321–330.
- Yoshida M, Fransén E, Hasselmo ME. 2008. mGluR-dependent persistent firing in entorhinal cortex layer III neurons. *Eur J Neurosci* 28:1116–1126.
- Zajaczkowski W, Quack G, Danysz W. 1996. Infusion of (+)-MK-801 and memantine — contrasting effects on radial maze learning in rats with entorhinal cortex lesion. *Eur J Pharmacol* 296:239–246.

- Zhang H-P, Xiao Z, Cilz NI, Hu B, Dong H, Lei S. 2014a. Bombesin facilitates GABAergic transmission and depresses epileptiform activity in the entorhinal cortex. *Hippocampus* 24.
- Zhang H, Cilz NI, Yang C, Hu B, Dong H, Lei S. 2015a. Depression of neuronal excitability and epileptic activities by group II metabotropic glutamate receptors in the medial entorhinal cortex. *Hippocampus* 25.
- Zhang H, Dong H, Cilz NI, Kurada L, Hu B, Wada E, Bayliss DA, Porter JE, Lei S. 2016. Neurotensinergic Excitation of Dentate Gyrus Granule Cells via Gq-Coupled Inhibition of TASK-3 Channels. *Cereb Cortex* 26.
- Zhang H, Dong H, Lei S. 2015b. Neurotensinergic augmentation of glutamate release at the perforant path-granule cell synapse in rat dentate gyrus: Roles of L-Type Ca²⁺ channels, calmodulin and myosin light-chain kinase. *Neuropharmacology* 95:252–260.
- Zhang H, Xiao Z, Cilz NI, Hu B, Dong H, Lei S. 2014b. Bombesin facilitates GABAergic transmission and depresses epileptiform activity in the entorhinal cortex. *Hippocampus* 24:21–31.
- Zhang S-J, Ye J, Miao C, Tsao A, Cerniauskas I, Ledergerber D, Moser M-B, Moser EI. 2013a. Optogenetic Dissection of Entorhinal-Hippocampal Functional Connectivity. *Science* 340.
- Zhang W-P, Ouyang M, Thomas SA. 2004. Potency of catecholamines and other l-tyrosine derivatives at the cloned mouse adrenergic receptors. *Neuropharmacology* 47:438–449.
- Zhang X-Y, Yu L, Zhuang Q-X, Peng S-Y, Zhu J-N, Wang J-J. 2013b. Postsynaptic mechanisms underlying the excitatory action of histamine on medial vestibular nucleus neurons in rats. *Br J Pharmacol* 170:156–169.
- Zhang Z, Reboreda A, Alonso A, Barker PA, Séguéla P. 2011. TRPC channels underlie cholinergic plateau potentials and persistent activity in entorhinal cortex. *Hippocampus* 21:386–397.
- Zhou F-M, Hablitz JJ. 1999. Dopamine Modulation of Membrane and Synaptic Properties of Interneurons in Rat Cerebral Cortex. *J Neurophysiol* 81:967–976.
- Zhou F-W, Xu J-J, Zhao Y, LeDoux MS, Zhou F-M. 2006. Opposite Functions of Histamine H1 and H2 Receptors and H3 Receptor in Substantia Nigra Pars Reticulata. *J Neurophysiol* 96:1581–1591.

Zlomuzica A, Ruocco LA, Sadile AG, Huston JP, Dere E. 2009. Histamine H1 receptor knockout mice exhibit impaired spatial memory in the eight-arm radial maze. *Br J Pharmacol* 157:86–91.

Zola-Morgan S, Squire LR, Amaral DG. 1989a. Lesions of the amygdala that spare adjacent cortical regions do not impair memory or exacerbate the impairment following lesions of the hippocampal formation. *J Neurosci* 9:1922 LP-1936.

Zola-Morgan S, Squire LR, Amaral DG, Suzuki WA. 1989b. Lesions of perirhinal and parahippocampal cortex that spare the amygdala and hippocampal formation produce severe memory impairment. *J Neurosci* 9:4355–4370.